AD-A110 621 GENERAL DYNAMICS SAN DIEGO CA ELECTRONICS DIV F/G 17/9
AREA INTRUDER TRACK STUDY.(U)
NOV 81 J B GEHMAN F30602-79-C-0189
UNCLASSIFIED RADC-TR-81-314 NL

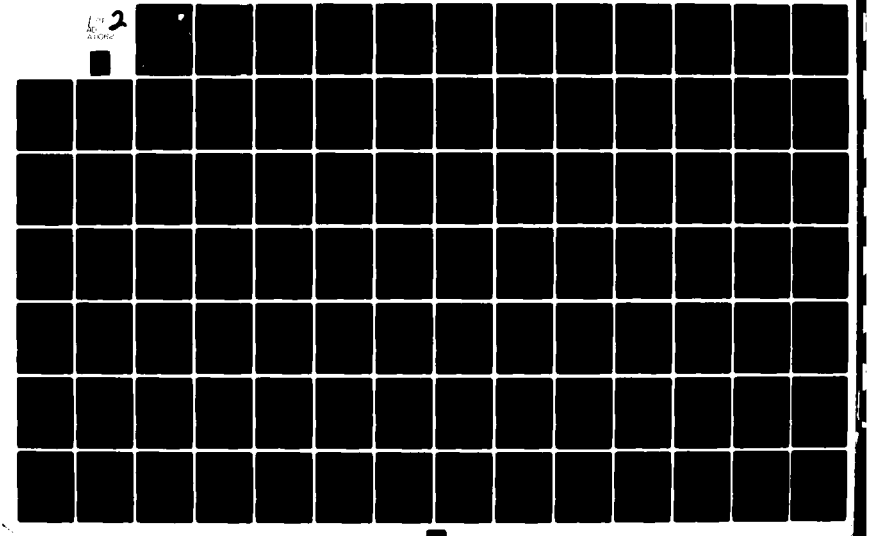

LEVEL II

12

RADC-TR-81-314
Final Technical Report
November 1981

AREA INTRUDER TRACK STUDY

General Dynamics

John B. Gehman

This effort was sponsored by the Defense Nuclear Agency

ROME AIR DEVELOPMENT CENTER
Air Force Systems Command
Griffiss Air Force Base, New York 13441

This report has been reviewed by the RADC Public Affairs Office (PA) and is releasable to the National Technical Information Service (NTIS). At NTIS it will be releasable to the general public, including foreign nations.

RADC-TR-81-314 has been reviewed and is approved for publication.

APPROVED: Nicholas V. Karas

NICHOLAS V. KARAS
Project Engineer

APPROVED: Allan C. Schell

ALLAN C. SCHELL, Chief
EM Sciences Division

FOR THE COMMANDER: John P. Huss

JOHN P. HUSS
Acting Chief, Plans Office

If your address has changed or if you wish to be removed from the RADC mailing list, or if the addressee is no longer employed by your organization, please notify RADC (EEC) Hanscom AFB NY 01731. This will assist us in maintaining a current mailing list.

UNCLASSIFIED

SECURITY CLASSIFICATION OF THIS PAGE (When Data Entered)

REPORT DOCUMENTATION PAGE		READ INSTRUCTIONS BEFORE COMPLETING FORM
1. REPORT NUMBER RADC-TR-81-314	2. GOVT ACCESSION NO. AD-A114	3. RECIPIENT'S CATALOG NUMBER 621
4. TITLE (and Subtitle) AREA INTRUDER TRACK STUDY		5. TYPE OF REPORT & PERIOD COVERED Final Technical Report Sep 79 - Apr 81
		6. PERFORMING ORG. REPORT NUMBER N/A
7. AUTHOR(s) John B. Gehman		8. CONTRACT OR GRANT NUMBER(s) F30602-79-C-0189
9. PERFORMING ORGANIZATION NAME AND ADDRESS General Dynamics/Electronics Division P. O. Box 81127 San Diego CA 92138		10. PROGRAM ELEMENT, PROJECT, TASK AREA & WORK UNIT NUMBERS 62704H DNAR0205
11. CONTROLLING OFFICE NAME AND ADDRESS Deputy for Electronic Technology (RADC/EEC) Hanscom AFB MA 01731		12. REPORT DATE November 1981 13. NUMBER OF PAGES 188
14. MONITORING AGENCY NAME & ADDRESS(if different from Controlling Office) Same		15. SECURITY CLASS. (of this report) UNCLASSIFIED 15a. DECLASSIFICATION/DOWNGRADING SCHEDULE N/A

16. DISTRIBUTION STATEMENT (of this Report)

Approved for public release; distribution unlimited.

17. DISTRIBUTION STATEMENT (of the abstract entered in Block 20, if different from Report)

Same

18. SUPPLEMENTARY NOTES

RADC Project Engineer: Nicholas V. Karas (EEC)
This effort was sponsored by the Defense Nuclear Agency

19. KEY WORDS (Continue on reverse side if necessary and identify by block number)

Radio Frequency Sensor
Intruder Detection
Multistatic Radar
Doppler Tracking
Personnel Detection

20. ABSTRACT (Continue on reverse side if necessary and identify by block number)

An investigation is made of a VHF bistatic doppler intrusion tracking system. A single CW transmitter illuminates an annular ring of 108 square meters, 8 km from its center. Multiple receiving sensors detect reflected signals from an intruder up to 1.5 km and compares its rotating phase with the direct signal. A data link connects all the sensors to a central computer which determines the track of the intruder. The track is visually displayed on a CRT and/or hard copy. Both theoretical

DD FORM 1 JAN 73 1473 EDITION OF 1 NOV 65 IS OBSOLETE

UNCLASSIFIED

SECURITY CLASSIFICATION OF THIS PAGE (When Data Entered)

14170

and test measurements were made to verify the signal-to-noise ratios, probability of detection , and false alarm rates. Although the original system was to be used in a Hybrid Sensor System (HSS) as a tracking device, and the supporting sensors were to be used to make the initial detection, a scheme has been devised to provide both the detection and tracking functions.

CONTENTS

CONTENTS (Continued)

ILLUSTRATIONS

ILLUSTRATIONS (Continued)

TABLES

SUMMARY

The objective of the Area Intruder Track Study was to investigate the feasibility of a bistatic VHF large area intrusion tracking system by theoretical analysis. The scope of the study did not include hardware verification. However, a parallel investigation was initiated by General Dynamics as a 1980, 1981 IRAD (Internal Research and Development) project to provide a limited amount of hardware study. This hardware study provided means for making field and laboratory measurements to collaborate the funded theoretical study. The results of the IRAD study have been included in the text and in the appendix.

The problem is to provide a Hybrid Sensor System (HSS) capable of tracking an intrusion within an annular ring 8 to 9 km from a central location. Supporting sensors in the HSS are supposed to provide the initial detection, after which the proposed equipment tracks the intruder within the surveillance zone. However, the initial detection problem has been included as an integrated system problem. The tracking zone area within the ring is 10^8 square meters. The system should be capable of tracking personnel 1 to 2 meters in height, weighing 30 to 100 kg. Vehicles weighing 200 to 2000 kg will also be tracked. The spread of velocities to be tracked will be 0.1 to 50 meters per second. The coverage from the central location is 360° in azimuth and vertically to 100 meters above the surveillance zone. The capacity of the proposed system will be to detect and track at least 30 simultaneous intrusions and have a false alarm rate (FAR) of less than 10 per day. The proposed system is used to protect nuclear processing, manufacturing or stockpiling sites, in addition to critical weapon installations. The perimeter of the 8 km radius surveillance zone is 52 km; therefore, such an installation needs to be located in an open and unpopulated area in order to reduce nuisance alarms from miscellaneous intrusions by local residents and large domestic animals.

The proposed system is based upon a bistatic VHF doppler tracking scheme. A VHF transmitter radiating 20 watts at 60 MHz illuminates an annular ring surveillance zone from its center. Reflections from moving targets entering the zone and the directly transmitted signal are received by multiple receivers distributed on the inside perimeter of the surveillance zone. The reflected intrusion and direct signals are compared in order to measure doppler and doppler sense. A data link connects the receivers to a computer which then determines the location of the intrusion and tracks it. The track is displayed on both a TV-type screen and a hard copy for a permanent record.

The investigation was divided into several study elements:

a. VHF propagation
b. Geometry-Computation Algorithm
c. Transmitter - Receiver requirements
d. Data Link requirements
e. System requirements
f. Display requirements

The selection of 60 MHz is based upon experience and work done previously on EMID (AN/GSQ160, Electro Magnetic Intrusion Detector); EPS (Electromagnetic Point Sensor); Model 174 Intrusion Detector, PEMID (Portable EMID) and literature surveys. Initial computations on VHF propagation losses indicating marginal signal-to-noise ratios were revised as a result of IRAD field strength surveys. These surveys provided factual data for transmission, reception, and reflection losses. It was determined that intruding personnel entering the surveillance zone would provide an intrusion signal 16.5 dB over the receiver noise limited to a bandwidth of 2.5 Hz and using a 20 watt, CW, 60 MHz transmitter with a vertical radiating antenna 80 feet high. Other intrusions such as vehicles and helicopters provide a greater radar cross section and a greater reflected signal.

A study of the geometry-algorithm indicated that two receiving sensors receiving a single doppler signal could provide accurate tracking data to within a few meters if an accurate starting location is specified. Errors in starting location would be maintained during the track as a type of integration constant error. A modification of the basic system is proposed where two CW signals are transmitted and received, 60.0 and 59.9 MHz. Two doppler signals at each receiver are compared to provide a type of range measurement. The accuracy of this range measurement is expected to be 20 meters; repeated average measurements during tracking could reduce the error to 2 meters.

The geometry used consists of a series of intersecting ellipses, each doppler cycle geographically defining an isophase locus ellipse about each receiving sensor. A pair defines a tracking point. Two basic algorithms were used to compute the intrusion track: one used a Kalman filter technique, the other an incremental step method. The Kalman filter determined velocity of the intruder and predicted the path; its advantage is that it will maintain a track with an intermittent loss of signal; its disadvantage is that it smooths out a track so much that it cannot accurately track when doppler rates change rapidly. The Kalman filter requires a "time tag" to be added to the doppler data in order to compute velocity. The Incremental Step Algorithm requires no time measurement. It depends upon the known location of each doppler cycle ellipse so that when a receiver detects a doppler transition, a new ellipse is located, providing a new intersection. Each doppler cycle represents a step of 2.5 to 5 meters, depending upon its elliptical orientation. The algorithm will track irregular paths but has no predictive capabilities and would be vulnerable to a loss in signal.

A dual doppler system using the incremental step algorithm would provide the best capabilities needing no initial location data; it would be capable of picking up the track after loss of signal, and would follow highly irregular paths with a terminal tracking accuracy of a few meters.

Studies on the receiver and the receiving antenna revealed direct signal overload which was in excess of 100 dB over the expected intruder reflected signal. A two-element automatic nulling antenna is proposed to reduce the direct signal 60 dB. Field tests showed this to be feasible and are described in the text. An additional 40 dB rejection of the steady state direct signal is removed by a synchronous tracking filter. The receiver proposed is a two-channel, dual frequency, multiple conversion type. The two channels receive the intruder reflected signal and direct transmitted signal. The two frequencies used in the dual doppler system are 60.0 and 59.9 MHz. These are converted to 5.000 and

5.100 MHz, followed by a conversion to 55 kHz and 45 kHz which are then product or phase detected. Crystal filters provide a very narrow bandpass, 2.5 Hz, and allow an equivalent noise input of -165 dBm.

1. INTRODUCTION

A security system consists of a number of interrelated functions: intrusion detection, discrimination, alarm and display, control, and deterrent functions; all are in response to an "attack function". The "attack function" can consist of a real threat, false alarms or nuisance alarms. False alarms are considered to be self-generated by internal noise of the equipment, while nuisance alarms are considered to be actual detections of external phenomena. Nuisance alarms can be caused by all sorts of flora and fauna, extreme weather conditions, e.g., wind, lightning. It is hoped the discrimination function will reduce false alarm and nuisance alarms. However, there will probably be human intrusions which are not aggressive. There is no foolproof way to determine intent of the intrusion, thus making it a nuisance alarm to which it is necessary to provide a response.

In any building complex requiring security, a prime necessity is to provide a detection zone which allows early detection of an intrusion so that a timely response can be initiated. As a complex becomes larger, the detection zone increases in size, and there is a need to track an intrusion to determine a convenient point to seize the intruder. Tracking also provides an indication of the intent by the path taken.

In protecting a nuclear processing, manufacturing, or stockpiling site, the surrounding detection zone is expected to be 8 km from the center location and approximately 1 km wide. This amounts to a 52-km long perimeter enclosing a 10^8 square meter area in the form of an annular ring. Such a complex needs to be located in an open and unpopulated area, in order to reduce alarms from miscellaneous intrusions by local residents and possibly large domestic animals.

The problem is to provide detection* and tracking capability within an annular ring 8 to 9 km from a central location. The tracking zone area within the ring is 10^8 square meters and intruders range from 1 to 2 meters in height and 30 to 100 kg in weight. In addition, vehicles weighing 200 to 2000 kg will also be tracked. Geometric cross sections provided by human targets are 0.5 to 1.5 m^2 moving at 0.1 to 3 m/s velocities, while vehicles present 1 to 4 m^2 cross sections at velocities of 2 to 50 m/s. Coverage from a central location is 360° in azimuth to an altitude of 100m above the surveillance zone. Probability of detection will be 95% with 90% of the intrusion tracked and located within 100m laterally and longitudinally. The capacity of the proposed systems will be to detect and track at least 30 simultaneous intrusions. False alarm rates must be less than 10 per day.

*Detection as indicated in the original USAF specification was to be provided by other sensors located on the outer periphery of the secure zone. These sensors would provide an initial alarm, alert the tracking system, and give a starting location. The funded study was called a Hybrid Sensor System (HSS) for this reason. We believe that both detection and tracking can be accomplished by the proposed equipments.

The objective of the study was to investigate the feasibility of a bistatic VHF large area intruder tracking equipment by a theoretical analysis. The investigation was divided into several study elements.

a. Propagation
b. Geometry - Computation Algorithm
c. Transmitter/Receiver requirements
d. Data Link requirements
e. System requirements
f. Display requirements

This study was without hardware verification. A parallel investigation was initiated by General Dynamics as a 1980 IRAD (Internal Research and Development) project to provide a hardware investigation. This hardware study provided means for making field and laboratory measurements to collaborate the theoretical study.

1.1 BRIEF SYSTEM DESCRIPTION

The intrusion tracking system covering a large area is based upon a VHF bistatic doppler scheme. The area to be monitored is 10^8 square meters, and is enclosed within an annular ring 16 km in diameter and about 1 km wide.

The basic principle of operation can be seen in Figure 1. A VHF transmitter located in a central location to the surveillance area illuminates the fixed and moving targets within this zone. Multiple receivers are distributed within the annular ring and pick up the reflections from these targets, as well as the direct signals from the transmitter. Only the moving targets produce a doppler in the receivers. The doppler information is transmitted via a data link, using wire, optical, or RF, to a computer in the central location. Doppler from adjacent receivers, when compared with spacings between receivers, computes tracking data; i.e., location, velocity, and direction of motion. Tracking data is then displayed on a properly formatted screen.

Previous experience in VHF intrusion devices indicated frequencies from 50 to 150 MHz provide a maximum available radar cross section relative to its geometric cross section while minimizing the response from smaller objects. In addition, these frequencies provide a good foliage penetration and immunity to environmental effect. (See Figure 2.) The study has tentatively selected 60 MHz as the operating frequency.[1]

A simple block diagram of the functions involved is shown in Figure 3. The transmitter provides an RF field at the intruder's site. The intruder reflects part of the signal back to a receiver (reflected signal channel). The transmitter also provides a direct signal to the receiver (direct signal channel). The outputs of the two separate channels are compared and their relative phase change is measured. When the intruder moves 8 to 16 ft toward a receiving site, 360° of phase change produces one doppler cycle.

---

[1]Merrill I. Skolnik, Radar Handbook; McGraw Hill Book Company, 1970.

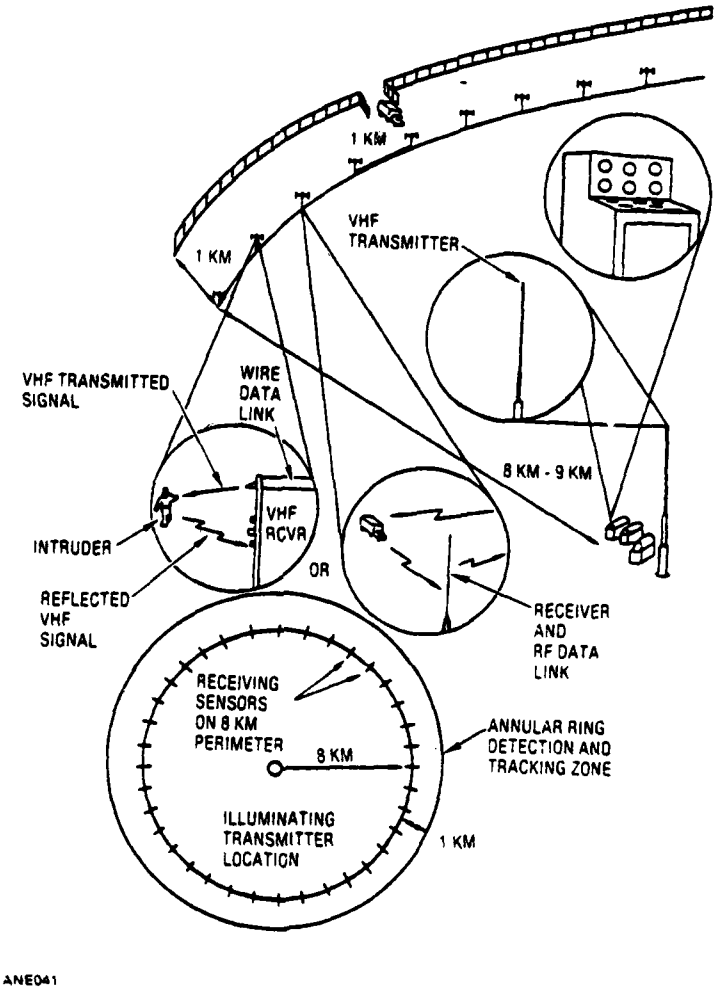

Figure 1. System Geometry

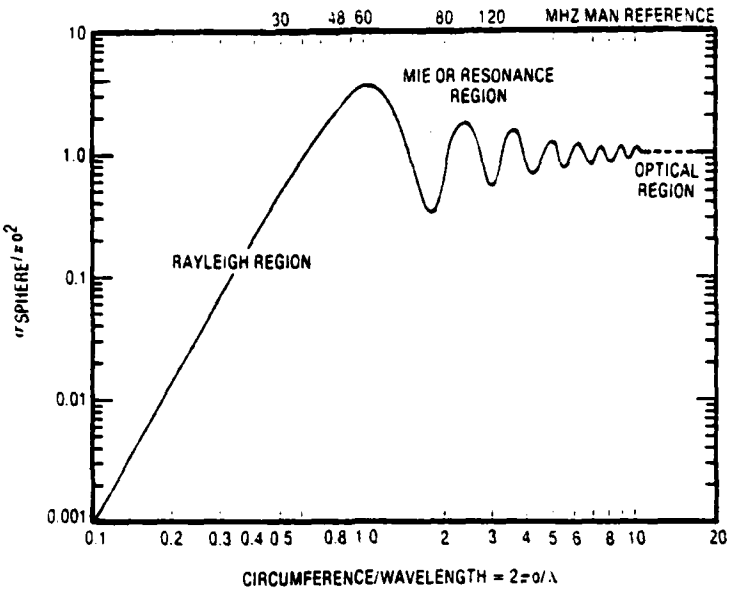

RADAR CROSS SECTION OF A SPHERE a = RADIUS, λ = WAVELENGTH

(A)

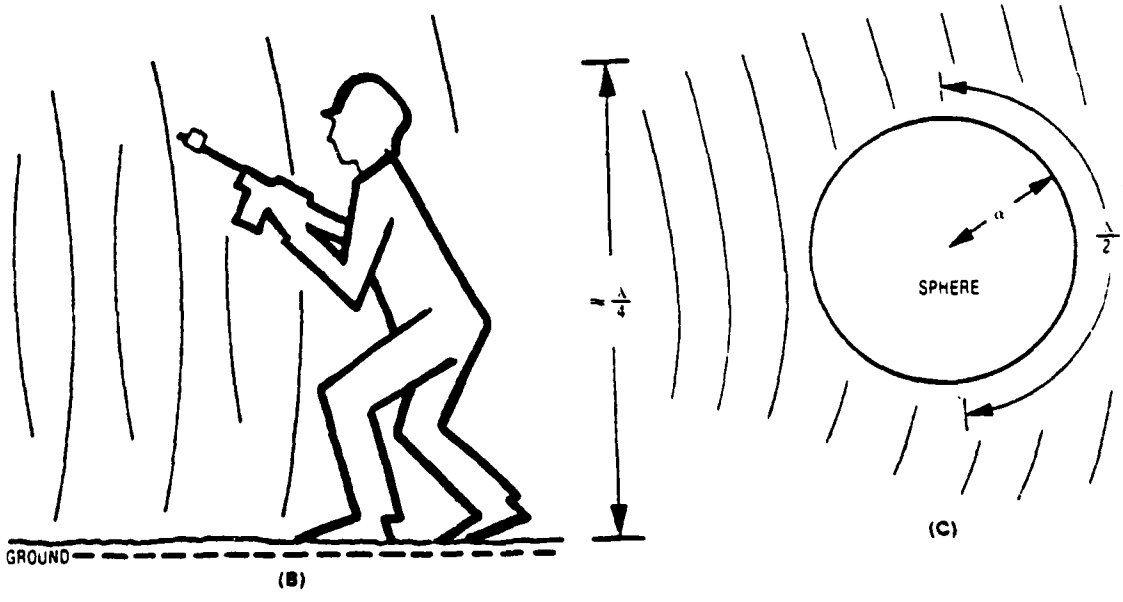

ALC002A

Figure 2. Frequency Selection

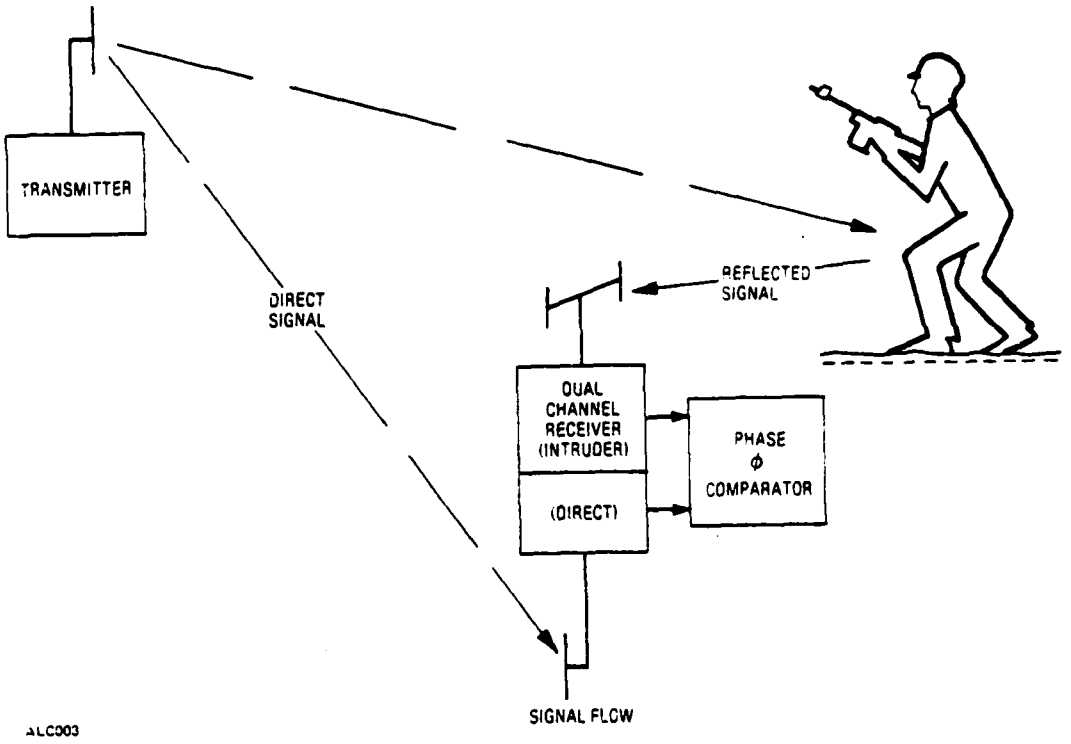

Figure 3. Signal Flow

2. THEORETICAL STUDY

Items covered in the study will deal with the propagation problems, the geometry-computation algorithm, transmitter/receiver requirements, data link requirements, display requirements, and system requirements.

2.1 PROPAGATION

2.1.1 COMPUTATION

The system studied consists of a central location where an omnidirectional transmitting antenna radiates to an annular ring that has an inner radius of 8 km and outer radius of 9 km. An intruder reflects the radiated signals at 9 km to the receiving antenna located on the 8-km radius. The frequency considered is 60 MHz; the transmitting antenna is 24m (80 ft) high; the receiving antenna is 2m (7 ft) high; the intruder is assumed to have a center of radiation 1m off the ground.

Signals transmitted to any location undergo a radiation loss due to a spreading signal and are expressed in decibel loss as:

$$\text{Free Space loss, dB} = -32.4 - 20 \log_{10} R_{km} - 20 \log_{10} f_{MHz}$$

where

R_{km} = The range in kilometers

f_{MHz} = The frequency in megahertz

The power radiated and received is related to an isotropic antenna.

The received signal is affected by the ground which reflects part of the transmitted signal adding vectorially to the direct signal. The reflected ground signal undergoes a phase and amplitude change due to the ground characteristics, in addition to the added phase delay for its longer path length. The complex value for this reflection factor is given by:[2,3]

$$R = \underline{\lfloor \phi} = \frac{\epsilon' \sin\psi - \sqrt{\epsilon' - \cos^2\psi}}{\epsilon' \sin\psi + \epsilon' - \cos^2\psi}$$

[2]Frederick Terman, Radio Engineers Handbook; McGraw Hill Book Company, 1943; p. 699.

[3]The Propagation of Radio Waves through the Standard Atmosphere, OSRD. Summary Technical Report of NRDC, Washington, DC 1946, Volume 3, pgs 53, 67, 71.

where

$\epsilon' = -J \cdot 6 \cdot \lambda \cdot \delta \cdot 10^{12}$

ϵ = Dielectric factor

δ = Conductivity EMU

λ = Wavelength $3 \times 10^8 / f_{MHz}$

ψ = Angle of incidence

$\rho \angle \phi$ = The complex reflectance factor containing amplitude and phase components

Values for typical wet and dry earth were used for various incidence angles to obtain earth reflectivity – $\epsilon = 20$, $\delta = 3 \times 10^{-13}$ (wet); and $\epsilon = 10$, $\delta = 2 \times 10^{-14}$ (dry). See graph Figure 4. The resultant change in signal when the reflected ground signal is added to the direct signal is given in decibels of reduced signal:

$$\text{Reduced Signal (dB)} = 20 \log_{10} \sqrt{(1-\rho)^2 + 4\rho \sin \frac{\Omega}{2}}$$

where ρ is reflectance, real portion of $\rho \angle \phi$, Ω is total phase delay. When $\Omega = \phi + \chi + 180$

$$\chi = \frac{4\pi h_1 h_2}{\lambda D}$$

h_1 and h_2 = Antenna height

λ = Wavelength

D = Range between antennas

$\angle \phi$ = Phase shift in ground

Figure 5 shows the loss in signal related to the incident angle . The incident angle is determined by

$$\psi = \tan^{-1} \left(\frac{h_2 + h_1}{R} \right)$$

Using the above equations the added loss due to ground reflections has been computed for each portion of the system range.

From Transmitter to Intruder	24m high 1m high	9 km range	Dry soil Wet soil	- 32.564 dB - 29.735 dB
	Range loss			- 87.05 dB
From Transmitter to Receiver	24m high 2m high	8 km range	Dry soil Wet soil	- 31.551 dB - 28.727 dB
	Range loss			- 86.05 dB

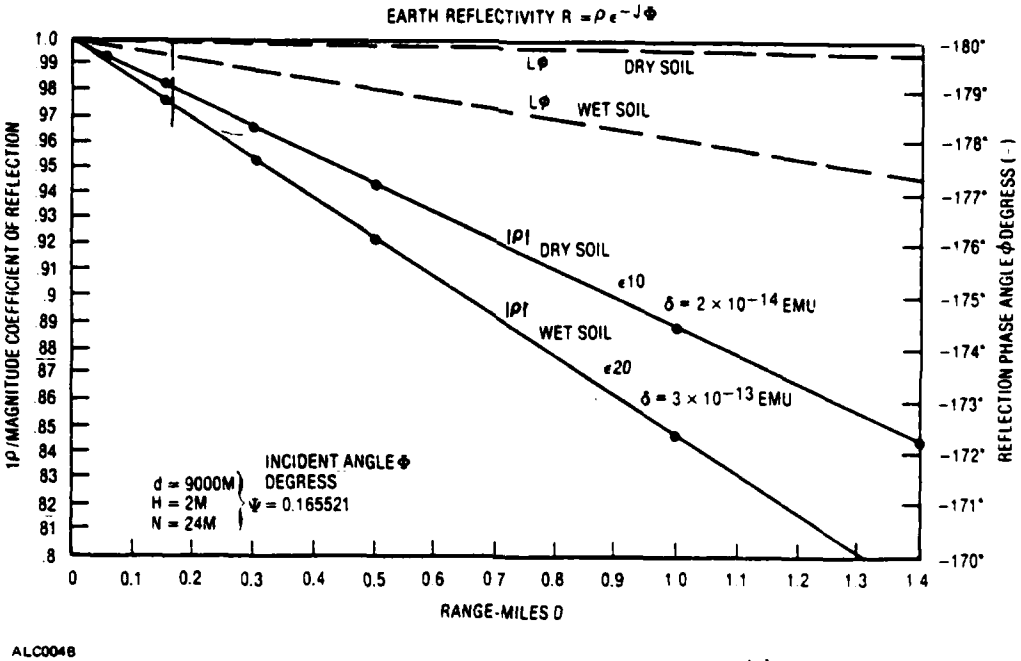

Figure 4. Earth Reflectivity $R = \rho_e^{-j\phi}$

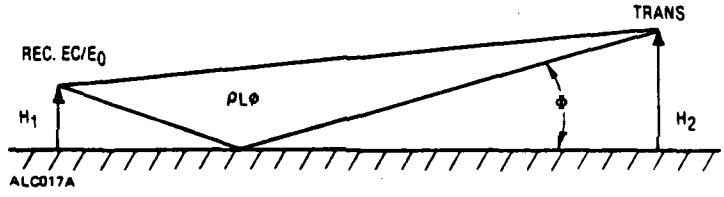

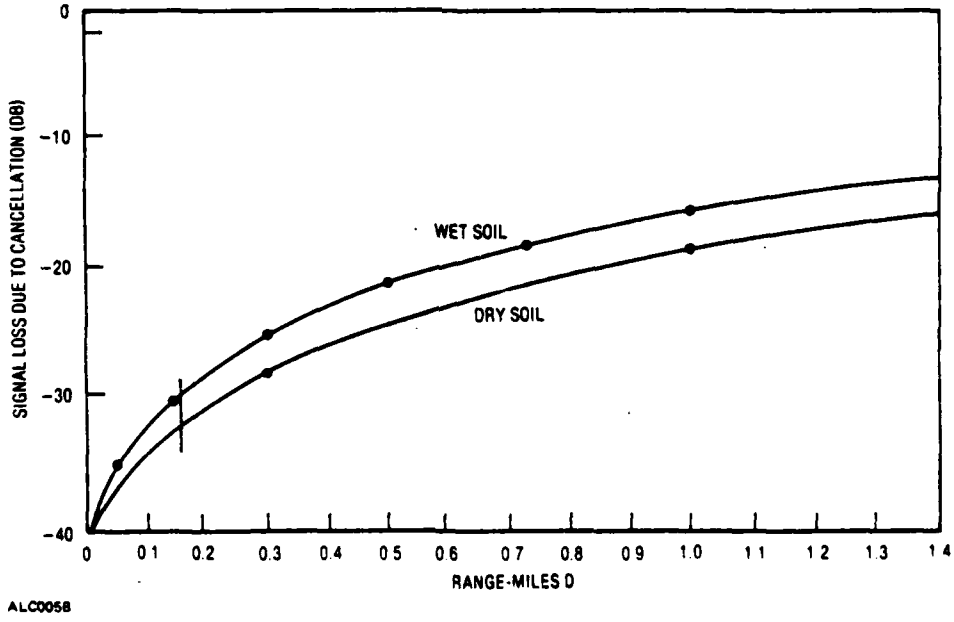

Figure 5. Signal Loss from Earth's Reflection

From Intruder to Receiver	1m high 2m high	1 km range	Dry soil - 30.938 dB Wet soil - 27.808 dB
	Range loss		- 67.96 dB

Total losses to the intruder and back to the receiving antenna are 218.5 dB for dry soil and 212.55 dB for wet soil.

Added to these losses is a 6 dB reflection loss from the intruder.

A transmitted signal of 20W with a 6 dB gain antenna radiates +49 dBm. The signal at the receiving antenna would be -170 dBm; with 6 dB gain over isotropic, the received signal was computed to be -164 dBm. A computed noise level in the receiver was -168 dBm giving a signal-to-noise ratio of 4 dB which was considered to be marginal.

2.1.2 FIELD TESTS

Experience at these frequencies (60 MHz) indicated much less ground reflection loss. It was decided to carry out a propagation test under the parallel GDE-sponsored 1980 IRAD program to verify or disprove these loss figures; standard EMI test equipment was used. An HP 8654 signal generator was connected to an IFI wideband amplifier which was then connected to an Empire Device DM 105-T1 dipole antenna. The measured radiated power was +23 dBm (200 mW) and was used as a CW transmitter. The transmitter equipment was located on top of the GDE antenna tower, 83 ft above the ground.

An International Travel-All 1200 Wagon, already equipped with a Singer 37/57 Field Strength Meter and its own power source, was calibrated for field strength measurements using an Empire Device 105-T1 dipole antenna (antenna factor 5). The wagon with its equipment made a survey, marking locations and the absolute field strength. Notes were made as to the visibility, i.e., line-of-sight, to the transmitter. A map in Figure 6 indicates the number of the test site. A relatively flat area was chosen for most of these tests. The receiving antenna was 5 to 6 ft from the ground (i.e., measured to the center of the antenna dipole). Readings were recorded in decibels above 1μ V/m. Table 1 presents the data taken on each site marked.

Clear line-of-sight locations at 9 km received about 20 dB more signal than the previous computations allowed. Where there were buildings, trees, fences, etc., still within line-of-sight, the signal levels were 5 to 10 dB more than the previous computations.

Further tests were made on a ground-to-ground basis, simulating intruder to receiving antenna conditions. A section of flat ground was located, 0.9 miles long (1.5 km), and field strengths were measured every 0.1 miles. The signal generator was located in the Wagon delivering 77 mW to an Empire DM 105-T1 located 15 ft away and about 10 ft high. A portable battery-operated NM37/57 field strength meter measured the field strength; its antenna was 5 ft off the ground. Measurements were made along a dirt road considered to have dry soil. Table 2 shows the results of these tests, which are referenced to the markings on the map Figure 6.

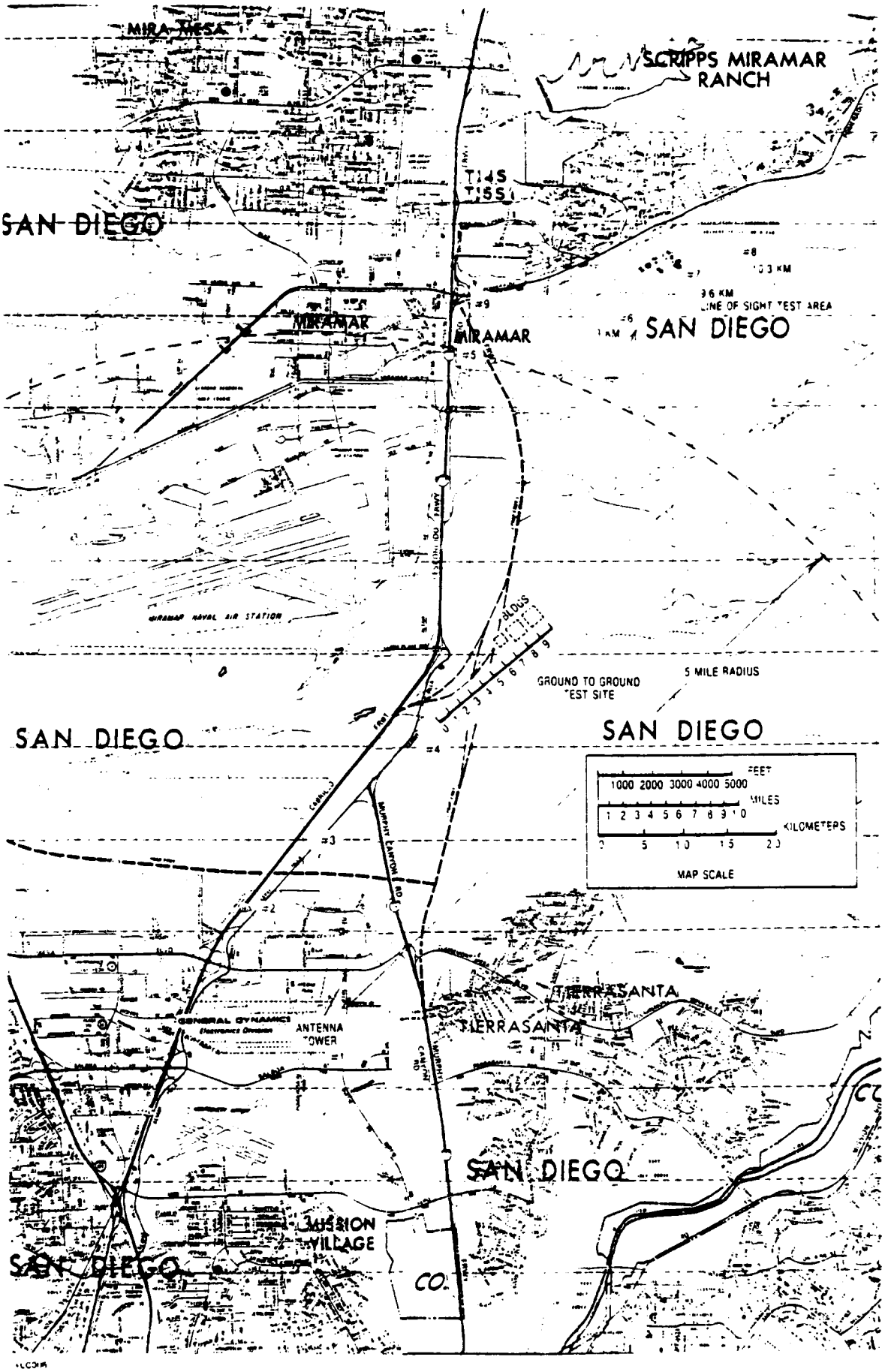

Figure [illegible] Test Sites

Table 1. Field Intensity Measurements in San Diego
(Miramar - Kearny Mesa Area) (3-17-80)

Frequency: 60 MHz; Antennas; Empire DM-105-T1 (transmitting and receiving);
Transmitting Power: +10 dB over 1V across 50 ohms, 0.2W, +22 dBm;
Field Meter: Singer NM 37/57
Transmitting Antenna Location: (on top of an antenna tower) 83 ft (Ht.) (25.3m)
Receiving Antenna Location: (per map locations) 5 ft (Ht.) (1.5m)
Antenna Factor: 5 dB; dB V/m to dBm = -107 Conversion factor (-107 + 5) = -102
Ground considered to be damp, generally flat as noted.

Location	Radial (Miles)	Distance (km)	Field Intensity dB V/m	Conversion Factor (dB)	dBm	Propagation Loss (dB)	Computed Loss (dB)	Difference (dB)
1	0.23	0.37	54	-102	-48	71	66	-5
2	0.9	1.4	39		-63	86	85	0
3	1.4	2.25	31		-71	94	93	-1
4	2.5	4.02	22		-80	103	105	+2
5	5.1	8.21	20		-82	105	115	+10
6	5.5	8.85	28-30		-74-72	9795	117	+21
7	5.8	9.33	25		-77	100	118	+18
8	6.0	9.66	27-28		-75-74	98-97	119	+21
9	5.4	8.69	14-16-18		-88, -86-84	111-109-107	117	+8
10	4.6	7.4	21		-81	104	114	+10
11	4.2	6.76	19		-83	106	113	+7
12	0.23	0.37	56	-102	-46	69	66	-3

Table 1. Field Intensity Measurements in San Diego
(Miramar - Kearny Mesa Area) (3-17-80) (Continued)

Notes on Site Locations

#1 At end of antenna range runway 1235 ft
#2 At end of Kearny Villa Rd. (through power lines)
#3 North of Chesapeake, South of I-15
#4 Camp Elliott
#5 South of Miramar overpass (not a clear view)
#6 Next to Aquaduct Marker, elevation 625 ft (line-of-sight)
#7 Next to Aquaduct Marker, 642 ft (line-of-sight)
#8 USIU on rise, slight elevation (line-of-sight)
#9 Pomerado overpass, wire fence close by (line-of-sight)
#10 Behind Miramar Airport Hangers (no line-of-sight)
#11 Terrain blockage in Miramar (no line-of-sight)
#12 Repeat #1

Assumed ground conditions $\epsilon = 20; \sigma = 3 \times 10^{-13}$ EMU

Table 2. Ground-to-Ground Transmission Test (3/25/80)

Signal Generator output: 110 mW
Signal Generator through antenna and cable: 15 ft, 77 mW
Antenna Factor: 5 dB; conversion mV/m to dBm -107 dB

Range Miles	Res. Sig. (dB on 1 μ V/m)	Conversion (dB)	Rec. Signal (dBm)	Power Output (dB)	Propagation Loss (dB)
0.1	41	-102	-61	19	80
0.2	31		-71		90
0.3	25		-77		96
0.4	23		-79		98
0.5	22		-80		99
0.6	18		-84		103
0.7	19		-83		102
0.8	8		-94		113
0.9	7		-95		114

Transmitting Antenna dipole height to center of antenna 5 ft
Receiving Antenna dipole height to center of antenna 10 ft

Notes: (1) 0.7, 0.8, 0.9-mile ranges influenced by small buildings and metal fences in the immediate vicinity.

(2) Ground was dry along dirt road.

2.1.3 FIELD TEST RESULTS

The losses for paths 9 km, and 1 km long have been plotted on a single graph showing their losses relative to free space loss and the computed ground reflection losses. It was concluded that the field strength at 8 km and 9 km was 10 to 20 dB greater than that computed. Apparently, the surface roughness reduces the ground reflection signal by scattering so that it is not as effective in cancelling the direct signal. It was also noted that on the ground-to-ground tests, the losses were greater within the 0.1 to 0.4-mile range by 6 to 8 dB. However, at 1 to 2 km (0.6 to 1.2 miles), the computed and measured values were comparable. See Figure 7.

The increase in signal over the 9-km range directly improves the signal-to-noise ratio from 4 dB to a value of 14 to 24 dB. This signal-to-noise ratio will be more than adequate and allow some degradation in the system.

2.1.4 INTRUDER REFLECTIVITY

As mentioned in paragraph 1.1, the frequency chosen to illuminate an intruder would be in the VHF band, specifically 60 MHz. The choice depended upon the apparent radar cross section being maximized when an isolated sphere's circumference is one wavelength (vertical section $\lambda/2$). (See Figure 2.) This also occurs for a hemisphere of the

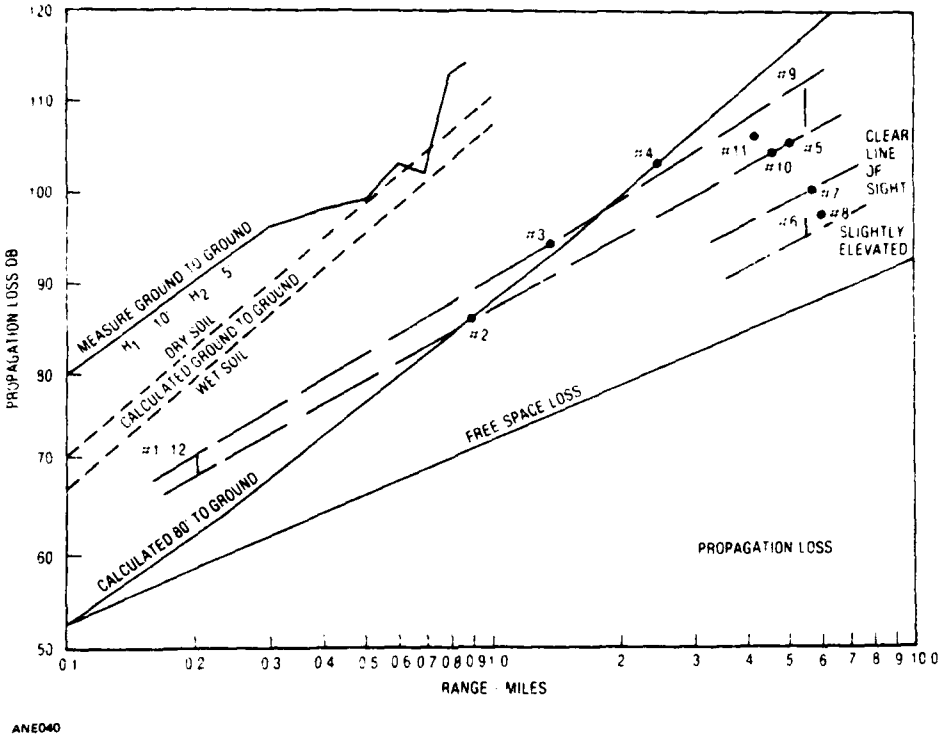

Figure 7. Propagation Loss

same diameter on the ground. A man-target responds in a like manner but with a less peaked response due to a lower conductivity. However, previous experiments on man-targets indicate 60 MHz gives a maximum reflected cross section. Small animals have only a minor response falling within the Rayleigh Region of the response curve.[4]

In order to obtain specific reflectivities, field tests were made using an EMID/EPS intrusion detector. This detector radiates and receives 60 MHz and can detect personnel at ranges greater than 40m. An 8-ft, 60-MHz resonant aluminum rod was used as a standard reflector; its characteristics are well known. A straight path was laid out with the closest approach to the EMID/EPS at 30m. Recordings were made of the detected responses for a rod, a man, and an auto traveling the 30m path. The auto was an International Harvester Travel-All 1200 Wagon. Point-by-point measurements were made and compared to the half-wave rod. Results indicated that the man-target response was 11.52 ±2 dB less than the half-wave rod. The Travel-All had a response 10.4 dB below that of the rod, about 1.1 dB more than that of a man. This response was averaged over the whole path. It should be noted that when the wagon was perpendicular to a radial from the EMID, a specular reflection (glint) was observed which had a response only 4.2 dB below that of the rod. Head-on vehicle tests were made when the vehicle took a radial path. Its response on this path was 7.8 dB less than the rod.

[4]Merrill I. Skolnik, Radar Handbook; McGraw Hill Book Company, 1970; p 21-27.

2.1.5 RECEIVING ANTENNA (GENERAL)

The main purpose of the receiving antenna is to pick up the reflected signals from an intruder. The sensitivity of the receiver and the antenna gain determine the effective intruder tracking range of the receiving site. The tracking range then determines the number of sites required to cover the annular ring security zone. The greatest coverage is obtained with the receiving site located half-way between the inner and outer radius of the annular ring and an antenna having an omnidirectional antenna pattern. However, the antenna not only receives the intruder signal but also the direct transmitted signal, which is calculated to be 103 dB greater than the intruder signal. Noise on the direct carrier would certainly exceed and mask any other received signals and would prevent adequate signal processing to determine doppler sense. The antenna can be made to reduce the direct signal by forming a null in its pattern toward the transmitter and providing general coverage elsewhere. There is no need to detect intrusions behind the receiving antenna since friendly personnel will be within the surveillance ring. In addition, as will be discussed in the geometry section, the doppler signals will be virtually reduced to zero for intrusions between the receiving antenna and transmitting antenna. The specific coverage of the surveillance area will be discussed in the receiving antenna design section.

2.1.6 SIGNAL BUDGET

The signal strengths at various points were computed using 20 watts of radiated power from a high gain vertical antenna assumed to be 6 dB over an isotropic source. The receiving antenna has a 6 dB gain (isotropic reference) and a -60 dB null (backward gain). The null permits a more favorable direct reflected signal ratio, i.e., -42.5 dB. A table of these relationships is shown in Table 3, Signal Budget.

2.1.7 HAZARD ANALYSIS OF RADIATING ANTENNAE

There is always a question of possible hazard due to radiation from an antenna to personnel within the radiating field. A standard of 10 milliwatts per square centimeter has been set up by MIL-R-9673B; AFR 161-7 and T.O. 312-10-4.[5] Basically, 60 MHz can cause only an RF heating effect within the first 0.2 inches of skin depth and only to the extent of power absorbed by the tissues.[6] Computations were made based upon 20 watts radiated at 60 MHz from an antenna 80 ft off the ground. The antenna has a vertical gain of 6 dB, reducing the signal strength at angles just below the antenna. The table below indicates the position of personnel at a distance from the base of the antenna structure, and the final power density in milliwatts per square centimeter. It should be noted that the sun's energy is equivalent to 100 milliwatts per square centimeter; in addition to the pleasant heating effect, it has an ionizing effect due to the ultraviolet (sunburn) radiation not present in the RF. Note: Solar constant is 1.94 cal/min/cm^2.

---

[5] MIL R 9673B Military Standard, Radiation Units, Microwave and X Radiation Generated by Ground Equipment (As Related to Personnel Safety).

[6] "How Dangerous Is Radiation," QST, September 1978, p 31.

Table 3. Signal Budget

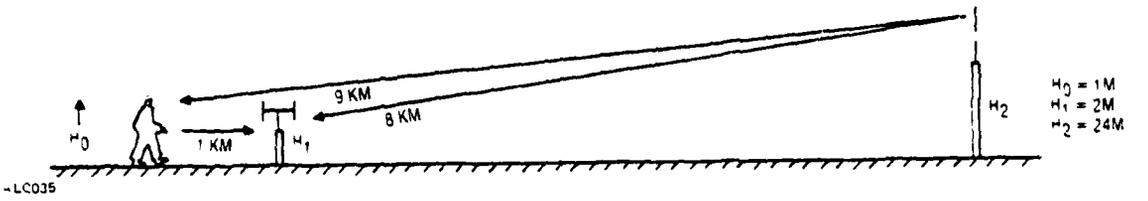

			Direct Signal	Reflected Signal
1.	Transmitter power	20W	+43 dBm	+43 dBm
2.	Transmitter antenna gain (over isotropic)	+6 dB	+49 dBm	+49 dBm
3.	Range loss @ 60 MHz free space	8 km-86.02 dB	-37 dBm	---
		9 km-87.04 dB	---	-38 dBm
4.	Ground reflection loss	8 km site -12 dB	-49 dBm	---
		9 km site -12 dB	---	-50 dBm
5.	Intruder (man) reflection loss	-5.5 dB	---	-55 dBm
6.	Range loss @ 60 MHz intruder-to-receiver	1 km -70 dB	---	-125.5 dBm
7.	Ground reflection loss intruder-to-receiver site	-32 dB	---	-157.5 dBm
8.	Receiving antenna forward gain (isotropic)	6 dB	---	-151.5 dBm
	(2-element array) backward gain	-60 dB	-109 dBm	---
9.	Receiving antenna reference channel (direct signal)	2 dB	-51 dBm	---
10.	Direct signal leak-through into reflected-signal channel			-42.5 dB

The greatest field strength is found to be at 160 ft from the base of the antennas where it is 0.0001 milliwatts per square centimeter. This is 1/100,000 of the permitted standard.

Table 4 shows RF power density at various ranges.

2.2 GEOMETRY - COMPUTATION ALGORITHM

2.2.1 GEOMETRIC PARAMETER

The geometric layout of the system is shown in Figure 1. The number of receiving stations on the perimeter depends upon receiving sensitivity, the redundancy desired, and the ability to handle multiple targets simultaneously.

Table 4. RF Power Density

Distance From Ant. Base x (feet)	Range to Personnel Y (feet)	(meters)	Antenna Gain at angle (dB - degrees)		Power Density Milliwatts/cm^2
0	80	24.4	-8	90	0.0
40	89	27	-12	-60	0.000013
80	163	34.5	-3	-45	0.0000665
160	179	54.6	+2.9	-27	0.000106
320	330	100.6	+5.2	-14	0.000052
640	645	196.6	5.8	-7	0.0000152

In order to investigate the geometry involved, a single element of the system is shown in Figure 8 using the common transmitter and one receiving sensor.[7,8,9] A direct signal from the transmitter travels from T_X to R_X over a distance D. An indirect signal travels from T_X to I_X (Intruder) and is reflected back to R_X over a combined path length of Z plus P. The difference in path length is (2R). If (2R) is made to be a constant with Z and P variable, an ellipse will be generated about two foci, T_X and R_X. When $\phi = 0^\circ$ P = R and Z = D + R. For variations in the constant R a new ellipse will be generated. If R is measured in terms of wavelength of the transmitted signal: Then $2R = N\lambda$ or $R = N\lambda/2$ (λwavelength); each ellipse is represented by a specific N, a whole number. Each ellipse then also represents a locus of points of constant phase delay of the reflected path when compared to the direct path, in increments of 360° (2 π radians). An intruder passing through "N" ellipses generates "N" doppler cycles of 360° of phase change at a phase comparator located at R_X. These are doppler cycles. It will be noted that each doppler cycle, represented by an ellipse, an isophase curve, has a specific geometric location with respect to its foci, T_X and R_X. Identifying "N" will identify an intruder crossing a specific ellipse.

An adjacent segment with the same transmitter (common) T_X and its own receiving sensor, R_X +1, will also receive reflections from an intruder, I_X. A family of ellipses will also be generated and will intersect its neighboring ellipses. If "N" for each segment is known, the intersection of two specific ellipses defines the intruder's location, I_X. This is shown in Figure 9.

---

[7]U.S. Department of Commerce NDS, Handbook of Mathematical Functions, U.S. Printing Office Applied Mathematics Series, 55; June 1964.

[8]Federal Telephone and Radio Corporation, Reference Data for Radio Engineers; 6th Edition ITT, 1975, H. Sams Co.

[9]Thomas E. Mason and Clifton T. Hazard, Brief Analytical Geometry; Ginn Co., 1935.

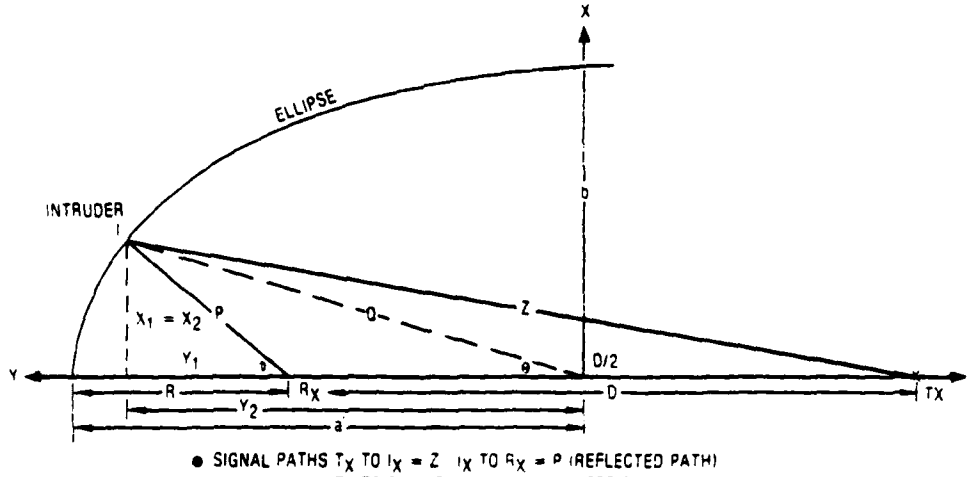

- SIGNAL PATHS T_X TO I_X = Z I_X TO R_X = P (REFLECTED PATH)
  T_X TO R_X = D (DIRECT PATH)
- SYSTEM MEASURES DIFFERENCE IN DIRECT AND REFLECTED PATHS
- THE LOCUS OF ALL POINTS SATISFYING (Z + P) − D = A CONSTANT (2R) IS AN ELLIPSE BY MATHEMATICAL DEFINITION
- THE MAJOR AXIS IS ALONG (a) AND THE MINOR AXIS ALONG b
  $a = R + D/2 \quad b = \sqrt{R^2 + (R \times D)}$
- $X_1 = P \sin \Phi$; $Y_1 = P \cos$ $\quad \frac{X_2^2}{b^2} + \frac{Y_2^2}{a^2} = 1$
- $X_2 = A \sin \theta$ $Y_2 = B \cos \theta$
- IN TERMS OF WAVELENGTH, λ, 2R = Nλ OR R = Nλ/2
- Z + P = 2R + D

LOCATIONS	DISTANCES	INTRUDER DIRECTION
WHERE T_X TRANSMITTER LOCATION	D DISTANCE BETWEEN T_X & R_X	Φ ANGLE FROM MAJOR AXIS AT R_X
R_X RECEIVER LOCATION	P DISTANCE TO I_X FROM R_X	θ ANGLE FROM MAJOR AXIS AT D/2
I_X INTRUDER LOCATION	Q DISTANCE TO I_X FROM POINT D/2	
	Z DISTANCE TO I_X FROM T_X	
	N NUMBER OF WAVELENGTHS ~ DOPPLER CYCLES	

ANE002

Figure 8. Elliptical Geometry

2.2.2 TRACKING

When receiving doppler signals only, identification of each cycle received cannot be made, only its directional sense (positive or negative) and the number of cycle crossings. If, however, a starting location is given, then a track can be made, updating the initial position by advancing one ellipse at a time as a cycle is received from the appropriate sensor. In the Hybrid Sensor System (HSS), it is assumed an auxiliary device will warn of an intruder, thus the proximity of the initial intrusion will be known. Figure 10 shows a simplified tracking procedure. An initial position of an intruder, I_X is given and located

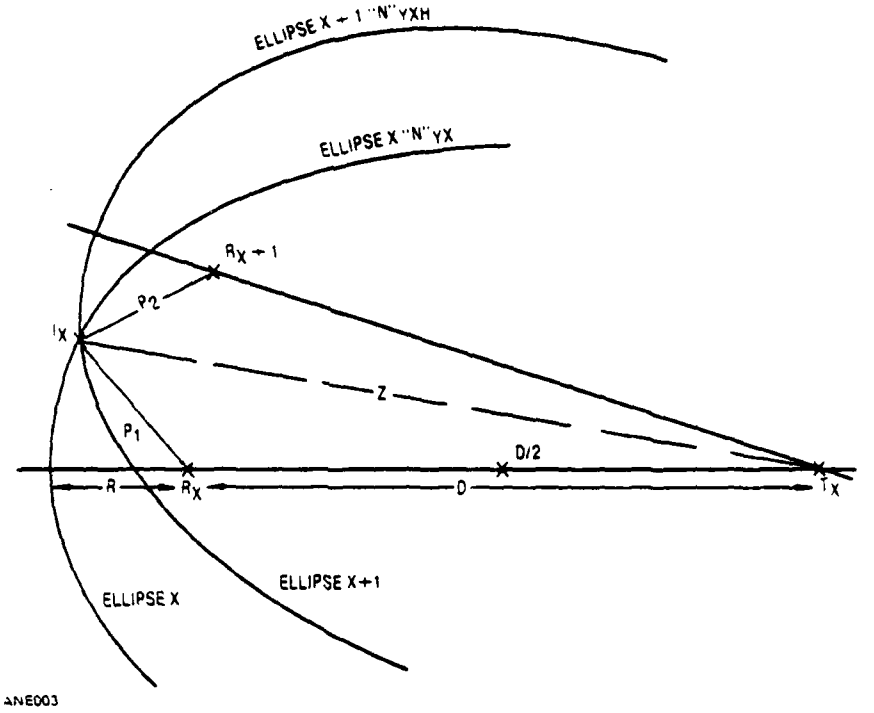

Figure 9. Intersecting Ellipses

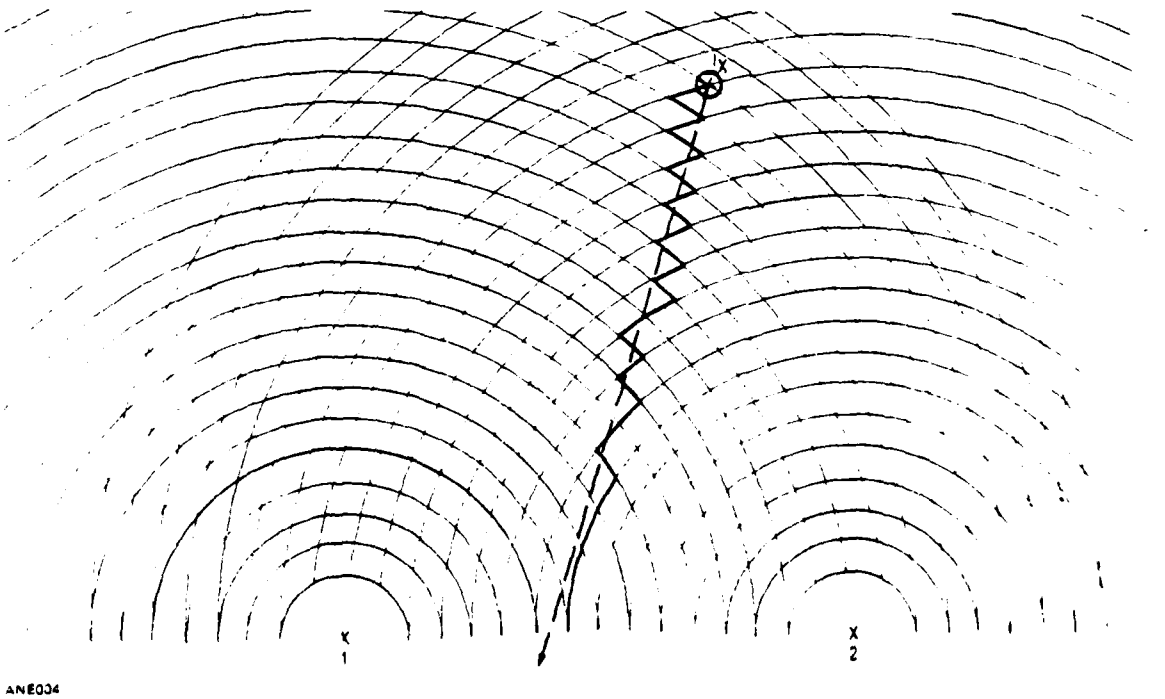

Figure 10. Tracking by Counting Doppler Cycles

on two intersecting ellipses. As a positive doppler cycle is received from 1, the position is updated by advancing one ellipse from sensor 1, sliding along the ellipse from sensor 2. Similarly, a signal from 2 advances one ellipse from 2, sliding on the ellipse from 1. A jagged track is shown in the illustration; each ellipse is 8 to 16 ft apart (8 ft (2.5m) along the major axis and 16 ft (5m) between sensors 1 and 2). Approximately 400 cycles are generated over a 1000-meter course. If drawn to scale, this would appear to be a smooth line.

It can be seen that an error in the initial location of the intruder will produce an error track which somewhat parallel the true track. The initial detection of an intruder can give an approximate radio range from computed sensitivities or by calibrating field tests. Two detections (2 sensors) could place an intruder within a 250m circle from where tracking could begin; however, the final accuracy would be no greater than the initial range assumptions.

It has been found during the study, a three-station response can provide a measurement of the intruder's velocity and direction from doppler only information. Three stations can by sensitivity range reduce the initial location assumption but still not accurately enough for the system requirements.

The study also found that a four-station response can uniquely pinpoint a location and track accurately; however, the range to be covered by four stations is excessive and would require considerably more transmitting power or many more receiving stations. The computation required to locate a single position is very involved. An alternate scheme is proposed to determine location and track simultaneously using two RF signals.

2.2.3 OPTIONAL DUAL DOPPLER SENSOR

If two signals were radiated from the transmitter T_X and received by R_X, then the two doppler signals received would differ by their wavelength. For example: one signal at 60 MHz (5m) would produce 400 cycles of doppler over a 1000m path along the major axis extension, where P = R and $R = N \cdot \lambda/2$. ($R = 1000$, $\lambda = 5$ $\therefore$ $N = 400$). A second signal of 59.85 MHz with a wavelength of 5.01253m will produce 399 cycles of doppler over the same 1000-meter course. If the phase of doppler 1 is compared with the phase of doppler 2, it will be found that they will be in phase at the receiving sensor and at 1000m. At 500m, they will be 180° out of phase; 250m, 90°; and 750m, 270°. The in phase condition at 0 and 1000m repeats every 1000m. Since there are 400 cycles of 60 MHz doppler between 0 and 1000m along the major axis, the second signal, 59.85 MHz, with doppler phase comparison can determine the ellipse number "N" of the 60 MHz signal. For every 0.9° of dual doppler phase shift difference one ellipse has been breeched, thus, 135° of phase difference would represent ellipse number 150.

An alternate method of describing the use of two frequencies for ranging is to make use of the difference frequency, i.e., 60 MHz - 59.85 MHz = 0.150 MHz, which has a wavelength of 2000m. Since $R = N \lambda/2$ then R = 1000; which is the range of the first doppler cycle based on 0.15 MHz frequency difference. A more suitable difference frequency might be 100 kHz, wavelength 3000 meters, with a repeating range of 1500m. This would reduce ambiguous ranges.

If the measurement of doppler phase is capable of 5° to 8° we could determine N to within 8 to 13 cycles out of 600 doppler cycles (1500m range). Eight to thirteen cycles represent 20 to 30m accuracy. Repeated measurements will reduce the RMS error by the square root of the number of measurements. Thus, by measuring each normal doppler cycle for tracking purposes, range can be measured and averaged to correct for an initial location error. In order to incorporate the ranging data into the tracking data, it is proposed that the initial location be obtained from the initial range data although only accurate to 33m or more. The ranging data is accumulated and averaged by updating the past measurements with each VHF doppler cycle. Tracking is accomplished as if doppler only was being used but periodically corrected when the range data differs significantly. See Figure 11.

2.2.4 ALGORITHM STUDY

A number of approaches were made to implement the tracking of an intruder from a doppler only signal from multiple receiving stations. Three methods were implemented: one used a Kalman filter, another was based upon incremental steps measured from each receiving station, and the third measured doppler difference phase. The basic difference in the algorithms is that the Kalman filter determines the velocity of the intruder and predicts a position while the incremental and doppler difference schemes step from one isophase intersection to another without a time reference. The Kalman Filter has the advantage of maintaining a track if the signal is momentarily lost while the incremental scheme loses data and position. The incremental scheme has the advantage of

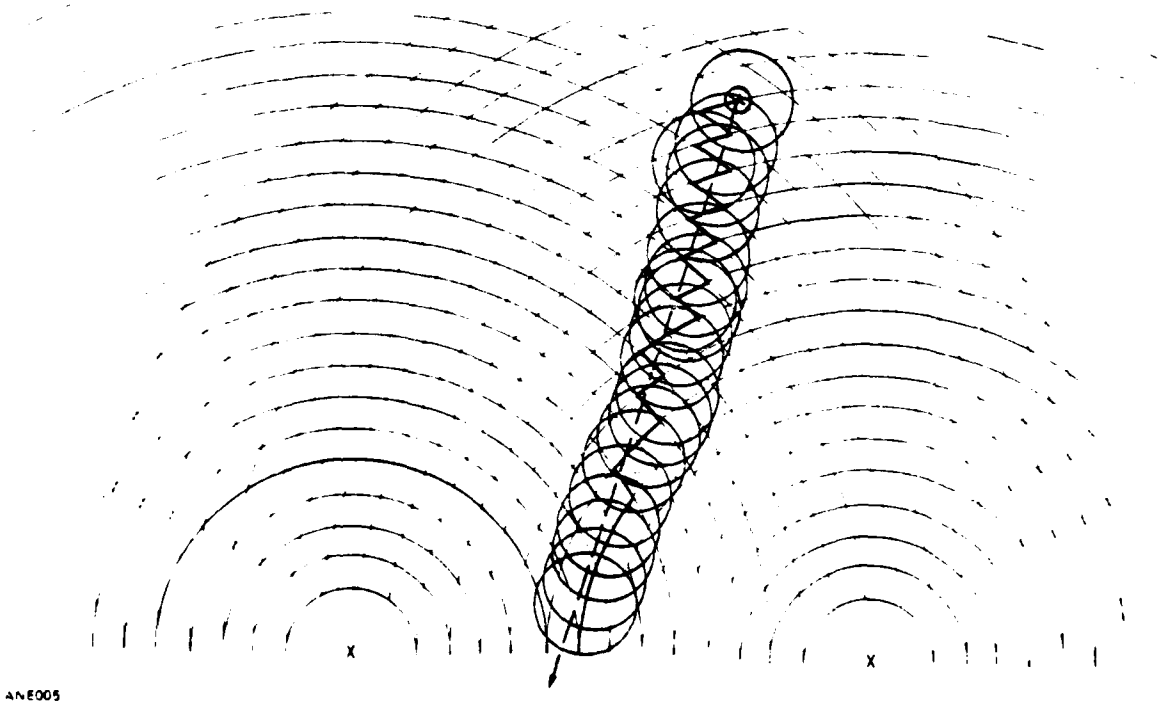

Figure 11. Tracking by Counting Doppler Cycles Plus Range Data

maintaining accurate position throughout the tracking regardless of random path motion, while the Kalman filter algorithm has considerable delay in correcting the velocity in order to track properly; delay is inherent due to the recursive nature of the filter. When doppler only is used, both algorithms require an accurate initial position. The Kalman filter algorithm was borrowed from another tracking program and had to be modified in order to accommodate this tracking problem. The algorithm is named SAINT X: Simulated Area Intruder Noncooperative Tracking.

A separate algorithm study was made using the optional dual doppler sensor where course range information only was used.

2.2.4.1 GENERAL DISCUSSION ON KALMAN FILTER TRACKING USING DOPPLER – During routine tracking operations, position and velocity data are determined using a recursive Kalman tracking filter. The recursive filter takes each measurement and computes a correction or update to the six tracking parameters: three components of target position and three components of target velocity. Each measurement is handled individually; i.e., each measurement is processed through the filter before another is taken. This simplifies some of the matrix operations and eliminates the need to correct all measurements to a common time base.

The Kalman filter is a time varying optimal filter which continuously adjusts its gains in accordance with the current tracking accuracy and the current measurement accuracy. Filter gains are set high during periods when the tracking accuracy is poor, and low during periods when tracking accuracy is good. This typically results in high filter gains during tracking start-up or restart procedures and low gain during steady-state conditions.

The Kalman filter weight is based on the estimation error covariance matrix, the predicted measurement accuracy, and the target-to-ground station geometry. The estimation error covariance matrix is a measure of the predicted accuracy of the current tracking data. A covariance matrix is the vector equivalent of the one-sigma error level of a scalar case. Each time the Kalman filter computes a correction or update, the covariance matrix is also updated to reflect the increased accuracy of the tracking data. Similarly, the covariance matrix is modified to account for the degradation of tracking accuracy between updates. Part of the tracking start-up procedure involves computing initial values of the covariance matrix which reflect the accuracy of the tracking parameters computed by the start-up procedures. In this way the Kalman filter maintains an estimate of the current tracking accuracy throughout the mission. The covariance matrix may be useful to the mission controller as a real-time indication of tracking accuracy.

The Kalman filter's covariance matrix also provides a convenient means for editing bad data.

A bad data evaluation prevents a particular measurement from being used to update the target tracking parameters.

The principal routine tracking functions using a Kalman filter are:

a. Estimate measurement
b. Propagate tracking parameters and covariance

c. Data conditioning
d. Residual
e. Reasonableness test
f. Update

The data conditioning function includes the operations necessary to convert raw time counts and raw measurement data into usable data. Specifically, what needs to be done to condition the raw data depends on the type of tracking system. The residual function takes the measurement provided by transformation and computes the difference between this measured quantity and an equivalent estimated quantity. For range rate measurements, the estimated quantity is the doppler between the target and the proper ground station computed from target tracking parameters and the known ground station locations.

The reasonableness test involves comparing the measurement residual with a decision criterion. If the measurement residual exceeds the criterion, the data is labeled bad and is not used to update the target track. A large number of bad data evaluations causes the system to reenter the initialization mode.

From the Kalman filter, the data reasonableness will be evaluated using:

$$E^2 \leqq S\,(MPM^T + Q)$$

where:

E - Measurement residual

S - Confidence factor

M - Measurement gradient vector

P - Estimation error covariance matrix

Q - Variance of Y reflecting the expected noise in the range measurement

T - Denotes matrix transpose

By definition, reasonable data satisfies the inequality; failure to satisfy the inequality results in an unreasonable data decision. The constant S is a measure of the statistical confidence of the reasonableness test and can be used to vary the data acceptance window.

Computational Logic - A logic diagram of the SAINT X algorithm is shown in Figure 12. The details of the computations follow with a list of symbols and definitions.

Geometry and Alternate Sensor Geometry for SAINT X Measurements are shown in Figures 13 and 14.

Kalman Filter Computations in SAINT X Program - See Figure 12 for details of implementation of equations in the program.

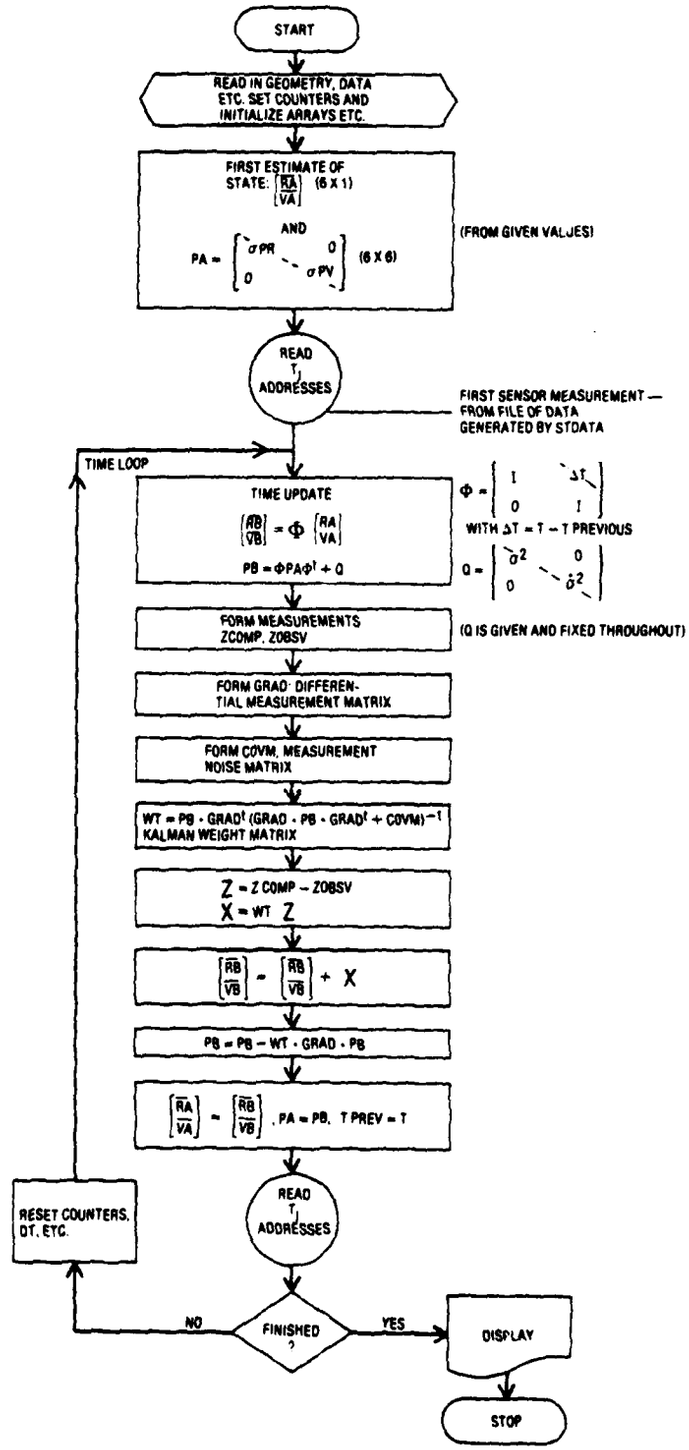

Figure 12. SAINT X Logic Diagram

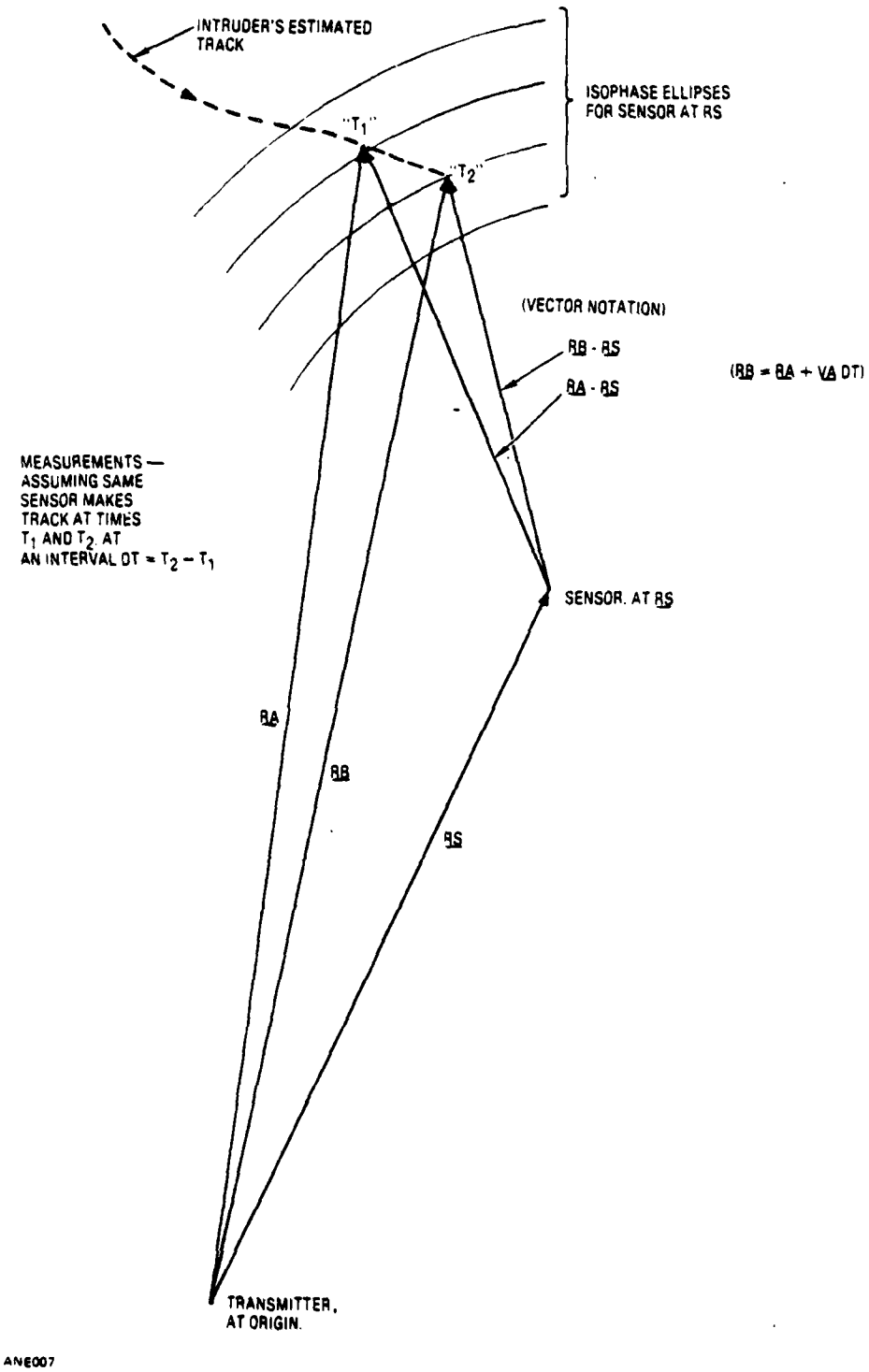

Figure 13. Geometry for SAINT X Measurements

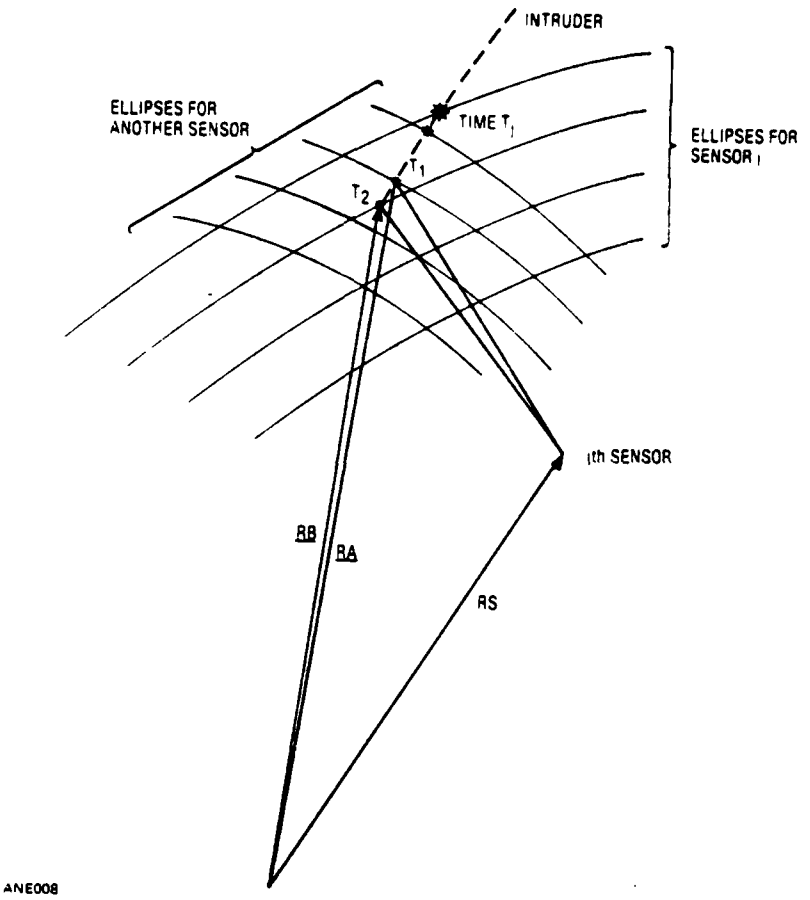

Figure 14. Alternate Sensor Geometry

Kalman filter equations:

$$\left.\begin{aligned} \hat{\underline{x}}_{k+1} &= \Phi_k \hat{\underline{x}}_k + \\ \underline{P}_{k+1} &= \Phi_k P_k + \Phi kt + Q_k \end{aligned}\right\} \text{Time update}$$

$$\left.\begin{aligned} K_k &= P_k H_k{}^t (H_k P_k H_k{}^t + R_k)^{-1} \\ \hat{\underline{x}}_{k+} &= \hat{\underline{x}}_k + K (\hat{z}_k - H_k \hat{\underline{x}}_k) \\ P_{k+} &= P_k - K_k H_k P_k \end{aligned}\right\} \text{Measure update}$$

where: P_k is state covariance; H_k is measurement matrix; R_k is measurement covariance, Q_k is process noise, Φ_k is the state transition matrix; K_k is the weight matrix; $\hat{\underline{x}}_k$ is the state, and $\hat{z}_k$ is the measurement; all at the kth iteration.

In the SAINT X program the following symbols are used in place of the above:

state $\hat{\underline{x}}_k = \begin{bmatrix} x \\ y \\ z \\ \dot{x} \\ \dot{y} \\ \dot{z} \end{bmatrix} : \begin{bmatrix} \hat{RA} \\ \hat{VA} \end{bmatrix}$ position and velocity,

$\hat{x}_{k+1} : \begin{bmatrix} \hat{RB} \\ \hat{VB} \end{bmatrix}$ new position and velocity,

P_k : PA, P_{k+1} : PB,

K_k : WT, H : GRAD,

R : COVM, Q : COVQ, COVQD

The update $\hat{\underline{x}}_{k+1} = \Phi_k \hat{\underline{x}}_k$ is accomplished by RB = RA + VA · DT, VB = VA. DT is the time interval between kth and (k + 1) iterations. The matrix Φ_k has the form, therefore, of:

$$\Phi_k = \begin{bmatrix} 1 & 0 & 0 & DT & 0 & 0 \\ 0 & 1 & 0 & 0 & DT & 0 \\ 0 & 0 & 1 & 0 & 0 & DT \\ 0 & 0 & 0 & 1 & 0 & 0 \\ 0 & 0 & 0 & 0 & 1 & 0 \\ 0 & 0 & 0 & 0 & 0 & 1 \end{bmatrix} = \begin{bmatrix} I & \diagdown & DT & \diagdown \\ O & & I & \end{bmatrix}$$

The measurement residual, written in the equations as

$$(\hat{z}_k - H_k \hat{\underline{x}}_k),$$

is formed in the SAINT X program as ZOBSV - ZCOMP. ZOBSV is a measurement of a change in range sum. It will be a scaler if only one sensor has sent in a time "mark!" at this iteration. It will be a vector if more than one sensor has tracked. (See Figures 13 and 14.)

ZCOMP is the diference in range sums for the same sensors; the difference being taken between range sums at positions RB and RA.

The matrices COVM, COVQ, and COVQD, (measurement, positional process noise, and velocity process noise covariance matrices) are formed from values input to the program, and remain fixed throughout the program. They are formed as follows:

$$COVQ = \begin{bmatrix} SIGQ(1) & 0 & 0 \\ 0 & SIGQ(2) & 0 \\ 0 & 0 & SIGQ(3) \end{bmatrix},$$

$$COVQD = \begin{bmatrix} SIGQD(1) & 0 & 0 \\ 0 & SIGQD(2) & 0 \\ 0 & 0 & SIGQD(3) \end{bmatrix}$$

(The matrix Q in Kalman equations has the form in SAINT X of

$$Q = \begin{bmatrix} COVQ & 0 \\ 0 & COVQD \end{bmatrix}$$

$$COVM = \begin{bmatrix} SIG1 + SIG2 & SIG2 & \cdots & SIG2 \\ SIG2 & SIG1 + SIG2 & & \\ \vdots & SIG2 & & \\ & & & \\ SIG2 & & & SIG1 + SIG2 \end{bmatrix}$$

n = number of sensors tracking

The values SIGQ, SIGQD, SIG1 and SIG2 are inputs.

The initial state covariance is formed as

$$PA = \begin{bmatrix} SIGPR(1) & & & & & \\ & SIGPR(2) & & & 0 & \\ & & SIGPR(3) & & & \\ & & & SIGPV(1) & & \\ & & & & SIGPV(2) & \\ & 0 & & & & SIGPV(3) \end{bmatrix}$$

where SIGPR and SIGPV are inputs.

The SAINT X algorithm simulates a system that receives time marks from sensors every time the direct and reflected signals are out of phase.

Two successive time marks from the same sensor are interpreted as meaning that the range sum for that sensor has changed by one wavelength. (Range sum is the sum of path lengths from transmitter to intruder and intruder to sensor.)

$$ZCOMP = \underset{\Delta DB - DA}{(|\underline{RB} - \underline{RS}| + |\underline{RB}|) - (|\underline{RA}| - \underline{RS}| + |\underline{RA}|)} \text{ (vector notation)}$$

$$Z\phi BSV = \text{WAVE2 (one wavelength)}$$

$$DT = T_2 - T_1$$

$$ZCOMP = \text{DB - DA, as before, but}$$

$$ZOBSV = \text{WAVE2}\frac{DT}{(T - T_j)},$$

reflecting the fact that the range sum from the jth sensor has not changed by a whole wavelength between times T_1 and T_2, but between times T_j and T_2. When the two successive time marks come from different sensors, the previous time that the presently tracking sensor tracked at, (T_j), is recalled, and used to decide how much the range sum has changed in the present time interval.

Summary, Definitions of Symbols

CAPX (X)	-	correction to state vector
CAPZ (Z)	-	measurement residual
COVM	-	measurement covariance matrix
COVQ	-	position plant noise
COVQD	-	velocity plant noise (together COVQ and COVQD form the process uncertainty matrix)
UT	-	time interval between successive iterations of Kalman filter
GRAD	-	(differential) measurement matrix
PA, PB	-	state covariances before and after incorporation of measurement info
RA, RB	-	positions (x, y, z) before and after incorporation of measurement info
SIG1	-	noise in transmitter to intruder path length
SIG2	-	noise in sensor to intruder path length
SIGQ(σ)	-	discrepancy between linear model and actual track, in position, during one time update (plant uncertainty)
SIGQD($\dot{\sigma}$)	-	same as SIGQ but for velocity
SIGPR	-	initial error in position estimate
SIGPV	-	initial error in velocity estimate
T	-	time after Kalman update
TPREV	-	time before update (VT = T - TPREV)
VA, VB	-	velocities before and after update
WT	-	Kalman gain (weight) matrix

ZCOMP - computed measurement

ZOBSV - actual measurement

DB, DA - total path length from transmitter to intruder and from intruder to receiving sensor (DB intruder at T_2) (DA intruder at T_1)

2.2.4.2 ALGORITHM RUN - KALMAN FILTER – Three preliminary Fortran listings were made which compute the track and the doppler cycles received by the receiving sensors. Three different tracks were considered: a straight-in approach, a curved path approach, and a zig-zag path. Incorporated in the computation were radio range limitations (1000 - 1500m) and noise (±1m). This resulted in three decks of cards which became the input to the Kalman filter algorithm, SAINT X. The input from the card deck indicates the doppler sign and the time a doppler cycle is received from up to 10 receiving sensors. Both a CDC - Cyber 7600 and a SEL Model 3277 (Systems Engineering Lab) were used to debug and evaluate the program.

Plots of a straight-in approach, curved course, and a zig-zag course were made and are found in Appendix G. The effect of initial location error was demonstrated in these runs. In Figure 15, the straight-in approach shows the real trajectory as "Os", and the computed trajectory as "Xs". The intiial starting position has a 15m error along the path, and is maintained over much of the track until it approaches the baseline where the error along the track becomes an error in cross path position. The skew in the track is due to poor velocity information since the path is parallel to the isophase (elliptical) curves (zero doppler).

In Figure 16, the curved course shows an apparent convergence of a tracking error. It should be noted that if the track ended between sensors 1 and 2 instead of directly at 2, divergence would result.

In Figure 17, the zig-zag course exercises the Kalman filter by a multiple change in direction. the computational delay depending upon velocity is demonstrated by the error paths. Again, path divergence is shown as it approaches the baseline between receiving sensors 2 and 3.

The Kalman Filter Algorithm is limited by its determination of velocity by relating a doppler cycle to the received time interval. Since the Kalman filter smooths the data by its recursive action, delays are incurred. At near zero doppler, it is most difficult to determine the velocity. This occurs when the track approaches a baseline, when all the nearby receiving sensors will have a very low doppler frequency.

2.2.4.3 INCREMENTAL TRACKING ALGORITHM – Another approach to a tracking algorithm was investigated which is not time dependent. Since each isophase (elliptical) curve is geographically located, crossing an ellipse locates the adjacent ellipse and a new intersection. The algorithm was developed using a microcomputer, (PET) Commodore 2001 with an 8k RAM, using Basic Language. The computation logic is shown in Figure 15.

The symbols are defined in Table 4. The geometry involved is shown in Figure 16. A listing of "Basic Commands" is shown in Table 5, TRACKER XV Program. The program

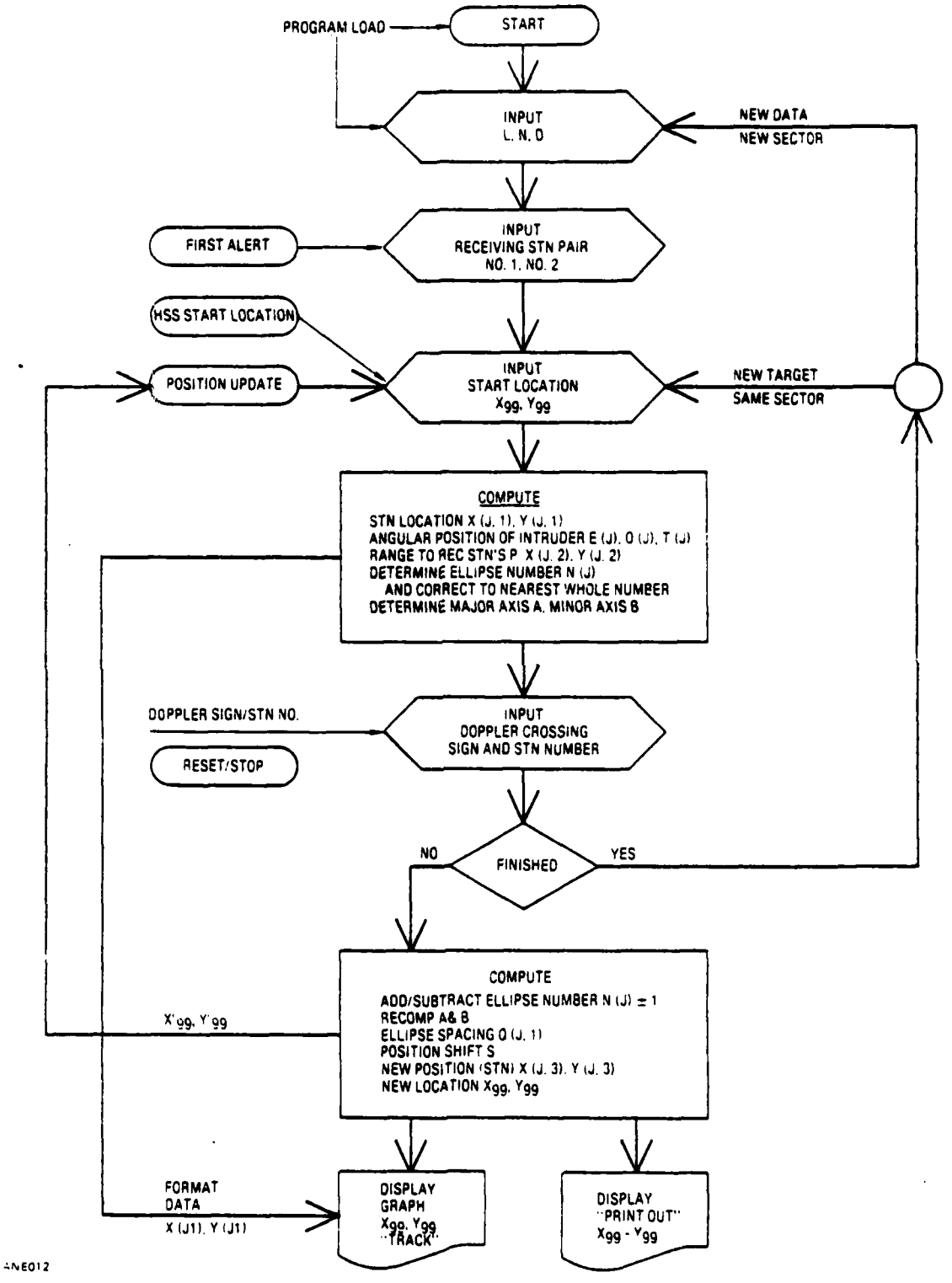

Figure 15. Incremental Tracking Algorithm Program Logic

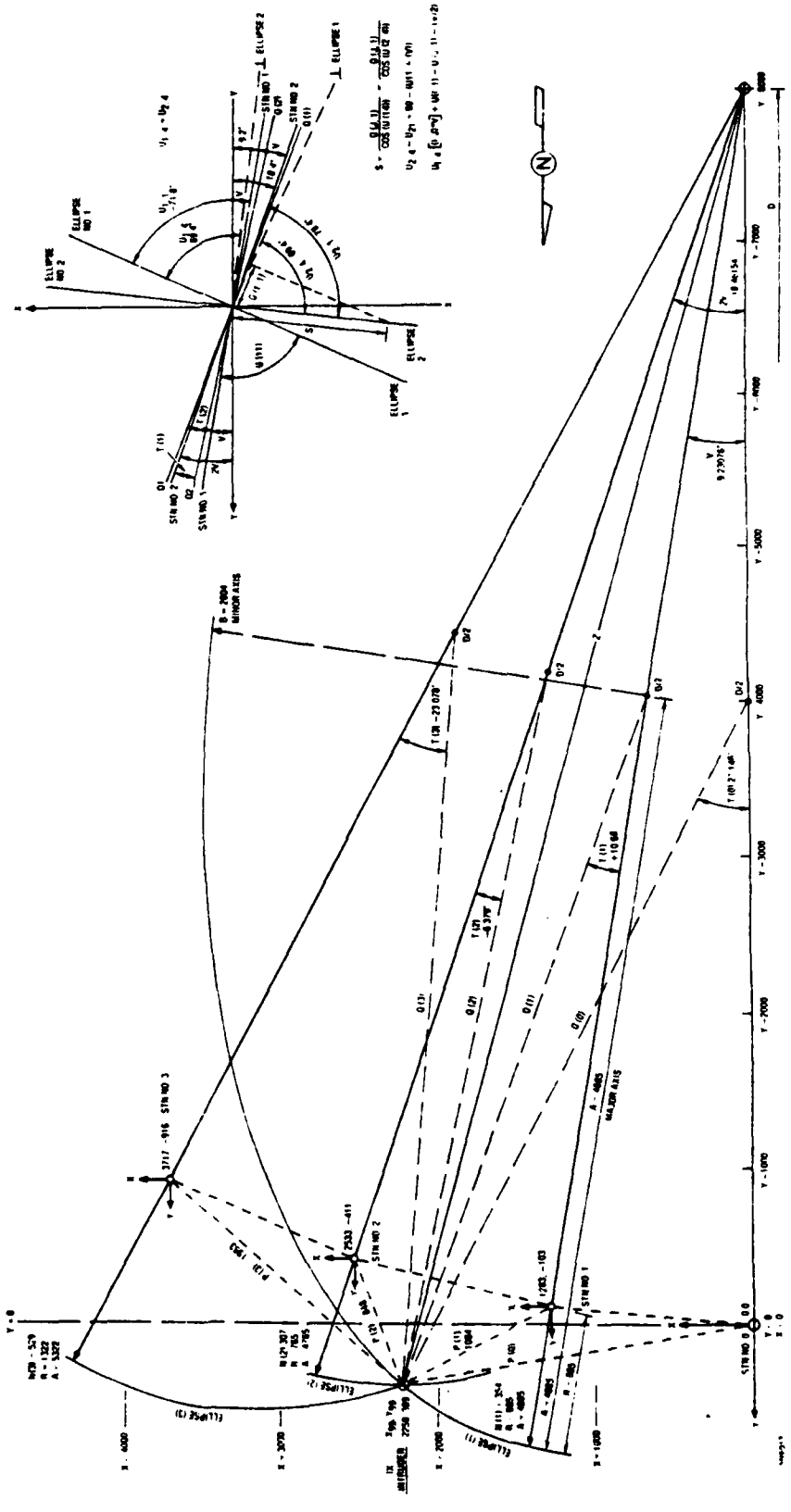

Figure 16. Computation Geometry

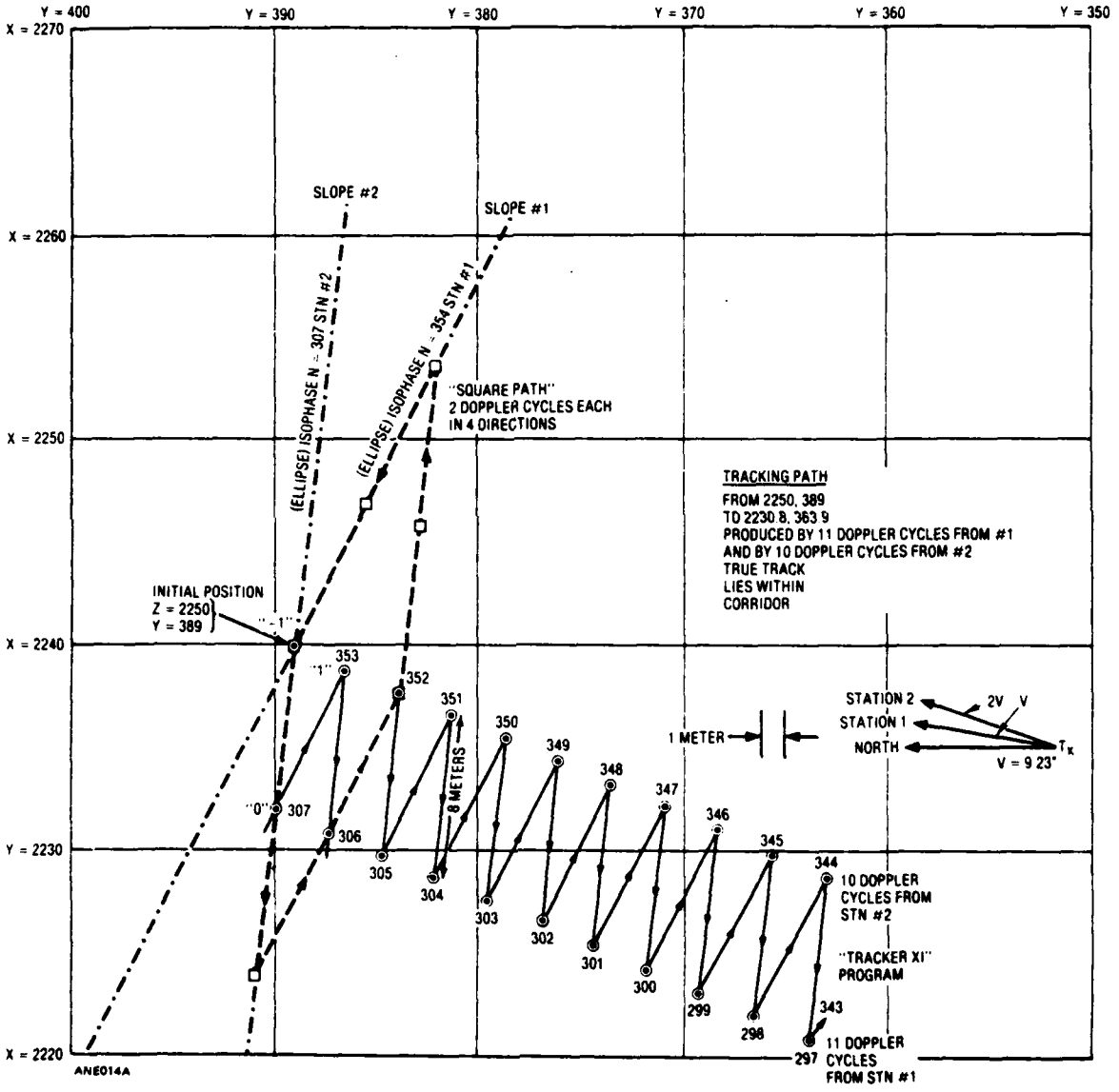

Figure 17. Sample Tracking Path

Table 4. Definition of Symbols for Incremental Tracking Algorithm

L	Wavelength meter (5 meters $\simeq$ 60 MHz)
N	Number of stations on periphery of surveillance zone
D	Distance between transmitter and receiving sensor (T_X and R_X)
V	Angle between stations from transmitter
W1, W2, W3, W4	Any 4 consecutive stations, W2 and W3 are central
X_{99}, Y_{99}	Intruder location x,y axis referenced to station #0 (north)
I(3)	Counting designator
Z	Distance from transmitter to intruder
J	Station designator; 1 to 4; designated by W1, W2, W3, W4
X(J,1), Y(J,1)	Station location (J) x, y, ref. STN O (north)
M1, M2	Temporary designator for distance to intruder from station
M3	Temporary designator for slope of M1/M2
E(J)	Angle to intruder reference y axis from station (J)
M4	Temporary designator to establish sign of E(J)
O(J)	Angle to intruder reference station axis station (J)
P(J)	Range to intruder from station (J)
X(J,2), Y(J,2)	Station location, station reference
T(J)	Angle to intruder from station axis measured at D/2
N(J)	Ellipse number from station (J)
R(J)	Distance to ellipse N(J), from station measured along major axis
A(J)	Major axis distance, station (J)
B(J)	Minor axis distance, station (J)
I(4), I(5)	Temporary designators to select W2 or W3 for a doppler cycle count
Q(J,1)	Distance between ellipse N(J) and (N-1) (J) at angle T(J)
U(I,1), U(J,1)	Angle between ellipse slope and station reference; station I or J.
U(I,4) U(J,4)	Angle between the perpendicular to ellipse and its intersecting ellipse (station I or J).
S	Measurement of shift from previous position X_{99} - Y_{99} to new X_{99} - Y_{99}
X(J,3), Y(J,3)	Coordinates of new position referenced to station (J)
T_X	Transmitter location y = -D
$R_{X(j)}$	Receiver location X(J,1), Y(J,1)
I_X	Intruder location $X_{(99)}$, $Y_{(99)}$
D/2	Midpoint between $R_{X(j)}$ and T_X

Table 5. TRACKER XV Program

Manual input for each doppler cycle. ±STN W1 to W4
OUTPUT typed coordinates X_{99}, Y_{99} and Ellipse numbers N(1)(N2)
BASIC LANGUAGE
PET COMMODORE 2001

COMPUTER LISTING	COMMENTS
100 REM EXAMPLE, 5, 39, 8000-1, 2-2250, 388	Typical example
110 REM STN2-Z=8684, P=1084, N=353, ANGLES 0=53, E=63, T=10.68-STN CORD 1283, -103	
120 REM INITIALIZE TRACKING ALGORITHM	
130 PRINT "L", "N", "D"	
140 INPUT L, N, D	
150 V=2*π/N	
160 PRINT "ANY ADJACENT STATIONS", "1 TO 8"	
170 INPUT W2, W3	Sector Selection
180 IF W2 <W3 THEN GO TO 200	
190 W5=W2:W2=W3:W3=W5	
200 W1=W2-1:W4=W3+1	
210 PRINT "INTRUDER INITIAL COORDINATES-X, Y	
220 INPUT X(9,9), Y(9,9)	
230 PRINT" "	Clear screen
235 PRINT	Line space
280 I(3)=-1	
290 Z=SQR(X(9,9)↑2+(Y(9,9)+D)↑2)	Entry for new position from 830
340 REM COORD OF REC STNS RX	
350 FOR J=W1TOW4	
360 X(J,1)=D*SIN(V*J)	Elliptical parameters
370 Y(J,1)=D*COS(V*J)-D	
380 M1=X(9,9)-X(J,1):M2=Y(9,9)-Y(J,1)	
390 M3=M1/M2	
400 E(J)=ATN (M3)	
410 M4=1	
420 IF M1 <0 THEN M4=-1	
430 IF M2 <0 THEN E(J)=E(J)+(M4* π)	
440 O(J)=E(J)-(J*V)	
450 P(J)=SQR((M1)↑2+(M2)↑2)	
460 X(J,2)=P(J)*SIN(O(J))	
470 Y(J,2)=P(J)*COS(O(J))	
480 T(J) =ATN(X(J,2)/(Y(J,2)+D/2))	
490 N(J) =(Z+P(J)-D)/L	
495 IF N(J)-INT(N(J)) >.5 THEN N(J)=1+IN	

Table 5. TRACKER XV Program (Continued)

COMPUTER LISTING	COMMENTS
T(N(J))	
497 IF N(J)-INT(N(J)) <.5 THEN N(J)=INT(N(J))	
500 R(J)=N(J)*L/2	
510 A(J)=R(J)+D/2:B(J)=SQR((RE(J))↑2+(R(J)*D))	Major and minor axis
520 NEXTJ	
530 REM INCREMENTAL CHANGE OF X,Y DUE TO DOPPLER FROM ANY STATION	
531 INPUT J	Manual input for tracking (±1, ±2)
532 I(3)-I(3)+1:I(2)=1	
533 IF J < OTHEN I(2)=-1	
534 J=SQR(J↑2)	
535 IF J >99TOTO 170:IFJ >9 GOTO 290	100 entry resets new section; 10 entry resets new coordinates
536 N(J)=N(J)+I(2)	
610 REM SPACING BETWEEN ELLIPSE	
620 R(J)=N(J)*L/2	
630 A(J)=R(J)+D/2:B(J)=SQR(R(J) 2+(R(J) *D))	
640 Q(J,1)=(L/2)*(1+SQR(((SIN(T(J)))*((A(J)/B(J))-1)))↑2))	Spacing between ellipses
650 REM INCREMENT OF X AND Y ON NEIGHBORING ELLIPSE	
660 IFJ=W1 THENGOTO700	
670 IF J=W2 THENGOTO710	
680 IF J=W3 THENGOTO720	
690 IF J=W4 THENGOTO730	
700 I=W2: GOTO740	
710 I=W3: GOTO740	
720 I=W2: GOTO740	
730 I=W3: GOTO740	
740 U(I,1)=ATN(B(I)/(A(I)*(TAN(T(I)))))	
750 U(J,1)=ATN(B(J)/(A(J)*(-TAN(T(J)))))	
760 U(I,4)=(I-J)*V+U(I,1)-U(J,1)-(π/2)	
770 S=I(2)*(I-J)*Q(J,1)/COS(U(I,4))	Vector shift in position

Table 5. TRACKER XV Program (Continued)

COMPUTER LISTING	COMMENTS
780 X(J,3)=S*COS(U(I,1)+(I*V)-(π/2))	Coordinate shift in position
790 Y(J,3)=-S*SIN(U(I,1)+(I*V)-(π/2))	
800 REM NEW X,Y COORDINATES	
810 X(9,9)=X(9,9)-X(J,3)	New coordinates
820 Y(9,9)=Y(9,9)-Y(J,3)	
825 PRINTI(3);X(9,9);Y(9,9);N(1);N(2)	Screen command
830 GOTO290	
840 PRINT"REND"	
845 X=USR(R)	Typing command
850 END	

requests wavelength, L, total number of peripheral stations, N, and distance between receiving stations and the transmitter, D. The second request is for which station pairs are receiving doppler. The program is instrumented for the first 8 stations. The third request is the initial starting coodinates, supplied by the HSS (Hybrid Sensor System). This information is initialized and awaits doppler data. The input in the form of the doppler sign and the station receiving the doppler, i.e., 1, -1, 2, -2, etc. A printout of the new coordinates is put on a CRT display or it is typed.

An example of a tracking plot for the first 30 meters on a magnified scale is shown in Figure 17. Four tracks are portrayed; (1) alternate doppler cycles from STN 1 and STN 2; (2) STN 1 only; (3) STN 2 only; and (4) a "Square Path" in which two doppler cycles are generated in 4 directions in order to show closure. Typed printouts of these paths are shown in Tables 6 and 7.

The time to generate a track position from a doppler cycle is 2.5 seconds with this program. No effort was made to reduce the computing time in the basic statements. If machine language was used the computing time could be reduced considerably. If the doppler cycles are accumulated, say every fifth cycle is computed, a time reduction of 1/5 could be realized. This would be necessary for tracking vehicles.

2.2.4.4 GRAPHICAL DISPLAY INCREMENTAL TRACKING – A simular program was developed to graph the intruder's track directly on the Commodore 2001 screen. The input to the sector established the scale and the position on the screen of two central responding stations. The standard screen displays 24 by 40 character elements: 20 out of 40 were allocated for the horizontal display, covering the area between two responding stations. Twenty spaces were allocated for the vertical display, covering the area perpendicular to the line between the two responding stations. Fifty peripheral stations would scale a sector, 1000m by 1000m, represented by 20 by 20 character elements. Each character element would be equivalent to 50m by 50m. The program labels the station numbers and the sector in degrees (W2). A plot of the track is designated by a series of "+" characters. It takes between 5 to 20 doppler cycles per station to cause a new position to be displayed (50m). Each character is generated by a dot matrix of 6 by 8. A high resolution modification to the computer can control these dots individually allowing an increase in resolution of 8-1/3m by 6-1/4m for the same scale.

A listing of TRACKER XII program and a typed printout of the screen display are shown in Figure 18. It shows an accelerated plot using 25m wavelength (X5 at 60 MHz), with 94 computations resulting in 18 discernable plots, and plot time 4.7 minutes. Initial position is 2250,389m (referenced from STN 0), and spacing between STN 1 and STN 2 is 1283m. There are 20 type elements between STN 1 and STN 2 is 20, or 64 meters/element. The path length is 640m and it ends near baseline, 550m from STN 2.

The input data used was 25m wavelength (X5 accelerated computation), 39 stations, 8000m transmitter-to-receiver spacing; STN 1 and STN 2 responding. Initial position 2250,389m from STN 0. Incremental steps were made with alternate doppler cycles from STN 1 and STN 2. The intruder is 700m from the baseline of STN 1 and STN 2, and a little to the right of the center. The track continues to the baseline 550m from STN 2. This program is used to demonstrate graphical tracking and does not have a separate

Table 6. TRACKER XI Program

Initial L=5 N=39 D=8000 STN 1, 2
x_{99}, y_{99} 2250, 389 N(1)354 N(2)307

0	2241.96828	389.964151	353	307	Automatic Advance
1	2248.87548	386.402548	353	306	1 cycle of doppler alternating
2	2240.85626	387.361471	352	306	at STN 1 and STN 2
3	2247.75178	383.80369	352	305	
4	2239.74507	384.757383	351	305	
5	2246.63187	381.20189	351	305	
6	2238.63767	382.150363	350	304	
7	2245.51278	378.598675	350	304	
8	2237.53109	379.541926	349	303	
9	2244.3945	375.994039	349	303	
10	2236.42534	376.932065	348	302	
11	2243.27704	373.387975	348	302	
12	2235.3204	374.320775	347	301	
13	2242.16039	370.780479	347	301	
14	2234.21629	371.70805	346	300	
15	2241.04456	368.171545	346	300	
16	2233.113	369.093885	345	299	
17	2239.92953	365.561165	345	299	
18	2232.01052	366.478274	344	298	
19	2238.81532	362.949336	344	298	

Doppler on STN 1 only

0	2241.96828	389.964151	353	307
1	2233.9537	390.901376	352	307
2	2225.95516	391.814051	351	307
3	2217.97749	392.699811	350	307
4	2210.01112	393.562007	349	307
5	2202.06517	394.397772	348	307
6	2194.13002	395.210429	347	307
7	2186.20953	395.99977	346	307
8	2178.30468	396.763773	345	307
9	2170.41395	397.504915	344	307
10	2162.54249	398.220764	343	307
11	2154.68062	398.914567	342	307
12	2146.83759	399.583497	341	307
13	2139.00369	400.230771	340	307
14	2131.1882	400.853577	339	307
15	2123.38141	401.455101	338	307
16	2115.59261	402.032545	337	307
17	2107.81206	402.589065	336	307
18	2100.0491	403.121879	335	307
19	2092.29397	403.634109	334	307

Table 6. TRACKER XI Program (Continued)

Doppler on STN 2 only

```
C  0     2256.90151    385.420228    354    306
   1     2263.79264    381.825299    354    305
   2     2270.66389    378.217538    354    304
   3     2277.52519    374.594577    354    303
   4     2284.36703    370.95877     354    302
   5     2291.19935    367.307709    354    301
   6     2298.01956    363.642843    354    300
   7     2304.82374    359.963579    354    299
   8     2311.61629    356.270433    354    298
   9     2318.39319    352.562855    354    297
  10     2325.15892    348.841306    354    296
  11     2331.90937    345.105284    354    295
  12     2338.65177    341.353717    354    294
  13     2345.3837     337.588003    354    293
  14     2352.10091    333.807713    354    292
  15     2358.80812    330.013155    354    291
  16     2365.50097    326.203954    354    290
  17     2372.1843     322.380352    354    289
  18     2378.86085    318.540823    354    288
  19     2385.5236     314.686507    354    287
```

Table 7. Closed Path Tracking Error TRACKER XV Program

	X_{99} 2 Dopplers	Y_{99} 4 Directions	N(1)	N(2)	
Initial	2250.000	389.00	354	307	
STN # & Sense					
? 1					
0	2241.95981	389.965168	354	307	Manual Input
? 1					
1	2233.93684	390.903348	353	307	
? 2					
2	2240.85206	387.356055	352	306	
? 2					
3	2247.75349	383.795232	352	305	
? -1					
4	2255.7602	382.841528	353	305	
? -1					
5	2263.78847	381.860315	354	305	
? -2					
6	2256.91717	385.468056	354	306	
? -2					
7	2250.026	389.063002	354	307	Closure error .026, .063m
6 doppler cy, 4 directions					
Result	2250.2657	289.114921	355	305	Closure error .2675, .1149m
10 doppler cy, 4 directions					
Result	2250.75054	389.080836	355	305	Closure error .75, .0808m

doppler input; the program automatically adds alternate doppler cycles. It can be modified as in program XV for manual doppler entry. If the wavelength L is changed to 25 instead of 5 the effect is to accumulate 5 doppler cycles of 60 MHz reducing the input entries and speeding up the tracking.

2.2.4.5 DUAL DOPPLER PHASE DIFFERENCE ALGORITHM – A program using the differential phase difference between two doppler frequencies 100 kHz apart was developed. The doppler was not included in the solution. With a measurement of phase from two adjacent sensor receiving stations, the ellipse number is computed by $\therefore N(J) = \phi \times 300/\pi$ (ϕ in radians) the algorithm XXB, requests wavelength (5m), the number of stations on the periphery, N, and the distance between transmitter and the receiving stations, D. The second request is the number of the two stations receiving the doppler signals. A graphical format is generated showing the relative position of the two

Table 8. TRACKER XII Graph Display

Automatic Input alternate doppler cycles added to W_2, W_3
OUTPUT Screen Display; output also typed.
PET COMMODOR 2001
BASIC LANGUAGE

```
100   EXAMPLE,5,39,8000-1,2-2250,388                    Typical example
110   REM STN2-Z=8684,P=1084,N=353,ANGLES
  0=53,E=63,T=10.68-STN CORD 1283,-103
120   REM INITIALIZE TRACKING ALGORITHM
130   PRINT"L","N","D"
140   INPUT L,N,D
150   V=2*π/N
160   PRINT"ANY ADJACENT STATIONS","1TO8"

170   INPUT W2,W3                                       Sector selection (in any
                                                        order)
180   IF W2<W3 THEN GOTO 200
190   W5=W2:W2=W3:W3=W5
200   W1=W2-1:W4-W3+1
210   PRINT"INTRUDER INITIAL COORDINATES-
          X,Y
220   INPUT X(9,9),Y(9,9)
230   PRINT"☑"                                          Clear screen
240   K1=.1*INT(10*V*W2*180/π)
250   PRINTTAB(7)K1"DEG.NORTH"
260   K2=W2+48:K3=W3+48
270   POKE33737,K2: POKE33757,K3
280   I(3)=-1
290   Z=SQR(X(9,9)↑2+(Y(9,9)+D)↑2)                      New position data from
                                                        830
                                                        Range from transmitter
                                                        to intruder
295   IFX(W2,2)=0 GOTO 340
300   F=.1*D*SIN(V/2)                                   Scale (depends upon STN
                                                        spacing)
310   G=(X(W2,2)/F)+10 :H=INT(25-Y(W2,2)/               Screen coordinates
F)
320   C=32768+(G-1)+(40*(H-1))                          Screen RAM Memory
                                                        Address
330   POKEC,43                                          "+" Point "poked" on
                                                        screen
340   REM COORD OF REC STNS RX
350   FOR J=W1T0W4
```

Table 8. TRACKER XII Graph Display (Continued)

```
 360   X(J,1)=D*SIN(V*J)
 370   Y(J,1)=D*COS(V*J)-D
 380   M1=X(9,9)-X(J,1):M2=Y(9,9)-Y(J,1)          Elliptical parameters,
                                                  4 stations
 390   M3=M1/M2
 400   E(J)=ATN (M3)
 410   M4=1
 420   IF M1  0 THEN M4=-1
 430   IF M2  0 THEN E(J)=E(J)+(M4*  )
 440   O(J)=E(J)-(J*V)
 450   P(J)=SQR((M1)↑2+(M2)↑2)
 460   X(J,2)=P(J)*SIN(O(J))
 470   Y(J,2)=P(J)*COS(O(J))
 480   T(J)   =ATN(X(J,2)/Y(J,2)+D/2))
 490   N(J)   =(Z+P(J)-D)/L:N(J)=INT(NCJ))
 495   IF N(J)-INT(J(J))>.5THEN N(J)=1+INT
(N(J))
 497   IF N(J)-INT(N(J))>.5THEN N(J)=INT(N
(J))
 500   R(J)=N(J)*L/2
 510   A(J)=R(J)+D/2:B(J)=SQR((R(J)) ↑ 2+(R(      Major axis, minor axis
J)*D))
 520   NEXTJ
 530   REM INCREMENTAL CHANGE OF X,Y DUE TO
   DOPPLER FROM ANY STATION
 540   I(3)=I(3)+1
 550   IF I(3)>400 GOTO 840                       I(3) count of plots (limited
                                                  to 400) (change as re-
                                                  quired)
 560   I(4)=I(3)/2:I(5)=I(4)-INT(I(4))
 570   J=W2
 580   IF I(5)>.01THEN J=W3
 590   J=SQR(J↑2)
 600   N(J)-N(J)-1
 610   REM SPACING BETWEEN ELLIPSE
 620   R(J)=N(J)*L/2
 630   A(J)=R(J)+D/2:B(J)=SQR(R(J)  2+(R(J)
*D))
 640   Q(J,1)=(L/2)*(1+SQR(((SIN(T(J)))*((    Spacing between ellipses
A(J)/B(J))-1))↑2))
 650   REM INCREMENT OF X AND Y ON
         NEIGHBORING ELLIPSE
 660   IFJ=W1 THENGOTO700
 670   IFJ=W2 THENGOTO710
```

Table 8. TRACKER XII Graph Display (Continued)

```
680   IFJ=W3 THENGOTO720
690   IFJ=W4 THENGOTO730
700   I=W2: GOTO740
710   I=W3: GOTO740
720   I=W2: GOTO740

730   I=W3: GOTO740
740   U(I,1)=ATN(B(I)/(A(I)*(-TAN(T(I))))
)                                          Slope of ellipse at T(I)
750   U(J,1)=ATN(B(J)/(A(J)*(-TAN(T(J))))
)                                          Slope of ellipse at T(J)
760   U(I,4)=(I-J)*V+U(I,1)-U(J,1)-(π/2))
770   S=(I-J)*Q(J,1)/COS(U(I,4))           Shift in position (vector)
780   X(J,3)=S*COS(U(I,1)+(I*V)-(π/2))     Coordinate shift in
790   Y(J,3)=-S*SIN(U(I,1)+(I*V)-(π/2))    position
800   REM NEW X,Y COORDINATES
810   X(9,9)=X(9,9)-X(J,3)
820   Y(9,9)=Y(9,9)-Y(J,3)
830   GOTO290
840   PRINTN(W2),N(W3)
850   END
855   X=USR(R)                             Typing command
```

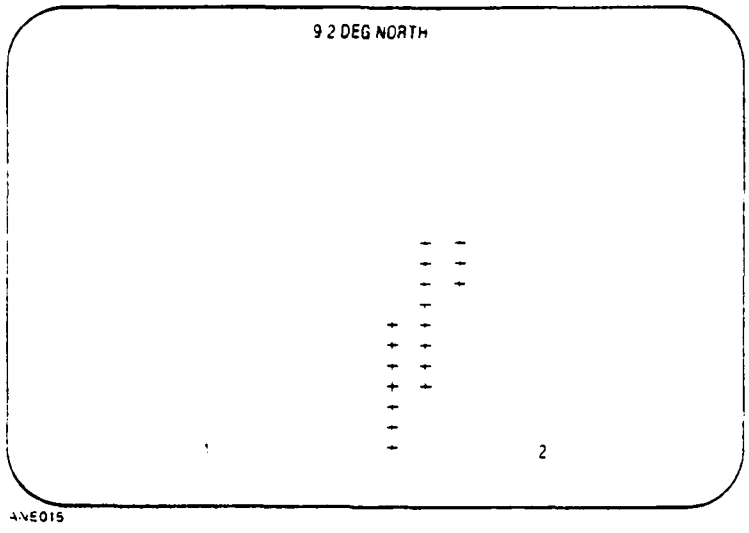

Figure 18. Typed CRT Display. (-X5 λ plot scans data as shown in Figure 17. Pairs of plotting result.)

receiving stations and identifying the sector by angle. An input request is made for the two ellipse numbers computed from ϕ. Computation is made by determining the intersection of the two ellipses and relating it to the reference axis and transferring it to the axis formed by the line between the two receiving stations and the perpendicular to this line at the low numbered station (left hand). A plot is made using "+". Table 9 shows the listing of the algorithm TRACKER XXB.

A typed CRT display is shown in Figure 19, was made using various N(1), N(2) combinations. The plots show some irregularities which is due to the course digital type intervals. A high resolution system using the dot elements would smooth the curve. Note the plots are not a track but show the latitude of computation. A true track would consist of adjacent type elements.

The accuracy of the phase measurements is estimated to be within one or two type elements. If the doppler computation of program XI were combined with the dual doppler phase, a high degree of accuracy could be obtained. The multiple phase measurements would be averaged and updated by each doppler cycle.

2.3 ANTENNA DESIGN

2.3.1 TRANSMITTING ANTENNA INVESTIGATION

The transmitting antenna provides the illumination for all the targets to be detected. It should provide an omnidirectional pattern in azimuth and provide a signal up to 300m above the area 8 km from the antenna. The 360° coverage in azimuth limits antenna gain to vertical directivity which could be as small as 3°. Vertical directivity is obtained by stacking halfwave (8 ft) elements; gain is nearly proportional to number of elements. A

Table 9. Dual Doppler Phase Input, CRT Screen Output
TRACKER XXB Program

COMPUTER	COMMENTS
100 PRINT"L","N","D"	Example 5,39,8000
110 INPUT L,N,D	Angle between sectors
120 V=2*π/N	
130 PRINT"ANY ADJACENT STATIONS","1 TO 8"	
140 INPUT W2,W3	
150 IF W2 W3 THEN GOTO 170	
160 W5=W2:W2=W3:W3=W5	Station selection
170 W1=W2-1:W4=W3+1	
180 PRINT"[▽]"	Clear screen
190 K1=.1*INT(10*V*W2*180/π)	Screen format
200 PRINTTAB(7)K1"DEG.NORTH"	Sector identification
210 K2=W2+48:K3=W3+48	and station numbers
220 POKE33737,K2: POKE33757,K3	
230 INPUT N(1),N(2) {Ellipse numbers. $N(J)=\frac{\phi rad}{\pi} \times \frac{1500}{5}$	ϕ phase difference; 1500 = λ/2 of 100 kHz; 5 = λ of 60 MHz
240 PRINT"[SEQ]" {Home, cursor down	
250 FOR J=1TO 2	
260 R(J)=N(J)*L/2 : A(J)=R(J)+D/2	Ellipse parameters for 1 & 2
270 E(J)=D/(2*A(J))	A=major axis,
280 Q(J)=(A(J)/E(J))*(E(J)↑2-1)	E=eccentricity
290 NEXT J	R=Distance STN to ellipse
300 S(1)=(Q(1)/E(2))-(Q(2)/E(1))	
310 S(2)=(Q(1)*COS(V))-(Q(2))	
320 S(3)= Q(1)*SIN(V)	Computation simplification
330 S(6)=S(1)↑2-S(3)↑2	
340 S(5)=-2*S(1)*S(2)	
350 S(4)=S(2)↑2+S(3)↑2	
360 U(1)=(-S(5)+SQR(S(5)↑2-(4*S(4)*S(6)	Quadratic solution of cos U2
	$\frac{-b \pm \sqrt{b^2-4ac}}{2a}$
))/(2*S(4))	(-solution rejected)
370 U(2)=ATN((SQR(1-(U(1))↑2))/U(1))	Arctan (of cos function)
371 S(6)=S(1)↑2-S(3)↑2	
372 S(5)=-2*S(1)*S(3)	
373 S(4)=S(2)↑2+S(3)↑2	Recompute using sin function
374 U(3)=(-S(5)+SQR(S(5)↑2-(4*S(4)*S(6)	to determine sign of U2
))/(2*S(4))	
375 U(4)=U(3)/(SQR(1-(U(1))↑2))	
380 I=1:IFU(4)<0THEN I=-1	I=-1 for negative angles
390 Z=-Q(1)/((1/E(1))-COS(U(2)))	

Table 9. Dual Doppler Phase Input, CRT Screen Output
TRACKER XXB Program (Continued)

	COMPUTER	COMMENTS
400	Y(9,9)=Z*COS(U(2)+V)-7990	Coordinates ref x=0 y=0
410	X(9,9)=Z*SIN((I*U(2))+V)	
420	FOR J=W1TOW4	
430	X(J,1)=D*SIN(V*J)	STN location ref x=0 y=0
440	Y(J,1)=D*COS(V*J)-D	
450	M1=X(9,9)-X(J,1):M2=Y(9,9)-Y(J,1)	
460	M3=M1/M2	
470	C(J)=ATN (M3)	Angle between STN "0"
480	M4=1	and intruder (ref. at STN)
490	IF M1<0 THEN M4=-1	
500	IF M2<0 THEN C(J)=C(J)(M4*π)	
510	O(J)=C(J)-(J*V)	Angle between major axis
520	P(J)=SQR((M1)↑2+(M2)↑2)	and intruder at station.
530	X(J,2)=P(J)*SIN(O(J))	Coordinates referenced
540	Y(J,2)=P(J)*COS(O(J))	to STN 1 & STN 2
550	NEXTJ	
560	F=.1*D*SIN(V/2)	
570	G=(X(W2,2)/F)+10 :H=INT(25-Y(W2,2)/F)	Plot on format.
580	C=32768+(G-1)+(40*(H-1))	
590	POKEC, 43	43 is "+"
600	GOTO230	New input return.
610	END	

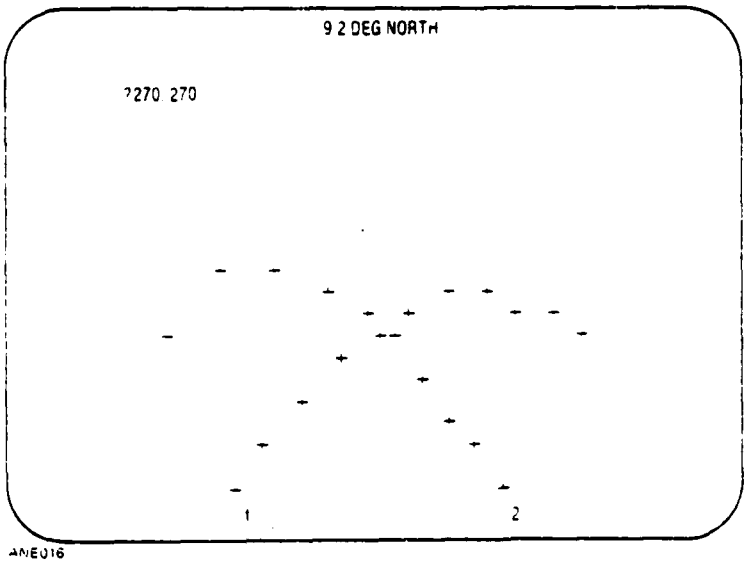

VARIOUS INPUTS OF STN1 STN2

STN1	STN2	STN1	STN2
10	270	270	10
50	270	270	70
100	270	270	100
150	270	270	150
200	270	270	200
270	270	270	300
300	270	270	350
350	270	270	400
400	270	270	425
450	270	270	470
470	270		

Figure 19. Typed CRT Display, Dual Doppler Phase Input

review of four types of vertical high gain antenna can be found in the Antenna Engineering Handbook[10]: the skirted coaxial, modified Franklin, Series Fed Collinear, and Mast mounted Collinear array. These antennae and a table of gain related to a halfwave dipole taken from Jasick are shown in Appendix F.

A three-element array takes at least 24 ft and gives about 3 dB gain over a dipole. In order to double this, the antenna would double its length to at least 48 ft. With an 80 ft-high antenna limit, the lower radiators will be at 30 ft and not be as effective as the upper ones due to ground multipath. A three-element array of the modified Franklin or the Series Fed Collinear seems to be the better configuration. The Series Fed Collinear is 1 dB greater than the Franklin and is longer by 6 ft; it also appears to be a bit more efficient.

No special development would be required for these antenna as these should be commercially available.

In combination with the above antenna which has 7 dB gain over isotropic and the computation/measurements of the propagation loss, 20 watts of radiated power would provide the necessary field intensity at the surveillance zone.

2.3.2 RECEIVING ANTENNA

The main purpose of the receiving antenna is to pick up the reflected signals from an intruder. The sensitivity of the receiver and the antenna gain determine the effective intruder tracking range of the receiving site. The tracking range then determines the

---

[10]Henry Jasik, Antenna Engineering Handbook; McGraw Hill Book Company, 1962; pp 22-2 - 22-9.

number of sites required to cover the annular ring security zone. The greatest coverage is obtained with the receiving site located halfway between the inner and outer radius of the annular ring and having an omnidirectional antenna pattern. However, the antenna not only receives the intruder signal but also the direct transmitted signal, which is calculated to be 103 dB greater than the intruder signal. This difference in signal level will most likely cause overload on the receiver. In addition, the noise on the direct carrier would certainly mask any other received signals and prevent adequate signal processing in determining doppler sense. The antenna can be made to reduce the direct signal by forming a null in its pattern toward the transmitter and provide general coverage elsewhere. A two-element array fits this requirement.

The study which involves the logic and computations on the antenna was made on this contract; the construction and the field measurements were made on the General Dynamics 1980 IRAD program.[11]

2.3.2.1 APPROACH – A passive array, i.e., a driven element and a parasitic reflector, can achieve 20 dB; 30 dB is unusual. Two driven elements can achieve 30 to 40 dB; however, with good controls of amplitude and phase on the driven elements we believed we could achieve 60 dB.

The operation of a two-element array is described as follows. Consider two elements, A and B; both are dipoles spaced "d" units apart. Energy received by both will be added vertorially. The dipoles are vertically polarized, and we view the arrangement from the top to show the azimuth responses.

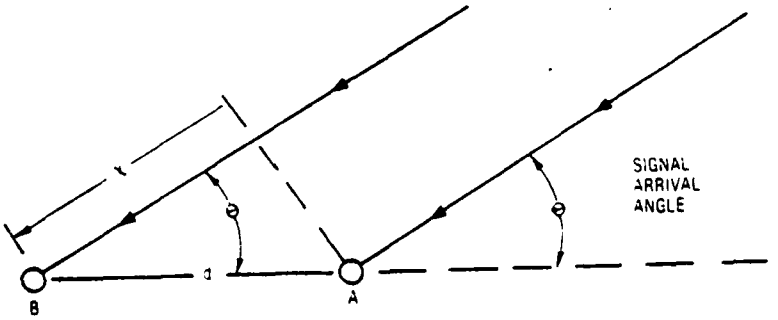

ALC008

[11]John B. Gehman, Large Area Intruder Sensor System, R-80-042; General Dynamics Electronics Division, December 1980.

The signal arriving at B is delayed $2\pi X/\lambda$ radians later than that received at A for angles less than $\pm\pi/2$ radians ($\pm 90°$). When signals arrive at B they are combined at A through a transmission line d long, adding an additional delay of $2\pi d/\lambda$.[12, 13]

The total delay "S" of Signal B is:

$$S = \frac{2 \cdot \pi \cdot X}{\lambda} + \frac{2\pi d}{\lambda}$$

$$\text{since } X = d \cdot \cos\Theta$$

$$\text{then } S = \frac{2 \cdot \pi \cdot d}{\lambda}(\cos\Theta + 1)$$

The two signals A and B are combined vectorially.

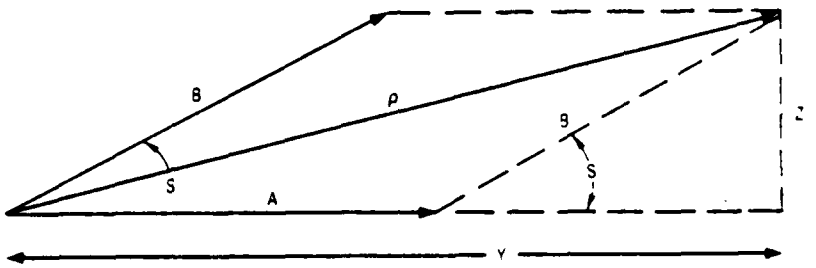

ALC009

The resultant signal

$$\rho = \sqrt{y^2 + z^2}$$

$$\text{since } y = A + B\cos(S)$$

$$\text{and } z = B\sin(S)$$

then,

$$\rho\sqrt{[A + B\cos(S)]^2 + [B\sin(S)]^2}$$

Since A and B takes energy from the same wavefront, A and B must divide the energy so that $A^2 + B^2 = 1$; if A = B, then, A and B are 0.707 (relative volts).

Computed antenna patterns are shown in Appendix F, Figure F-1 for various spacings of d. Wavelength λ is 5m; when $d = \lambda/4$ (1.25m), then at this value, a perfect cardioid pattern is formed. Nearly uniform gain is obtained over 220°, and a sharp null is noted at

---

[12]Keith Henney, Radio Engineering Handbook; McGraw Hill Book Company, 1935, p 746.

[13]Frederick Terman, Radio Engineers Handbook; McGraw Hill Book Company, 1943, p 802.

180°. For d = 1.35m and 1.3m, a backlobe bubble in the pattern is generated, and for d = 1.2m, only a shallow null is formed. For unbalances in A and B, shallow nulls are generated for all values of d.

2.3.2.2 ANTENNA DEVELOPMENT – An initial test using 1/8 in. copper tubing produced a deep null 50 to 60 dB but was extremely unstable and not repeatable. A better electrical design was needed.

The length of a dipole is approximately $\lambda/2$ but varies with the thickness of the elements and is given as:[5]

$$\frac{5905 \times K}{F} = \text{Reasonant Length L}$$

where K is a factor determined by antenna diameter to length; F is the frequency, F = 60 MHz.

Approximate diameter 3/8 in. and length 98 in. (ratio 262) for a ratio of 262, K = 0.968 Resonant length 47.63 in. L.

The impedance at the center of the dipole is found from data by King and Blake.[14] (See Appendix E.) At H ($\approx\lambda/2$) and for $a/\lambda = 0.0019$; $R_{11} = 57$ ohms, and $X_{11} = 30$ ohms, where H_R = resonant length, and a/λ = the ratio of diameter to wavelength (0.375/196.8). Since the two elements are coupled to each other, a mutual impedance will influence the center impedance of each element.

Z_{11} and Z_{22} is the self impedance of half wave dipole 57 + j30 (rectangular)

Z_{11} and Z_{22} is the self impedance of half wave dipole 64 $\angle 28°$ (polar)

Z_{12} is the mutual impedance, coupling the elements

Z_{12} = 43 + j30 (rectangular coordinate)

Z_{12} = 52 $\angle 35.5°$ (polar coordinate)

$$\text{Center Impedance } Z_D = Z_{11} + \frac{\left(Z_{12}\right)^2}{Z_{22}}$$

Z_D = 26.95 - J1.67 (rectangular coordinate)

Z_D = 27 $\angle -3.55°$ (polar coordinate)

Z_D is the center impedance of either element, A or B in the presence of the other.

---

[14] Ronald King and F. G. Blake, Jr., Proceedings of the IRE, July 1942; Volume 30, pp 336-349.

2.3.2.3 ADJUSTMENT OF NULL BY AMPLITUDE CONTROL – In order to combine A and B, a transmission line $\pi/4$(d = 1.25m) long is used. If Z_o is equal to the antenna impedance Z_{DB}, the antenna impedance is transferred directly across to Z_{DA}. Then the total impedance at A will be:

$$Z_T = \frac{Z_{DA} \cdot Z_{DB}}{Z_{DA} + Z_{DB}}$$

which works out to be 13.5 $\angle -3.55°$ polar coordinate or 13.47 - J.84 rectangular coordinate.

The output impedance of the antenna Z is too low for suitable impedance matching and too low for a balanced transmission line between the two elements. A folded dipole configuration was selected. The drive point impedance is raised four times. The same length antenna and diameters of the elements then produce

Z_{DA} or Z_{DB} = 26.95 - J1.67 $\qquad Z_{DB} \times 4$ = (107.8 - J6.68) (rectangular)

Z_{DA} or Z_{DB} = 27 $\angle -3.55°$ $\qquad Z_{DB} \times 4$ = (108 $\angle -3.55°$)

If the transmission line Z_o is made to be 108 ohms, then the parallel circuit of A and B

$$Z_T = 53.88 - J3.35 \text{ (rectangular)}$$
$$= 53.98 \angle -3.57° \text{ (polar)}$$

A Z_T of 54 ohms is easily matched to the receiver through a standard coaxial line.

The surge impedance (characteristic impedance), Z_o, is determined by the diameter of the transmission line, its spacing, and the dielectric between the lines.[15]

$$Z_o = 120 \cosh^{-1} \frac{D}{2R}$$

where

D = Spacing of the lines
R = Radius of the lines

For an impedance Z_o of 108 ohms and a line radius R = 0.1875 in., a center-to-center spacing of 0.537 in. is computed. Space between lines is 0.162 in.

When signals arrive at azimuth angles of 0° or 180° (A and B are in line), A or B will shadow the other element reducing its share of the incident power. At ± 90°; equal

---

[15]Henry Jasik, Antenna Engineering Handbook; McGraw Hill Book Company, 1962; pp 3-13, 3-15, 30-3.

distribution of power is realized. It will be necessary to adjust the contribution of A and B for the null at 0° (in-line case). A change in the surge impedance, Z_o of the connecting transmission line between A and B, will change the contribution of B to the point at A. The $\lambda/4$ line acts as a transformer such that the product of the input and output impedance is equal to the square of the surge impedance.

$$Z_{DB} \; Z_{DBout} = Z_o^2 \quad 108 \cdot 87.3 = (97.1)^2$$

thus, if Z_o = 97.1 ohm, and Z_{DB} = 108 ohms, then 87.3 ohms would appear out of the line (Z_{DBout}). The power contributed by each element divides as follows:

$$P_t = \underbrace{\left(\frac{Z_A}{Z_B + Z_A}\right)}_{(A)} Pi + \underbrace{\left(\frac{Z_B}{Z_B + Z_A}\right)}_{(B)} Pi$$

where Pi is the incident power and Pt the total power.

$P_A/P_B = Z_B/Z_A$ in terms of current or voltage $I_A/I_B = \sqrt{Z_B/Z_A}$

If A = 0.4470046

B = 0.5529954

Substituting A and B into the antenna pattern equation, having null at 0°, will produce a null of -9.75 dB rather than something in excess of -100 dB.

2.3.2.4 ADJUSTMENT OF NULL BY PHASE CONTROL – We have considered taking an output from the array at element A. If the point of output is moved along the transmission line (Z_o), the delay of signal from B will be less and an "a" delay from A will be vectorially added. The relative delay of signal B with respect to A, i.e.

$$S = \frac{2\pi d}{\lambda}(\cos\Theta + 1)$$

will now be

$$S = \frac{2\pi d}{\lambda}(\cos\Theta + (1 - 2\alpha))$$

where "a" is a small increment along "d" from the element A; and $\alpha = \frac{a}{d}$.

Computations have been made showing the attenuation at various signal incident angles (azimuth) for d = 1.25 ($\lambda/4$), and for a slightly longer d, d = 1.275 with various pickoff points "α". "α" is measured as a percent of "d". See Table 10 and Figures 20 and 21.

The variation of the pickoff "α" will shift the angle where a null is found, or correct for construction tolerances by putting the null at 180° incident angle.

Table 10. Offset Null Versus "a" Tap

Θ ANGLE (degrees)	$\alpha = 1$		$\alpha = 0.01275$			$\alpha = 0.01976$			
	d = 1.25m (dB)	d = 1.275 (dB)	1% x d	1.25% x d	1.45% x d	1.55% x d	1.65% x d	1.65% x d	1.75% x d
0	-190	-27.05	-36.17	-41.6	-51.91	-69.08	-54.91	-49.79	-44.25
5	-47.48	-27.94	-39.00	-47.95	-	-	-	-	-39.65
10	-35.46	-31.30	-55.53	-41.02	-	-	-	-	-32.64
15	-28.44	-44.69	-32.74	-30.38	-	-	-	-	-26.89
20	-23.49	-33.44	-25.55	-24.44	-	-	-	-	-22.57
25	-19.66	-24.20	-20.86	-20.20	-	-	-	-	-19.00
30	-16.56	-19.39	-17.33	-16.88	-	-	-	-	-16.05

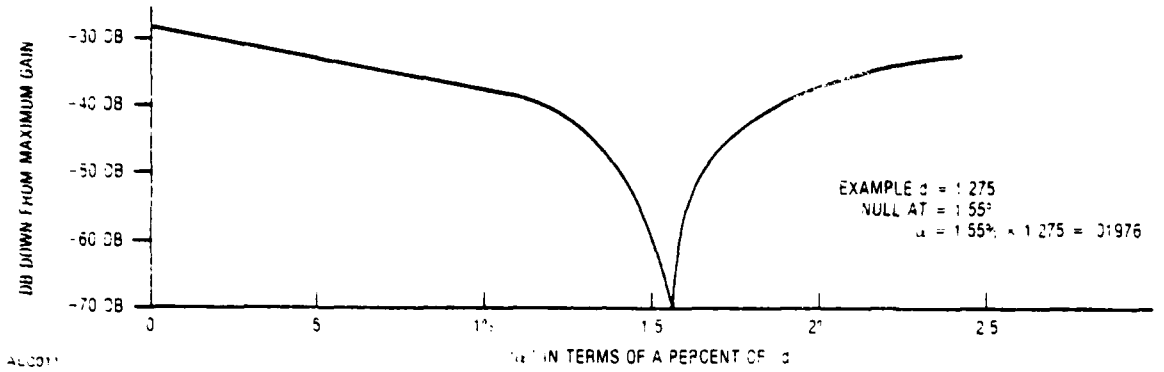

Figure 20. Offset Null

2.3.2.5 ANTENNA CONSTRUCTION – An antenna was built with the computed parameters in mind. Soft aluminum tubing 3/8-in. diameter was used. The folded dipoles were bent as illustrated in Figure 22 and fitted with aluminum plugs at the feed points. The transmission lines were fitted on the other end of the plugs. The plugs were then held in place with 4-40 screws on both the antenna side and the transmission line side. Electrical connection was made by a copper shim stock sleeve 3-in. long wrapped around the plugs and transmission lines. The sleeve had a small exposed 1/8-in. lip. An external line was connected to the exposed lip by miniature clips which were adjusted to provide the proper phasing. Blocks of nylon were used to clamp the transmission lines and provide a means for mounting the complete array. The antenna length was 92 1/4 in.; the spacing between elements was 44 3/8 in.; the folded dipole spacing was 1 1/2 in.; and the transmission line spacing varied between 3/8 in. to 7/8 in. An 8-ft long fiber tube was used to hold the antenna, fastening through the nylon clamps. The fiber tube was parallel to the interconnecting transmission line. External connection was made by cable taped to the fiber tube.

2.3.2.6 ON BOARD OSCILLATOR* – Tests on the antenna gave a fairly good null about 40 dB; however, it was soon discovered that a small motion of the feed line would cause the null to completely disappear. The problem was traced to the line reradiating

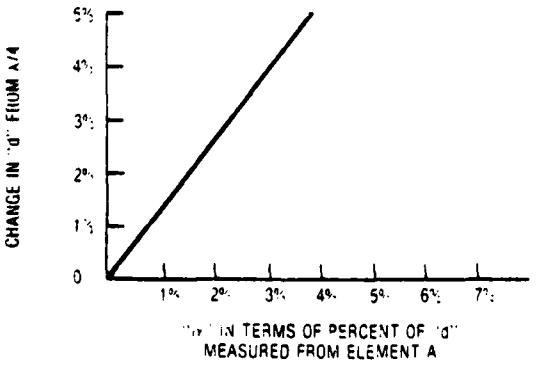

Figure 21. Transmission Line Length Change Versus Change in Line Tap

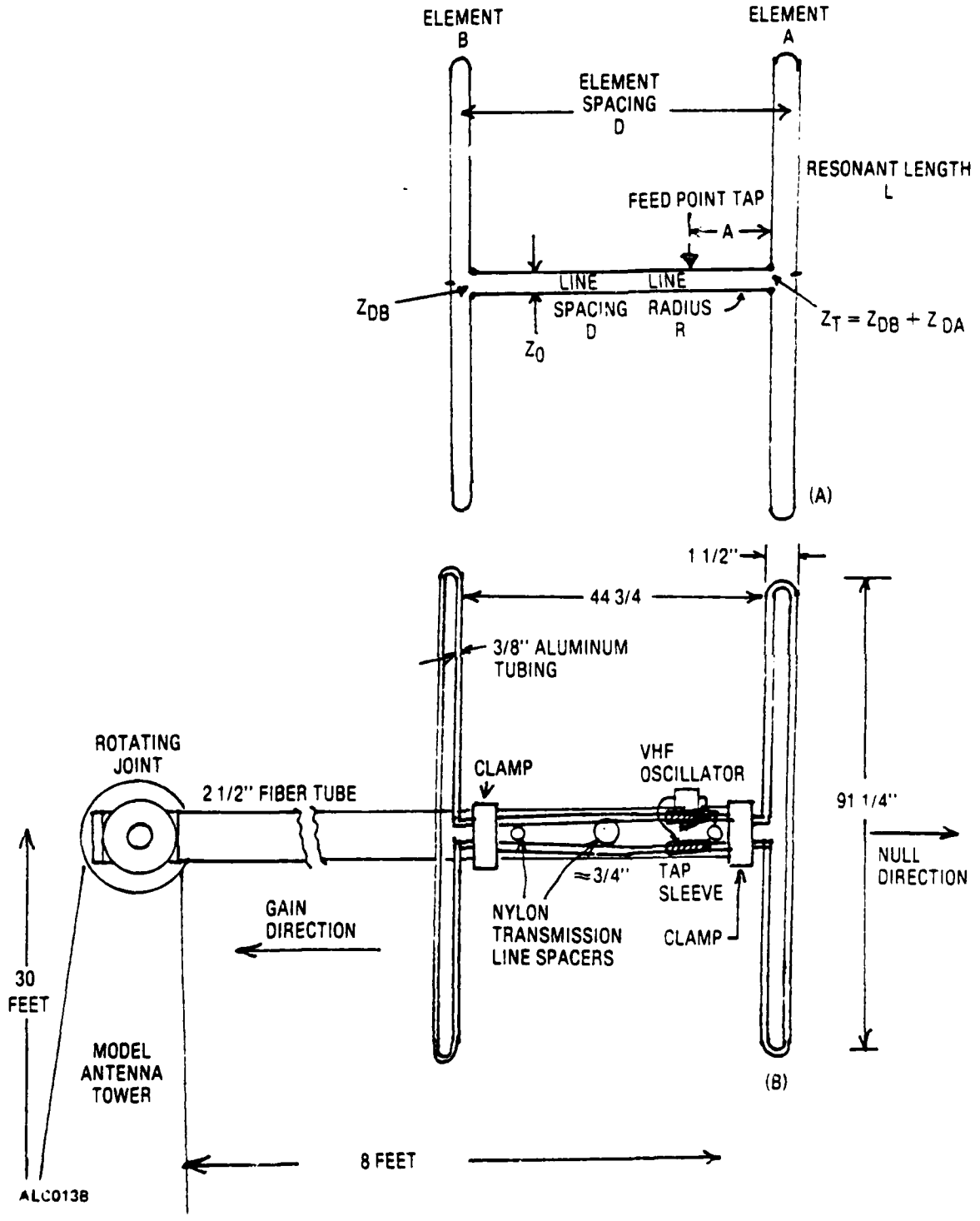

Figure 22. Antenna Configuration

signals from the antenna. In addition, it was found that moving personnel within 20 ft of the antenna would cause drastic changes in the null portion of the pattern. It was decided to eliminate the feed line problem by making a self-contained 60-MHz oscillator with its own 9V battery connected directly to the feed point. Tests would then be performed on the antenna test range, placing the antenna more remote from the ground and moving personnel.

The oscillator was constructed on a printed circuit board using a 2N706 in a Colpitts circuit. Approximately 10 mW at 60 MHz was generated using a 9V battery. The circuit was inductively tuned with a powered iron core. The battery and oscillator were taped to the antenna with clips connected to the copper adjustment sleeve on the transmission line for phase adjustment. A schematic of the oscillator is shown in Appendix H, Figure H-1.

2.3.2.7 FIELD ADJUSTMENT AND TEST OF RECEIVING ANTENNA* – The antenna testing range consists of a Scientific Atlanta Model 5836 tower unit located 185 ft from a control observation booth. The booth contains a control console (PC4D polar chart recorder), amplifiers, and Scientific Atlanta 1600 and 1710 receivers. The model tower has a drive mechanism which raises a 25-ft fiberglass pole which rotates in azimuth. A separate drive also turns a rotating joint at the top of the pole. All parts of the pole are nonconducting. The base which positions the pole adds another 5 ft to the pole's height (30 ft total). The 60-MHz two-element array is mounted to the top of the pole via its fiber tube placing it about 5 ft from the tower pole. A diagram of the antenna testing arrangement is shown in Figure 23. Controls are such that the antenna rotates in azimuth and elevation. Since the oscillator is built on and connects to the antenna, it becomes a transmitting rather than a receiving antenna. A separate receiving antenna, a quarter-wave ground plane, is mounted on top of a 13-ft ladder located 180 ft from the model tower. It is connected via coaxial cable to one of the Scientific Atlanta receivers in the control booth about 50 ft away. The output of the receivers feeds a demodulator and an amplifier which operate the polar plotting chart. Various locations were tried for the receiving antenna site to minimize multipath effects.

Some basic measurements were taken to adjust relative gain, azimuth, and elevation starting points. The chart's format plotted 360° in azimuth and 40 dB in gain. A technique to plot 60 dB required that the first plot be the normal 0 to 40 dB and then add 20 dB gain where the normal plot indicated 20-dB loss in signal. A second curve plotted at the higher gain would then show a -20 to -60 dB plot.

Thirty-one patterns were run in which the spacing between the transmission lines was varied in order to change the relative power in the array elements. The feed positions (designated as "a") was changed in order to change the relative phase between the two elements. The feed position "a" was measured from the nylon clamp point; the spacing was measured by the size of wedges placed between the lines. The spacing was not uniform: 3/8-in. at each element end, and 3/8-in. to 7/8 in. in the center, producing a bow in the middle. (See Figure 22.)

---

*1980 IRAD Sponsored

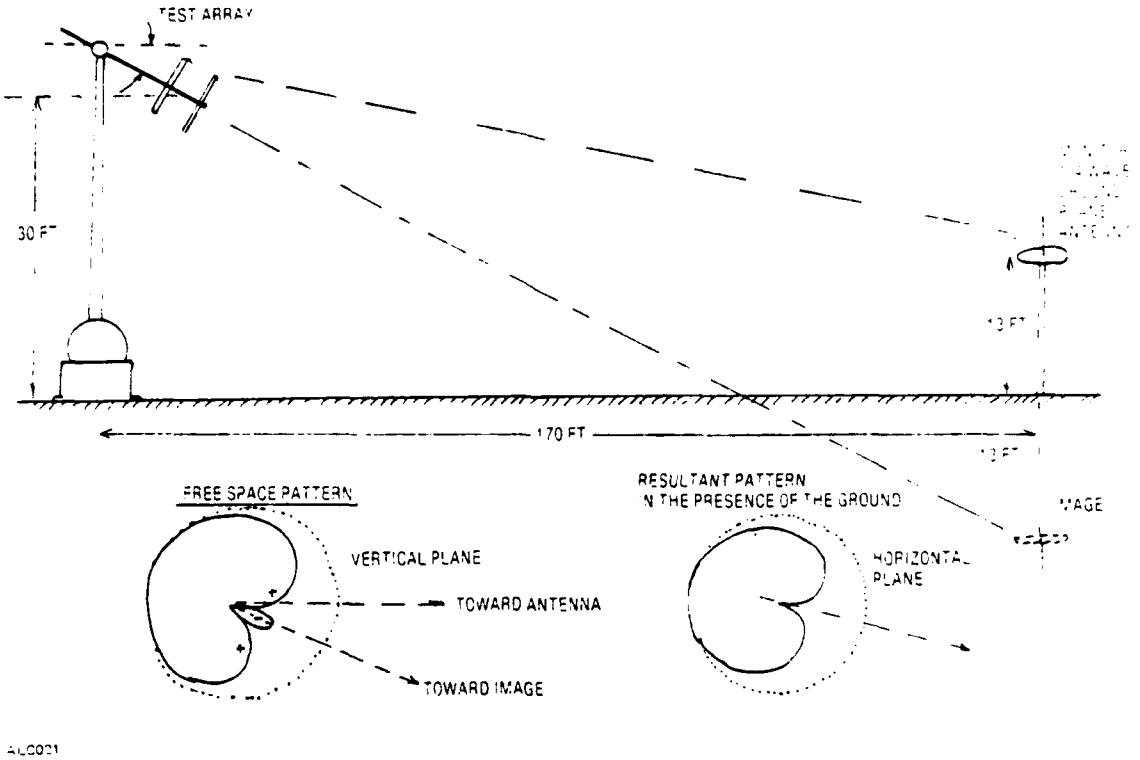

Figure 23. Antenna Test Range

Variations in the tap and spacing were made to improve the null response in the initial tests of the antenna. These are shown in Cut Nos. 4, 7, and 17 which are shown as Figures F-5, F-6 and F-7 in Appendix F. Improvement in the null was obtained; from 23 dB, to 38 dB, and to 60 dB. When the adjustments were near optimum, specific effects were noticed by varying phase only, i.e., varying tap position and maintaining transmission line spacing. (NOTE: Cut Nos. 29, 27, and 28 (Figures F-8, F-9 and F-10) vary the tap position, 3 3/8 in., 3 in., and 2 5/8 in. The transmission line block spacings were 5/8 in., 11/16 in., and 5/8 in. for all three measurements. A sharp null in No. 29 (Figure F-8) becomes a small bubble in No. 27 (Figure F-9) and a large bubble in No. 28 (Figure F-10).)

Note, Cut Nos. 29, 30, and 31 (Figures F-8, F-11, and F-12) show the effect of varying the power between elements by varying the block spacings and maintaining the tap position. Tap position was 3 3/8 in.; the block spacings were 5/8 in., 11/16 in., and 5/8 in.; 5/8 in., 5/8 in., and 5/8 in.; and 5/8 in., 3/8 in., and 5/8 in. The null varies from -60 dB, -40 dB, and -30 dB.

During the tests the effect of building reflections was noticed and a new location was sought to minimize this multipath. Cut No. 16(a) (Figure F-13) shows a bad multipath; the reflections produced an unsymmetrical null 10° off center. It was also noted that the ground reflections caused the largest multipath, and that nulls could be produced regardless of these multipaths; there seems to be an adjustment which produces a null. An example of this is shown by varying the antenna elevation from a normal -15° angle to -16°, -17° and -20° below the horizon. (NOTE: In Cut Nos. 29, 30(a), and 31(b) (Figures F-8, F-14 and F-15) each of the elevation angles are compensated by varying

the transmission line spacing: 5/8 in., 11/16 in., and 5/8 in.; 5/8 in., 5/8 in., and 5/8 in.; and 5/8 in., 3/8 in., and 5/8 in., while the tap remains at 3 3/8 in.)

The effect of the wind is shown in Figure B-11 where the curve is quite jagged due to movement of the elements, causing as much as 10 dB variation. This variation could be a noise source and would require a rigid mechanical structure. Figure F-3 shows an optimal adjustment for a null; at a -15° depression angle, tap is 5 1/8 in. from the near dipole, and transmission line spacing is 5/8 in.

2.3.2.8 DISCUSSION OF PHASE AND AMPLITUDE ADJUSTMENTS IN FIELD USE – The antenna test pointed out an important requirement feature. A null must be maintained at all times in order to minimize the direct signal in the intruder receiver channel. Since the antenna receives energy over 220°, all nonmoving objects (including the ground) reflect back signals from directions not included in the null. We have been able to compensate for this miscellaneous multipath experimentally by over correcting the phase and amplitude controls. Basically, the total signal contribution by all nonmoving objects in the field (static clutter) produces a fixed phase and amplitude which may shift due to changes in weather. This static clutter can be cancelled by allowing a small portion of the direct signal to enter. The polarity and magnitude of the direct signal depend upon the amplitude and the phase shift controls. The pattern with the small bubble and the pattern with a shallow null actually produce "leak-through" signals of opposite phase (Figures F-5 and F-9). Phase changes within the bubble or shallow null are controlled by the tap adjustment.

It appears that the total static clutter may change drastically during rain. In order to maintain a constant 60 dB atttenuation an automatic control will be required.

2.3.2.9 AUTOMATIC NULL CONTROL OF RECEIVING ANTENNA – If the null is 20 dB when it should be 60 dB (assume infinity), then the energy in the antenna elements are unbalanced by 10%, A = B± 0.1B. In order to correct this, a change in the surge impedance Z_o, of the transmission line between elements A and B, must also change about 10%. The normal impedance Z_o is 108 ohms with a computed spacing 0.555 in.; a change in Z of ± 10% will change the spacing ± 5%.

However, the apparent impedance of the transmission line can be varied by the addition of a capacitor at the middle of the line, an eighth wavelength from each element. An eighth wavelength rotates the impedance 90°. The addition of a capacitor across one of the dipole elements will vary the phase angle as a function of the added capacitance.

A Smith chart computation was made; see Appendix F, Figure F-4.

As an example, assume an antenna element impedance Z_B to be 108 +J0, and a transmission line impedance, Z_o of 97.1; the transformation on the quarter wave line is 87.39 ohms. $[(97.1)^2/108 = 87.39]$. This can be found on the Smith chart by first normalizing all impedances from Z_o = 97.1 to Z_o = 1.0. Then, 108 +J0 = 1.11 +J0 located at point (a). The transformation occurs when (a) is rotated 180° a quarter wavelengh clockwise to (b), found to be 0.9 +J0. The midpoint of the transmission line, 90° clockwise or an eighth wavelength on the chart is found at point (c). The addition of a reactance of -J100 across will change the impedance to (d) 1 -J.09. Continuing toward

the feed point at element A, an eighth wavelength clockwise, will locate a point (e) 0.91 +J0. Multiplying the value by the normalizing impedance, $Z_o = 97.1$, we have 88.36 ohms. This is a change of 0.97 ohms (88.36 - 87.39) for an added reactance of 9,710 ohms (97.1 x J100) or 27.3 pF at 60 MHz. This change in transfer impedance of approximately 1% causes a change in contribution of power of 1% delivered to the feed point of antenna element B over A.

In a similar manner, the addition of a like reactance 27.3 pf (9,710 ohms) across element B rotates point (a) 0.014 wavelengths to a normalized impedance of 1.1 - J.02 at point (f). Adding the mid-line reactance to point (g) (0.975 - J.95) reduces the impedance to (h), 0.915 - J.8. The impedance when transferred to the feed point at A now has a normalized impedance of 0.915 + J.02 (j). The normalized impedance has had a change of J.02 from an input of -J.02. Thus, amplitude and phase are controlled by two reactances (capacitors), one at mid-line, and one at the end of the connecting transmission line.

In order to make these adjustments automatic, varactors are used so that control voltages vary the capacitance at the two control points. The control voltages are developed in the receiver output phase detectors. The receiver has a direct or reference channel and an intrusion signal channel. The intrusion signal channel will have an in-phase and quadrature phase detector referenced to the direct signal channel. The dc output from each phase of the detector represents the leak-through phase of the direct signal in the intrusion channel. These voltages amplified, scaled, and filtered, control the varactor diode capacitance. The feedback sense is such that the detected output voltages are driven to a minimum, the detected signal thus adjusting the antenna null to a minimum. If it should rain, causing the static clutter to change, it will be detected and corrected over a period of minutes. An expected time constant for such a change would be five minutes. A functional diagram of the automatic null control system is shown in Figure 24.

2.3.2.10 RECEIVING SENSOR COVERAGE AND DISTRIBUTION – A plot of the effective range of a receiving station using the two-element array with the null directed toward the receiving station is shown in Figure 25. The effective range pattern was then used to determine total coverage for 1, 2, 3, and 4 stations tracking an intruder within the 8 and 9 km zone. Figure 26 shows that a spacing of 450m requires 112 stations. Fair coverage is available for two-station coverage with 150m notches on the 9 km perimeter. Four-station coverage is small. Figure 27 shows a spacing of 450m, increased range of 1.1 km and 112 stations for the system. A further increase in signal level or sensitivity to increase the range to 1.35 km and an increase in spacing to 675m is shown in Figure 28; 75 stations are required for the system. Figure 29 shows coverage for two stations spaced 600m but with an increase in range to 1.1 km; 84 stations were required for the system.

Placement of the receiving stations other than on the 8 km perimeter is not possible since the back lobe (null) reduces the range toward the transmitter. In addition, the doppler is practically zero for an intruder since the isophase lines run parallel to the major ellipse axis.

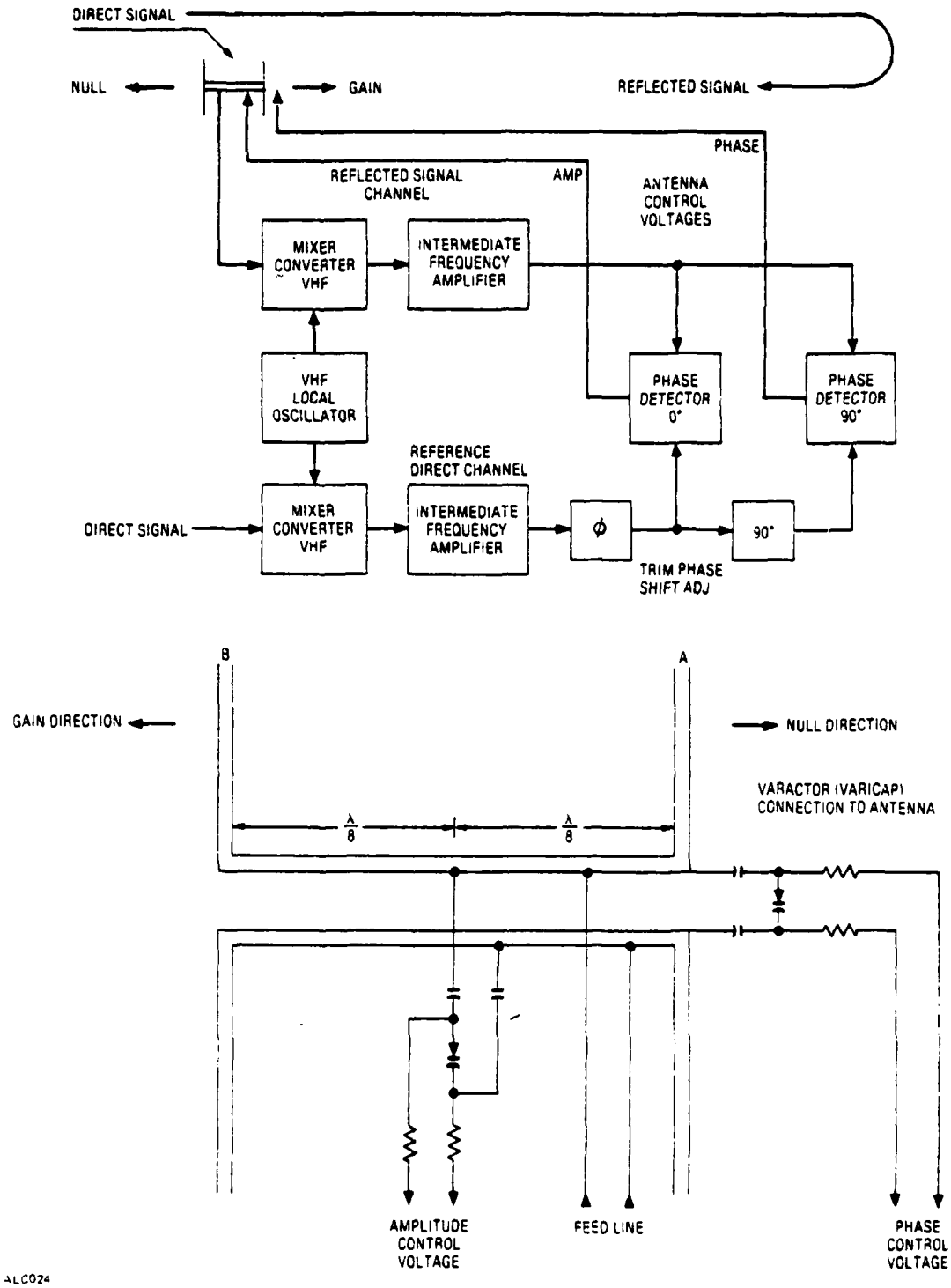

Figure 24. Antenna Null Control, Functional Block Diagram

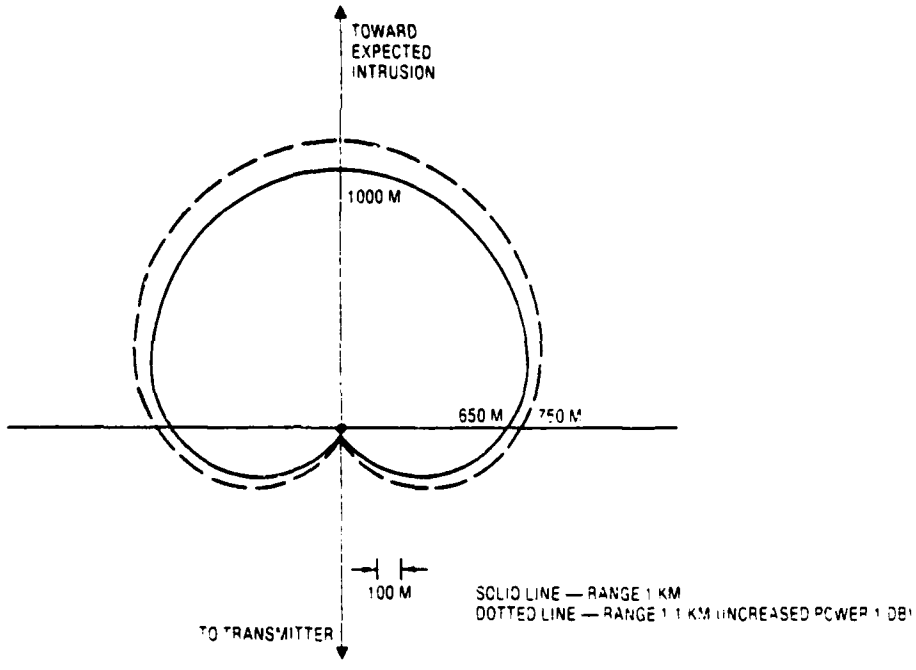

Figure 25. Sensitivity Plot for Receiver and Receiving Antenna

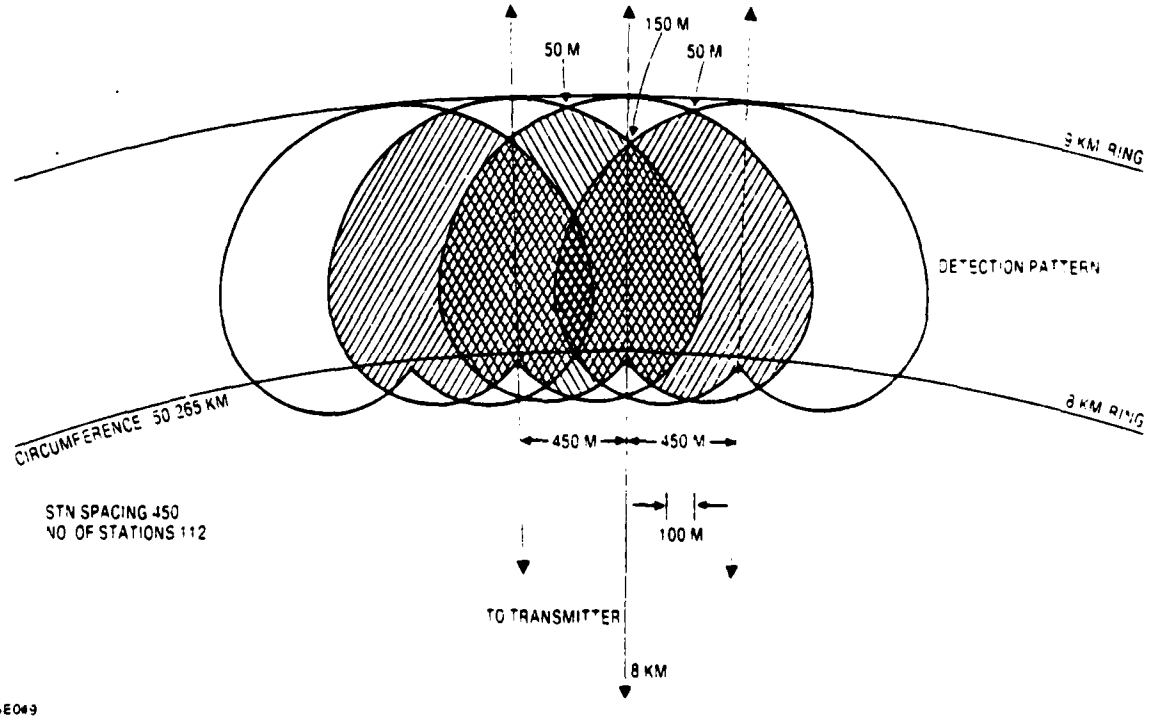

Figure 26. Multiple Receiving Station Plots Showing Single, Dual, Triple, and Quadruple Coverage Detection Areas. Range Limited to 1 km. Station Spacing 450m. Number of Stations: 112

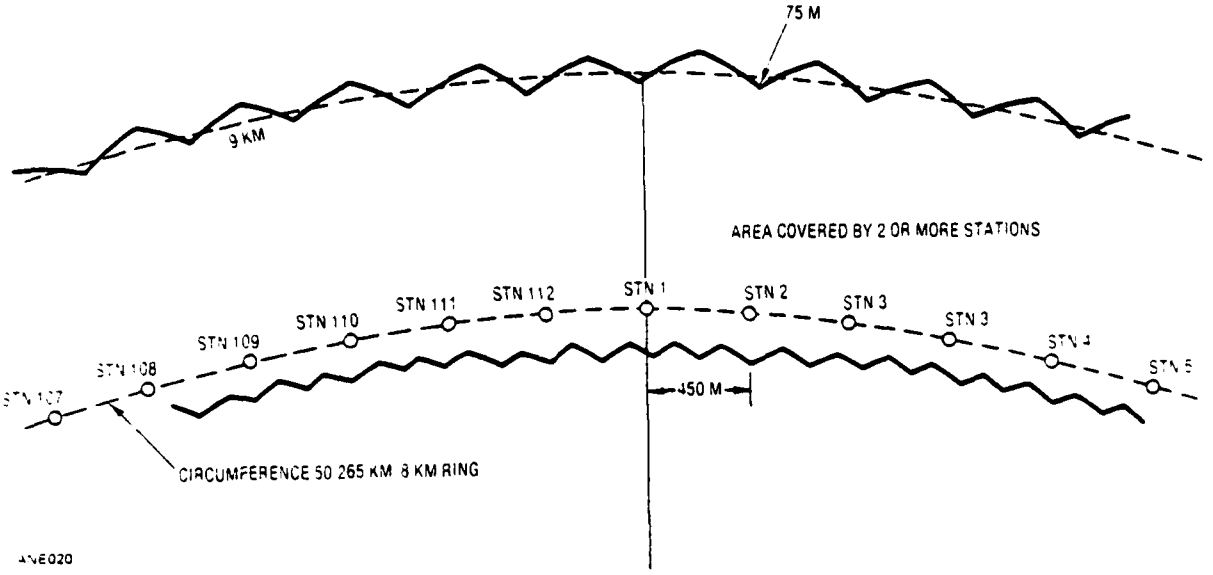

Figure 27. Multiple Receiving Stations Area Coverage for Two Stations. Range Limited to 1.1 km. Station Spacing 450m. Number of Stations: 112

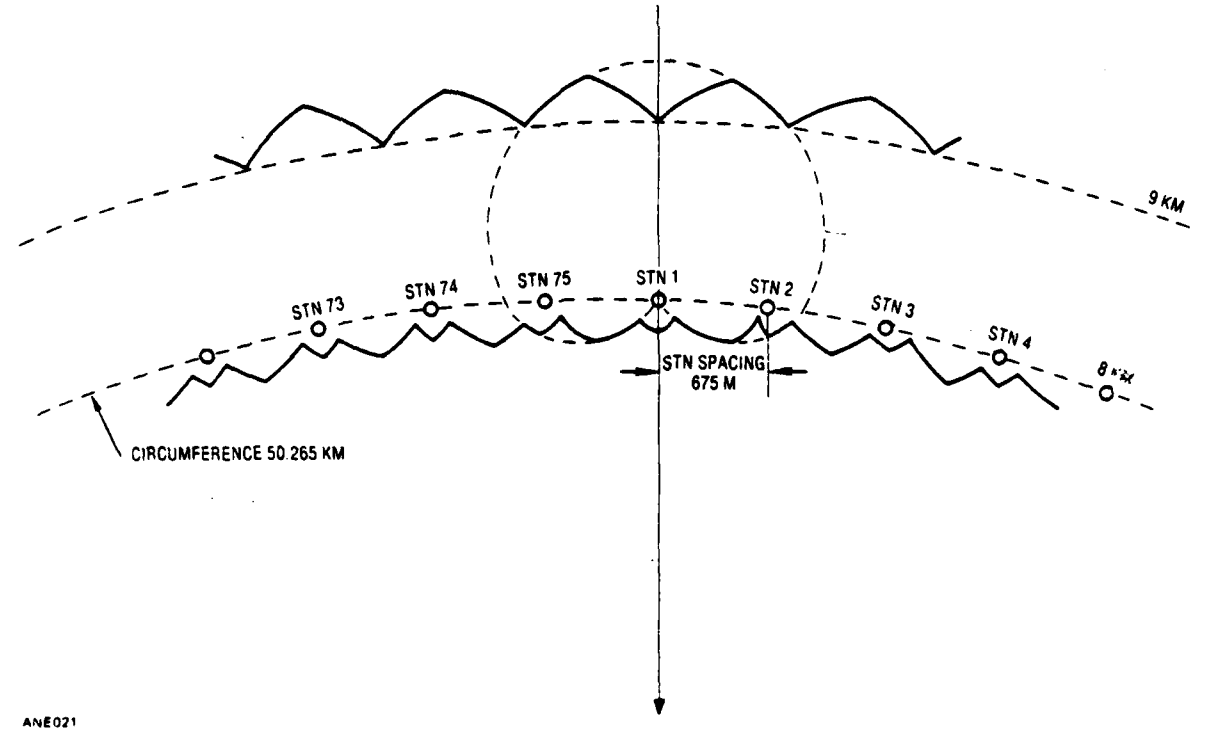

Figure 28. Multiple Receiving Stations Area Coverage for Two Stations. Range Limited to 1.35 km. Requires +2.6 dB Increase in Sensitivity. Station Spacing 675m. Number of Stations: 75

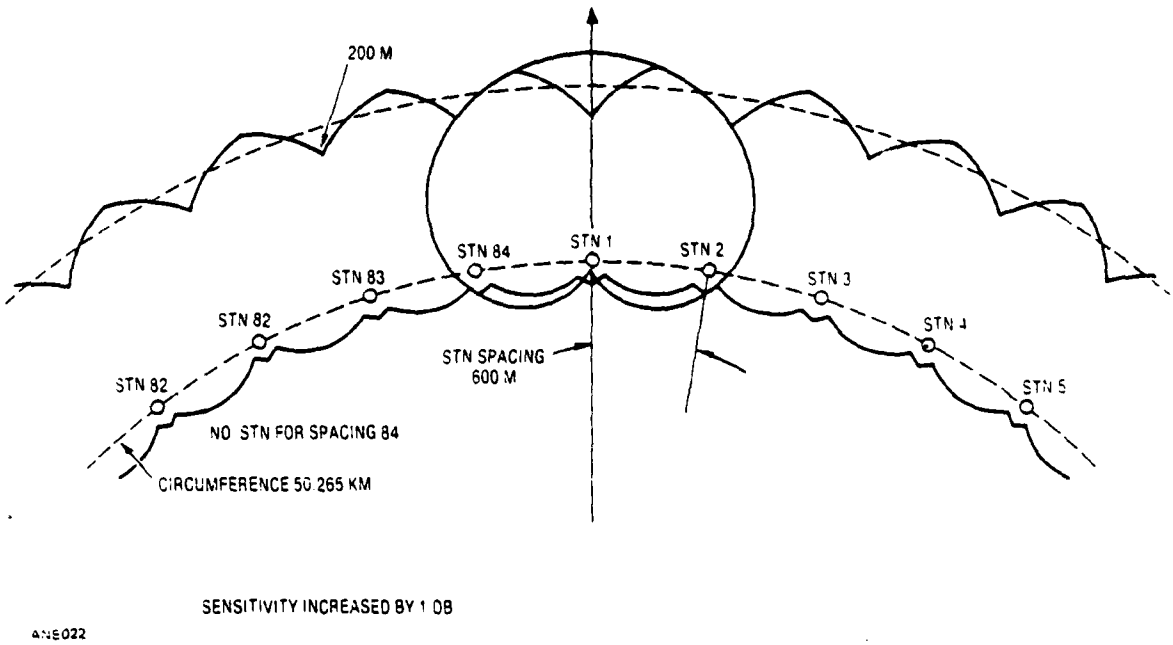

Figure 29. Multiple Receiving Stations Area Coverage for Two Stations. Range limited to 1.1 km. Station Spacing 600m. Sensitivity Increased by 1 dB. Number of Stations: 84.

By using the data from Figures 25, 26, 27, 28, 29 and other data, maximum intrusion range in terms of transmitter power is plotted against the number of system stations required for 100% coverage of the 8 to 9 km zone. It appears that a 20 to 40 watt increase in power at the transmitter will reduce the system station requirement from 120 to 30.

It should be noted that further reduction of the number of system stations is limited by multiple intrusion isolation. Doppler information at any one station is the sum of all intrusions within the station's range. In order to isolate one intrusion from another each intrusion must be handled by another pair of receiving stations. Therefore, the greater number of stations with limited range can better isolate intruders. Note from Figure 30, 90 watts will require 15 stations and be able to isolate 7 intrusions; 20 watts will require 120 stations and isolate up to 60 intrusions simultaneously. Multiple intrusions detected by a receiving station combine the intrusions into a single target.

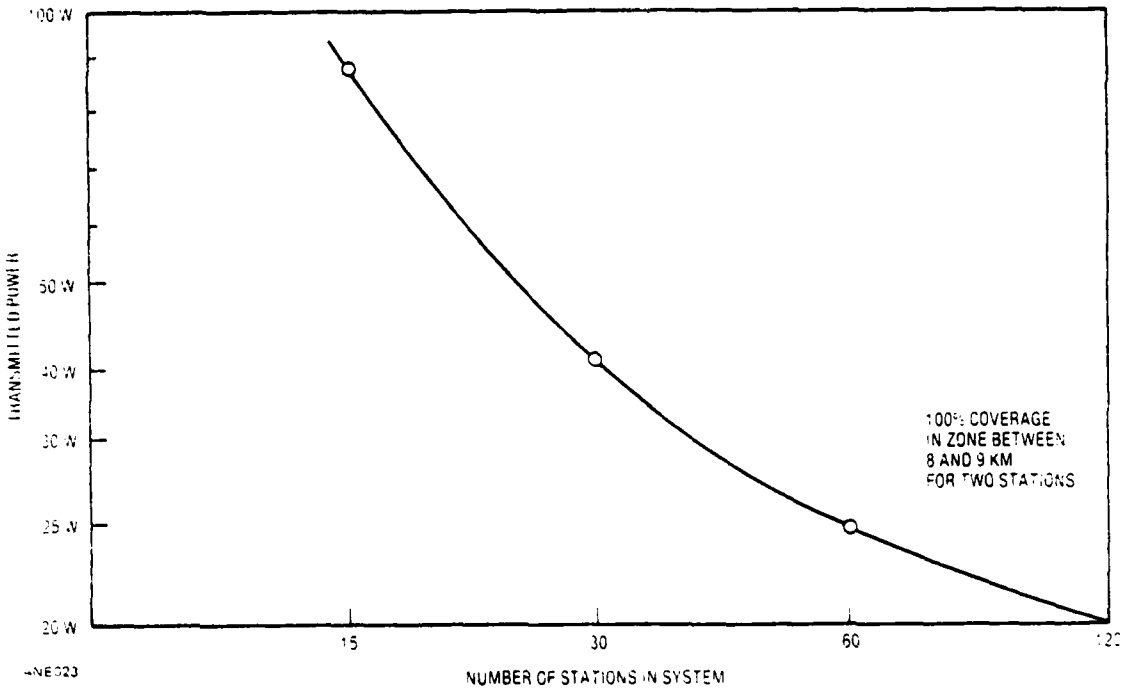

Figure 30. 100% Coverage Dependent on Power Transmittal and Station Numbers

2.4 DATA LINK

A more detailed discussion of a data link may be found in General Dynamics Electronics Division 1979 IRAD Report, Security Systems Development.[16] This IRAD investigated the problem of netting a large number of sensors and means to implement it.

The data to be transferred to the central computer for computation of the intrusion track and final displays consists of the individual addresses of each receiving sensor, the doppler sense and differential doppler phase. Two additional data items may be required: time and the number of accumulated doppler cycles between transmissions. Time generally will not be required since a transmission will be quick and time could be added at the computer if required. Timing of each doppler cycle would be required if the Kalman filter technique of tracking is used. The incremental tracking or doppler ranging scheme does not require time in its computations. The doppler received from intruding vehicles at 60 MPH could be as much as 10 doppler cycles per second. In order to limit the data rate transmitted, doppler in excess of 1 per second would be accumulated by counting cycles. After 1 second, the doppler count would be dumped and the count

[16]John B. Gehman, Security Systems Development, R-79-083; General Dynamics Electronics Division, December 1979.

number transmitted. Differential doppler phase data would only be necessary if the doppler ranging technique is used.

A pulse code scheme was selected over a multifrequency type since this type can accommodate a large number of sensors and data in its format. In our 1979 IRAD report a "CMOS IC", "ED-15" manufactured by Supertex was used for coding and decoding a 15-bit manchester NRZ code format. The chip permits pulse repetition rates of 0.01 Hz to 25 kHz. The chip also has a transmit-receiving function controlled by a "1" or "0" on the IC chip; this permits a self-test mode, identified by the sensor address. In the system described in the report a double code burst was used. The first burst 15 bits (32,768 selections) was used to identify the system and used a pseudorandom code, the second burst provided address and data. See Figure 31. The pseudorandom code (PRC) identification was necessary for an RF data link which may be subject to interference; the PRC eliminates any interfering repetitions code from entering the system.

Three types of media were considered to be used for the data link; wire, RF, and optical (fiberglass).

RF is probably the least costly to install, but it is subject to interference since data links are relegated to specific frequencies by the FCC; these frequencies usually have many users. Wire and optical links must be installed, either underground or on poles. Underground is the safest but most costly; the pole mounted is subject to weather problems. The optical links have the least interference cross talk and can be used in

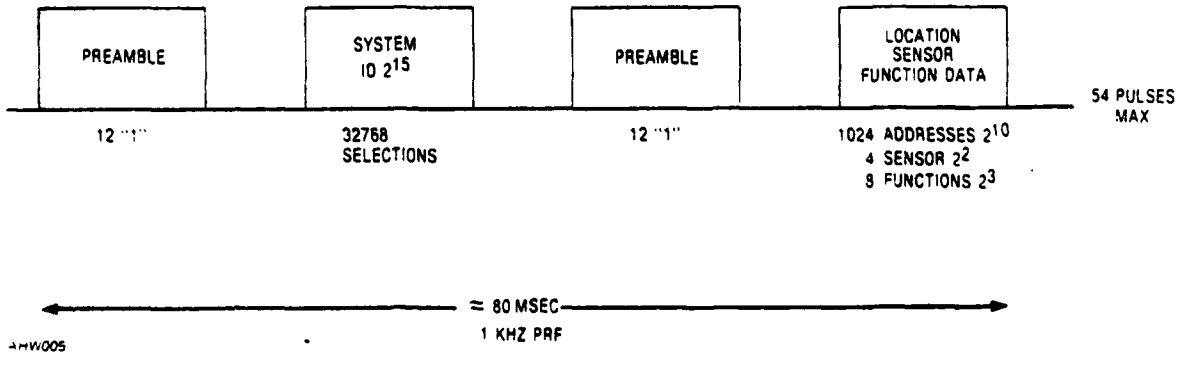

Figure 31. Code Format, Two Bursts

areas of high electrostatic and magnetic field activity. The wired system has the main advantage of being bidirectional. When using the ED15 transmission and reception is made on a single line pair to all sensors operating on a party line. Wire links have a problem with limited bandwidth which will determine the pulse repetition rate (prf) of the code. A 1000 prf was selected and tested over a 1 to 2 mile line.

The wired system would be a good choice since the line pair can also supply the power necessary to operate both the data link and the receiving sensor along with the data link transmission. It would be expected that self-test signals could interrogate each sensor to determine if it still functions.

The coding format provides 15 bits for address, and data. We could expect to use up to 128 receiving stations which would use 7 address bits; 1 bit to indicate doppler sense; 7 bits for differential phase measurements. The differential phase measurement represents 1500m (N=600) along the major axis; and therefore the 7 bits provide 11.7m increments (N = 4.7). If the peripheral stations are divided in half or quarters with separate lines brought into the central computer less bits would be required for the address. Probably the best arrangement would be to have all stations on the party line with multiple lines coming back to the computer to provide redundancy in case the lines are broken. If more data is required or more stations are needed, a double burst code could be used providing a 30-bit code.

The time to transmit a burst is approximately 25 milliseconds which also includes a short preamble burst for synchronization. A double burst requires 60 milliseconds prf is 1000).

At 25 to 60 milliseconds and at expected intrusion speeds of 2.5m in 2.5 seconds (1 doppler in 2.5 seconds), there is a 1-in-40 to 1-in-100 change for codes to overlap between responding pairs. To eliminate this chance happening each data link will be in a receiving mode until it has data to transmit. This is also necessary in order to receive self-test commands. If data is being transmitted by another link, a subsequent transmission by another link will be delayed until the line is free.

Block diagram of a coder, decoder and coder-decoder is shown in Figures 32, 33, and 34. These block diagrams show a pseudorandom code identifier which could be easily used as the address code for each sensor. If the decoder is used (Figure 33), separate decoders would be used for each sensor at the computer center; however, it is expected that the computers will provide the decoding function, decoding up to 128 addresses and routing the data from each sensor station.

The Coder-Decoder in Figure 34 is basically an encoding device that has receiving capabilities. It consists of same blocks that the Coder has (Figure 32) but has an additional switch and connections to the code IC. The ED-15 is set in a receive mode. Upon receiving the system code and the location code, two pulses are generated from the ED-15 which constitute a self-test command output. If a sensor responds, the normal receive mode is switched to transmit. The function ROM provides the ASCII code and initiates switching action between the pseudorandom code, the location code, and the receive/transmit function. R-C values control transmit/receive pulse repetition rates.

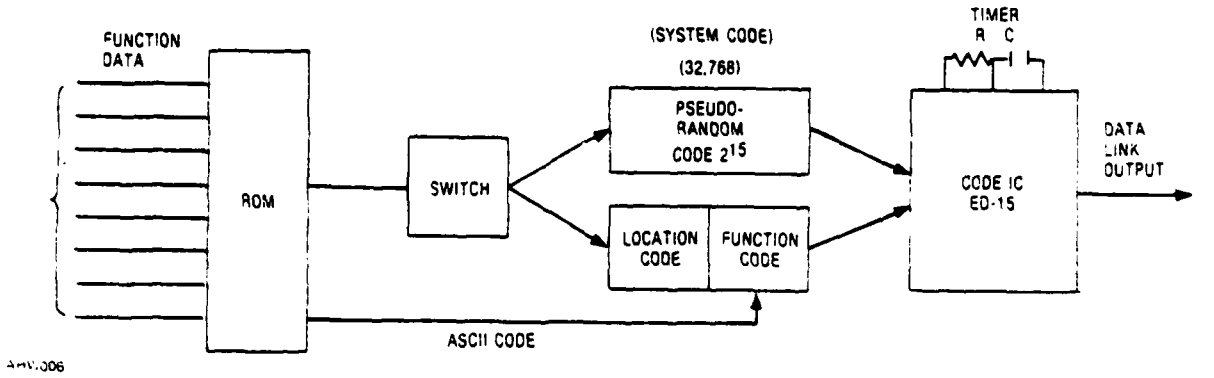

Figure 32. Coder

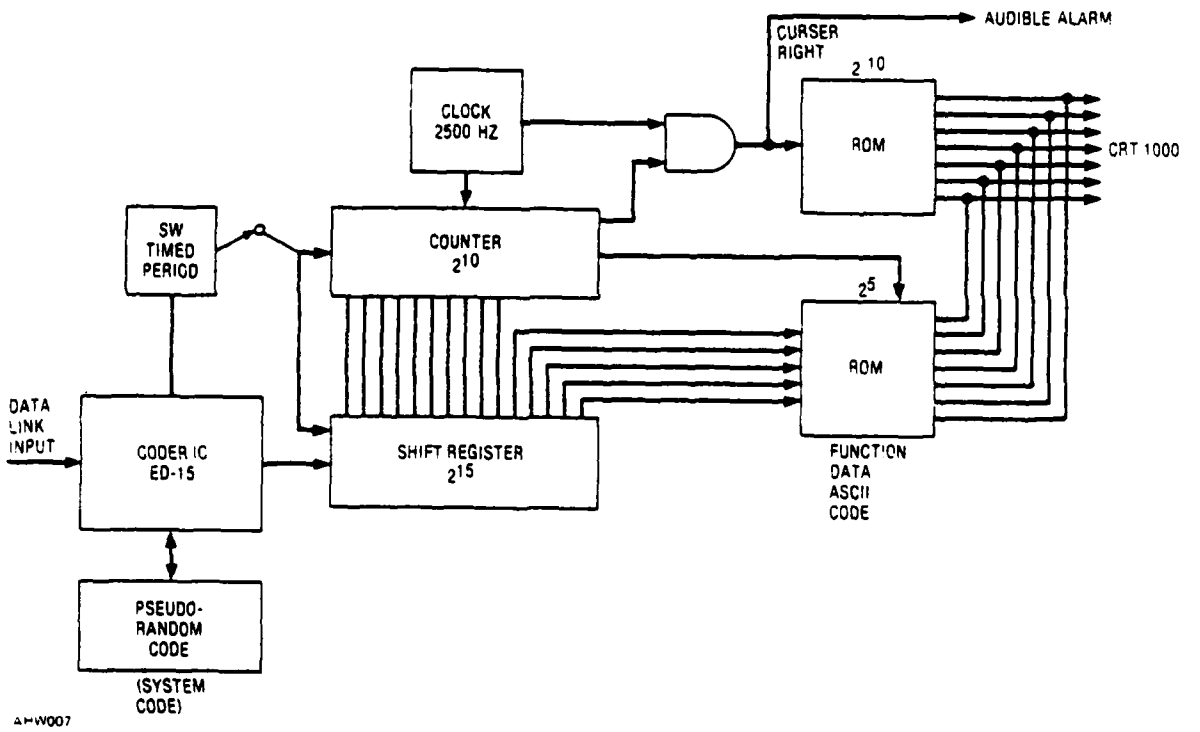

Figure 33. Decoder

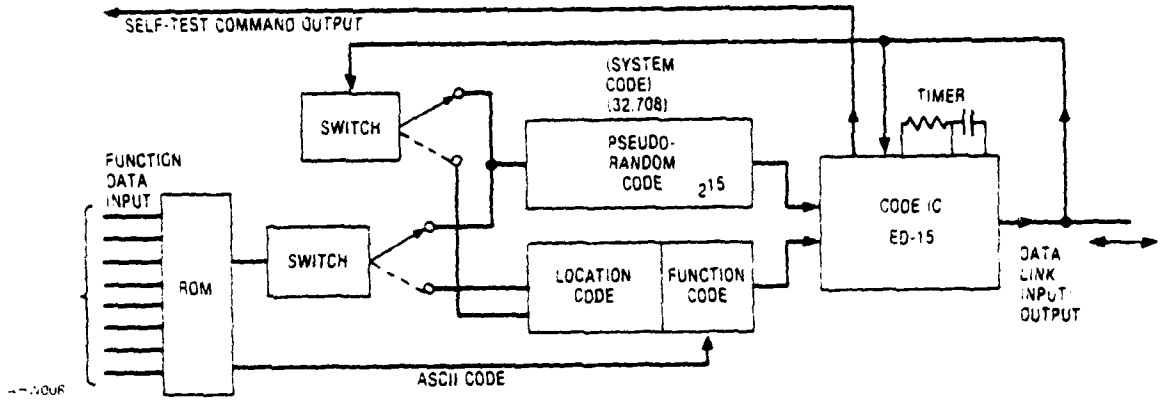

Figure 34. Coder-Decoder

Specifications for coder, decoder and combined coder-decoder are shown in Table 11. The values shown would also be valid for the Area Intruder Track equipment. Figure 35 shows the wired data link with power and redundant connections.

2.5 TRANSMITTER

Computations show that 20 watts radiated from a high gain antenna should provide the necessary operational signal level in the surveillance area. A single 60 MHz CW is used. The transmitter frequency control should be stable, variations should be less than 1 Hz per minute, and controlled within 1000 Hz of the assigned frequency. Noise on the carrier, AM or FM should be 50 to 60 dB down from the carrier. Depending upon the coaxial cable to feed the antenna (which is 85 ft high needing at least 100 feet of coax), it is expected to have a loss of 0.3 to 1.5 dB (RG 267U, 0.32 dB/100 ft; RG 17/U, .78 dB/100 ft; RG-8U, 1.48 dB/100 ft). If RG 17/U was selected, the transmitter would be required to have an output of 24 watts to radiate 20.

Transmitter power from 20 to 100 watts at 60 MHz should be quite available commercially. A special frequency control might be necessary to obtain the required stability but with not too much difficulty.

If the dual doppler system is used, two CW signals must be radiated approximately 100 kHz apart. Two separate transmitters of 20 watts each fed to a multiplexer to add the signals to the antenna feed could be used with a special frequency controller. The controller is similar to the single doppler control oscillator device and would be modulated by 100 kHz, the carrier and one sideband would be extracted to provide the control frequencies for the transmitter. The 100 kHz would be generated by a count down from the 60 MHz carrier.

This method is necessary to provide coherence between the two frequencies so that there is no phase drift due to slight variations in frequency. Figure 36 shows the dual channel CW transmitter block diagram.

Table 11. Specifications for Coder, Decoder, and Coder-Decoder

CHARACTERISTIC	CODER	DECODER	CODER-DECODER
Input Impedance	290 k	1 M min.	500 k
Input Voltage for Operation Vcc = +6 Vdc	4.0V min.	4.0V min.	4.0V min.
Output Impedance	550	–	400
Bias Current Vcc = +6 Vdc	1.4 A standby 2.0 mA transmit	0.46 mA standby 0.60 mA decoding	1.2 A standby 4.0 mA transmit
PRF rate variable, .01 Hz to 25 kHz	1 kHz nominal	1 kHz nominal	1 kHz nominal
Clock Frequency	2500 Hz	2500 Hz	2500 Hz
Processing Time	110 ms	90 ms	110 ms
Inputs	6 Alarm Functions 2 Alarm Total 10 Location Selections	Data Words from Coder or Coder-Decoder	6 Alarm Functions 2 Alarm Total 10 Location Selections Self-Test
Outputs	2 Data Words: 1. Pseudorandom Code 2. Address, Function, Total	ASCII code for Address, Function, and Number in serial order	2 Data Words: 1. Pseudorandom Code 2. Address, Function, Total Self-Test Command

Common Characteristics:

1. Pulse Code: NRZ Manchester Type
2. Code Selection: $2^{15} = 32,768$
3. Plug-in IC for pseudorandom code (system ID)
4. Data Word Format: Word 1. Preamble of 12 "1's" followed by 15-bit pseudorandom code ID
   Word 2. Preamble of 12 "1's" followed by 10-bit address (1024 locations), 3-bit alarm function, 2-bit alarm total

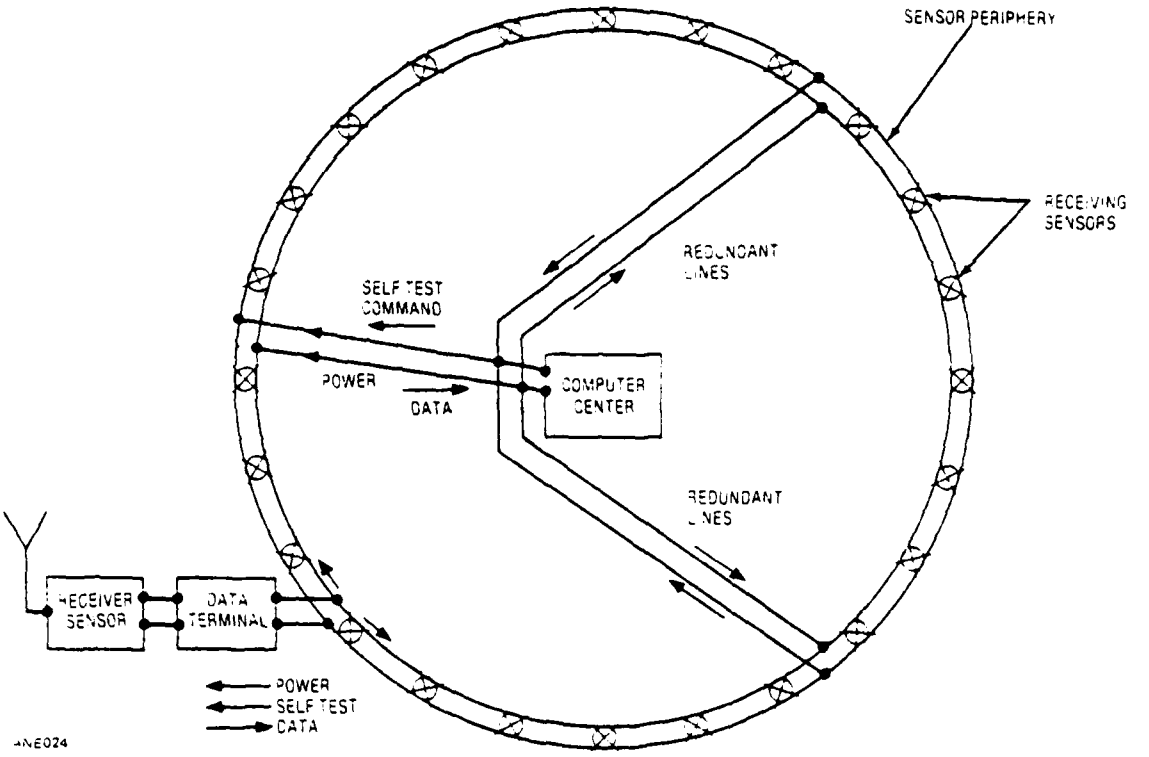

Figure 35. Wired Data Link with Power and Redundant Connections

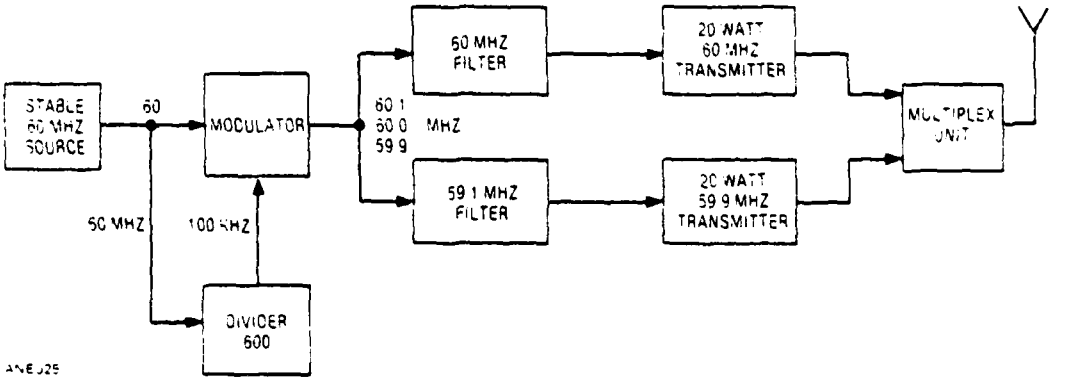

Figure 36. Dual Channel CW Transmitter Block Diagram

2.6 RECEIVER

As mentioned previously multiple receiving sensors are used to detect reflected signals generated by intruders entering a 1 km zone, 8 km from a central location. The receivers compare the direct signal from an illuminating transmitter and reflected intruder signal which produces a rotating phase vector, a doppler. Multiple receivers located on the 8 km perimeter provide a much larger signal from the intruder than that possible if it were located at the center. In addition, the multiple receivers also provide the means to track a moving target by comparing signals from each receiving sensor and computing the reflected signal's origin.

The receiver has two basic elements: a detection-phase comparison component, and a detection signal processor. The detection signal processor also has two sections, one to receive the reflected intruder signal, the other to receive the direct transmitted signal. The two signals are compared to obtain a varying phase output. The detected signal processor measures the rotating phase vectors, determines its polarity and continuity, and rejects discontinuous or oscillating motions. Each cycle is counted and formatted for data link transmission.

An optional system was considered which will use two frequencies - 50 kHz to 100 kHz apart at 60 MHz. The purpose is to obtain two doppler signals which, when compared, will provide a measure of range from each receiving sensor. Each receiving section, i.e., direct and reflected signals, is a dual-channel device, demodulating both VHF signals. This actually requires four VHF channels.

2.6.1 RECEIVER FUNCTIONAL DESCRIPTION

A block diagram of the multichannel RF and signal processor section is shown in Figure 37. Figure 38 shows a simplified diagram of how the dual-frequency doppler system functions. Its inputs come from two separate antennas. The reflected signal comes through the antenna described in section 2.3.2; the direct signal comes via a simple short rod located away from the special nulling antenna. The expected signals to the receivers are -150 dBm (intruder) and -50 dBm (direct). If the range option is considered, two frequencies 100 kHz apart are processed, such as 60.0 and 59.9 MHz. The signals are mixed and amplified with each section providing a 100-kHz output. The reflected signal, when compared with the direct, will have a phase relationship which varies from 0° at the receiving site to 360° (one cycle) at 1500m (measured along the major axis). At angles off the major axis, the range for 360° change in phase is greater. Two explanations can be used to visualize the operation of the phase range measurement. (1) Consider the doppler resulting from motion along the major axis (in line with receiver and transmitter at 60 MHz and 59.9 MHz; a doppler cycle will be generated every 2.5m at 60 MHz and 2.5041736m at 59.9 MHz. The two dopplers will be in phase at the receiving site and depart in phase as range increases. At 750m, there will have been 300 doppler cycles generated by 60 MHz, and 299.5 cycles by 59.9 MHz; they will be 180° out of phase. At 1500m, the two dopplers will be in phase, the 60 MHz doppler gaining one cycle in the 1500m. Therefore, the measurement of the difference in doppler phase between the two signals will indicate the number of doppler cycles between the intruder and the receiving site. (2) Another method of visualizing the system is to consider the difference frequency, 100 kHz (60-59.9), as the transmitted carrier or modulation on

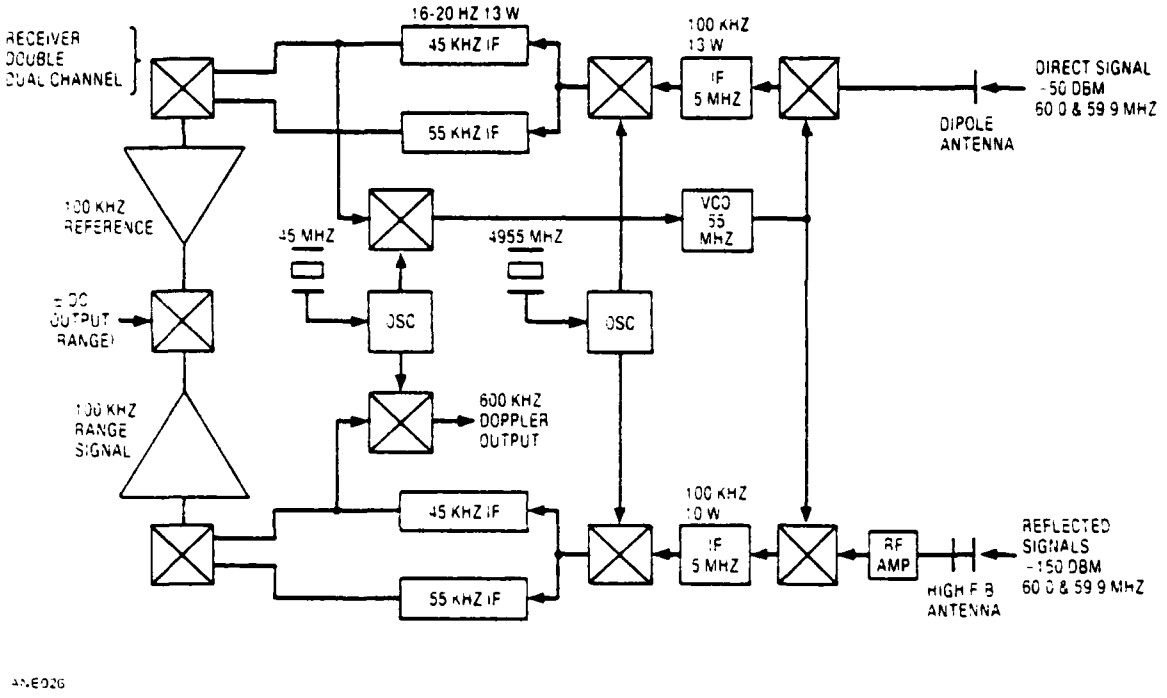

Figure 37. Multichannel RF Receiver

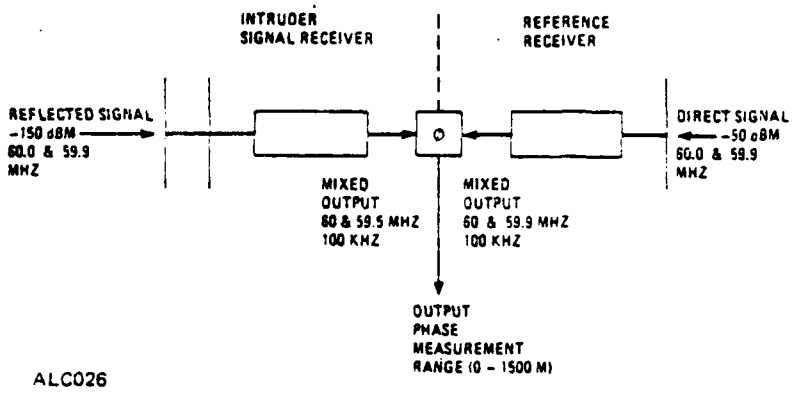

Figure 38. Dual Frequency Doppler System

60 MHz. Either way a doppler cycle is generated every 1500m. Therefore, the measurement of phase within 1500m is unambiguous. The cycle repeats every 1500m. In both cases the actual range varies off axis, but each doppler cycle has a geographic location relative to the transmitting and receiving site. When two such stations have intersecting cycles the intruder can be specifically located. Without a starting location or a method of specifying which doppler cycle is being received, whereas only the distance traveled can be computed from the basic single frequency scheme.

Figure 37 shows two inputs, i.e., two separate antennas. The reflected intruder signal is amplified by a low noise amplifier. Both signals are mixed and converted to 5 MHz by a common local oscillator at 55 MHz; 60 MHz becomes 5.00 MHz, and 59.9 MHz becomes 4.90 MHz. Both 5.0 and 4.9 MHz are amplified through filters and reconverted by a common oscillator, 4.955 MHz, to 45 kHz and 55 kHz. Very narrow-band filters (2.5-Hz wide) are used in this low frequency IF amplifier. This is accomplished in both the direct and reflected signal sections of the receiver. The outputs from the 45-kHz channels are product-detected (zero IF conversion) by a common 45 kHz oscillator. The dc output from the direct channel signal is amplified, filtered, and fed back to the 55-MHz local oscillator. The 55-MHz oscillator is voltage-controlled and will be phase-locked to the input direct signal. The common oscillator's 55 MHz, 4.955 MHz, and 45 kHz, and the phase-lock scheme provide a coherent detector for the reflected signal. The 45 kHz and 55 kHz can be recombined to produce 100 kHz. Each output (direct and intruder signal) can then be compared in a product detector (phase detector) whose output will be dc. Assuming the 100-kHz signal is limited, the dc level will be a measure of range specifying an ellipse which is a locus of constant phase difference about a receiver and transmitter.

PROBLEMS AFFECTING DESIGN – The study indicated two areas of improvement necessary to produce a suitable receiver.

(1) The direct signal feed-through is a problem. Computations show 100-dB difference between the reflected intruder signal and the direct signal. By using the nulling antenna, 60-dB attenuation of the direct signal could be realized leaving about 40 dB coming in to the intruder channel. The direct signal, a fixed-phase signal with a small intruder signal riding on top of it, results in a large signal with a small oscillating phase of $1/2^{\circ}$. The intruder signal can only be recovered as amplitude modulation, "in-phase" with the direct signal, thus eliminating the possibility of determining sense. Therefore, it is necessary to remove 40 dB or more so that the intruder signal is larger than any leak-through signal. A synchronous filter was suggested.

(2) A study of the original receiver concept resulted in an improved system which would tend to cancel carrier noise. Instead of a common 45 kHz LO to demodulate both the direct and reflected signals, the direct channel signal is used to demodulate the reflected signal; a separate 45 kHz LO demodulates the direct signal to provide phase lock VXCO control. A wideband amplifier would have greater capture bandwidth and a shorter lock-up time. The direct signal demodulates the intruder signal allowing all noise signals common to both channels to cancel. A block diagram of this configuration is shown in Figure 39.

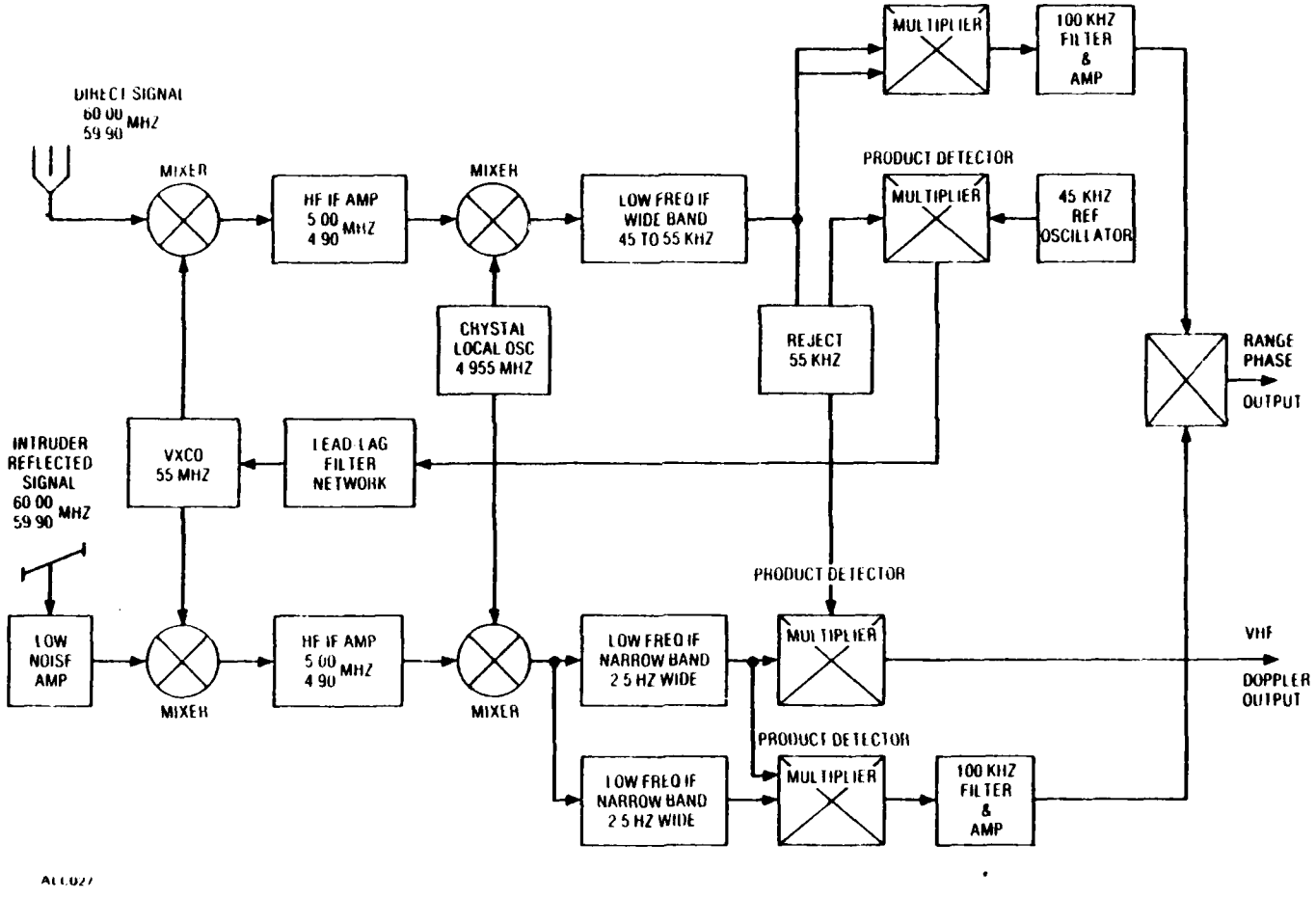

Figure 39. Dual Frequency, Dual Channel Receiver Block Diagram

2.6.2 RECEIVER DESIGN

Construction of a number of breadboards was started on the GDE-sponsored 1980 IRAD program. It consisted of a dual-channel (two-frequency) single section representing the direct signal portion (reference channel) of the receiver. The dual frequencies were set 67.89 kHz apart to accommodate crystal filter availability; they had originally been discussed as being 100 kHz apart. The breadboard design was not completed; it required closing the feedback loop on the VHF local oscillator and was held up in favor of development work on a tracking synchronous filter.

2.6.2.1 VHF FRONT-END DESIGN – The front-end design consists of an active mixer, a VXCO, and a variable crystal local oscillator for the reference channel. An added stage, a low-noise amplifier (LNA), is used in front of the mixer for the reflected intruder signal section.

A 40673 FET was used as an active VHF mixer. The schematic is shown in Appendix H, Figure H-2.

A stable crystal voltage controlled oscillator, VXCO, was used to drive the VHF mixer. A schematic of the circuit is shown in Appendix H, Figure H-3. Current drain is approximately 2.5 mA at 6V.

The total variation in frequency for a 6V change in control voltage is +1360 Hz. The control is nonlinear, following a hyperbolic function typical of the varactor (IN5461). The variation is adequate and necessarily restrictive since the tracking of the input signal must be held to less than 1 Hz.

An LNA is shown in Appendix H, Figure H-4.

A 3N159 FET replaced a 3N200 with a noise factor of 2 dB.

Total noise factor with contribution of mixer noise is given by

$$F = F_1 + \frac{F_2 - 1}{G_1}$$

F_1 = 2 dB = 1.5849 power ratio

F_2 = 3.4 dB = 2.1878 power ratio

G = 23 dB = 199.53 power ratio

F = 1.5908 = 2.016 dB

Overall noise factor is computed to be 2.016 dB. This assumes no contribution to the noise by the image frequency. This is made possible by the use of a tuned trap to the image frequency (55 MHz) coupled to the output of the LNA circuit. Power is transferred from the LNA to the mixer tuned circuits by a single turn link. Q of these circuits is about 15 to 30 loaded.

2.6.2.2 HIGH FREQUENCY IF SECTION – The high frequency IF section receives the converted 60.0 and 59.993 MHz as 5.000 and 5.067 MHz. These two frequencies are amplified by a dual-channel IF. The two frequencies are further converted in a mixer to two lower frequencies, 33.36 kHz and 34.53 kHz, by a 5.035-MHz crystal local oscillator.

Figure H-5, Appendix H, is a schematic of the high frequency IF. The high frequency IF consists of a separate crystal filter stage which uses a 2N930, a unity gain phase splitter. The emitter of 2N930 drives two crystals (5.000 and 5.067 MHz); the crystal capacitance is neutralized by a variable of 60 pF capacitor. A small trimming capacitor is added in series with the 5.067-MHz crystal for moving the resonant frequency a few hundred hertz in order to match the subsequent low-frequency filters. Another 2N930 is used to impedance match the crystal filter output to the high gain "IC" amplifier. The gain of the 2N930 pair is 10 dB. The 3-dB bandwidth is 900 Hz at each frequency. An MC1950G provides up to 50 dB of gain with an AGC (automatic gain control) range of 60 dB (6 to 9V). Maximum output from the MC1590G is 2.5V RMS. The 2N930 requires 1.5 mA at 6V while the MC1590G requires 15 mA at 12V.

A crystal oscillator shown in Figure H-6, Appendix H, drives a SRA-1 mixer. The SRA-1 is a commercial diode ring mixer made by MINI-CIRCUITS. It has a 6-dB conversion loss in converting from 5 MHz to 33 or 34 kHz. The crystal oscillator uses a 2N918 in a modified Colpitts circuit. The crystal is operated between base and ground. A 60-pF trimming capacitor is used to adjust both converted frequencies. The circuit requires takes about 2.5 mA at 6V.

Crystals for the high frequency IF filter and its local oscillator had to be moved on frequency since those which were available were 1 to 5 kHz off frequency. The crystals were reground using aluminum oxide No. 302. Final frequency was set to within 100 Hz where the trimming capacitors could make the further adjustment to 1 Hz.

2.6.2.3 LOW FREQUENCY IF SECTION – Two parallel IF amplifiers were made, one at 33.36 kHz, the other at 34.53 kHz. The circuit is similar to the crystal circuit used at 5 MHz, except for using a single frequency response and 2N2222s instead of the 2N930s. The circuit phase splits the input, drives the crystal from the emitter, and neutralizes the crystal holder capacity by a 60-pF capacity connected to the collector. The second 2N2222 provides impedance matching and 18-dB gain. Figure H-7, Appendix H shows the frequency response of these parallel IF stages.

Two MC1596 multiplier ICs are used to mix the 33.36 kHz and 34.53 kHz upward to 67.89 kHz and mix the 34.53-kHz downward to zero (product detector). The up-converter, MC1596, actually produces 1.17 kHz as well as the 67.89 kHz, but it is easily filtered in subsequent circuits. The down-converter, MC1596, acts as a well-balanced product detector with a dc output representative of the phase difference between the incoming signal and the reference oscillator. The reference oscillator consists of an LM358 and a buffer FET amplifier 2N3823.

In order to stabilize the feedback, the connection to the 65-MHz VXCO requires a filter to provide the proper lead-lag and gain network.

2.6.2.4 SIGNAL-TO-NOISE RATIO – From the Signal Budget, Table 10, the signal levels have been computed and verified by tests. Three RF bandwidth were assumed for determining the noise power developed at the input. These widths were 2.5 Hz for man-

type targets, 15 Hz for vehicle type targets, and 50 Hz for aircraft (helicopter). An expected receiver noise factor of 2 dB is used.

Noise Power

BW 2.5 Hz	-168 dBm
BW 15 Hz	-160 dBm
BW 50 Hz	-155 dBm

Signal-to-Noise

Rec. Signal	(Man) 151.5 dBm	16.5 dB
	(Vehicle) 150.5 dBm	9.5 dB
	(Aircraft) 136.5 dBm	18.5 dB

2.6.2.5 SYNCHRONOUS FILTER – When an investigation was made of the intruder signal parameters, it was found that although the direct signal was attenuated 60 dB by the receiving antenna, 40 dB of direct signal remained. This residual signal could prevent a variable phase measurement of the intruder signal. A tracking filter was considered and breadboard circuitry tried to determine the practicability of removing the leak-through signal.

The basic logic for this signal cancellation circuit is shown in Figure 40. The interfering signal and the data signal are applied to a summing circuit; the interfering signal has a constant amplitude and phase. Both signals pass to the output through a bandpass filter. A very narrow bandpass filter permits only the interfering signal to pass. The output will be phase-inverted (assuming no other phase shift) to cancel out the input signal at the summing amplifier. Since this is a feedback circuit the degree of feedback determines the degree of cancellation. Therefore, 40 dB of cancellation requires 40 dB of feedback. Since the IF frequency involved is 34 kHz, and the changes in amplitude must be less than 3 dB in a minute, the Q of the filter would be in excess of 2,000,000. A tracking-synchronous filter can achieve this.

The operation of a synchronous filter is shown in Figure 41. A multiplex switch samples the incoming signal in eight samples per cycle; the sampling rate is phase-locked to the input frequency. Each sample will monitor a specific phase which will have a specific dc average value for a steady signal. Variations in the input signal are filtered out depending on the time constant of the RC network. The output switch is synchronized with the input frequency and selects the potential of each phase, reconstituting the steady state input frequency.

The output, although highly distorted, contains all the fundamental energy of the input wave. This signal is phase-inverted and added to the input signal cancelling the fundamental; the stairstep distortion products are removed in the following bandpass filter. Varying signals are not cancelled since they were not accepted by the RC network. The RC time constant will be reduced by the feedback ration, i.e., 40 dB will reduce an RC TC of 10 sec to 0.1 sec. It will be necessary to increase the RC TC to 1000 sec to maintain an overall 10 sec response.

A test circuit was made to determine the degree of cancellation obtainable (see Appendix H, Figure H-8). The input signal, V_{in} at 33 kHz, was phase-locked by a

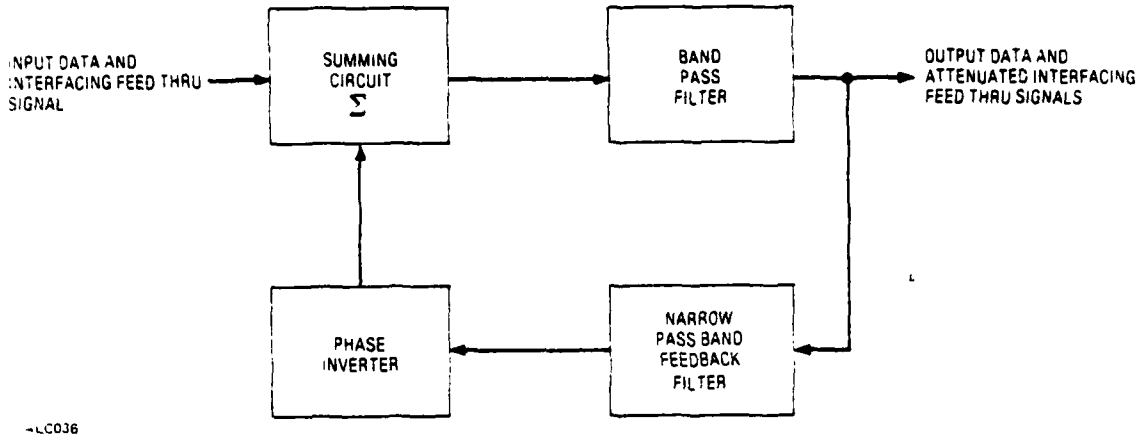

Figure 40. Information Flow for Interfering Signal Cancellation

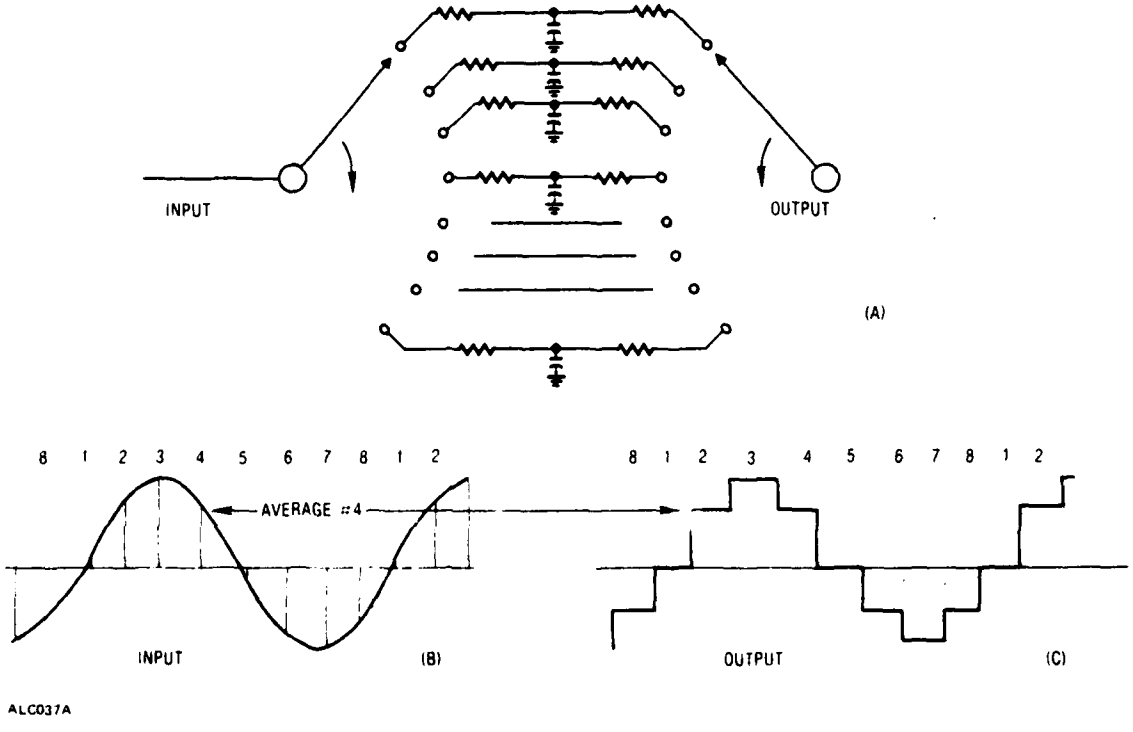

Figure 41. Operation of a Synchronous Filter

CD4046B operating at 264 kHz (8 x 33). The 264 kHz was divided by 8 in a CD4024 binary counter and fed back to the phase-locked IC, U_1 (CD4046B). The CD4024, U_2, produces outputs of 132, 66 and 33 kHz which are used to key a multiplex-demultiplex IC, U_3 (CD4097B). The output represents binary counts of 264 as 2^1, 2^2, and 2^3 which slices 33 kHz into eight bits. The CD4097B has two sections; each is switched by the same binary input (A,B,C). The X_{in} is sliced into eight bits and stored in separate IC integrators, U_5 and U_6 (two RC4136Ds); the time constant is 10 sec. The output of the integrators is fed back to the y inputs of the CD4097 where these are synchronously switched to a single output Y_{out}.

The summing amplifier is U_6, and LM 108. The input signal from V_{in} is attenuated by R31 and R32 and represents the leak-through signal which is cancelled in U_6. The crystal filter, Q_1 and Q_2, removes the distortion products generated by the CD4097B. Its output is the desired signal; any residual signal is reprocessed for additional cancellation.

Tests on this circuit showed 32 dB cancellation. Since the breadboard was built on a proto-board, considerable cross coupling was experienced; a better circuit layout would probably give better results. In actual use the direct signal section would drive the phase-locked loop, while the reflected signal section would be applied to pin 3 of U_6. An overall schematic including the synchronous filter is shown in Figure H-9, Appendix H.

Another approach using a tracking filter is shown in Figure H-10, Appendix H. This approach does not use feedback, but uses a balance scheme. The signal containing the steady-state 33 kHz and the variable 33 kHz signal are applied to the LF356 out of phase and are cancelled. However, the addition of a CD4051 multiplexer loads one line to the LF356, unbalancing its input. This unbalance continues until the charging on the capacitors is complete; then it will appear unloaded and cancelled in the LF356. A varying signal will continually change and discharge C_o, unbalancing the circuit to the extent that it varies.

2.7 RECEIVER/TRANSMITTER/PROPAGATION NOISE STUDY

The quality of the tracking data supplied to the tracking algorithm is degraded by noise. Five sources of noise have been identified as influencing the doppler data:

a. Transmitter AM/FM noise transmission
b. Receiver input noise (ENI)
c. Multipath effects
d. Clutter effects
e. Intruder path instabilities

2.7.1 TRANSMITTER AM/FM NOISE AND REFERENCE CHANNEL PHASE LOCK LOOP (PLL) INVESTIGATION

A signal flow diagram, Figure 42, was prepared in the course of analyzing the extent of cancellation of noise modulation of the transmitter carrier at the inputs to the product detectors of a sensor receiver.

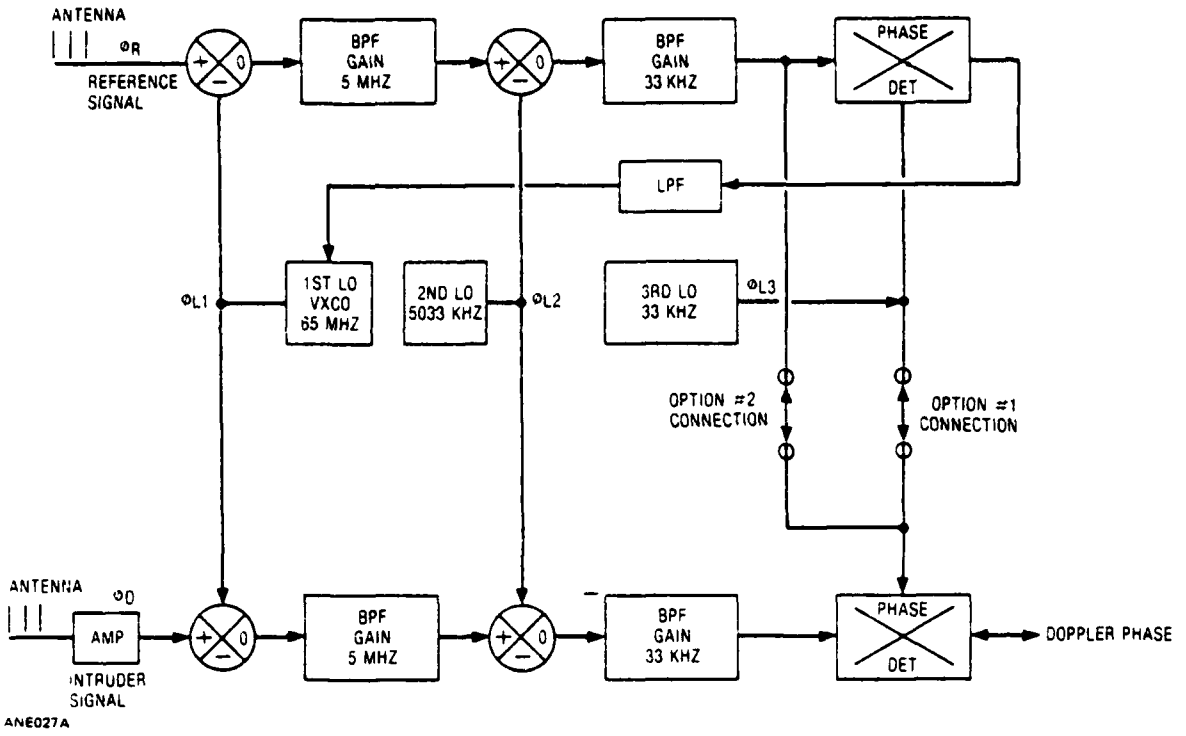

Figure 42. Tracking Receiver Basic Information Flow Diagram

The bandwidth of the sensor receiver, ahead of the final doppler phase difference detector, is set at 2.5 Hz by crystal filters. A phase lock loop (PLL) is employed in the receiver in order to keep the received reference and doppler signals centered in the receiver passband. The PLL is designed to remove frequency drift of the transmitter and the local oscillators of the receiver. The time constant of the PLL is of the order of several minutes; therefore, the loop does not affect phase modulation noise in incoming reference and doppler signals.

The receiver heterodynes the incoming signals (reference and doppler) down to the input frequency of the phase (or product) detector (nominally 33 kHz) in two steps.

Identical frequency conversion processes are applied to both signals at each step. Therefore any phase modulation of the IF signals that is caused by either the first or second local oscillators appears on both signals that are available for application to the output phase (product) detector in Option 2 of Figure 42. Therefore all phase noise added by the local oscillators is cancelled at the output of the phase detector.

Use of the third oscillator signal (Option 1) as the reference signal for the output phase detector would result in loss of oscillator noise cancellation, and would also result in output data error due to failure of the PLL to accurately track drifts and phase modulation of the transmitter's carrier.

The use of the Option 2 implementation results in virtually complete cancellation of transmitter phase noise as seen at the output of a doppler phase detector.

The effective signal flow for Option 2 and carrier phase modulation is shown in Figure 43. Given that the transmitter carrier is phase modulated (with a modulation index B) at an angular frequency of w radians per second, and that the difference in time delay for the reference at doppler signals at the sensor is t_d seconds and the product wtd is much less than 1. Then the residual phase modulation, at the output of the sensor's phase detector is given by

$$\Delta\phi(t) = BA \cos (wt + \Delta\phi)$$

where

$$\begin{aligned} A &\quad \omega t\lambda/\sqrt{2} \\ \Delta\phi &= \omega t_d/2 \text{ radians} \\ \beta &= \text{carrier modulation index} \\ \dot{\omega} &= \text{carrier modulation frequency} \end{aligned}$$

For modulation frequency of 5π rad/sec (2.5 Hz) and a time delay of 13 microseconds (4 km path difference), then (Appendix B):

$$\begin{aligned} A &= \omega t_d/\sqrt{2} \\ &= 3.25 \times 10^{-5} \text{ Amplitude ratio} \\ &= -89.76 \text{ dB} \end{aligned}$$

The RMS error which would result from a specific phase noise spectrum of the oscillator can be obtained by integration of spectral noise power of the transmitter phase noise, as modified by the factor A^2, across the passband of the receiver. The error would be negligible for any reasonable transmitter phase noise spectrum.

Amplitude noise modulation on the transmitter could be eliminated in the reference channel since limiting could be incorporated in the low frequency IF stages. However, AM noise can be accepted in the signal channel since this channel must be linear. If the AM noise is 60 dB below the carrier, and the direct signal leak-through the intruder signal channel, the noise will be 60 dB below the leaked signal. The noise on this signal

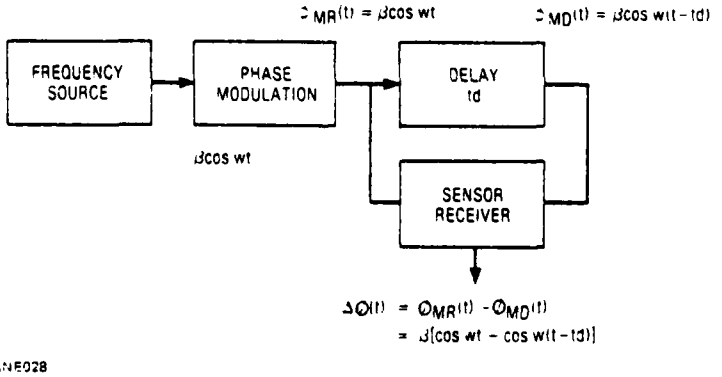

Figure 43. Information Flow Diagram for Analysis of Effect of Transmitter Phase Noise

would then be 60 dB less or 20 dB below the intruder signal. Removing the leak through signal by cancellation techniques will not further reduce the noise, since cancellation will be on the carrier only and not its sidebands to within 1/100 of a hertz.

2.7.2 RECEIVER INPUT NOISE (ENI)

The noise in the receiver has been calculated to be -168 dBm at a 2.5 Hz bandwidth; the expected signal is -151.5 dBm, a signal-to-noise-ratio of 16.5 dB. The noise has a random phase and amplitude distribution which adds to the incoming signal. Since both incoming signal and noise are converted to 0.01 to 2.5 Hz, an analysis is made at the phase detector in which only the change of state (+ or -) is noted. The time of change is our key interest. Noise signals added to a normal doppler signal can cause an early or late change of state depending upon the relative magnitudes of the signals near the time of transition. A detailed analysis is found in the next subparagraphs.

2.7.2.1 AXIS CROSSING ERROR DUE TO NOISE – False alarm rate and time interval (functions of):

a. Hysteresis/$\sqrt{\text{S/N ratio}}$
b. Noise bandwidth

Axis crossing angle time error (functions of):

a. S/N ratio and V_t/A ratio
b. Noise bandwidth and doppler offset (angular rate)

2.7.2.2 HYSTERESIS/$\sqrt{S/N}$ =Z – The ratio of hysteresis to $\sqrt{S/N}$ determines how far out on the probability curve tails the Up or Down axis crossing thresholds lie when the true value is centered. A $V_t/\sqrt{2t}$ ratio of 2.18 gives a 1×10^{-3} probability of an axis crossing detection for the + or - direction when the detector outputs are centered between the thresholds.

Noise Bandwidth[24,25] – The noise bandwidth determines the average time between successive noise voltage peaks.

The average time between successive noise peaks is given by the quotient of average time, τ, between noise pulses and probability, $(P(\chi > V_t)$,

$$T = \tau/P(\chi > V_t) = (1/BW)\, P(\chi > V_t)$$

2.7.2.3 S/N AND V_t/A RATIOS – S/N ratio and V_t/A ratio set the angle at which threshold is reached in absence of noise.

Assume constant $V_t/\sqrt{S/N}$ ratio and varying S/N ratio. Then increasing S/N (signal amplitude) reduces the angle at which threshold is reached as well as the 1σ range sum of axis crossing time error.

$\Delta\chi$ = $\chi_2 - \chi_1$
= Integration band
$\chi_1 + \Delta\chi/2$ = Center of integration band
V_t = Threshold of decision

and

$$\sum_{-\infty}^{\infty} K(T_X \Delta X/\dot{X}) = 1$$

2.7.2.4 NOISE BW AND DOPPLER OFFSET – Noise bandwidth determines the average time interval between noise pulses.

$$(\tau = 1/BW)$$

Doppler offset determines the duration of dwell at any particular window (Δ Phase) for which a hit probability is computed. Probability of hit in a given Δ Phase is a function of

$$\dot{X},\ P(X \geq V_t) \text{ and } \tau = 1/BW$$

$$P_H(X, \dot{X}, \Delta X\ BW) = KT_X \Delta X/\dot{X}$$

where

$$T = \tau/P\left[(X_1 + \Delta X/2) > V_t\right]$$

Detection Time/Phase Error

a. Compute crossing probability

$$= 1/2 \text{ erfc } (z)$$

where $Z = V_t/\sqrt{2N}$

b. Select ΔZ increment, Zmax, $\dot{Z}$ values

c. Compute, for each Z, time in ΔZ

$$T_{\Delta Z} = \Delta Z/\dot{Z}$$

d. Compute ratio

$$\text{Ratio} = T_{\Delta Z}/\tau$$

where $T_{\Delta Z}$ = time in ΔZ increments
= average time between noise pulses

e. Compute for each ΔZ increment at Z(i) product

$$\left[1/2 \text{ erfc } (Z)\right]\left[T_{\Delta Z}/\tau\right]$$

f. Compute

$$P_H(I) = P_{HX(I)} P_S(I)$$

where

$$P_{S(I)} = 1 - P_{H(I-1)}$$

and

$P_{H(I)}$ = probability of axis crossing detection for I-th ΔZ segment

$P_{(I)}$ = probability of not being detected before I-th segment

$P_{H(I)}$ = probability of a hit (if in I-th segment)

$= \left[1/2 \text{ erfc } (Z)\right] \left[T_{\Delta Z}/\tau\right]$

Compute axis crossing error as function of

Threshold/Noise and S/N ratio

$S/N = A^2/2\sigma^2 = A^2/2N$

$Y = V_t = (KA)/(\sqrt{2}\cdot N) = K\sqrt{S/N}$

$\chi_o = A \sin \emptyset$

$\emptyset_t = \sin^{-1} (Y/A)$

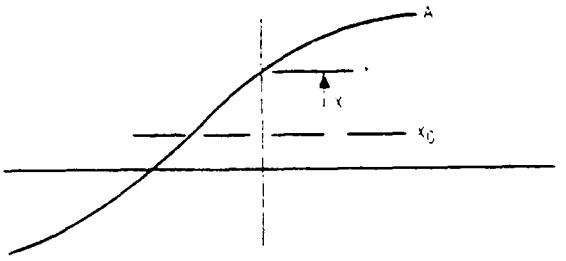

ANE 129

2.7.2.5 EFFECT OF GAUSSIAN NOISE ON AXIS CROSSING DETECTION – The presence of thermal noise at the output of a doppler channel product detector will result in a random variation of the apparent phase difference between the input reference and doppler data signals.

In a typical phase difference tracking system, if the range increment is sufficiently small compared to noise induced error, the error parameter of interest is standard deviation of phase. See Appendix C.

Data processing in this system utilizes direction and time of reported axis crossing from several sensors in the determination of the location and travel of moving intruders. Also, the increment size is large relative to the expected variation of apparent phase difference caused by Gaussian noise.

This analysis is directed toward determining the nature of axis-crossing jitter as a function of hysteresis and signal-to-noise ratio, and to the effect of such variations upon apparent travel of an intruder.

AD-A110 621 GENERAL DYNAMICS SAN DIEGO CA ELECTRONICS DIV F/G 17/9
AREA INTRUDER TRACK STUDY.(U)
NOV 81 J B GEHMAN F30602-79-C-0189
UNCLASSIFIED RADC-TR-81-314 NL

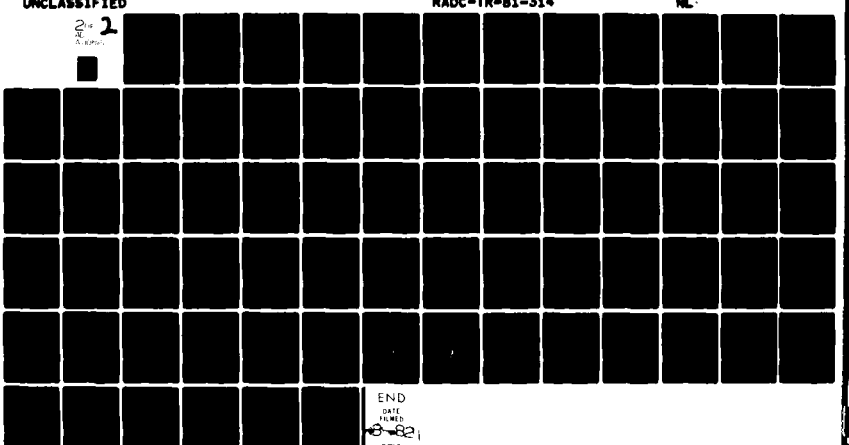

The axis crossing detection process will require a dead zone (hysteresis) in order to avoid excessive jitter, as a result of noise when an axis crossing is approached.

Consider a detection process in which the time of axis crossing is defined as the time at which a positive going crossing reaches a value $+V_t$ or a negative going crossing reaches a value $-V_t$.

The probability that signal plus noise will cross a particular threshold is given by (see Appendix C)

$$P(X > Y) = 1/2 \text{ erfc}(Z)$$

where

$$Z = \frac{Y - \chi_o}{\sigma \sqrt{2}}$$

and

Y = Threshold voltage
σ = Mean square noise voltage
χ_o = Bias voltage

If $Y = KA$ where A = is amplitude of the signal, $\sigma^2 = N$ where N = signal noise power, and $\chi_o = 0$, then

$$Z^2 = K^2 \frac{A^2}{2N}$$

and

$$Z = K \sqrt{S/N}$$

Given an S/N value, and a detection threshold Y, set at factor K times the signal amplitude then, with $X_o = 0$, the probability of crossing one of the next threshold is obtained by solving for

$$P(X > Y) = 1/2 \text{ erfc}(Z) = 1/2 \text{ erfc}\left(K \sqrt{S/N}\right)$$

Conversely, given a desired probability, then obtain the corresponding Z and solve for

$$S/N = (Z/K)^2$$

or

$$K = Z/\sqrt{S/N}$$

to find the required S/N for a given threshold choice or the required threshold factor for a given S/N.

For example, Z must be 2.182 to obtain a 10^{-3} probability value. If K = 0.5, corresponding to a ± 30° hysteresis, then S/N 2.182/.5 = 4.364

$$S/N = 12.78\ dB$$

2.7.2.6 SPEED/NOISE INVESTIGATION – An investigation was directed toward the effects of noise with changes in the intruder's speed at various signal-to-noise ratios. The analysis shows that noise superimposed upon the signal causes a random early triggering of the threshold crossing detector. Recrossing the threshold is prevented by having dual level thresholds which provides hysteresis. Once a positive threshold (or negative) is crossed, only a negative threshold (or positive) can be crossed.

Upon selecting a ± threshold voltage of 2.18 times the RMS noise voltage, computations show that the probability of noise triggering the threshold without a signal input with the above setting will be 1 part in a 1000 within a time period defined as 1/BW (Bandwidth).

This probability was considered small; averaging one crossing in 400 seconds for 2.5 Hz bandwidth. With the addition of signal the probability of crossing threshold increases to a probability of unity when the instantaneous detected signal voltage is equal the threshold. Noise will randomly cause an early crossing. There is a small possibility that noise pulses may inhibit a threshold crossing, however, as soon as the noise pulse fades the threshold will be crossed within a very short period. Our analysis accounts for only the early triggering of the threshold and neglects any inhibiting action of the noise. A peak signal voltage twice the threshold setting previously adjusted for no signal, low probability threshold triggering will have a signal-to-noise ratio of 12.77 dB. In section 2.6.2.4, the signal-to-noise was computed to be 16.5 dB at a 1 km range for a man-type intruder. The peak signal will be 3 times the threshold setting.

Computations are made for the mean value of variations from the true value in terms of doppler phase angle as a function of doppler frequency representing the speed of an intrusion.

The greater the speed of an intrusion, the lower the probability that a significant noise pulse will cause a significant change in threshold crossing time. Figure 44 shows the standard deviation from the mean value as a function of doppler for 14.5 dB, 20.5 dB, and 26.5 dB signal-to-noise ratios. The mean value and standard deviations are in degrees; two timed pulses are generated per cycle of doppler or 8 ft; 5° of 180° represents approximately 1/8 ft. Tables 12 and 13 also show these values.

Note that a variation of the threshold voltages will change the doppler shift timing, however the timing as used is related to the preceding timing so that any time variations in threshold are normalized. Variations in the threshold within a doppler cycle will cause errors.

2.7.3 MULTIPATH EFFECTS

Large objects within the surveillance field will reflect some of the transmitted illuminating energy on the intruder's path. The addition of the two signals can cause the transmitted signal to have an apparent phase shift at the target not seen by the receiver as the direct signal but included in the intruder's reflected signature. The maximum

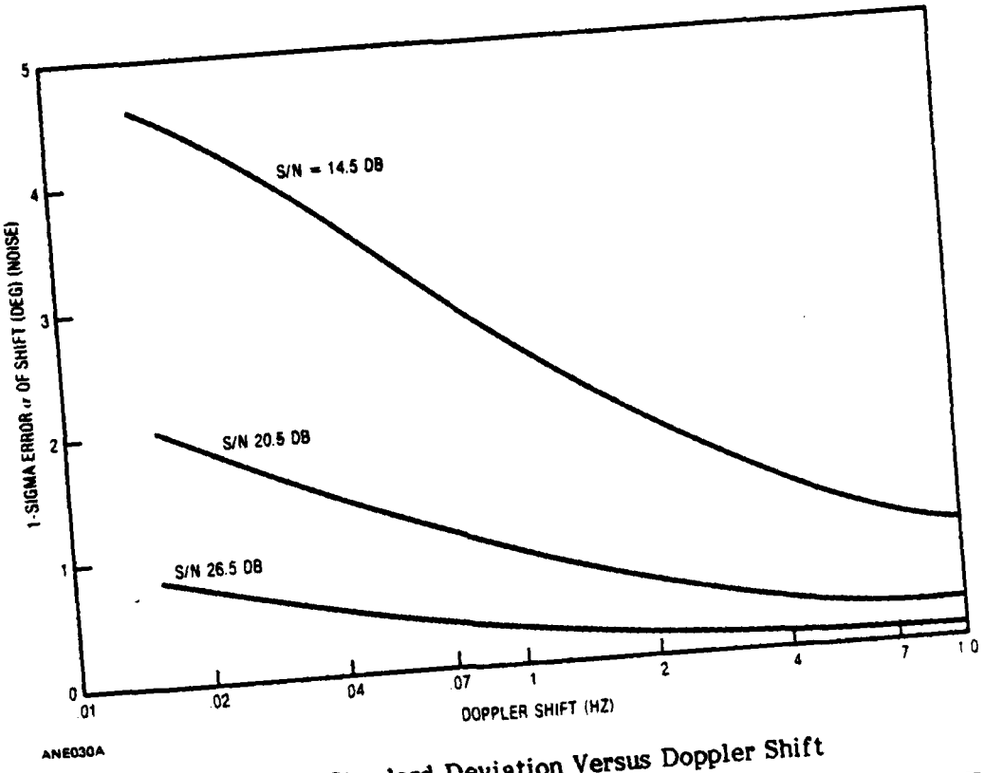

Figure 44. Standard Deviation Versus Doppler Shift

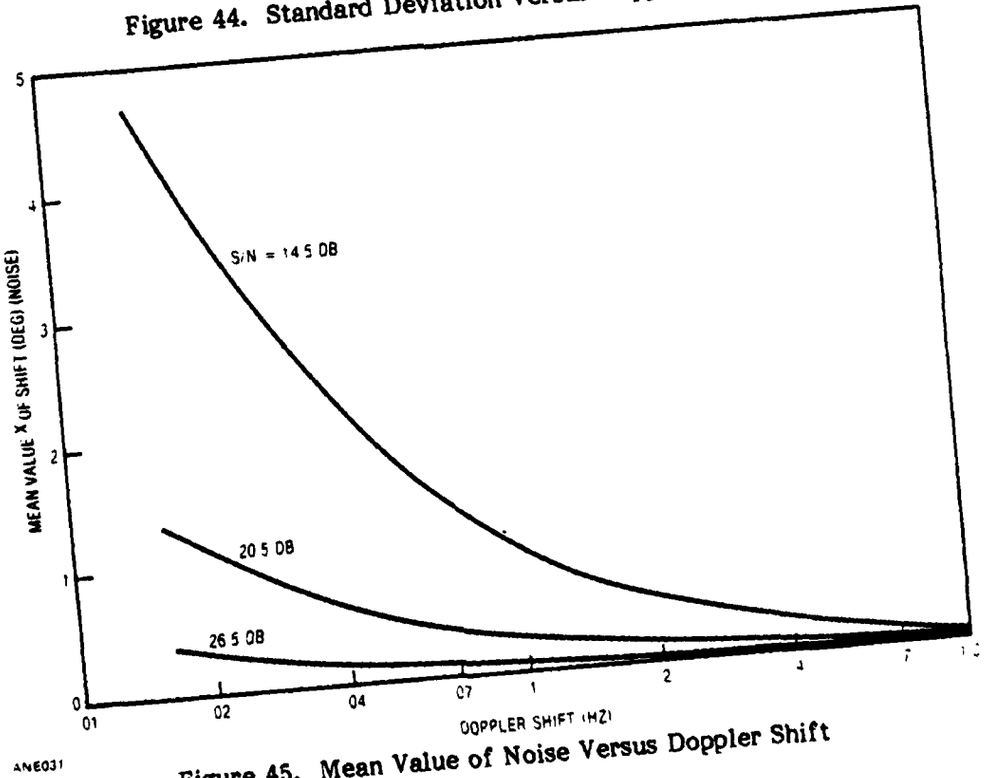

Figure 45. Mean Value of Noise Versus Doppler Shift

Table 12. 1-Sigma Error of Axis-Crossing in Degrees as Function of S/N and Doppler Shift

DOPPLER (Hz)	SIGNAL/NOISE RATIO (dB) 14.5	20.5	26.5
0.015625	4.6037	2.0131	0.8019
0.03125	4.0140	1.5986	0.6027
0.0625	3.1867	1.2013	0.4397
0.125	2.3943	0.8763	0.3158
0.25	1.7465	0.6295	0.2251
0.5	1.2545	0.4486	0.1598
1	0.8941	0.3185	0.1132

effect occurs when the intruder's path is closest to a fixed object when it may reflect a quadrature component to the transmitted signal at the intruder. At a very short range the interfering objects reflected signal is lost: at 5m a 40 dB loss is incurred; at 20m a 50 dB loss is incurred. At worst case, the doppler measurement will vary 0.3% at 5m, and 0.1% at 20m, causing a slight warp in the computed tracking path.

2.7.4 CLUTTER

Clutter, unwanted reflections from the ground, rain, trees, grass, and wind-moved objects such as telephone or electric lines, comes in two classifications; static and dynamic. Static clutter comes from the ground, building and other non-moving reflectors. Dynamic clutter comes from moving objects intruders and trees. The static clutter is not detected through the system but could overload the receiver. The receiving antenna can eliminate this type of clutter by readjusting its "null." Dynamic clutter can produce a noise output if it is within the bandpass of the receiver.

Table 13. Mean Offset of Axis-Crossing in Degrees as Function of S/N and Doppler Shift

DOPPLER (Hz)	SIGNAL/NOISE RATIO (dB) 14.5	20.5	26.5
0.015625	4.6446	1.3607	0.3719
0.03125	2.7096	0.7404	0.1944
0.0625	1.4741	0.3869	0.0944
0.125	0.7703	0.1979	0.0503
0.25	0.3939	0.1001	0.0253
0.5	0.1993	0.0504	0.0127
1	0.1002	0.0252	0.0064

In order to generate one doppler cycle, the object in motion must move 1/2 wavelength, however, a partial cycle can be generated which will produce a reduced output. The reduced output is equal to the sin $(4\pi d/\lambda)$, where λ = wavelength, d = motion of object. The oscillating motion of a tree in wind would simulate a doppler signal. We intend to reduce this possibility by separately measuring positive and negative doppler signals; therefore a fixed object in oscillation has no net motion and will be eliminated. Most of the clutter will be reduced due to the choice of frequency, 60 MHz. Individual small objects less than 3 to 4 ft high will not present a suitable reflecting surface at 60 MHz. (See Figure 4.) There is, however, a real source of noise from tall grass; each blade has virtually no reflection, but together over a large area they do present a sizeable reflection. It has been observed that gusts of wind causing the grass to move in unison generate a real target with a positive doppler even through each blade has no net movement. A field with various shrubs 3 to 4 ft high will have a random motion with respect to wind and produce a random noise output. These observations have been made on an EMID, AN/GSQ.160 which also operates at 60 MHz. The total clutter can be considerable since our antenna looks over more than 270° of the ground out to one or more kilometers; keeping the average foliage down to less than one foot would effectively reduce such noise.

2.7.5 INTRUDER PATH INSTABILITY

A computed irregular path may not be due to noise. It is virtually impossible and most unlikely an intruder will walk or run a straight or smooth curve path. Irregularities in the ground, occasional stones, etc., will cause a conscious deviation of the path plus an unconscious deviation of the path direction due to mental inattentiveness. We will have to expect a noisy input and perhaps expect the tracking algorithm to smooth out the information as more data becomes available during the tracking.

2.8 PROCESSOR

2.8.1 DOPPLER COUNTER

The receiver section provides a signal processor which reduces the internally generated noise by narrow bandwidth filters. The logic processor which counts the doppler cycles provides discrimination logic to reduce nuisance alarms and operates from a relatively clean signal provided by the receiver section.

The logic processor-doppler counter consists of a chain of phase detectors referenced to a sequential phase of 90° for eachdetector. See Figure 46. The reference phase "A" is applied to the chain and a common signal phase "B" is applied in parallel. As the phase shifts in each phase detector, a polarity change triggers a Schmitt bistable circuit, and triggers a 1-shot monostable multivibrator. The Schmitt circuit provides hysteresis to prevent retriggering on noise signals. The Schmitt and the 1-shot are cross connected to a second phase detector to perform a sampling function. The polarity of the Schmitt circuit is sampled by the adjacent 1-shot, producing a positive or negative pulse indicating doppler phase rotation. A complete cycle of doppler will produce four pulses of the same polarity; a reverse in polarity indicates a change in direction and an incomplete cycle. See Figure 47. The pulse output is counted in an up-down counter IC;

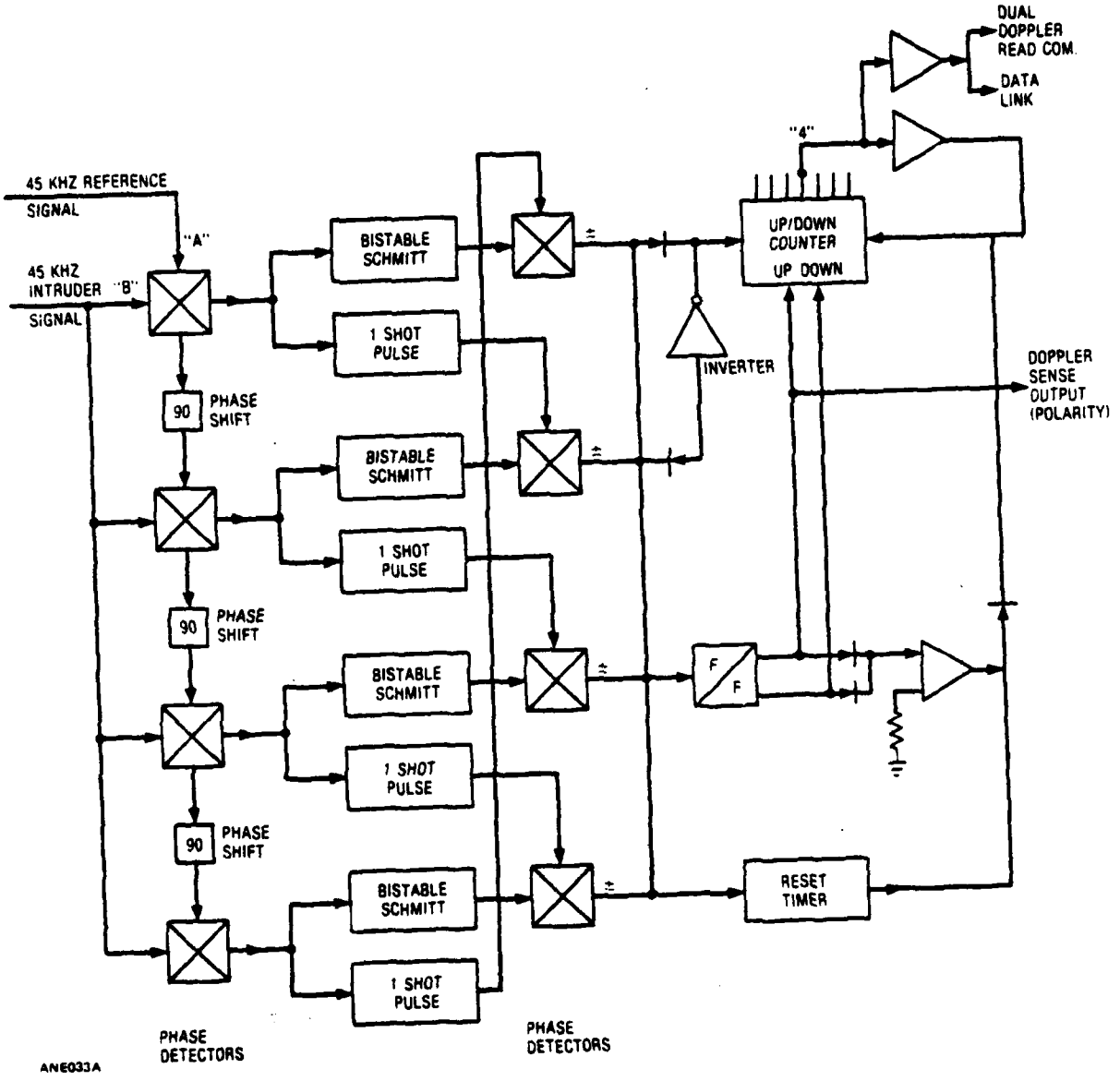

Figure 46. Processor Block Diagram

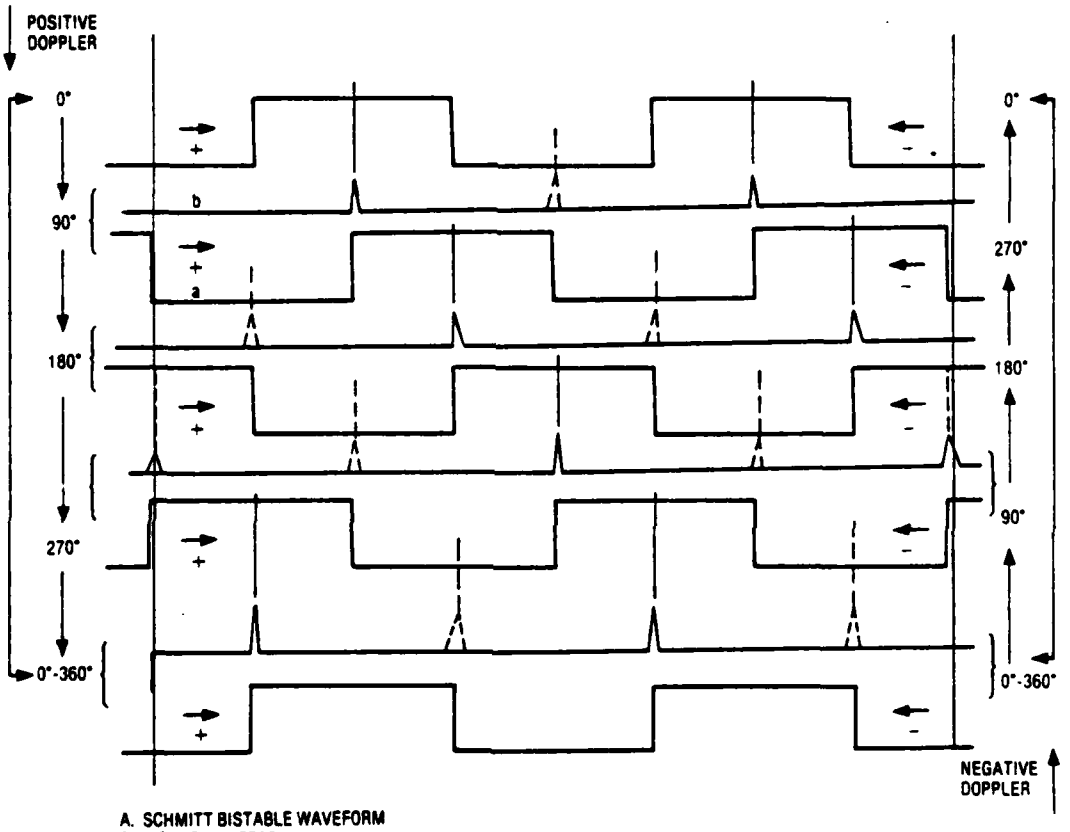

A. SCHMITT BISTABLE WAVEFORM
B. 1 SHOT WAVEFORM

1. INPUT SIGNAL GENERATES (A) AND (B) WAVEFORMS IN SEQUENCE.
2. SEQUENCE DEPENDS UPON SIGN OF DOPPLER; RIGHT HAND DOWN POSITIVE DOPPLER; LEFT HAND UP NEGATIVE DOPPLER.
3. ONE SHOT (B) CLAMPS (SAMPLES), BISTABLE SCHMIDT WAVEFORM. (A) OF ONE SHOT OPERATES ON POSITIVE GOING WAVEFORM (B).
NEGATIVE (DOTTED) DOPPLER READ RIGHT TO LEFT. POSITIVE (SOLID) LEFT TO RIGHT.

ANE034A

Figure 47. Waveform Relationship in Processor Phase Detector

positive or negative pulses are rectified for a pulse input to the counter. The pulse polarity is monitored by a bistable flip-flop IC, the output of which controls the up or down count of the counting IC. The output of the flip-flop also provides a reset pulse to the counting IC for every change in polarity, starting its count from zero. A reset timer produces a pulse after a time considered too long to be a legitimate quadrature doppler pulse.

The counter IC provides an eight count; the count of "four" is arrived at either from counting plus four or minus four, at which time it is reset to zero. The count of "four" is monitored as a doppler cycle output.

In a dual doppler scheme, the doppler cycle output may be used to command a differential phase measurement; otherwise, it commands only the data link to transmit the polarity of the doppler, and the station address.

2.8.2 DUAL DOPPLER PROCESSOR

Refer to Figure 39 for the block diagram of the receiver having an output at 100 kHz for the differential doppler phase. A block diagram for processing this signal is shown in Figure 48. The reference phase and the signal phase are both amplitude limited and fed into an "AND" gate and in turn fed into another "AND" gate shared with a clock pulse generator operating at 1,280 kHz. As the two signals shift in phase, pulses from 0 to 64 are generated for 0°to 360° of phase shift. 64 bits was chosen since the accuracy may not be better than 5.6°. Each bit represents 5.6° or 9.395 ellipses. ($\phi \times 1500/5\pi$). If the frequency of the dual doppler was chosen to be 93.75 kHz, the repeating range would be 1600m containing 640 ellipses (along major axis); 1/64th would represent 10 ellipses. This number could be transmitted directly as N(J) 10 (an ellipse number). The pulses generated per (93.75 or 100 kHz) cycle is counted and stored in a 2^6 parallel latch IC. At the end of each count the number is transferred and reset. The parallel output is connected to the data link.

Note, the doppler-only processor can also be used with the dual doppler scheme in order to use its discrimination characteristics and provide for reading commands. In addition, added accuracy could be obtained by using data from both.

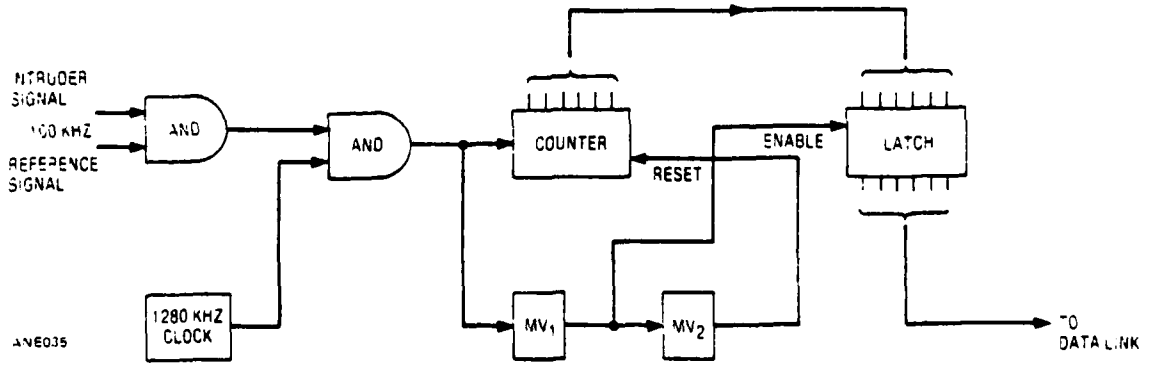

Figure 48. Dual Doppler Processor Block Diagram

2.8.3 PROCESSOR/DATA LINK INTERFACE

A doppler-only interface block diagram is shown in Figure 49. The interface circuitry provides a "Busy/Hold" circuit which delays a transmission if the party line is "Busy." The circuit also limits transmissions to one per second, allowing for storage and transmitting the number of doppler cycles stored in one second. Provision has been made for two other inputs of data, doppler sense (polarity) and tamper alarm.

The "Busy/Hold" circuit monitors the potential across the isolation diode at the output of the ED15 code generator. Normally both sides are ground potential; upon transmission, both are positive producing no change in output at "X" (normally positive). A signal on the party line has only a positive signal at "Y," resulting in a change at "X," a negative pulse. A negative pulse at "X" causes a nonretriggerable monostable multivibrator to trigger on for 20 milliseconds, an estimated time of transmission. A signal at "Z," representing the initiating doppler cycle, generates a 25 millisecond pulse. If the signal at Z arrives first, the leading edge triggers the ED15; if the signal X arrives before Y, it will inhibit Z up to 20 milliseconds depending upon the degree of coincidence. It should be noted that if the ED15 starts to transmit other Data Link outputs will be inhibited. The doppler storage circuit operates by allowing the first doppler cycle to be transmitted through U5 and allowing a 1 count which is automatically reset by the signal from U3. MV_1 is triggered and inhibits additional cycles from being counted for 1 second. At the end of 1 second the next pulse triggers MV_2, V_3 resetting the counter. The resetting pulse is the trailing edge of the 25 millisecond pulse so that the count (0 to 32) is fully transmitted before resetting. A small delay is added in front of MV_1 to allow the first pulse to operate U5 before MV_1 inhibits its output.

2.8.4 COMBINED DOPPLER, DUAL DOPPLER AND SELF-TEST

A simplified block diagram of a combined data link is shown in Figure 50. It incorporates the inputs shown in Figure 49 plus the addition of the dual doppler input and self-test. The ED15 coder IC is set to a normal receive mode (T/R). The MV_2 $\bar{Q}$ output keeps the tristate buffer "on," so that the address set by switches is connected. Upon receiving a coded signal, the ED15 compares the input code to the address switch code, if matched an output will be generated to the self-test terminal. When a doppler cycle is generated, MV_1 and MV_2 are sequentially operated; each for the duration of a code sequence, producing a double coded burst. The output switches the T/R function to transmit, operates the first burst sequence, i.e., address, doppler polarity, doppler storage, tamper, and operates the second burst by disconnecting the previous data and connecting the dual doppler data. Upon completion it switches back to a receive mode. A schematic of a coder/decoder can be found in Figure 50.

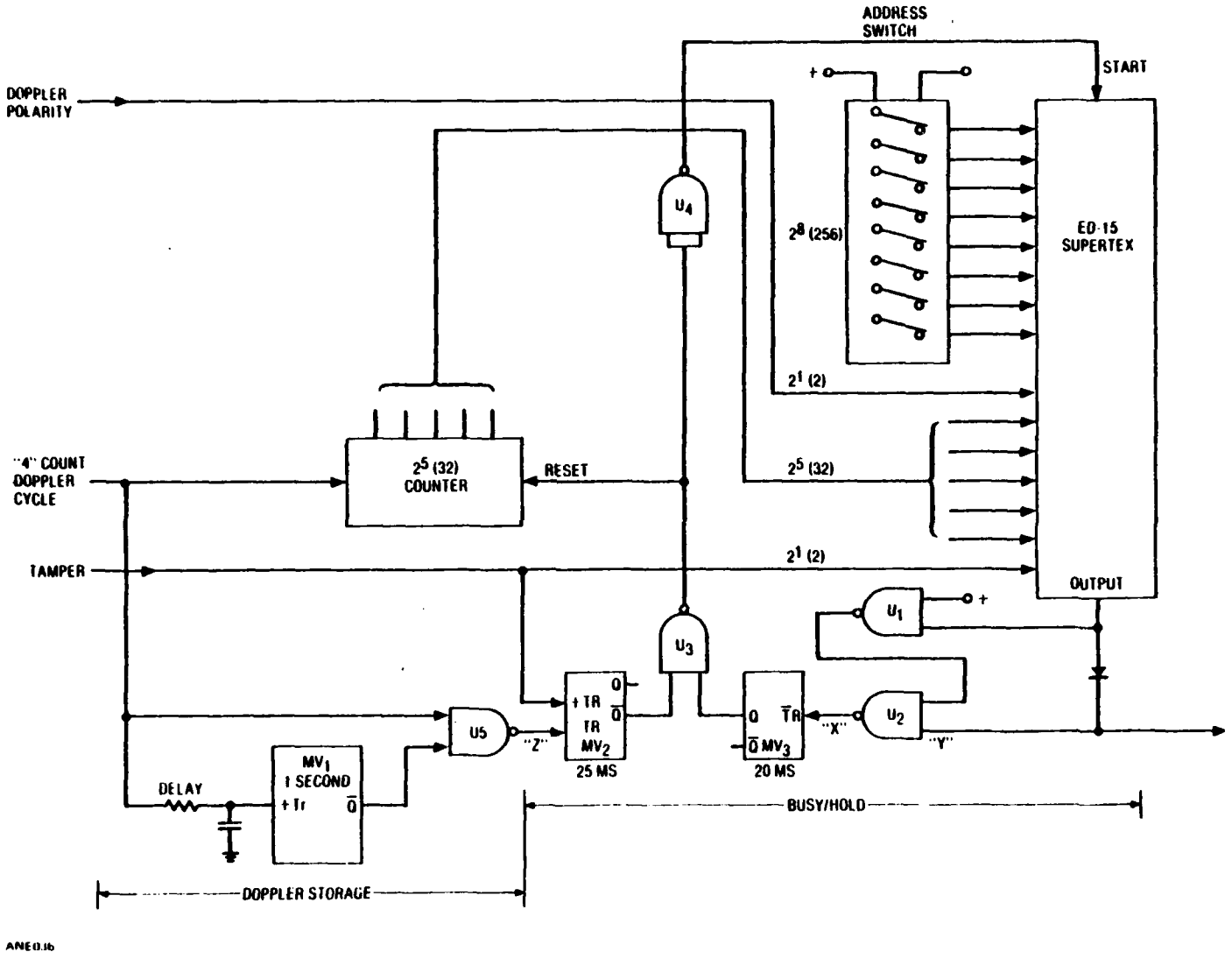

Figure 49. Processor/Data Link Interface Block Diagram, Doppler Only

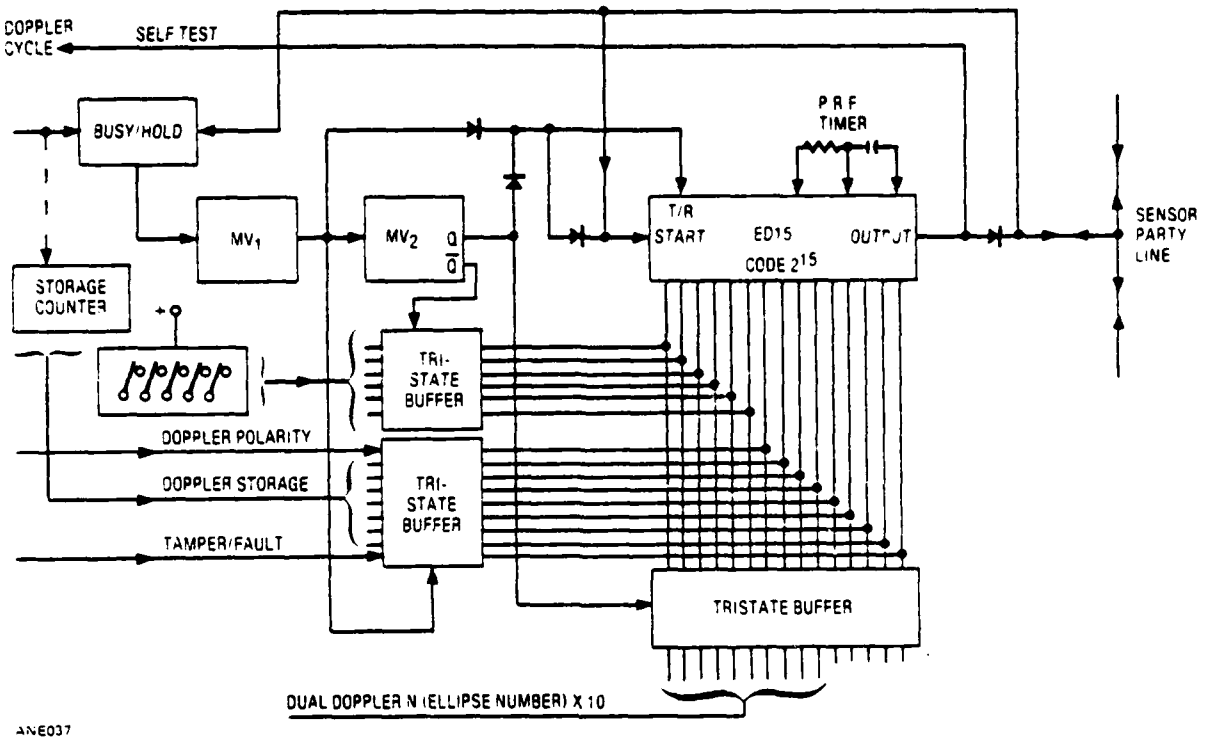

Figure 50. Processor/Data Interface Block Diagram (Simplified), Combined Doppler, Dual Doppler and Self Test

3. SYSTEM CONSIDERATIONS

3.1 GENERAL

The previous sections have described the technology of the various portions of the Area Intrusion Tracker. The purpose of this section is to consider all the portions interacting and the cost/complexity, accuracy, reliability and possible regulatory problems.

In Section I, "Brief Description of the System," the basic concept was described. A CW transmitter illuminated an annular ring from the center 8 km away a surveillance zone 1 km wide. Receiving sensors are distributed on the periphery of the ring and have antennae directed outward and with a "null" directed toward the transmitter. The configuration is designed to improve the intrusion signal to direct transmitted signal ratio. Doppler is measured in the receiver and as each doppler cycle is generated a coded address, doppler sense and other data is transmitted via a data link to the transmitter location where the data is used to pinpoint and track the intruders as they traverse the surveillance zone. The tracking data is displayed in a coordinate grid and/or on a map-like monitor.

3.2 DETECTION CHARACTERISTICS

Detection is dependent upon intruder-reflected signal strength and doppler frequency. Signal strength is dependent upon antenna coverage and target size, while doppler is dependent upon intruder location, direction of motion and the magnitude of the velocity.

For a normal-sized intruder, 20 watts of transmitted power and a two-element array, a single receiving station will cover a cardioid shaped area 1 to 1.5 km outward from the surveillance ring, 0.65 to 1.0 km along the perimeter (90°); 200 to 300m at 135°, 25m at 180°. See Figure 25.

In order to have full coverage for two receiving sensors, the spacing must be approximately 600m. The relation of power/sensitivity and the number of stations on the perimeter is shown in Figure 30. Between 60 and 120 stations are required for a transmitter power of 20 to 25 watts. If the tracking algorithm requires 3 or 4 stations to provide data, then a 30% increase in power or receiver sensitivity or doubling the number of stations on the perimeter would be necessary.

As indicated in Figure 2, the size of the intruder determines the reflected signal magnitude. This characteristic helps discriminate against small animals, but will also reduce the response to children and very small stature adults. The frequency chosen should suitably detect people 4.5 ft high and upward. Larger targets produce reflected signals in proportion to their silhouette. Note that the purpose of Figure 2 is to show a response greater than the apparent silhouette by operating on the first large peak.

Signals can also be attenuated in the presence of foliage. The lower the frequency the greater the penetration through the foliage. Measurements made at 60 MHz under dense

jungle conditions indicate an attenuation factor of 0.2 dB per foot. This of course is a limiting condition and much less attenuation should be expected.

Detection depends upon the measurement of doppler cycles; the lower limits of measurement are close to zero and the upper limit approaches the bandwidth of the receiver. An RF bandpass suggested for personnel is 2.5 Hz, giving ±1.25 Hz of doppler as an upper limit. This occurs when tracking personnel moving at a rate of 10 ft per second directly toward the receiving sensor. At angles away from the sensor, the doppler will be reduced as a cosine function. To detect vehicles and aircraft which may have velocities up to 600 mph to 120 mph (88 to 176 ft/sec) a greater bandwidth is necessary, 50 Hz. A 50 Hz bandwidth receiver will have a greater ENI (noise power), but compensating for this is that the vehicles/aircraft will have a greater reflected signal.

Low frequency doppler measurement is dependent upon the system low frequency cutoff. This cutoff is necessary to eliminate system electrical drift from causing false alarms. It is expected that cutoff will be as low as 0.01 Hz, an equivalent velocity of 1 inch per second toward a receiving sensor. At a normal walking gate, 6 ft per second, frequencies less than 0.01 Hz are generated at angles between 89.25° and 90° to a radial from the receiving sensor. It should be noted that zero doppler for two or more receiving sensors does not exist except inside and at the sensor perimeter.

Multiple targets within a sector provide only one set of doppler outputs. When two targets approach an area using doppler-only tracking, the centroid of the two targets is tracked. If the two targets have different velocities, the higher speed target is tracked. Two targets moving in opposite directions along a radial will cause the processor to cancel the counting and no tracking will result. In a range only system, two targets separated and moving at different speeds will alternately measure one, then the other. This would also happen if they were moving in opposite directions and there were no positive/negative doppler cancelling circuit. The accuracy of tracking would be affected.

Multiple targets around the perimeter, spaced so that each were detected by a separate pair of receiver sensors, would track each independently. There is an advantage in having a large number of sensors on the perimeter: to permit the separation of multiple intrusion.

3.2.1 COVERT DETECTION[16]

If there is a desire to completely hide a receiving sensor, it can be installed on the surface or just under the surface. Vertical whips disguised as weeds could be used. The signal levels would be reduced, limiting the detection range to about 200 to 250m. Tests were made using an underground antenna, a wire 100 ft long buried 1 in. below the surface. Detection was achieved 20 meters from the antenna using a local FM station as an illuminating source. Detection past the ends of the antennas (10m) was also observed; however, only the area in front of the antenna was usable, and no detection was noted in the back direction, i.e., toward the transmitter. A more sensitive receiver as proposed in this report could increase the detection zone to 60m.

---

[16] John B. Gehman, Line Sensor Intrusion Detector System, R-71-008, General Dynamics Electronics Division, March 1972.

3.3 COMPUTATION OF FALSE ALARM RATE (FAR)

For the purposes of definition, false alarms are to be considered as originating from internal electrical noise. External generated noise supplied by unwanted targets (animals), environmental effects of wind, rain and electrical discharges will be considered as nuisance alarms. False alarms can be calculated, whereas "nuisance alarms" must be found experimentally for each general location.

False alarm rate (FAR), based upon a single doppler tracking signal only is determined as follows:

The probability of an impulse of noise crossing a threshold detection circuit is given by the equation (refer to section 2.7.2):

$$P(x > y) = 1/2 \operatorname{erfc}(Z)$$

where $$Z = \frac{y - x_o}{\delta\sqrt{2}}$$

and

erfc = complex error function

y = threshold voltage

δ = *mean square noise voltage*

x_o = signal voltage (minimum usable)

where $x_o = A \sin\phi$

$\phi = \sin^{-1}(y/A)$

under no signal conditions $x_o = 0$

In previous accounts when a minimum usable signal was considered we have used 12.78 dB as a signal-to-noise ratio and specified the threshold to be 1/2 the peak signal voltage (A). In this case $z = y/\delta\sqrt{2} = 2.18$. The probability for a noise pulse to exceed y will be:

$$P(x>y) = 1/2 \operatorname{erfc}(2.18) = 1.014 \times 10^{-3}$$

(See Table C-1, Appendix C.)

The average time, T, an impulse will cross the threshold y, will be:

$$T_f = \frac{1}{BW \cdot P_{(x>y)}}$$ BW = 2.5 Hz the bandwidth of the system

then

$$T_f = \frac{1}{2.5 \cdot 1.014 \times 10^{-3}} = 394.48 \text{ seconds}$$

approximately 1 pulse crossing in 400 seconds on the average.

Since there may be time limiting circuits which require incoming signals to be received at intervals no greater than T_M, the probability that a pulse will be detected is $P_M = T_M/T_f$. If 40 seconds between pulses are required before the system is reset, the $P_M = 40/394.48 = 0.1014$ (one chance in ten that there will be a threshold crossing in a 40-second gate).

If a quadrature detector is used and a phase sequence is required, a threshold crossing coherent with any of four phases must be followed by its specified adjacent phase. The first pulse becomes the standard; the second pulse can have two positions out of four which determine rotating sense; the third pulse can only have one position out of four, and the fourth pulse only one position out of four, thus completing one cycle of doppler: $P_{p1} = 1$, $P_{p2} = 0.5$, $P_{p3} = 0.25$, $P_{p4} = 0.25$, $P_m = 0.1014$

$$P_{pt} = (1) \cdot (P_m \cdot P_{p2}) \cdot (P_m \cdot P_{p3}) \cdot (P_m \cdot P_{p4})$$

$$P_{pt} = 0.0000326 \text{ (1 in 30698)}$$

In order to produce an output, 1 cycle of doppler must be received without a reverse in doppler sense. On the average, noise might produce a 1 cycle count in T_{f_T} seconds

$$T_{f_t} = \frac{T_f}{P_{pt}} = \frac{40 \times 4}{3.3 \quad 10^{-5}}$$

$$T_{f_t} = 4.85 \times 10^6 \text{ seconds}$$

$$T_{f_t} = 56.116 \text{ days}$$

assuming 40-second maximum gate before reset.

If the maximum gate was 400 seconds before reset,

then

$$P_{pt} = (1) \times (1 \times 0.5) \times (1 \times 0.25) \times (1 \times 0.25) = 1/32 = 0.03125$$

$$T_{ft} = 4 \times 400/_{0.03125} = 51200 \text{ seconds}$$

$$T_f = 14.22 \text{ hours}$$

It was assumed that a clear choice of one of four phases would be chosen if a noise pulse entered a phase detector; this is not true. In a product detector where the pulse appears, it is multiplied by the reference sine wave in whatever phase it happens to be. The normal signal at a slightly different frequency than the reference sweeps through the phase detector always reaching a maximum (A) and in sequence, triggering each phase when reaching the threshold. Noise is an impulsed signal occurring in a selected phase or in between two phases. If it occurs in between two phases a reduction of apparent noise results. A reduction in noise voltage reduces the probability it will cross a threshold. Noise pulses in the form of (sin X/X) multiplied by sin y for various random phase angles will vary the efrc(Z) error function. A computation was made, integrating noise pulses over π radians and erfc was found to be 8.73×10^{-4} instead of 1.014×10^{-3} for a Z = 2.18. The effect will be to increase the time between crossings from 394 seconds to 1145 seconds on the average. Therefore, the timed gate probability, Pm, will be 40/1145 0.03493 (40-second gate); four-phase probability Pp will be 1.3×10^{-6}; $T_{f_t} = 1.232 \times 10^8$ sec. $(4.40/1.3 \times 10^{-6})$ average time to generate 1 cycle or $T_{f_t} = 3.9$ years.

In addition, noise impulses can possibly cause two-phase detectors to trigger whereas a doppler can only trigger one at a time. If logic is used to determine that two phases were triggered within 0.4 seconds X 1/BW, a reset could be ordered, further reducing the false alarm rate.

Assuming a series of noise pulses does get through to send an alert, a second pulse train must be sent to indicate a change in position as going from one doppler cycle to the next, reducing the probability still further.

Consider a more simplified system: no phase quadrature detection, just a doppler cycle indication; with the S/N and threshold as before, the false alarm rate would be as follows:

(a) $P(x>y) = 1.014 \times 10^{-3}$ and $T_f = 394.48$ seconds. (BW = 2.5 Hz)

(b) Each pulse would then indicate a cycle of doppler in error.

(c) It would take two pulse position computations to establish motion.
Tf x 2 = 788.96 seconds (average).

(d) To establish a track, two stations must report with the same noise probability 788.96 seconds.

(e) Therefore, it would be expected that a false track would be highly irregular and would on the average make a new tracking point every 13 minutes, each tracking point 8 to 16 ft toward the receiving station.

(f) If we added a time gate, Tm, of 40 seconds,

then $P_{(x>y)} = 1/10 \cdot 1.014 \cdot 10^{-3}$:

to establish the first pulse, 394.48 seconds:

to establish two pulses, $\frac{394.48}{1/10} = 3944.8$ seconds:

for the two pulses from an arbitrary start,

$$T_f = 3944.8 + 394.48 = 4339.28 \text{ seconds.}$$

$$\text{average } T_f = 1.2 \text{ hours}$$

1.2 hrs. = average time to generate a false track of 2 points
2.3 hrs. = average time to generate a false track of 3 points
3.4 hrs. = average time to generate a false track of 4 points
4.5 hrs. = average time to generate a false track of 5 points

It becomes obvious if a target does not move more than 8 to 16 ft toward a receiving site in one hour, it ceases to be a bona fide target and can be rejected.

3.4 PROBABILITY OF TRACKING AND DETECTION

The probability of detection and tracking is defined as

$$P_D(t) = \lim_{N \to \infty} \cdot \frac{n(t)}{N}$$

$$P_T(t) = \lim_{N \to \infty} \cdot \frac{n(t)}{N}$$

where n is equal to the number detections or tracking outputs that exceed a threshold (t) out of a total number of tries N. This assumes paths evenly distributed about the periphery but selected at random. The threshold has been selected to be 2.182 times the noise to reduce false alarms to less than 1×10^{-3} as described in Section 2.7.2. In order to compute the probability, it is assumed that the reflected signal is dependent only on range; this is not necessarily true, but to reduce complications this assumption is made. The antenna patterns of each sensor overlapping vary the detection sensitivity as is shown in Figures 27, 28, and 29, see Table 14. To make a detection and determine the probability P_D (t), approaches are made normal to the surveillance zone at random noting the range. Any station picking up an intrusion constitutes a detection. Tracking, P_T (t), require at least two stations to pick up an intrusion.

Table 14. Probability Table

Figure	Power (watts)	Range Limit (km)	Number of Sensors	Sensor Spacing (meters)	90% Probability Detect (km)	90% Probability Track (km)
27	24	1.1	112	450	9.05	8.94
28	30	1.35	75	675	9.25	9.06
29	24	1.1	84	600	9.02	8.8

Note Noise figure = 2 dB, antenna gain = 7 dB transmitter, antenna gain = 6 dB receiver

Figures 27, 28 and 29 have been used as examples to graphically compute the probability of detection and tracking at various ranges from the center. Figure 51 shows probability of detection and tracking by range.

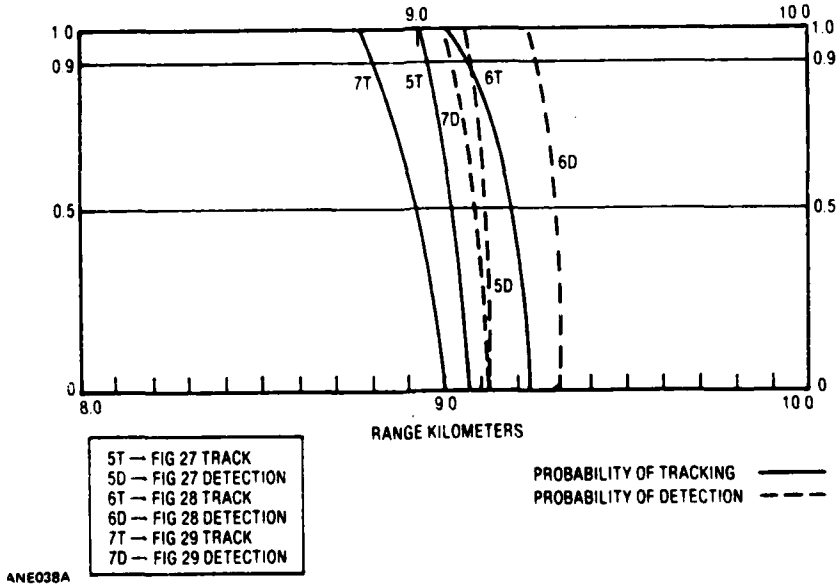

Figure 51. Probability of Detection and Tracking

3.5 TRACKING SYSTEMS

In this study two types of measurements can be made. Measure only doppler cycles, and measure range by a dual-doppler differential phase scheme. Actually three systems can be generated, doppler only, range-dual doppler and a combination of both.

The doppler-only system must be given an initial starting location by supporting sensors sited on the outer perimeter of the surveillance zone. This system is in accordance with the original study request for an HSS, Hybrid Sensor System. The starting location can be determined by a more complicated computation using four receiving stations; however, the receiving range must be increased or the number of receivers on the perimeter doubled. The computations would require more time; the overall effect is a more costly system if four sensors are needed for tracking.

A dual-doppler system which uses the doppler from two close CW carriers provides a means for determining range, eliminating the need for additional sensors to provide an initial starting location of an intruder. Actually, it is a phase measurement between two doppler responses which in the illustrated case (100 kHz) has 0 to 360 represent 600 ellipse-type isophase loci. Along the major axis it represents 1500m. Determining the ellipse number from two receiving sensors pinpoints the location of an intruder. However, the tracking accuracy of this measurement, 20m, is much less accurate than measuring the 60 MHz doppler. The advantage is that a tracking point is independently determined for each measurement pair. A loss of signal would not impair the final tracking points.

A highly accurate system can be developed using a combination of phase range and 60 MHz doppler. The less accurate phase range establishes a starting location. The range is updated by doppler and compared to a new range measurement. The repeated range measurement reduces the RMS error as the square root of the number of samples. The computation is more complicated and requires more time to compute the track.

3.6 RECEIVING SENSOR

As described in Section 2.6, the complication in designing a dual receiver with dual channels of 59.9 and 60 MHz that are phase-lock-looped tuned and mixed to 5 MHz, further mixed to 45 and 55 kHz and product-detected, is quite feasible. The critical part of the design involves the "nulling" antenna which should maintain a 60 dB reduction in direct signal reception. A second critical design is the synchronous filter, which should provide a 40 dB reduction of a constant phase signal (static clutter - direct signal). Both of these critical designs permit the phase measurement, determination of sign, and discrimination of the doppler signal to eliminate foliage-type nuisance signals.

A 0.01 Hz low frequency detected passband cutoff is considered to be adequate to measure personnel at very slow walking speeds, while 1.25 Hz is specified as the high frequency passband cutoff. Separate channels, 10 to 50 Hz, for a wider band are recommended to allow higher speed targets such as vehicles and aircraft to be tracked.

A 2 dB noise figure can be easily achieved. Lower noise figures are achievable, i.e., to 1 dB at an additional cost. It would cost less to raise the transmitting power 1 dB, or the antenna gain 1 dB.

3.7 TRACKING CENTER

The installation at the center of annular ring consists of the illuminating transmitter, data link terminal, tracking computer, displays and alarms, monitoring personnel and a security force.

The transmitter has been discussed as being a 20-watt highly stable CW, VHF equipment feeding a vertical omnidirectional antenna array 80 ft high. The data link is a wire pair either underground or above the ground with parallel redundant connecting lines to the central location. The data terminal is required to decode the pulse code transmissions. The decoding can be done separately or within the computer.

3.7.1 COMPUTER REQUIREMENTS

Two computer approaches were made during the study. One was the use of a CYBER 7600 made by CDC, and the other an SEL Model 3277 (System Engineering Lab) computer; both have high speed and considerable memory capability but are much too expensive; a smaller computer such as the NOVA II (Data General Corporation) could do the decoding, computation and display for all stations. The other approach was to use small microcomputers of the Commodore 2001, Apple or TRS80 type. The latter types cost under $1000 while the NOVA II runs $20,000. All the computers have the capability of accepting data link information and decoding it to computer language at the expected speeds. Considering 30 intrusions around the periphery with pairs of stations reporting, 60 data bursts per second, 60 ms long can be expected to overload the data link rather than computer decoding. Possibly 3 or 4 separate lines would be necessary to bring in data from each quadrant. An alternate solution is to increase transmission speed from 1000 pps to 5 kbps; each transmission could then be made in 10 ms. The transmission time also varies with the type of system used, i.e., doppler only or doppler and range (one or two burst transmissions).

The CYBER, SEL, and NOVA II can decode each transmission and direct it to the proper computer address. In the case of a Kalman Filter computation, each address must have a time tag added to the input data. No time tag is necessary for the incremental doppler or range measurement algorithms.

If the small microcomputer of the Commodor 2001-8 is used, a separate computer can be reserved for each intrusion. One computer can be used to display the complete 60 to 120 stations; an alarm from any segment would be displayed and would activate a second computer displaying just that sector as shown in Figure 15. Additional intrusions would be added to the first computer and directed to display the sector response on additional devices. The displays would be held until reset.

3.7.2 DISPLAYS AND ALARMS

Security personnel monitoring the intrusion system are required to direct a security force to intercept the intruders. How many sectors and the speed of the attack will determine the reaction. How efficiently this can be done depends upon the display and alarm.

As soon as a discriminated detection is made on one station, an "alert alarm" should be sounded (audible) and a display showing which sector of the 120 is being activated. A second detection on an adjacent station should indicate a "full alarm" and a single sector display which is activated. A second detection not adjacent would provide a second "alert" and display it on the overall display. Additional "full alarms" would be displayed on a separate device.

There are a number of means for displaying an intrusion track. The most common is the CRT (cathode ray tube) generally available on all computers. Second, there is the hard copy printer, using either type or high resolution dot matrix printing. The typewriter necessary to make the hard copy would need to have tractor feed to allow reverse paper feed. The advantage of hard copy is that a permanent copy sometimes necessary in legal controversies. Another type of hard copy is an X-Y pen plotter; it provides a continuous curve and it can also provide a much larger plot, 36 in. x 36 in. with much greater resolution. It would be reasonable to have both the CRT display and a hard copy.

Additional algorithms could be added to the program to predict the time the intrusion will cross the baseline between receiving stations. Visually, this could be estimated by security monitor personnel. It would be difficult to put the computation on hard copy for curved or zig-zag paths; the prediction would be constantly changing, causing overprinting of previous prediction. This is more easily done on a CRT. The size of the display depends upon the number of personnel using the display and the resolution necessary. For a very large group a large screen display can be used. These displays are 8 ft x 8 ft and are projection CRT types; their usefulness is probably limited to VIP demonstrations.

4. CONCLUSIONS

From experience and investigations, we conclude a VHF (60 MHz) bistatic CW doppler intrusion sensor can be made and is practical for protecting the proposed surveillance zone.

The results of the study have shown that we will have sufficient signal level to track an intruder within a surveillance zone, 1 km wide and 8 km from a center, forming an annular ring containing 10^8 square meters. The propagation values were verified by field tests on the illuminating signal, reflective measurements on personnel and vehicles, and receiving site measurements. The study indicated a severe problem in separating the direct transmitted signal from the reflected intruder signal which is 100 dB below the direct signal. Two solutions have been presented, one using two-element receiving antenna producing a 60 dB null toward the transmitted signal, the other solution adding another 40 dB attenuation by using a synchronous notch filter.

Three algorithms were developed: one based on a Kalman Filter, the second based on an incremental tracking algorithm, and the third using a differential doppler phase measurement to produce a pseudo-range algorithm.

The Kalman Filter algorithm uses doppler only from two or more sensors and adds a time tag to the data to compute the intruder's velocity. An initial starting location is necessary to start the tracking. The algorithm is able to track an intruder with a temporary loss in signal through its velocity memory. A starting location is necessary to start the tracking. Large errors are generated by initial starting location errors, some causing divergence, other convergence depending upon geometry. Errors are also developed where the controller takes an erratic course. Errors are within a few meters given a proper starting location and a reasonable straight path.

The Incremental Tracking Algorithm uses doppler-only data with no time tag. Its tracking is not time dependent but requires an accurate starting location and cannot tolerate a loss in signal during the tracking. Tracking accuracy is within a few meters and not sensitive to erratic paths.

The dual doppler differential phase measurement which produces a pseudo-range establishes an intruder location continuously. No starting location is necessary nor does an erratic path disturb the computation of the track. However, no experimental data is available in verifying the expected range data to be within 20m. A scheme has been worked out which will improve the 20m accuracy to 2m by using the VHF doppler signal to updating the pseudo-range measurements; however, this algorithm has not been completed.

Criteria have been developed to determine RF coverage, which depends upon the number of receiving sensors and power (or sensitivity) to give a high probability of detection with a low false alarm rate. It can be expected to have a 90% probability of detection at 1.25 km from the sensor ring, and a 90% probability of tracking at 1.06 km with a false alarm rate of 1 in 56 days using quadrature detection processing. The processing

circuitry can be simplified, which will produce alarm rates of one in 1.2 hours or more elaborate considerations producing FARs of one in 3.9 years.

Jeep and helicopters were used in scenarios to intercept walking and running personnel, vehicles, and helicopter attacks. It was found that the jeep security force could respond adequately for intrusions involving personnel and vehicles but would require help from a helicopter if another helicopter was involved. It was found that the seven jeeps should be deployed on a concentric circular road 7 miles from the center to reduce the interception time. Security forces must stay out of the surveillance zone in order not to be detected and disturb the tracking.

Although the system can track multiple intruders around the surveillance zone, up to 30 or 40 depending upon the total number of receiving sensors, only a single target can be tracked within any segment composed of two sensors. The centroid of multiple targets within a segment would be tracked if they were moving as a group. Unpredictable tracking would occur if the group would scatter in all directions, producing positive and negative dopplers.

5. REFERENCES

The following references were used for information and data, especially on antennas and circuitry.

Antenna Engineering Handbook; Jasik, Henry, editor; McGraw Hill Book Company, 1962.

Area Intruder Track Study, P9131005 Technical Proposal; General Dynamics Electronics Division, August 1979.

Area Intruder Track Study Monthly Status Reports 1-14; Gehman, John B.; General Dynamics Electronics Division, March 1980 – April 1981.

Brief Analytical Geometry; Mason, Thomas E. and Hazard, Clifton T.; Ginn Company, 1935.

Communications Systems Engineering Theory; Sunde, Erling D.; John Wiley and Sons, Inc., 1969.

Computer Approximations; Hart, J. F. et al.; John Wiley and Sons, Inc., 1968.

Electronic Point Sensor, EPS; Gehman, John B., General Dynamics Electronics Division Tech Manual for Sandia Laboratories, USAF Prime Contract F-19628-77R-0229, SANDIA CONTRACT 03-9715, April 1980.

Estimation of Zone of Detection of the Single Wire Individual Resource Protection Sensor; Poirier, J. Leon; RADC TR-80-256, August 1980.

Handbook of Mathematical Functions, Applied Mathematics Series, 55; U.S. Department of Commerce NDS; U.S. Printing Office, June 1964.

"How Dangerous Is RF Radiation," QST; September 1978 p. 31.

Large Area Intruder Sensor System, R-80-042; Gehman, John B.; General Dynamics Electronics Division, December 1980.

Line Sensor Intrusion Detector System, R-71-008; Gehman, John B.; General Dynamics Electronics Division, March 1972.

MIL R 9673B Military Standard, Radiation Limits, Microwave and X Radiation Generated by Ground Equipment (as Related to Personal Safety).

Proceedings of the IRE, Volume 30; King, Ronald and Blake, F. G., Jr.; July 1942.

"The Propagation of Radio Waves through the Standard Atmosphere, OSRD," Summary Technical Report of the NDRC, Volume 3; Washington, D.C., 1946.

Radar Handbook; Skolnik, Merrill L. ; McGraw Hill Book Company, 1970.

Radio Amateur's Handbook, 54th Edition; ARRL; 1977.

Radio Engineering Handbook; Henney, Keith; McGraw Hill Book Company, 1935.

Radio Engineer's Handbook; Terman, Frederick; McGraw Hill Book Company, 1943.

Reference Data for Radio Engineers; Federal Telephone and Radio Corporation; 3rd Edition, Knickerbocker Printing Company, 1949; 5th Edition, ITT, H. Sams Company, 1972; 6th Edition, ITT, H. Sams Company, 1975.

San Diego County (Map) 1980 Edition; Thomas Brother Company, 1980.

Security Systems Development, R-79-083; Gehman, John B.; General Dynamics Electronics Division, December 1979.

"Two Remote Unattended Sensors Employing Electromagnetic Motion Sensing Techniques," Nineteen Annual Tri-Service Radar Symposium, Volume II, 1973.

"Weed an Intrusion Detection System," Gehman, John B.; First National Symposium on Law Enforcement, March 1967.

Patents related to intrusion detection sensors:

3,836,960	Sensor System, filed September 1974
3,761,908	Object Detection System, filed September 1973
3,731,305	Object Detection System, filed May 1973
3,706,982	Intrusion Detection System, filed December 1972
3,550,106	Object Detection System Utilizing Electromagnetic Waves, filed December 1970

APPENDIX A

MATHEMATICAL DERIVATIONS

APPENDIX A MATHEMATICAL DERIVATIONS

A.1 DERIVATION OF P AT F

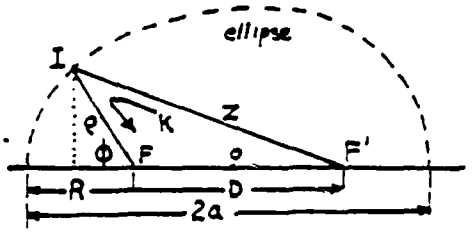

ANE046

I = intruder
Z = range to intruder from F^1
P = range to intruder from F
K = reflected range from F^1 to F
K = Z + P
R = distance to ellipse from F along major axis
D = distance between F and F^1
a = major axis
o = center of ellipse

$$Z^2 = (P\cos\phi+D)^2 + (P\sin\phi)^2$$

$$(K-P)^2 = (P\cos\phi+D)^2 + (P\sin\phi)^2$$

$$K^2 - 2KP+P^2 = P^2\cos^2 d+2DP\cos d + D^2 + P^2\sin^2 d \qquad \left\{ P^2\cos^2 d + P^2\sin^2 d = P^2 \right\}$$

$$K^2 - 2KP+P^2 = 2DP\cos d + D^2$$

$$P = \frac{K^2 - D^2}{2(K - D\cos\phi)}$$

A.2 DERIVATION OF Z AT F^1

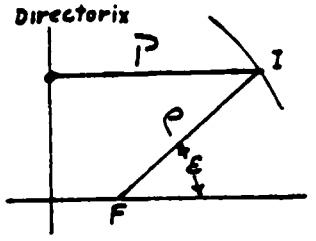

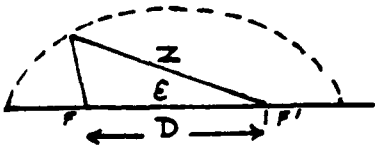

ANE047

ellipse defined by

$$P = \frac{eP}{1 - e\cos E}$$

where e is the eccentricity

$$e = D/2a$$

$$P = \frac{a}{e} = \frac{2a^2}{D}$$

correcting for a change in pole

$$Z = P\ P = \left(\frac{2a^2}{D} - \frac{D^2}{2}\right)$$

then: $$Z = \frac{eP}{1 - e\cos\epsilon}$$

$$Z = \frac{\frac{D}{2a}\left(\frac{2a^2}{D} - \frac{D^2}{2}\right)}{1 - e\cos\epsilon}$$

$$Z = \frac{a - \frac{D^2 a}{4a^2}}{1 - e\cos\epsilon}$$

$$Z = \frac{a - ae^2}{1 - e\cos\epsilon}$$

for use in computer program

$$Z = \frac{\frac{a}{e}(e^2 - 1)}{1/e - \cos\epsilon} = \frac{Q}{1/e - \cos\epsilon}$$

where $$Q = \frac{a}{e}(e^2 - 1)$$

A.3 DERIVATION ANGLE ϵ

Intersection of two ellipses rotated about F^1 measured from STN 1

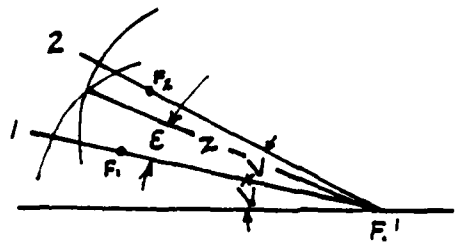

ANE048

Z is common to both ellipses at intersection

$$Z = \frac{Q_1}{1/e_1 - \epsilon_1} = \frac{Q_2}{1/e_2 - \cos\epsilon_2}$$

$$Q_1 = \frac{a_1}{e_1}(e_1^2 - 1)$$

$$Q_2 = \frac{a_2}{e_2}(e_2^2 - 1)$$

$$Q_1\left(\frac{1}{e_2} - \cos\epsilon_2\right) = Q_2\left(\frac{1}{e_2} - \cos\epsilon_1\right)$$

$$\left(\frac{Q_1}{e_2} - \frac{Q_2}{e_1}\right) = Q_1\cos\epsilon_2 - Q_2\cos\epsilon_1$$

let $S_1 = \left(\frac{Q_1}{e_2} - \frac{Q_2}{e_1}\right)$

$$S_1 = Q_1\cos(V - \epsilon_1) - Q_2\cos\epsilon_1$$

$$S_1 = Q_1\cos V \cdot \cos\epsilon_1 + Q_1\sin V \cdot \sin\epsilon_1 - Q_2\cos\epsilon_1$$

$$S_1 = \underbrace{(Q_1\cos V - Q_2)}_{S_2}\cos\epsilon + \underbrace{Q_1\sin V}_{S_3}\sin\epsilon$$

$$S_1 = S_2\cos\epsilon + S_3\sin\epsilon$$

to find $\cos\epsilon$

$$S_1 = S_2\cos\epsilon + S_3\sqrt{1 - \cos^2\epsilon}$$

$$(S_1 - S_2\cos\epsilon)^2 = S_3^2(1 - \cos^2\epsilon)$$

$$S_1^2 - 2S_1S_2\cos\epsilon + S_2^2\cos^2\epsilon = S_3^2 - S_3^2\cos^2 E\cos^2\epsilon$$

$$\underbrace{(S_2^2 + S_3^2)}_{(a)\ S_4}\cos^2\epsilon \underbrace{- 2S_1S_2\cos\epsilon}_{(b)\ S_5} + \underbrace{(S_1^2 - S_3^2)}_{(c)\ S_6} = 0$$

then

$$S_4\cos^2\epsilon + S_5\cos\epsilon + S_6 = 0$$

quadratic formula

$$\frac{-b \pm \sqrt{b^2 - 4ac}}{2a}$$

$$\underline{\cos \epsilon} = \frac{-S_5 \pm \sqrt{S_5^2 - 4 \cdot S_4 \cdot S_6}}{2 \cdot S_4}$$

positive sign only used in computation

in a similar manner

the sin ϵ can be found substituting $\sqrt{1 - \sin^2 \epsilon}$ for cos ϵ

the sin function is used to determine sign of the angle about zero.

A.4 DERIVATION "S"

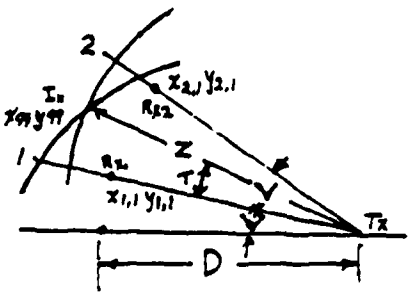

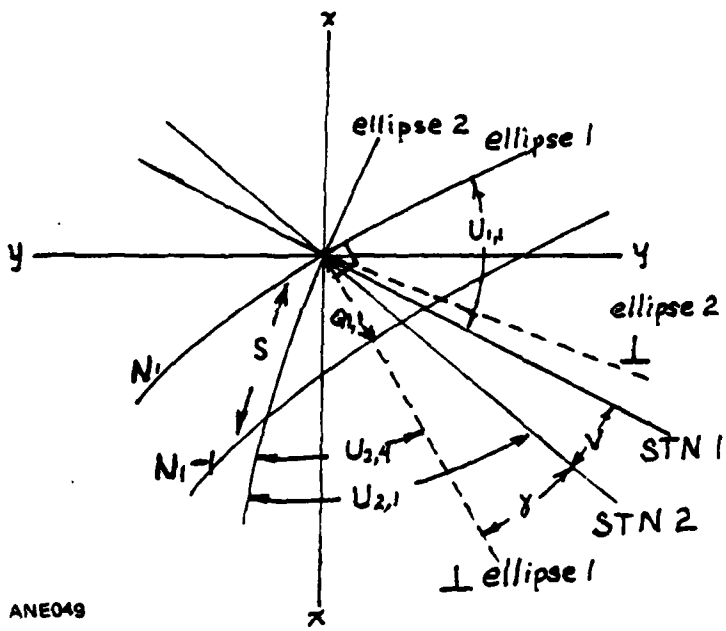

General Relations

D distance between Rec. and trans

L wavelength (RX & TX)

V sector angle (STN 1 & STN 2)
(STN 0 & STN 1)

Z distance from transmitter to intruder

N_1 ellispe number on STN 1

X_{99}, Y_{99} Intruder coordinates zero reference

X_{11}, Y_{11} coordinates of Rec. 1

X_{21}, Y_{21} coordinates of Rec. 2

R, range from receiver to ellipse along major axis

a_1 $R_1 = N_1 \times L/2$

a_1 1/2 major axis

$a_1 = R_1 + D/2$ 1/2 major axis

$b_1 = \sqrt{R_1^2 + R_1^2 D}$ 1/2 minor axis

Q_1 spacing between ellipses 1 & 1^1

$\angle T_1$ = angle between STN 1 and Z

$\angle T_2$ = angle between STN 2 and Z

$\angle U_{2,4}$ angle between ellipse 2(slope) and the perpendicular ⊥ to ellipse 1(slope)

$\angle U_{1,1}$ angle between ellipse 1 slope and station 1 major axis

$\angle U_{2,1}$ angle between ellipse 2 slope and station 2 major axis

$$Q_{1,1} = L/2 \quad 1 + \sqrt{(\sin T_1)\left(\frac{a_1}{b_1 - 1}\right)^2} \quad \text{approximation}$$

In incrementing one ellipse 1 to 1' (N_1 to $N_1 - 1$)
we slide along ellipse 2 to 1'(N_1–1)
the length of the slide is "S"

$S_1 = Q_{1,1}/\cos(\angle U_{2,4})$

$\angle U_{2,4} = \angle U_{2,1} - \gamma$

$\gamma = 90 - \angle U_{1,1} - V$

or $\angle U_{2,4} = \angle U_{2,1} - (90° - \angle U_{1,1} - \angle V)$

accounting for proper signs

$U_{2,4} = V + U_{2,1} - \angle N_{1,1} - 90°$

$$\angle U_{1,1} = \text{ARCTAN}\left(\frac{b_1}{a_1 \times (-\text{TAN}(T_1))}\right) \quad \text{slope of ellipse 1 at } \angle T_1$$

$$\angle U_{2,1} = \text{ARCTAN}\left(\frac{b_2}{a_2\ (-\text{TAN}(T_2))}\right) \quad \text{slope of ellipse 2 at } \angle T_2$$

APPENDIX B

DIFFERENTIAL PHASE ERROR DERIVATIONS

APPENDIX B

The residual differential phase error for the signal flow represented in Figure 63 is derived herein. Parameters used in this derivation are defined as follows:

β = Modulation index at transmitter

w = Angular frequency (rad/sec) of modulation

t = Time of observation

t_d = Time delay of reflected (doppler) signal relative to direct (reference) signal

$\Delta\phi(t)$ = Residual modulation signal time function

The carrier modulation is represented by

$$\phi_m(t) = \beta \cos wt$$

The differential modulation for a delay t_d is therefore

$$\begin{aligned}(t) &= \beta\cos wt - \beta\cos w(t - t_d) \\ &= \beta\left[\cos wt - \cos wt \cos wt_d - \sin wt \sin wt_d\right] \\ &= \beta\left[\cos wt\,(1 - \cos wt_d) - \sin wt \sin wt_d\right] \\ &= \beta A \cos(wt + \Delta\theta)\end{aligned}$$

where

$$\begin{aligned}A &= \left[\sin^2\theta + \cos^2\theta + 1 - 2\cos\theta\right]^{\frac{1}{2}} \\ &= \sqrt{2}\,(1 - \cos\theta)^{\frac{1}{2}} \\ \Delta\theta &= \tan^{-1}\left[(-\sin\theta)/(1 - \cos\theta)\right]\end{aligned}$$

and

$$\theta = wt_d$$

since

$$\cos X = 1 - \frac{X^2}{2!} + \frac{X^4}{4!} - \frac{X^6}{6!} + \cdots\cdots$$

$$\sin X = X - \frac{X^3}{3!} + \frac{X^5}{5!} - \frac{X^7}{6!} + \cdots\cdots$$

$$(1 \pm X)^{\frac{1}{2}} = 1 \pm 1/2X - 1/8\, X^2 + 1/16\, X^3 \cdots\cdots$$

then

$$A = \frac{wt_d}{\sqrt{2}} \left[1 - \frac{(wt_d)^2}{2!} + \frac{(wt_d)^4}{4!} - \cdots\cdots \right]^{\frac{1}{2}}$$

and

$$\Delta\phi = \tan^{-1} \frac{wt_d}{2} \left[\frac{1 - \frac{(wt_d)^2}{2!} + \frac{(wt_d)^4}{4!} - \cdots\cdots}{1 - \frac{(wt_d)}{3!} \quad \frac{(wt_d)^5}{5!} - \cdots\cdots} \right]$$

For wt_d much less than 1:

$$A \simeq wt_d / \sqrt{2} \qquad \text{(a ratio)}$$

$$\Delta\phi = \tan^{-1} (wt_d / 2) \qquad \text{(radians)}$$

APPENDIX C

PROBABILITY OF THRESHOLD CROSSING BY A GAUSSIAN RANDOM VARIABLE

APPENDIX C

Calculation of Probability of Threshold Crossing by a Gaussian Random Variable

The probability density function for a Gaussian single variable (noise) is given by (Reference 24):

$$p(x) = \frac{1}{\sigma\sqrt{2\pi}} e^{-(x - x_o)^2/2\sigma^2}$$

where

σ^2 = variance of random variable

x_o = mean value of variable

The parameters are normalized so that:

$$P(-\infty \leq x \leq \infty) = \int_{-\infty}^{\infty} p(x)dx = 1$$

$$m_1 = \int_{-\infty}^{\infty} xp(x)dx = x_o$$

$$m_2 = \int_{-\infty}^{\infty} x^2 p(x)dx = x_o^2 + \sigma^2$$

$$\mu_2 = m_2 - m_1 = \sigma^2$$

The probability distribution function is

$$P(x \leq y) = \int_{-\infty}^{y} p(x)dx$$

$$= 1/2 \left[1 + \text{erf} \left(\frac{x - x_o}{\sigma\sqrt{2}}\right)\right]$$

where

$$\text{erf } Z = \frac{2}{\sqrt{\pi}} \int_0^Z e^{-\lambda} \, d\lambda$$

The probability that the variable will exceed a given value is -:

$$P(x > y) = \int_y^{\infty} p(x)dx$$

$$= 1/2 \text{ erf} \left(\frac{x - x_o}{\sigma \sqrt{2}} \right)$$

$$= 1/2 \text{ erfc} \left(\frac{y - x}{\sigma \sqrt{2}} \right)$$

Table C-1 lists erfc(Z), erfc(Z1/2) and 20 $\text{Log}_{10}(Z)$ for $1 \leq Z \leq \sqrt{10}$

Evaluation of the function erfc(Z) is based on the polynomial approximation 5703 from Hart* (see Table C-2).

$$\text{erfc}(x) \approx e^{-x^2} \frac{P(x)}{Qx}$$

where

$$P(x) = P_o + Px + P_2x^2 + P_3x^3 \cdot$$

$$Q(x) = Q_o + Q_1x + Q_2x^2 + Q_3x^3 + Q_4x^4$$

and

$$P_o = 6.13375290544$$

$$P_1 = 6.1772457672$$

$$P_2 = 2.8501392633427$$

---

*J. F. Hart, et al.; Computer Approximations, John Wiley and Sons, Inc. 1968.

$P_3 = 0.56409091955032$

$Q_o = 6.13375455943$

$Q_1 = 13.098326849962$

$Q_2 = 11.497651079822$

$Q_3 = 5.0472398277593$

$Q_4 = 1.$

Table C-3 is a listing of the BASIC program which used to produce Table 1.

Table C-1. erfc(Z), erfc(Z)/2, and 20 Log_{10}Z for $1 \leq Z \leq \sqrt{10}$

Amplitude Ratio Z	Decibels 20 Log_{10} Z	erfc(Z)	Error Rate erfc(Z)/2
1			
2	6		2.339E-03
2.108	6.48		1.435E-03
2.182	6.78		1.014E-03
2.390	7.57		3.616E-04
2.626	8.39		1.020E-04
2.828	9.03		3.167E-05
3.015	9.59		1.004E-05

Table C-2. Evaluation of Function erfc(Z)

1/X*2	TABLE VAL	PARAM	ERFC(PARAM)	PROB. ERROR	RATIO	SNR/DB
.500	0.4754641	1.414	4.550E-02	2.275E-02	1.41	3.01
.490	0.4766765	1.429	4.335E-02	2.168E-02	1.43	3.10
.480	0.4779026	1.443	4.123E-02	2.061E-02	1.44	3.19
.470	0.4791426	1.459	3.913E-02	1.956E-02	1.46	3.28
.460	0.4803973	1.474	3.706E-02	1.853E-02	1.47	3.37
.450	0.4816664	1.491	3.501E-02	1.751E-02	1.49	3.47
.440	0.4829507	1.508	3.301E-02	1.650E-02	1.51	3.57
.430	0.4842503	1.525	3.103E-02	1.552E-02	1.52	3.67
.420	0.4855657	1.543	2.910E-02	1.455E-02	1.54	3.77
.410	0.4868972	1.562	2.720E-02	1.360E-02	1.56	3.87
.400	0.4882454	1.581	2.535E-02	1.267E-02	1.58	3.98
.390	0.4896105	1.601	2.354E-02	1.177E-02	1.60	4.09
.380	0.4909931	1.622	2.178E-02	1.089E-02	1.62	4.20
.370	0.4923936	1.644	2.007E-02	1.004E-02	1.64	4.32
.360	0.4938124	1.667	1.842E-02	9.211E-03	1.67	4.44
.350	0.4952501	1.690	1.683E-02	8.414E-03	1.69	4.56
.340	0.4967072	1.715	1.529E-02	7.647E-03	1.71	4.69
.330	0.4981842	1.741	1.382E-02	6.912E-03	1.74	4.81
.320	0.4996817	1.768	1.242E-02	6.210E-03	1.77	4.95
.310	0.5012003	1.796	1.109E-02	5.543E-03	1.80	5.09
.300	0.5027406	1.826	9.823E-03	4.912E-03	1.83	5.23
.290	0.5043032	1.857	8.636E-03	4.318E-03	1.86	5.38
.280	0.5058889	1.890	7.526E-03	3.763E-03	1.89	5.53
.270	0.5074983	1.925	6.496E-03	3.248E-03	1.92	5.69
.260	0.5091322	1.961	5.546E-03	2.773E-03	1.96	5.85
.250	0.5107914	2.000	4.678E-03	2.339E-03	2.00	6.02
.240	0.5124767	2.041	3.892E-03	1.946E-03	2.04	6.20
.230	0.5141891	2.085	3.190E-03	1.595E-03	2.09	6.38
.220	0.5159293	2.132	2.569E-03	1.284E-03	2.13	6.58
.210	0.5176984	2.182	2.028E-03	1.014E-03	2.18	6.78
.200	0.5194975	2.236	1.565E-03	7.827E-04	2.24	6.99
.190	0.5213276	2.294	1.177E-03	5.884E-04	2.29	7.21
.180	0.5231899	2.357	8.581E-04	4.291E-04	2.36	7.45
.170	0.5250856	2.425	6.036E-04	3.018E-04	2.43	7.70
.160	0.5270161	2.500	4.070E-04	2.035E-04	2.50	7.96
.150	0.5289826	2.582	2.607E-04	1.304E-04	2.58	8.24
.140	0.5309869	2.673	1.571E-04	7.853E-05	2.67	8.54
.130	0.5330303	2.774	8.770E-05	4.385E-05	2.77	8.86
.120	0.5351148	2.887	4.456E-05	2.228E-05	2.89	9.21
.110	0.5372421	3.015	2.008E-05	1.004E-05	3.02	9.59
.100	0.5394141	3.162	7.744E-06	3.872E-06	3.16	10.00

ANE050

Table C-3. Basic Program Used to Produce Table C-1

```
100   Rem ***** PROGRAM ERRORFUN.BAS *****
110   Rem *****       R.C.WEAVER       ******
120   Rem *****  4/07/80 (Rev 6/26) ******
130   Rem ***** ERFC(X) CALCULATION WITH INDEX 5703 *****
140   Dim A$(80)
150   A$=".###   &.&&&&&&&   ##.###   #.####!!!!   #.####!!!!   ##.##   ##.##"
160   Fact1=1 : Fact2=Log(10)
170   Data 6.13375290544,6.1772457672,2.8501392633427
180   Data 0.56409091955032,6.1337S455943,13.098326849962
190   Data 11.497651079822,5.0472398277593,1
200   Restore 170
210   Read P00,P01,P02,P03,Q00,Q01,Q02,Q03,Q04
220   Goto 230
230   @ P00 : @ P01 : @ P02 : @ P03
240   @ Q00 : @ Q01 : @ Q02 : @ Q03 : @ Q04
250   Input"START, STOP, INCREMENT   ",S1,S2,S3
260   Q=0
270   @ : @ : @ : @
280   Start'printer$=Chr$(23)+Chr$(23)
290   @"PRINT TABLE: 1=YES"; : Input Q1
300   If Q1=1 Then @ Start'printer$
310   Print"1/X*2  TABLE VAL    PARAM  ERFC(PARAM) PROB. ERROR";
320   Print"   RATIO  SNR/DB"
330     For Y=S1 To S2 Step S3
340     X=1/Sqr(Y)
350     P=(((P03*X)+P02)*X+P01)*X+P00
360     Q=((((Q04*X+Q03)*X+Q02)*X)+Q01)*X+Q00
370     Ratio=P/Q
380     Error'funct=Ratio/Exp(X*X)
390     Table'val=Ratio*X
400     Snr'amp=Fact1*X : Snr'db=20*Log(Snr'amp)/Fact2
410     @ Using A$,Y,Table'val,X,Error'funct,Error'funct/2,Snr'amp,Snr'db
420     Next Y
430   Stop'printer$=Chr$(20)+Chr$(20)
440   If Q1=1 Then @ Stop'printer$
450   @ : @ : @ : @
460   End
```

ANE051

APPENDIX D

ANTENNA IMPEDANCE

(Referenced in Section 2.3.2.2)

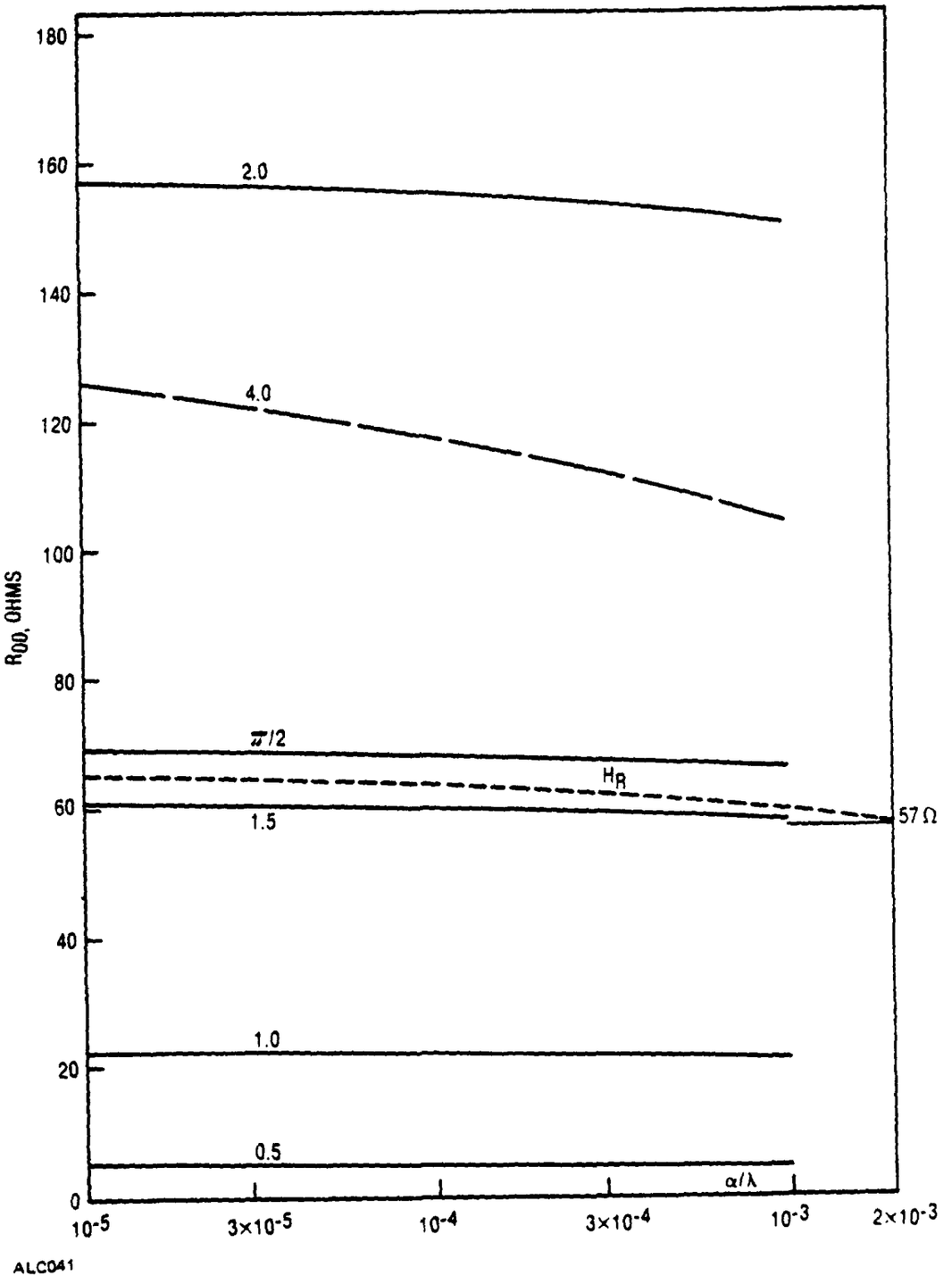
180
160
140
120
100
80
60
40
20
0
R_{00}, OHMS
2.0
4.0
$\pi/2$
H_R
1.5
57 Ω
1.0
0.5
α/λ
10^{-5}
3×10^{-5}
10^{-4}
3×10^{-4}
10^{-3}
2×10^{-3}
ALC041

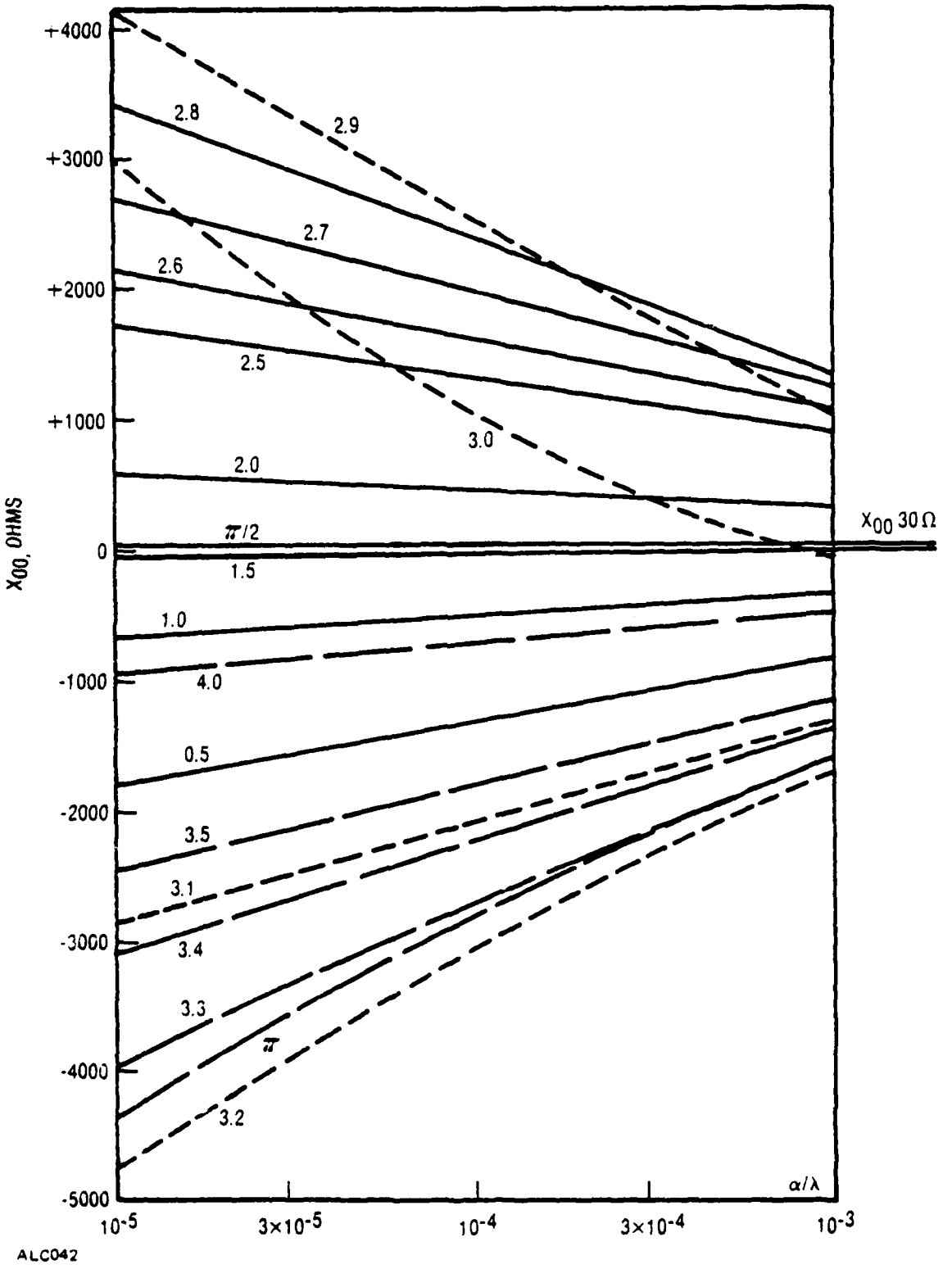
+4000
+3000
+2000
+1000
0
-1000
-2000
-3000
-4000
-5000
X_{00}, OHMS
2.8
2.9
2.7
2.6
2.5
3.0
2.0
$\pi/2$
X_{00} 30 Ω
1.5
1.0
4.0
0.5
3.5
3.1
3.4
3.3
π
3.2
10^{-5}
3×10^{-5}
10^{-4}
3×10^{-4}
10^{-3}
α/λ
ALC042

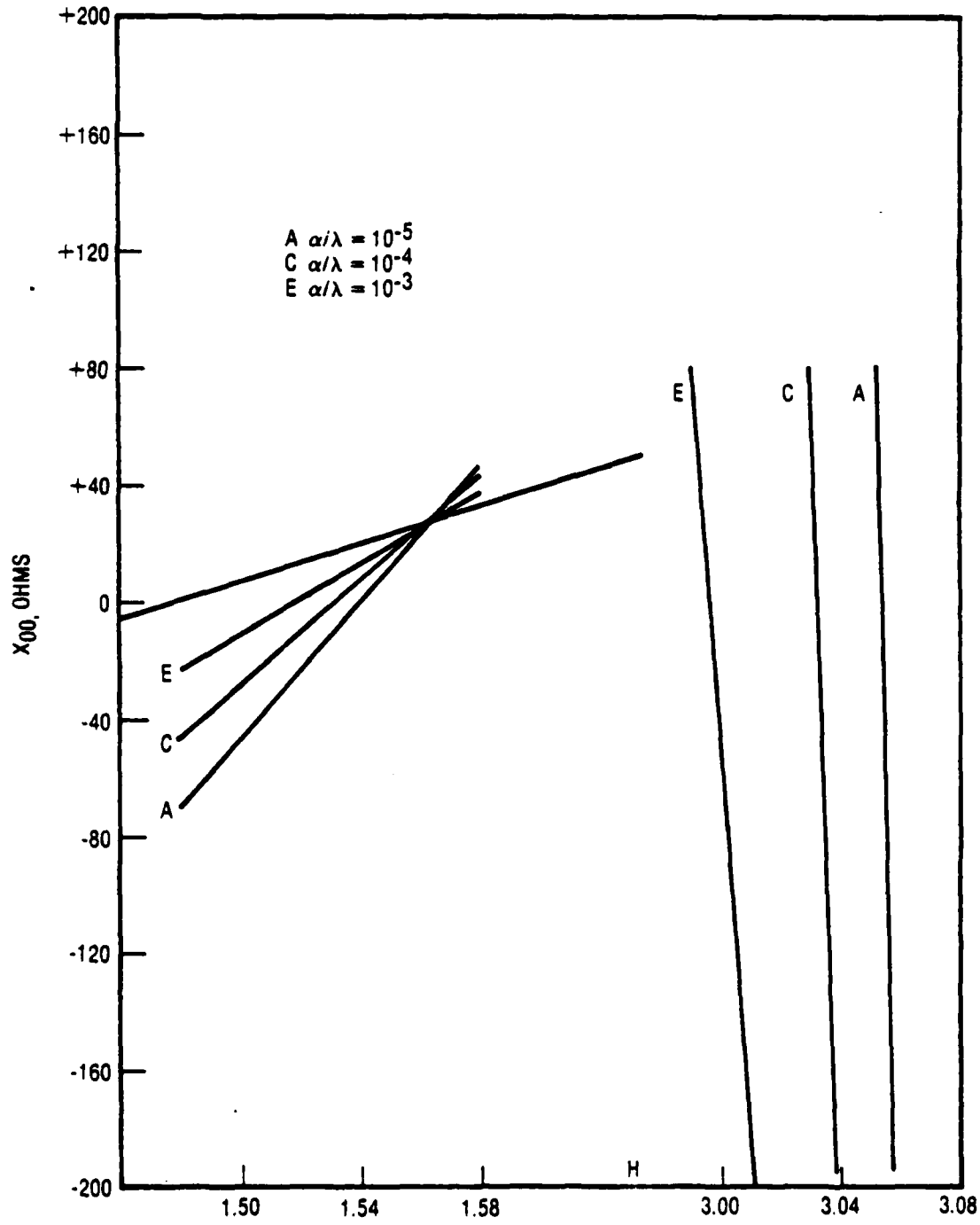
+200
+160
+120
+80
+40
0
-40
-80
-120
-160
-200
A $\alpha/\lambda = 10^{-5}$
C $\alpha/\lambda = 10^{-4}$
E $\alpha/\lambda = 10^{-3}$
E
C
A
E
C
A
H
1.50
1.54
1.58
3.00
3.04
3.08
X_{00}, OHMS

ALC043

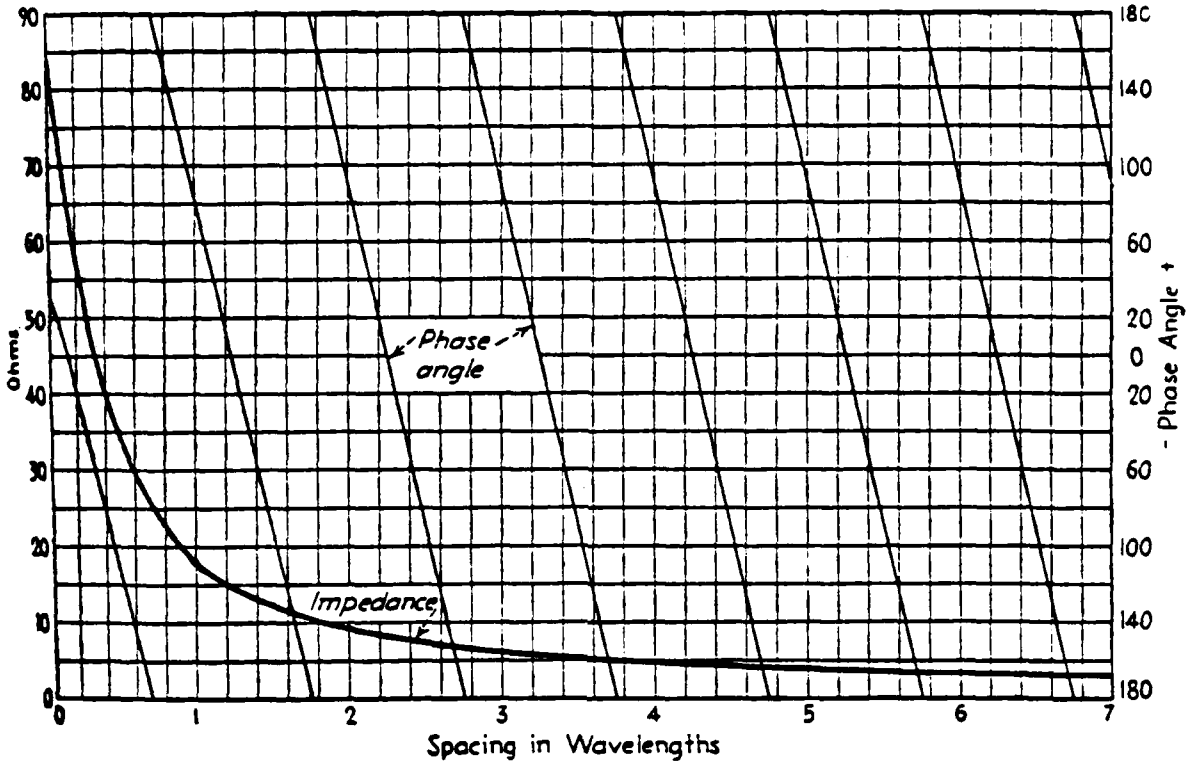
90
80
70
60
50
40
30
20
10
0
Ohms
0
1
2
3
4
5
6
7
Spacing in Wavelengths
180
140
100
60
20
0
20
60
100
140
180
- Phase Angle +
Phase angle
Impedance

ALC044

APPENDIX E

POLAR ANTENNA PLOTS

(Referenced in Section 2.3.2.7)

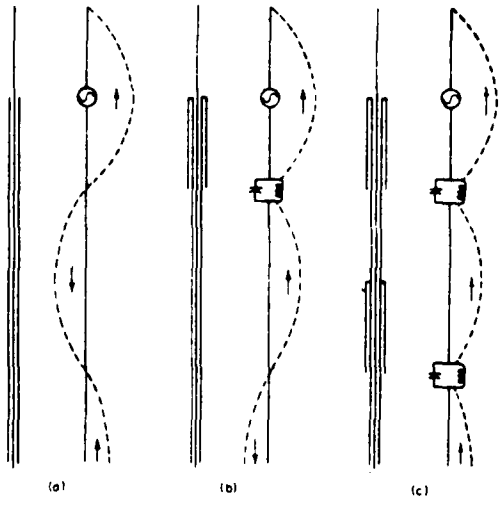

A. Evolution of multiple-skirt coaxial antenna.

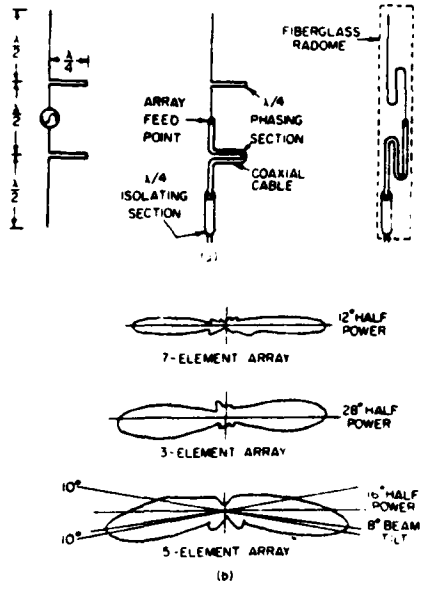

B. Development of modified Franklin array.

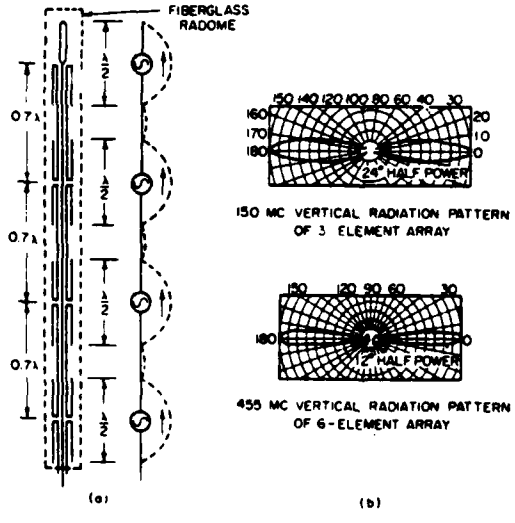

C. Series-fed, collinear array.

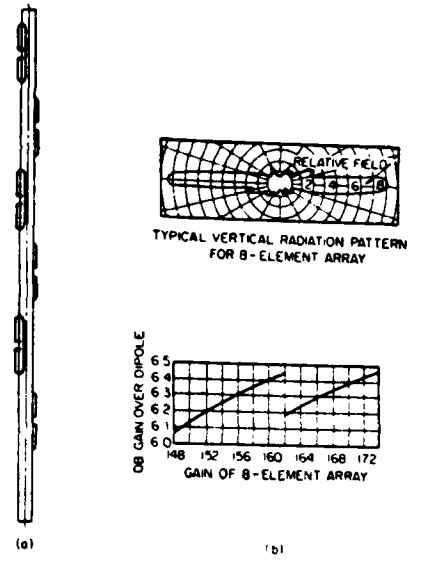

D. Mast-mounted, collinear array.

E. Gain in Decibels over a Half-wave Dipole for Various Arrays.

Antenna	Number of elements					
	2	3	4	6	7	8
Shirted coaxial	1-2	2-3				
Modified Franklin	...	3.2	4.0	...	7.2	
Series-fed collinear	...	4.23	...	6.5		
Mast-mounted collinear array	...	....	3.1	6.2	...	6.3

ANE017

Figure E-1. Antennae and Gain Table (from Jasick)

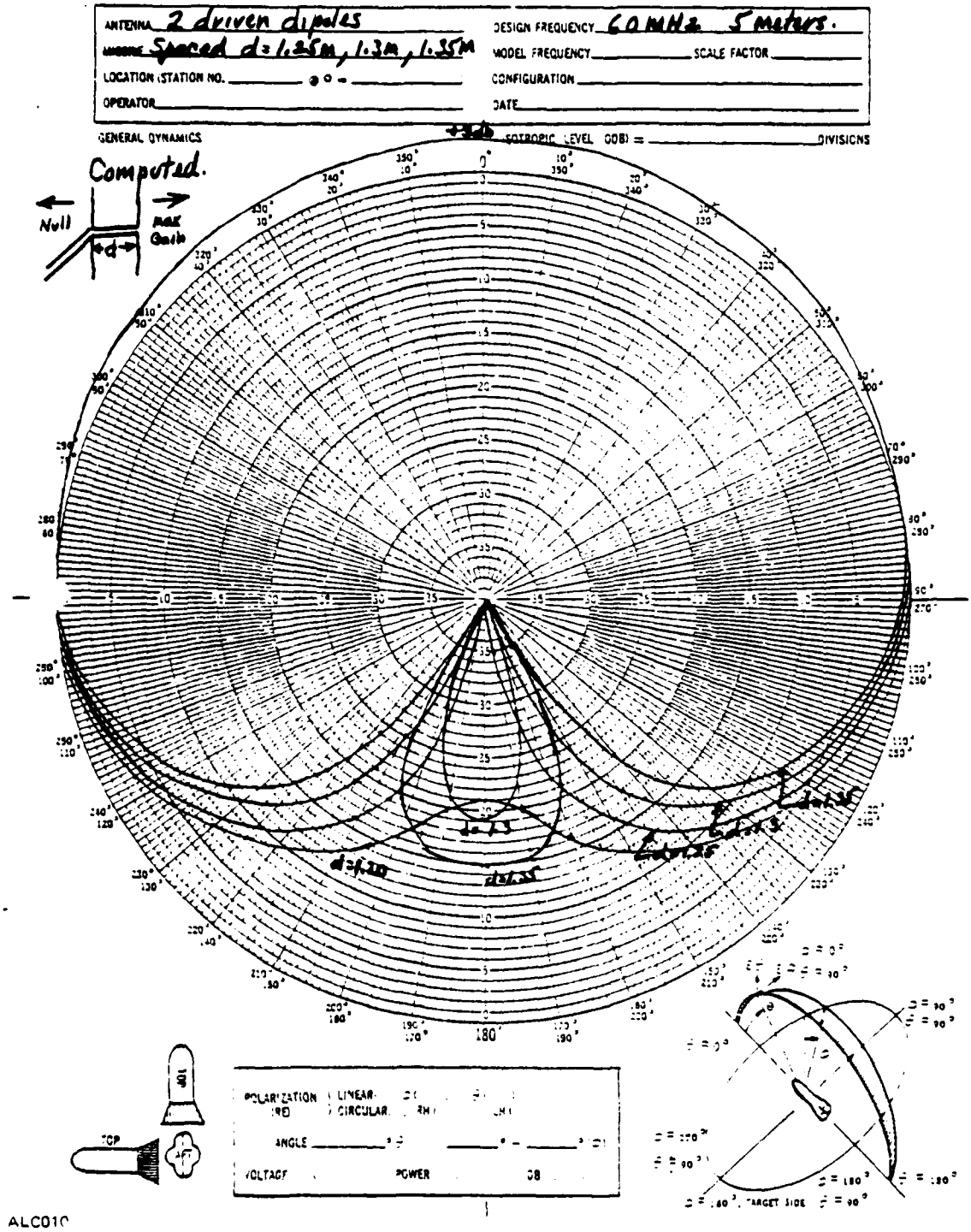

Figure E-2. Antenna Pattern

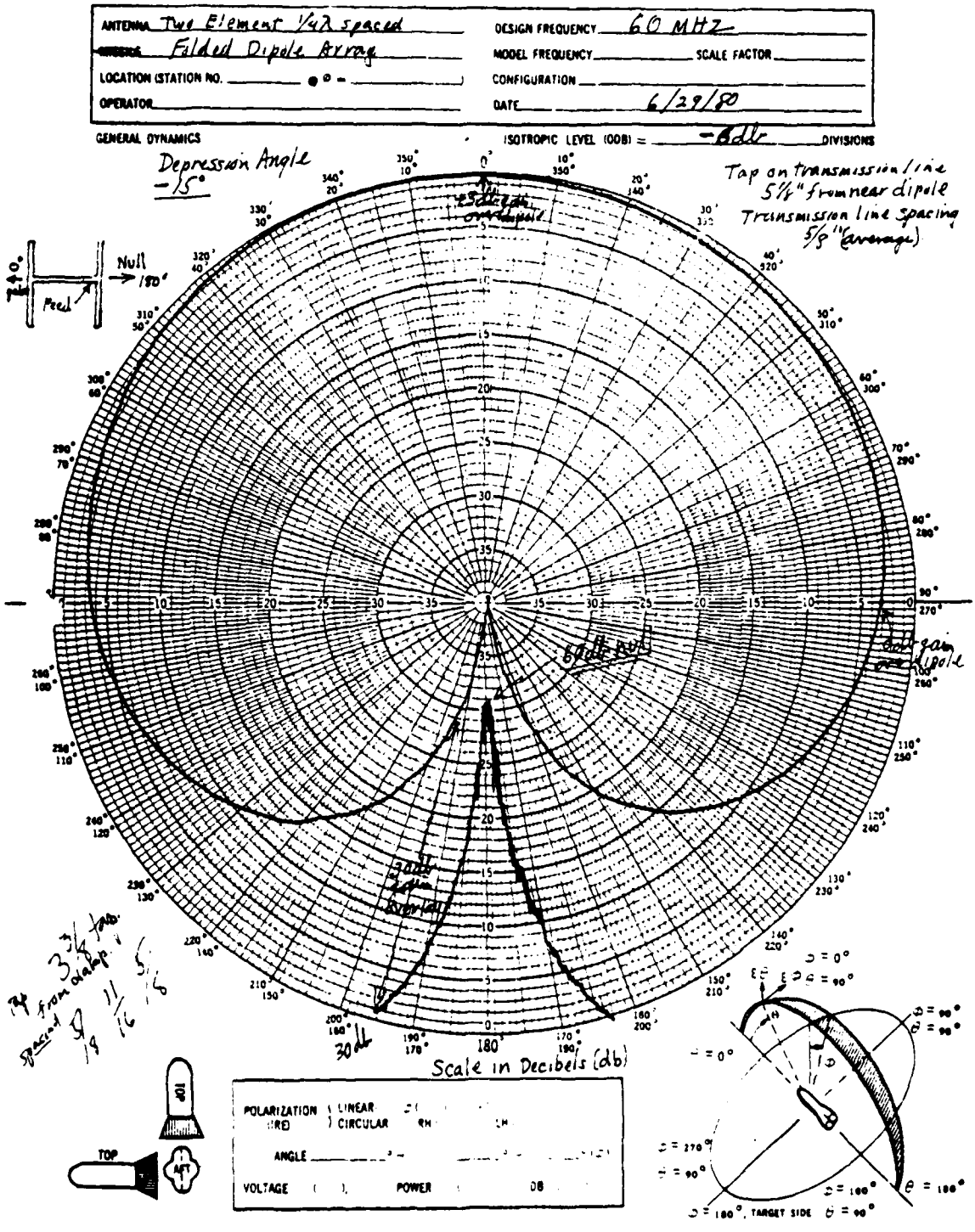

Figure E-3. Antenna Pattern Test

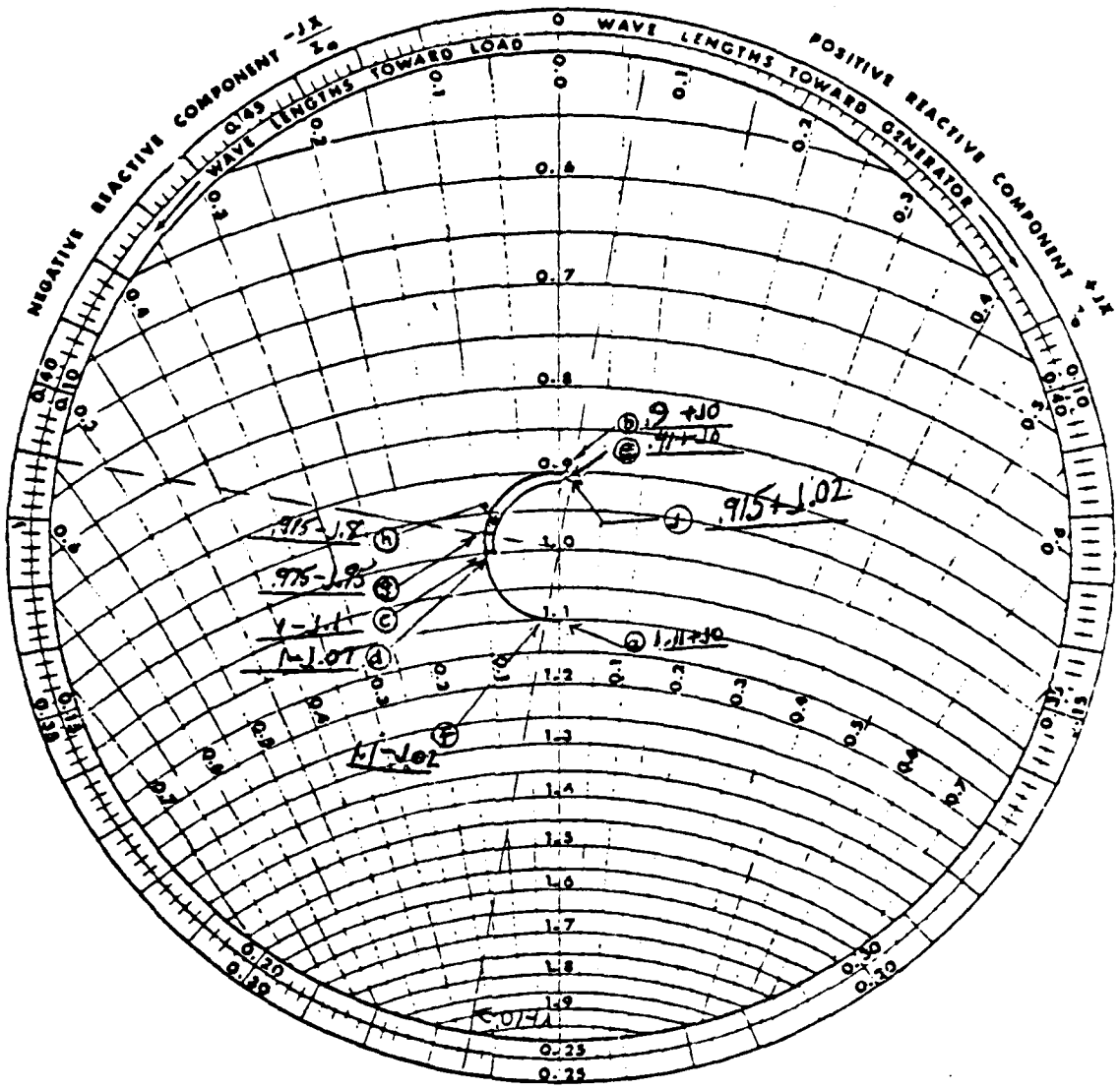

SMITH CHART REFERENCES

MICROWAVES	APR 1964 P46
MICROWAVES	NOV 1967 P38
QST	JAN 1960 P28
QST	JAN 1966 P22
QST	FEB 1961 P30
MICROWAVES	JUN 1962 REPRINT
JASICK 1462	ANTENNA ENGINEERING HANDBOOK PG 31-4

ALC023

Figure E-4. 2:1 Smith Chart

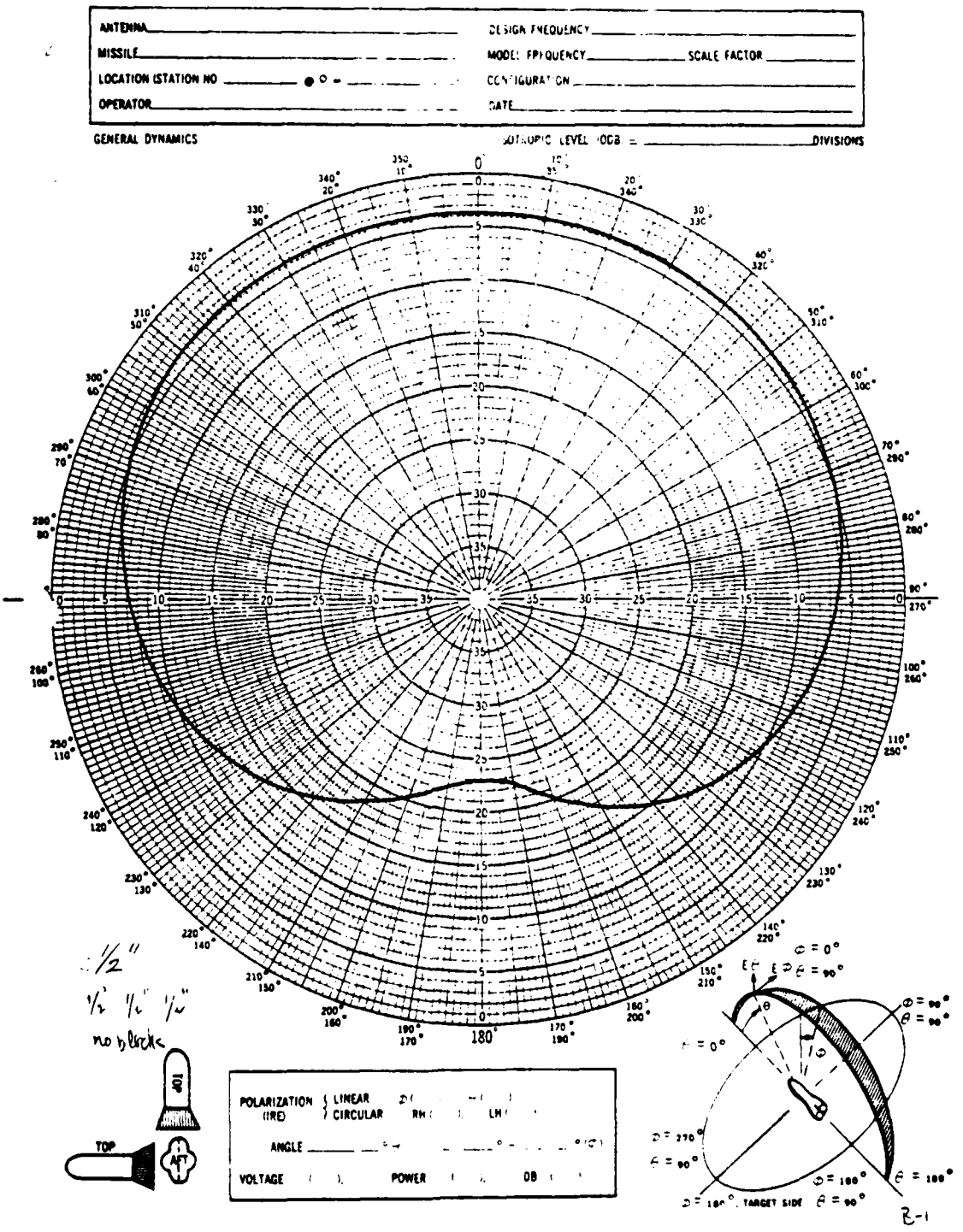

Figure E-5. Cut No. 4

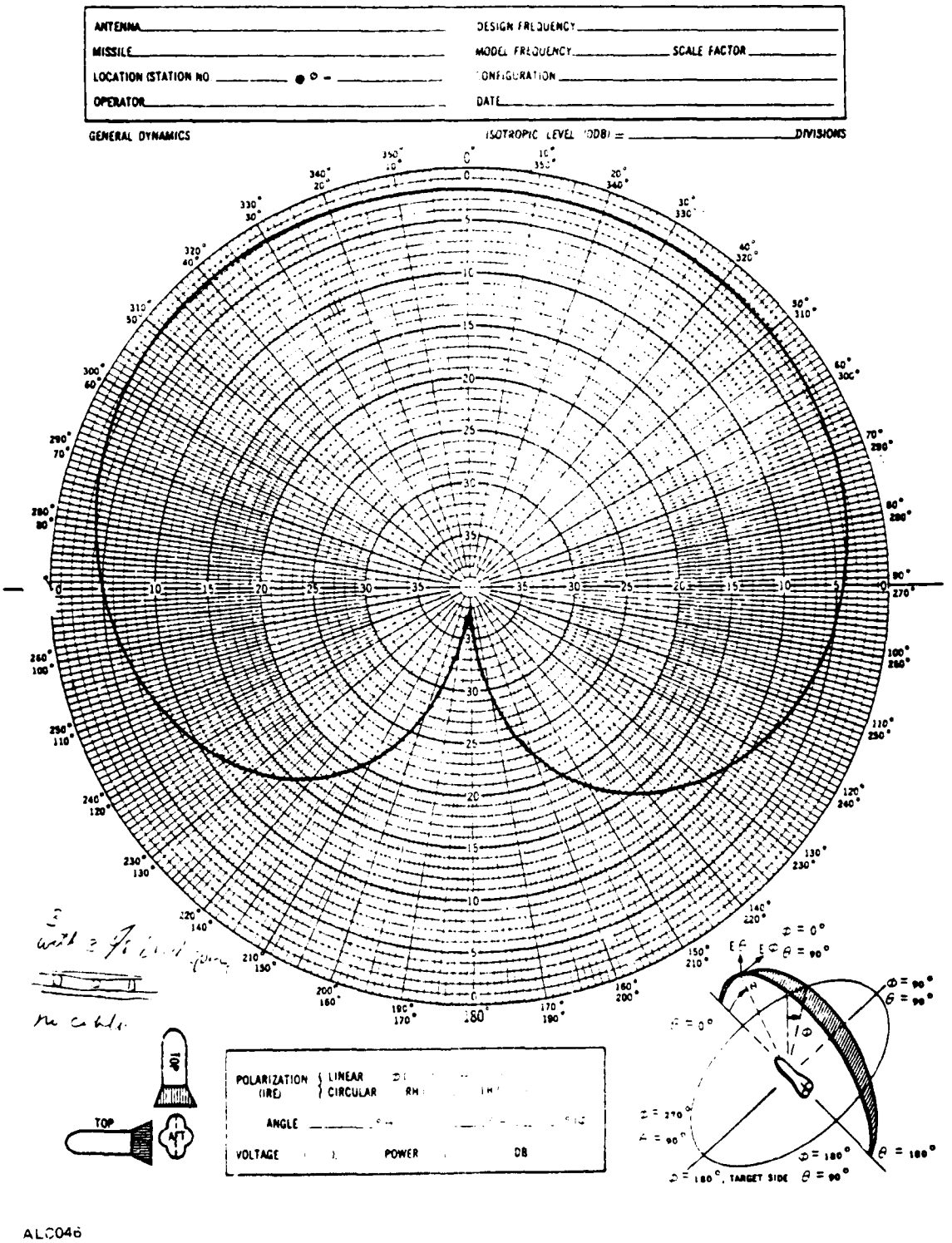

Figure E-6. Cut No. 7

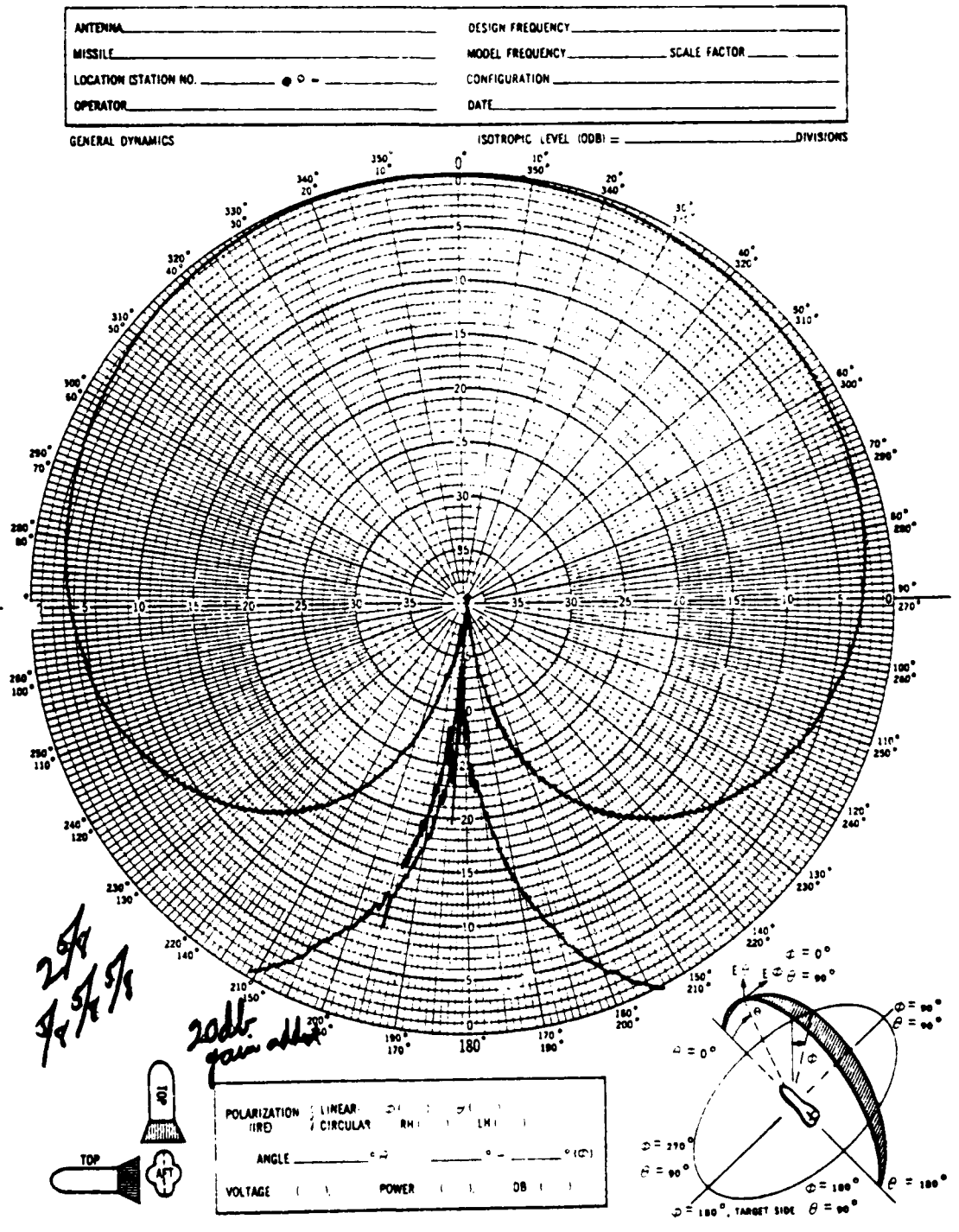

Figure E-7. Cut No. 17

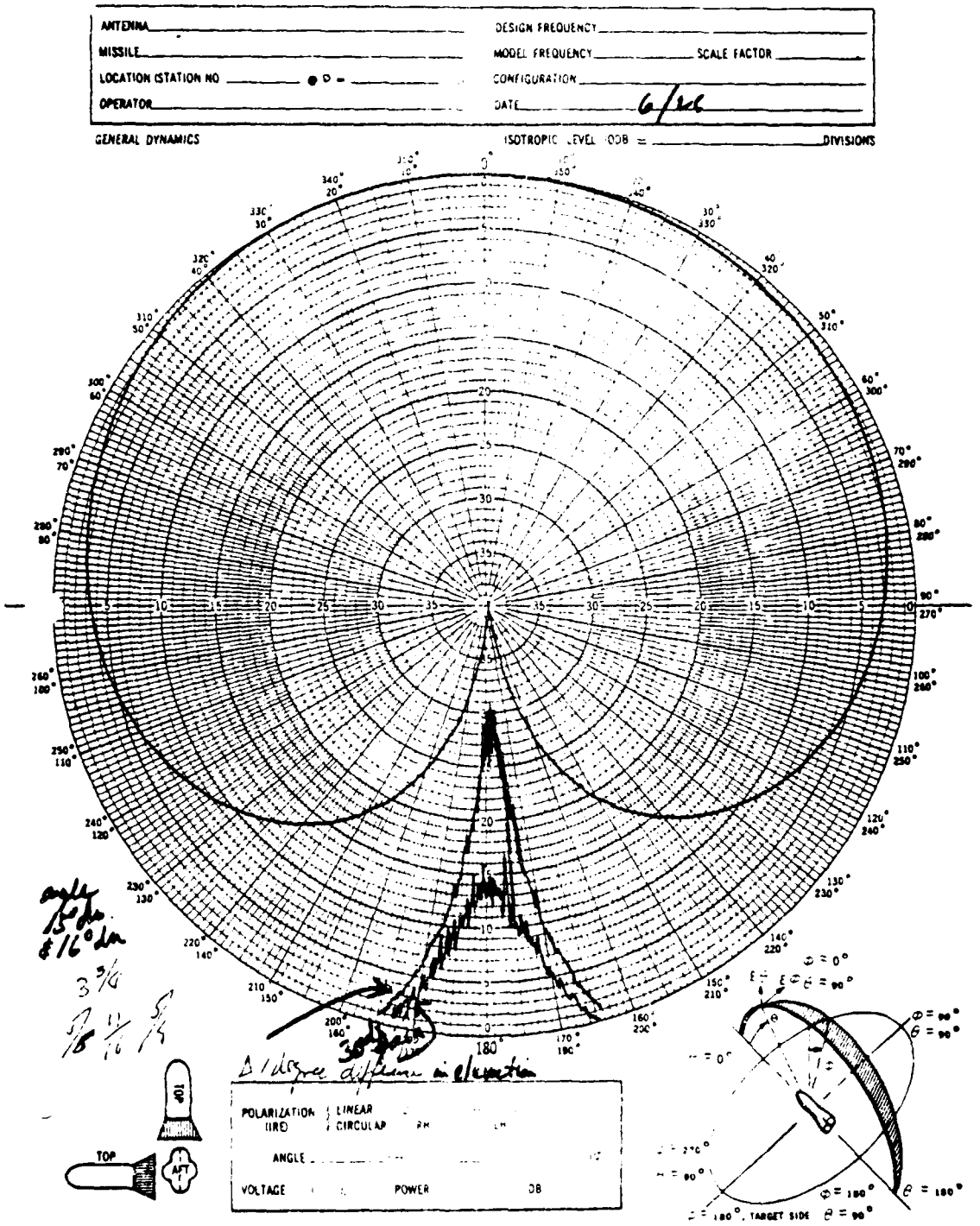

Figure E-8. Cut No. 29

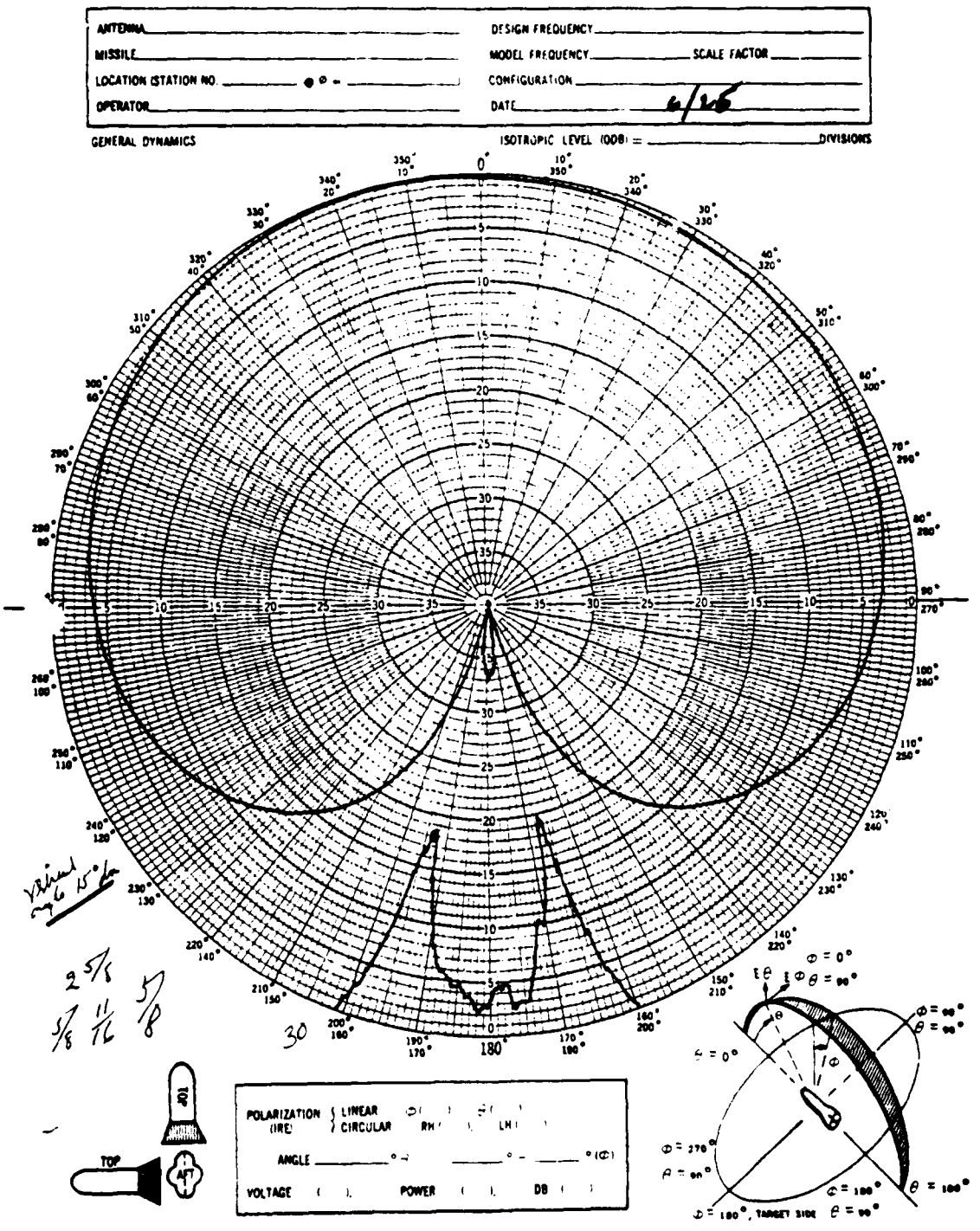

ALC049

Figure E-9. Cut No. 27

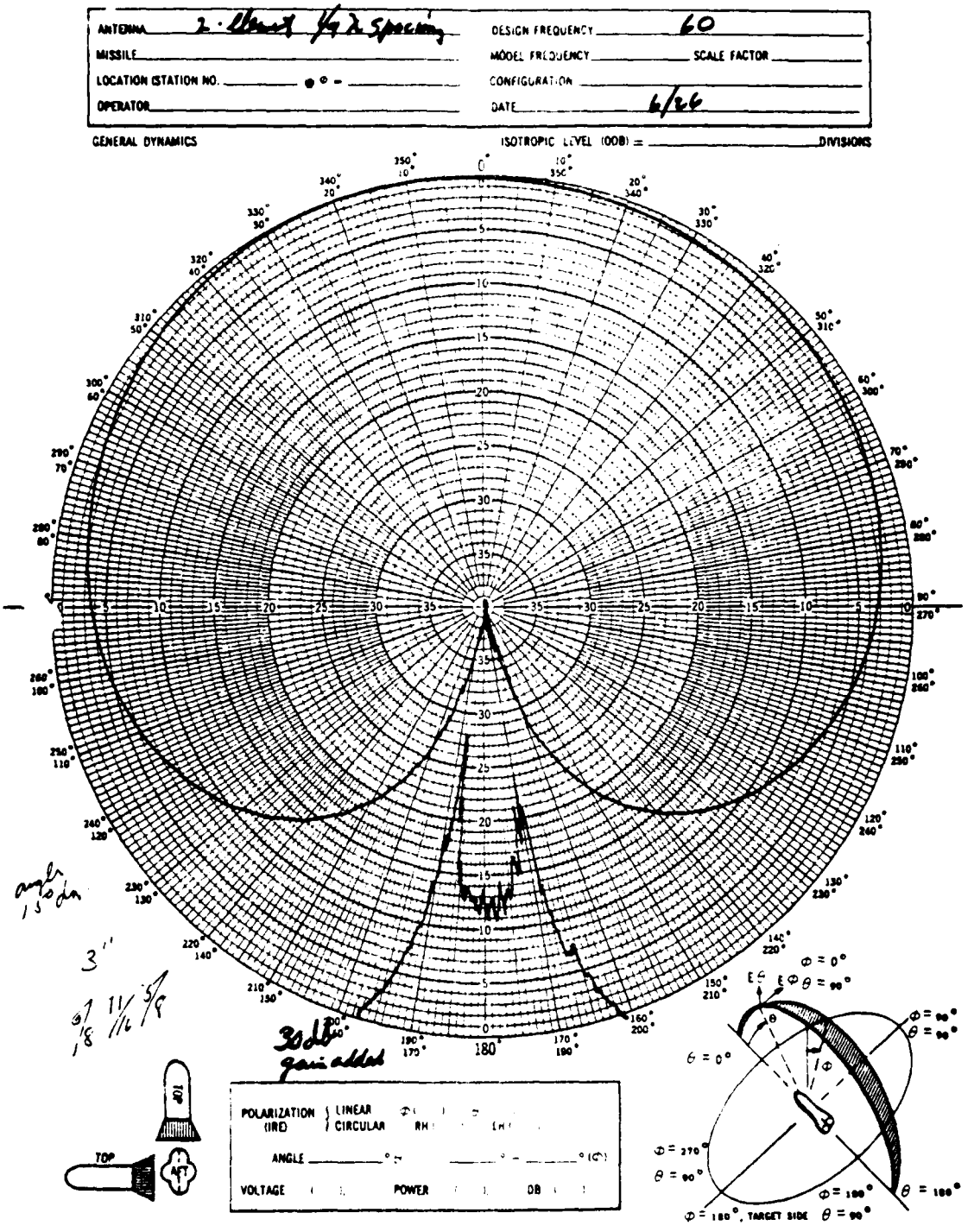

Figure E-10. Cut No. 28

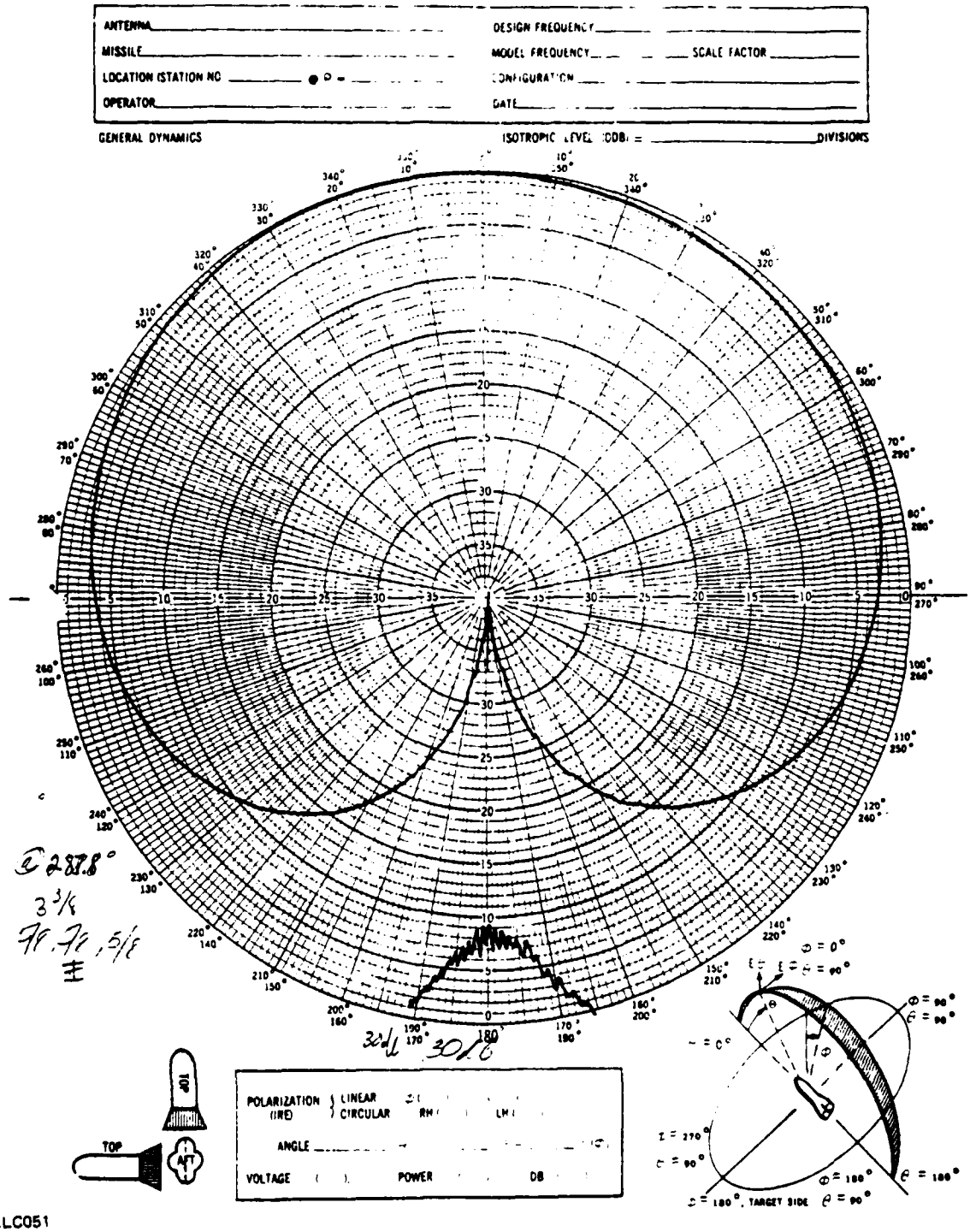

Figure E-11. Cut No. 30

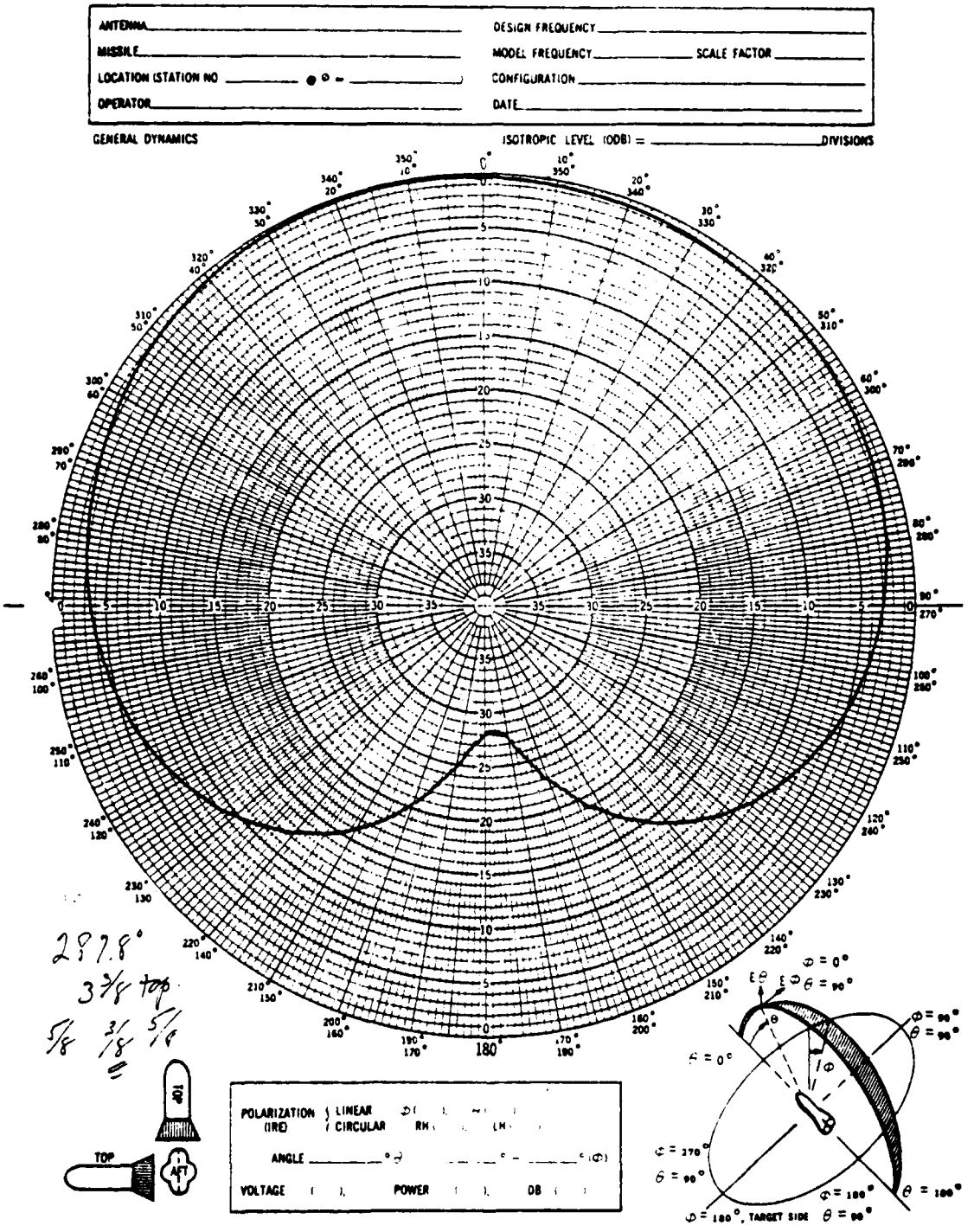

Figure E-12. Cut No. 31

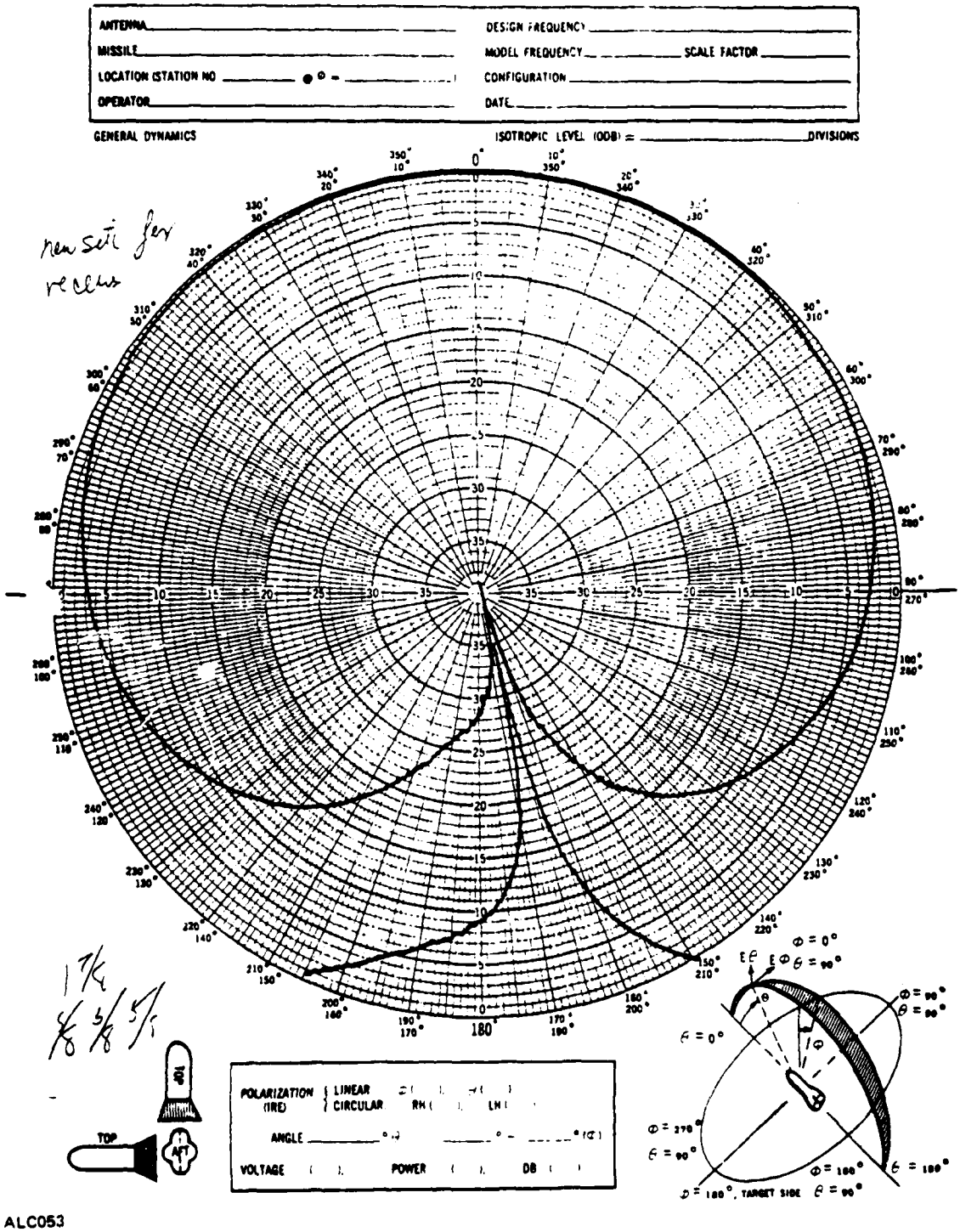

Figure E-13. Cut No. 16(a)

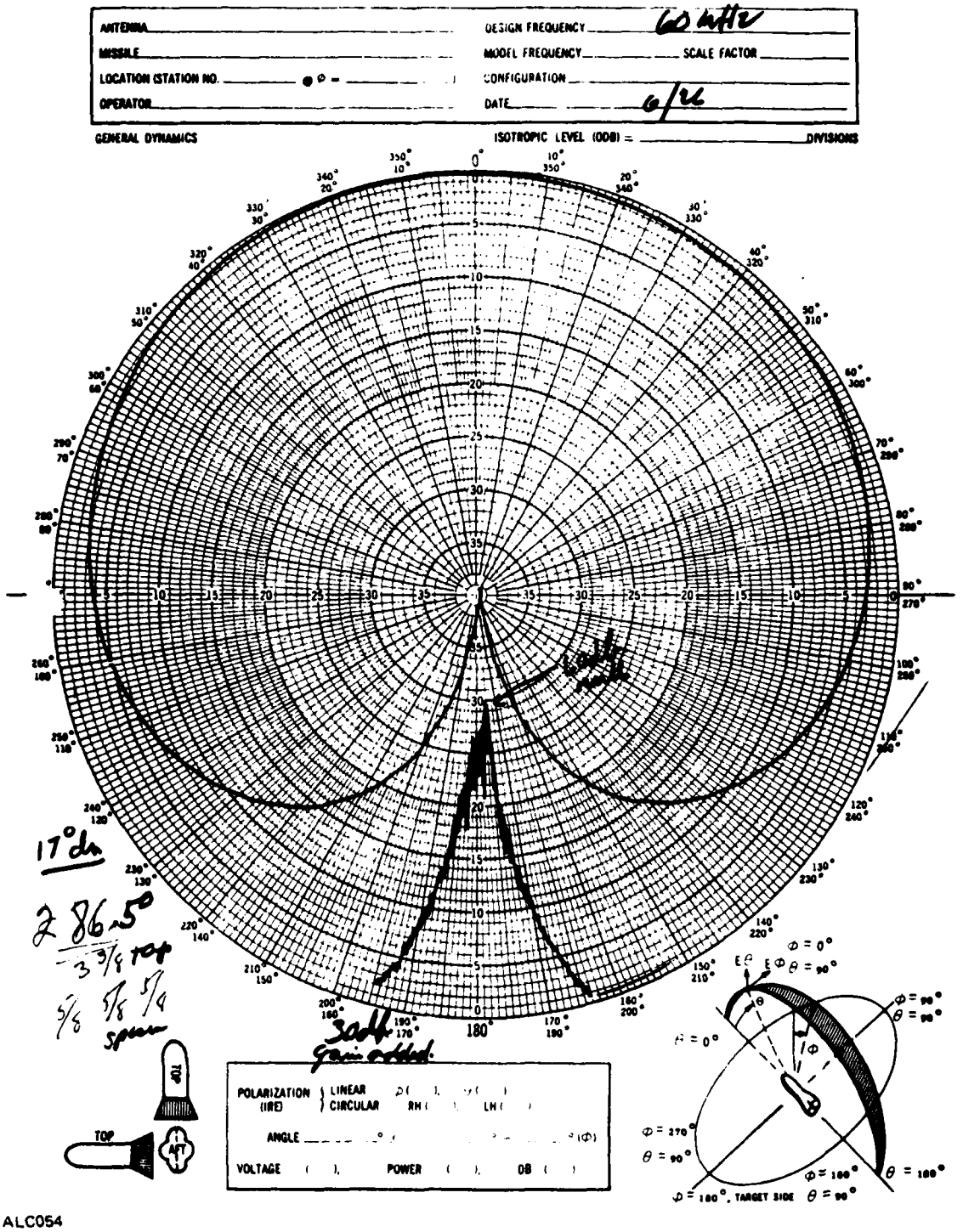

Figure E-14. Cut No. 30(a)

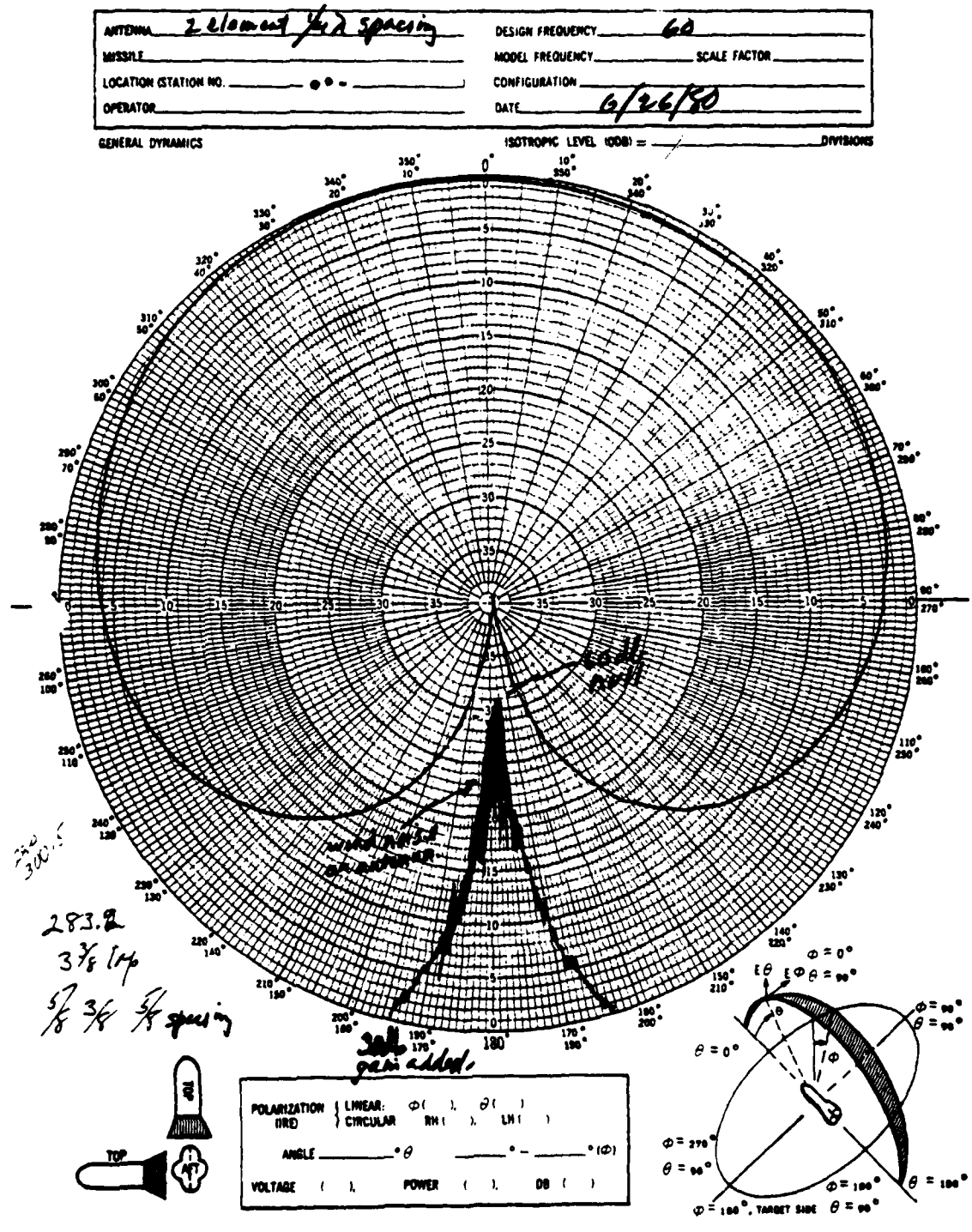

ALC055

Figure E-15. Cut No. 31(b)

APPENDIX F

TRACKING SIMULATIONS

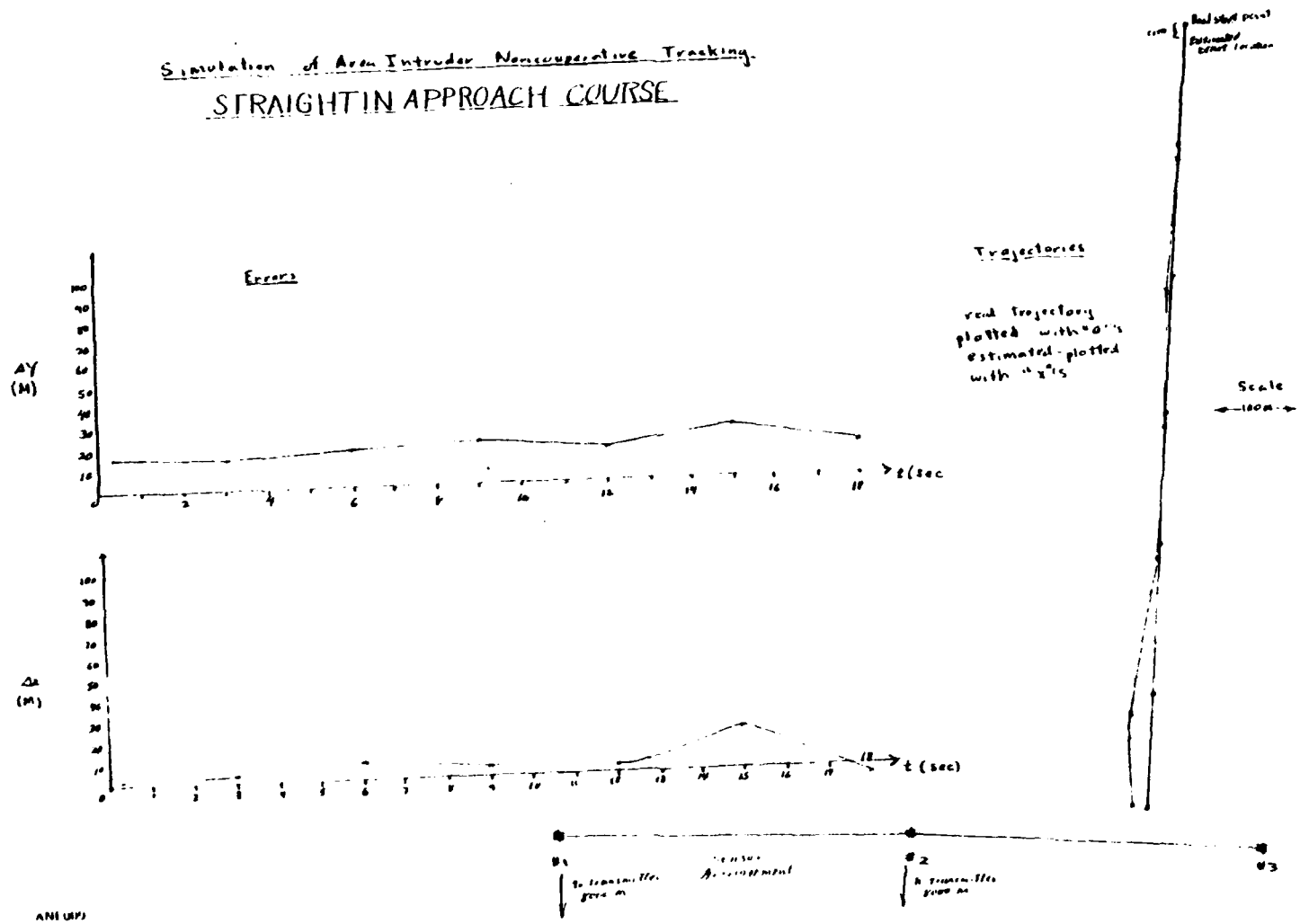

Figure F-1. Straight-In Approach Course

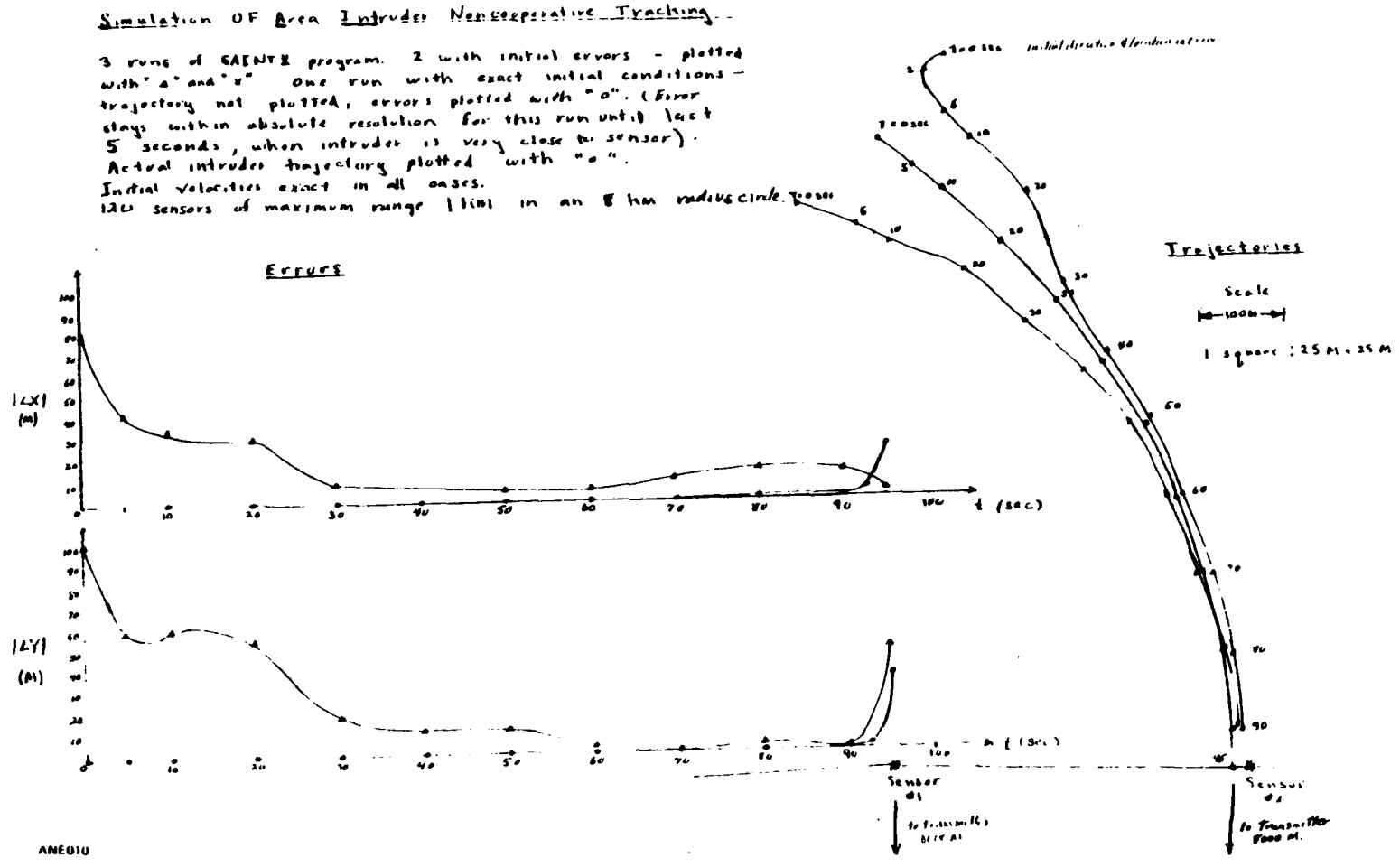

Figure F-2. Curved Course

APPENDIX G

SCHEMATIC DIAGRAMS

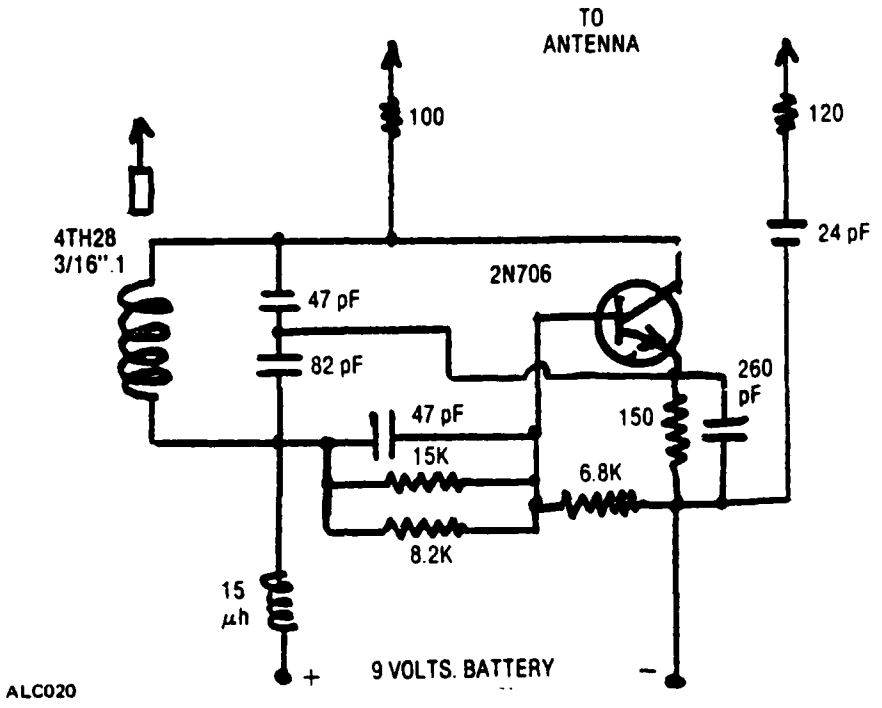

Figure G-1. Colpitts Oscillator Circuit

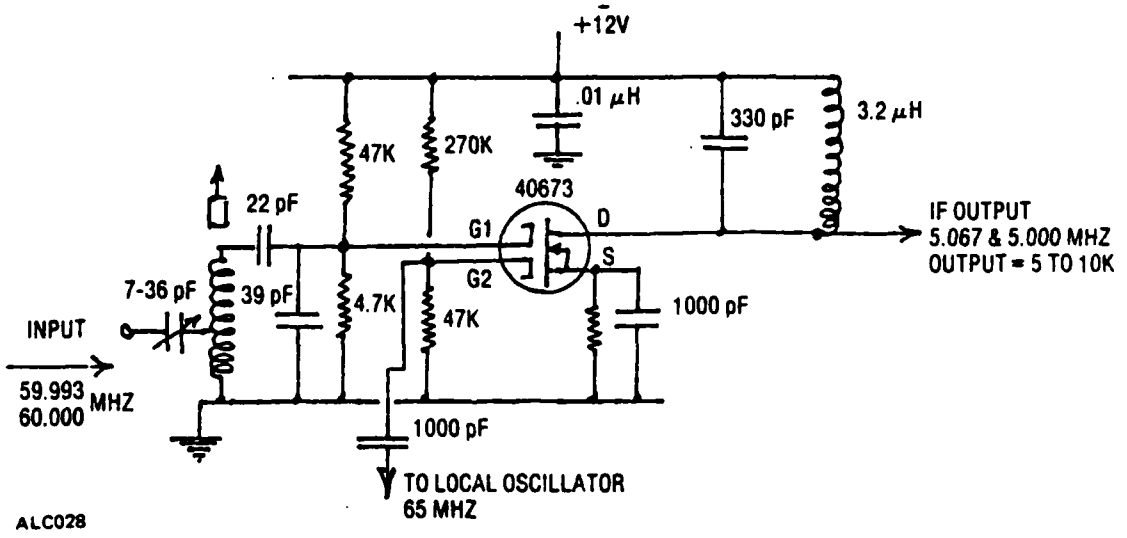

Figure G-2. VHF Mixer

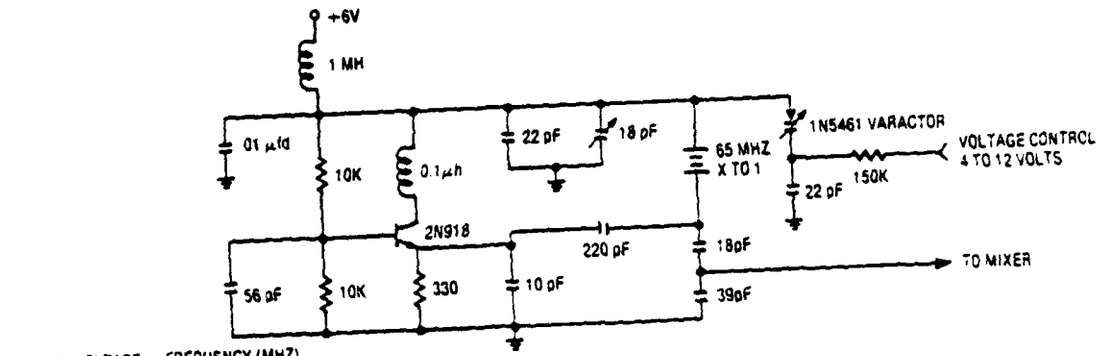

CONTROL VOLTAGE	FREQUENCY (MHZ)
12	65.00138
11	65.00135
10	65.00132
9	65.00125
8	65.00112
7	65.00065
6	65.00002

ALC029

Figure G-3. VXCO

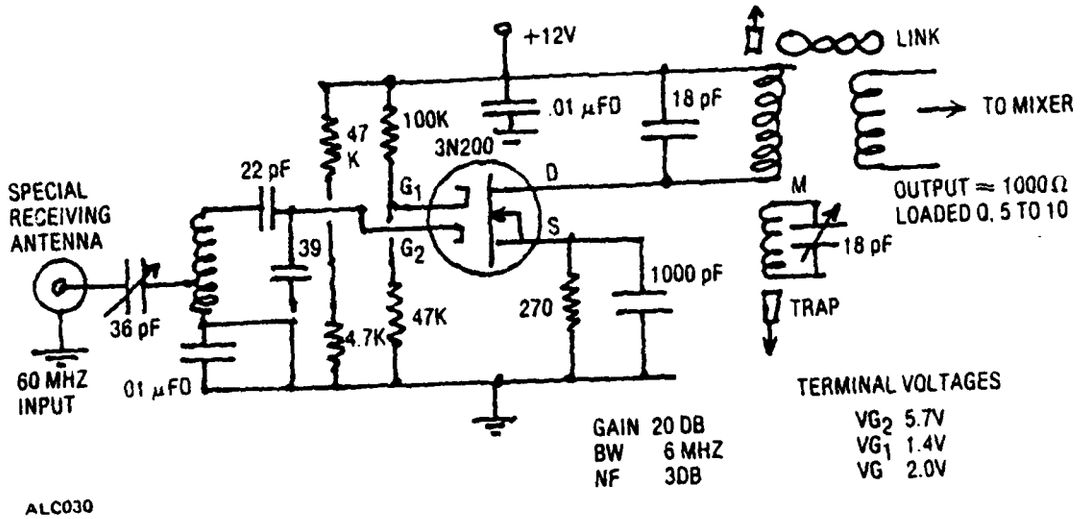

Figure G-4. Low Noise Amplifier (LNA)

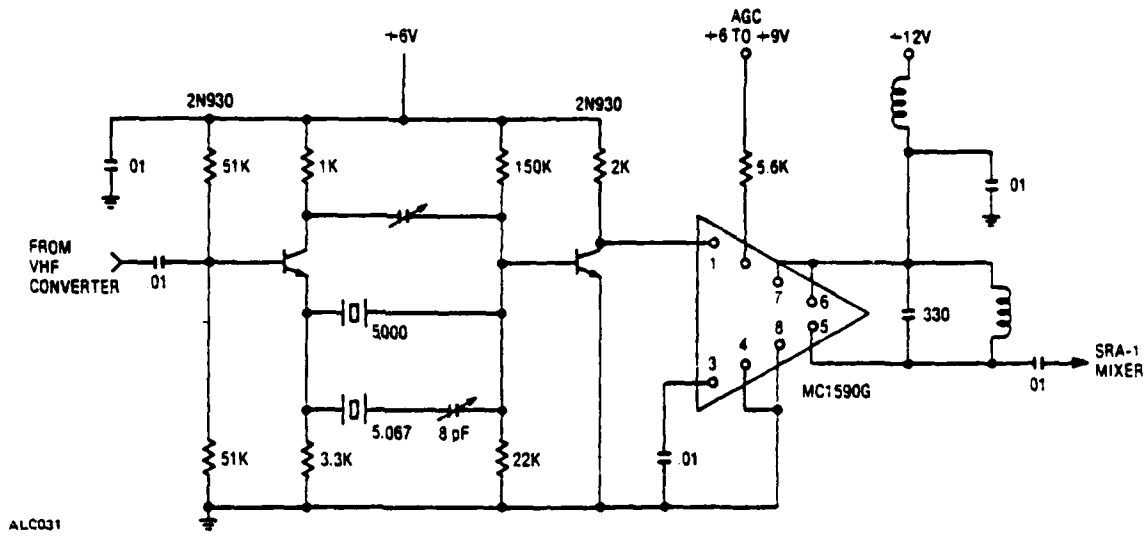

Figure G-5. High Frequency IF Stage

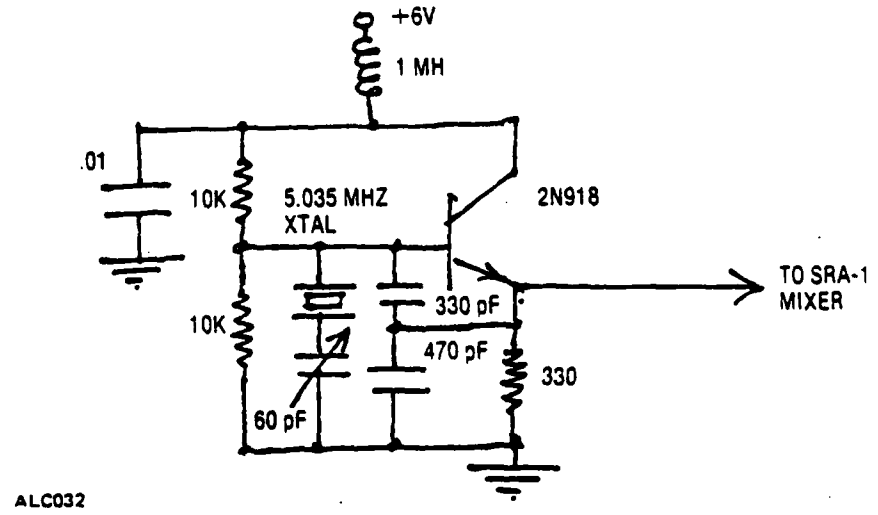

Figure G-6. High Frequency Crystal Oscillator

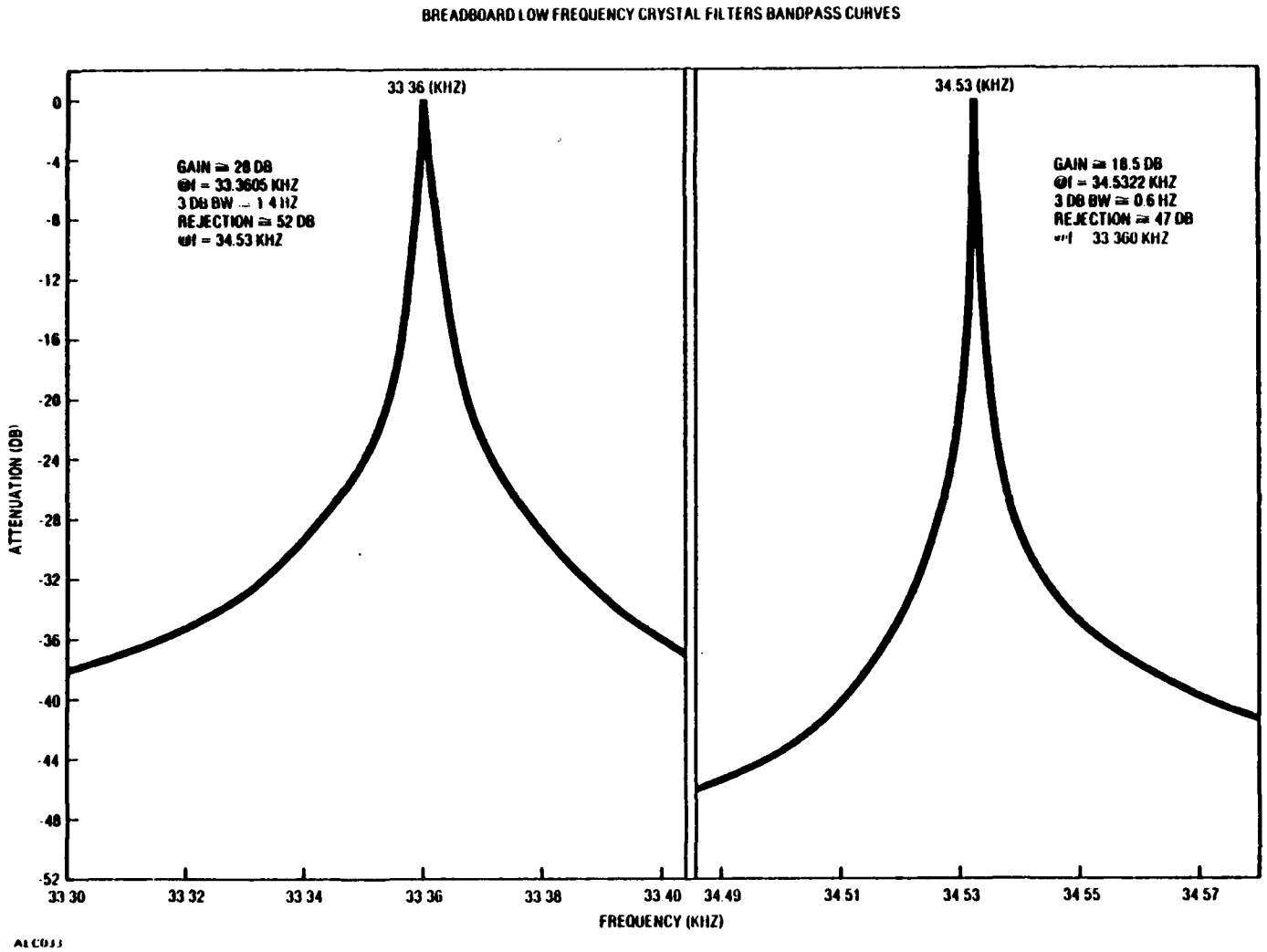

Figure G-7. Frequency Response of Parallel IF Stages

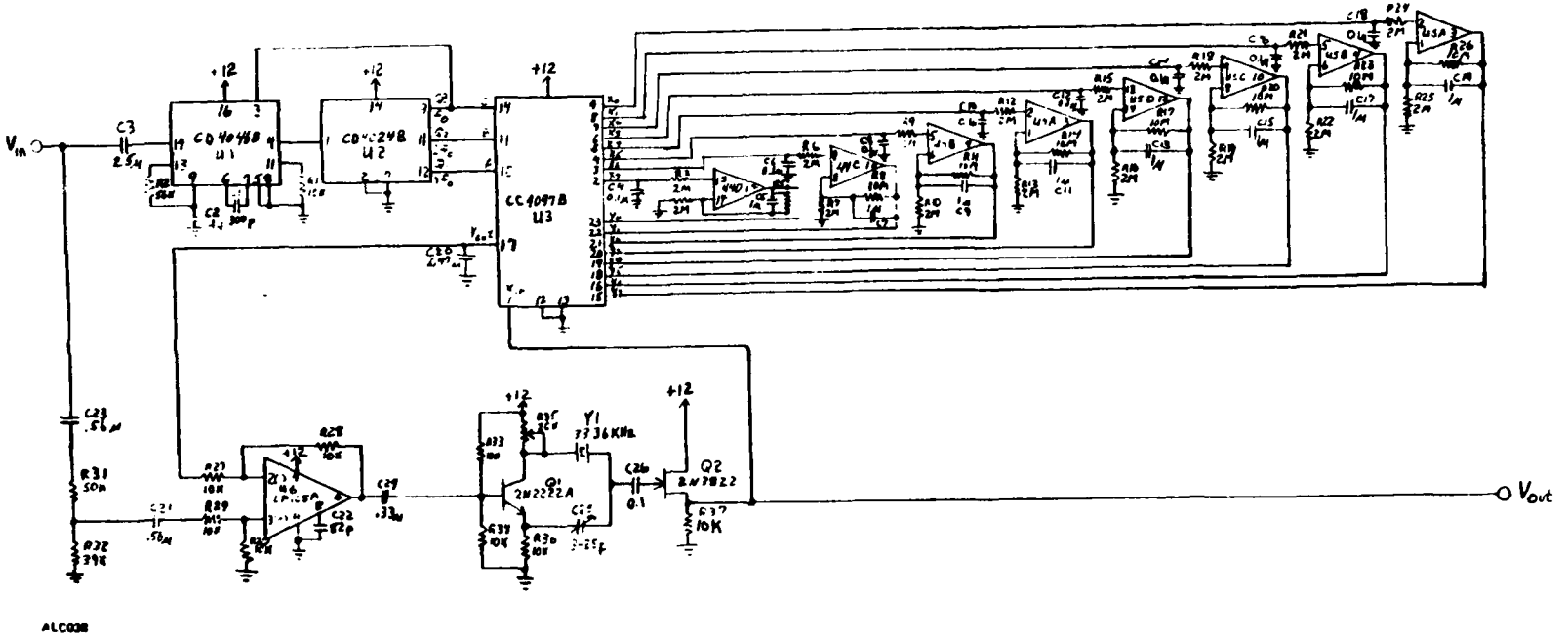

Figure G-8. Synchronous Filter Schematic

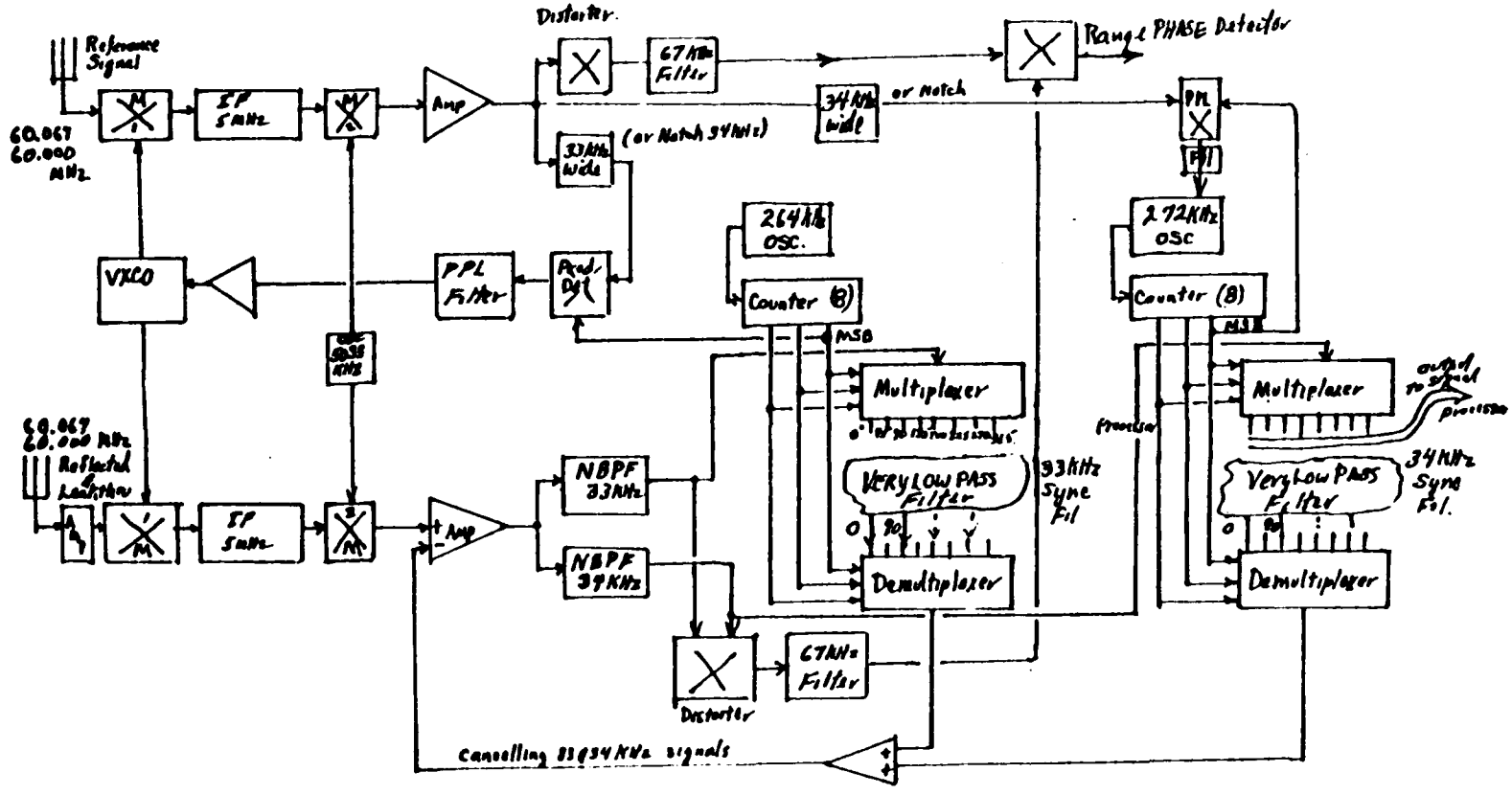

Figure G-9. Dual Channel Receiver Using Synchronous Filters at 33 and 34 kHz for Cancelling Feed-Through Signals

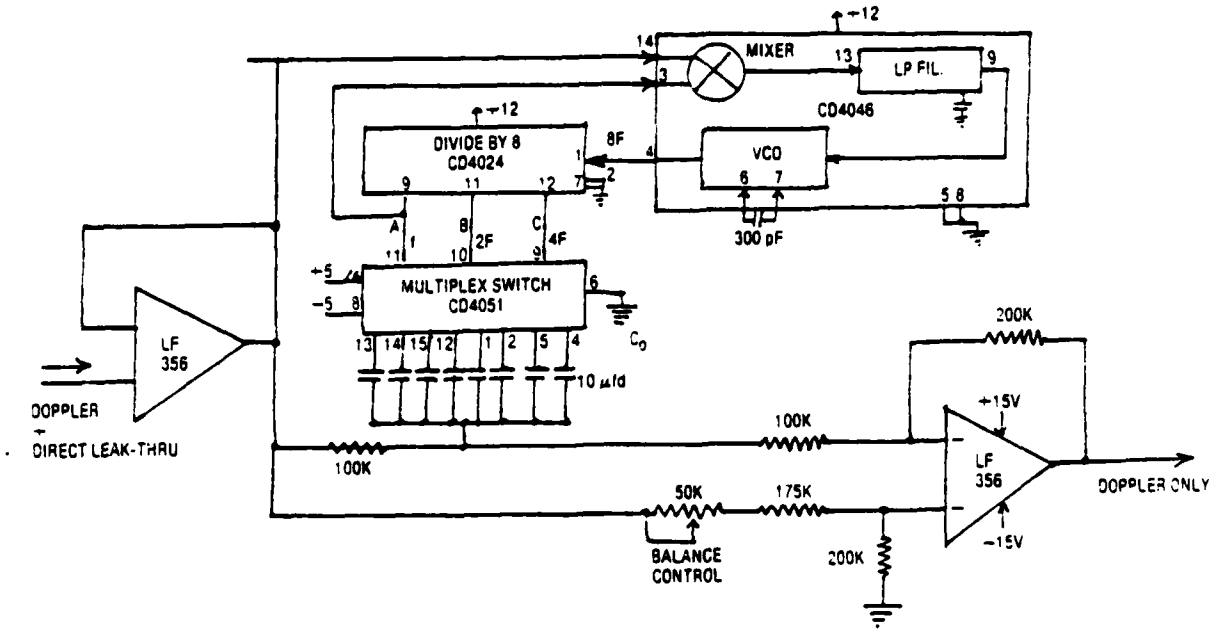

ALC040

Figure G-10. Synchronous Notch Filter

MISSION
of
Rome Air Development Center

RADC plans and executes research, development, test and selected acquisition programs in support of Command, Control Communications and Intelligence (C^3I) activities. Technical and engineering support within areas of technical competence is provided to ESD Program Offices (POs) and other ESD elements. The principal technical mission areas are communications, electromagnetic guidance and control, surveillance of ground and aerospace objects, intelligence data collection and handling, information system technology, ionospheric propagation, solid state sciences, microwave physics and electronic reliability, maintainability and compatibility.

Printed by
United States Air Force
Hanscom AFB, Mass. 01731


DATE
FILMED
8